ISSN 1007-9327 (print)
ISSN 2219-2840 (online)

World Journal of *Gastroenterology*

World J Gastroenterol 2022 May 28; 28(20): 2152-2250

Published by Baishideng Publishing Group Inc

World Journal of Gastroenterology

Contents

Weekly Volume 28 Number 20 May 28, 2022

MINIREVIEWS

ORIGINAL ARTICLE

Basic Study

Retrospective Cohort Study

Retrospective Study

Observational Study

CASE REPORT

LETTER TO THE EDITOR

ABOUT COVER

Editorial Board Member of *World Journal of Gastroenterology*, Donatella Barisani, MD, MSc, Associate Professor, School of Medicine and Surgery, University of Milano Bicocca, Via Cadore 48, Monza 20900, Italy. donatella.barisani@unimib.it

AIMS AND SCOPE

The primary aim of *World Journal of Gastroenterology* (*WJG*, *World J Gastroenterol*) is to provide scholars and readers from various fields of gastroenterology and hepatology with a platform to publish high-quality basic and clinical research articles and communicate their research findings online. *WJG* mainly publishes articles reporting research results and findings obtained in the field of gastroenterology and hepatology and covering a wide range of topics including gastroenterology, hepatology, gastrointestinal endoscopy, gastrointestinal surgery, gastrointestinal oncology, and pediatric gastroenterology.

INDEXING/ABSTRACTING

The *WJG* is now indexed in Current Contents®/Clinical Medicine, Science Citation Index Expanded (also known as SciSearch®), Journal Citation Reports®, Index Medicus, MEDLINE, PubMed, PubMed Central, and Scopus. The 2021 edition of Journal Citation Report® cites the 2020 impact factor (IF) for *WJG* as 5.742; Journal Citation Indicator: 0.79; IF without journal self cites: 5.590; 5-year IF: 5.044; Ranking: 28 among 92 journals in gastroenterology and hepatology; and Quartile category: Q2. The *WJG*'s CiteScore for 2020 is 6.9 and Scopus CiteScore rank 2020: Gastroenterology is 19/136.

RESPONSIBLE EDITORS FOR THIS ISSUE

Production Editor: *Yu-Xi Chen*; **Production Department Director:** *Xu Guo*; **Editorial Office Director:** *Ze-Mao Gong*.

NAME OF JOURNAL
World Journal of Gastroenterology

ISSN
ISSN 1007-9327 (print) ISSN 2219-2840 (online)

LAUNCH DATE
October 1, 1995

FREQUENCY
Weekly

EDITORS-IN-CHIEF
Andrzej S Tarnawski

EDITORIAL BOARD MEMBERS
http://www.wjgnet.com/1007-9327/editorialboard.htm

PUBLICATION DATE
May 28, 2022

INSTRUCTIONS TO AUTHORS
https://www.wjgnet.com/bpg/gerinfo/204

GUIDELINES FOR ETHICS DOCUMENTS
https://www.wjgnet.com/bpg/GerInfo/287

GUIDELINES FOR NON-NATIVE SPEAKERS OF ENGLISH
https://www.wjgnet.com/bpg/gerinfo/240

PUBLICATION ETHICS
https://www.wjgnet.com/bpg/GerInfo/288

PUBLICATION MISCONDUCT
https://www.wjgnet.com/bpg/gerinfo/208

ARTICLE PROCESSING CHARGE
https://www.wjgnet.com/bpg/gerinfo/242

STEPS FOR SUBMITTING MANUSCRIPTS
https://www.wjgnet.com/bpg/GerInfo/239

ONLINE SUBMISSION
https://www.f6publishing.com

World Journal of Gastroenterology

Submit a Manuscript: https://www.f6publishing.com

World J Gastroenterol 2022 May 28; 28(20): 2152-2162

DOI: 10.3748/wjg.v28.i20.2152

ISSN 1007-9327 (print) ISSN 2219-2840 (online)

MINIREVIEWS

Artificial intelligence: Emerging player in the diagnosis and treatment of digestive disease

Hai-Yang Chen, Peng Ge, Jia-Yue Liu, Jia-Lin Qu, Fang Bao, Cai-Ming Xu, Hai-Long Chen, Dong Shang, Gui-Xin Zhang

Specialty type: Gastroenterology and hepatology

Provenance and peer review: Invited article; Externally peer reviewed.

Peer-review model: Single blind

Peer-review report's scientific quality classification

Grade A (Excellent): A
Grade B (Very good): B
Grade C (Good): 0
Grade D (Fair): 0
Grade E (Poor): 0

P-Reviewer: Salvi M, Italy; Shafqat S, Pakistan

Received: September 24, 2021
Peer-review started: September 24, 2021
First decision: November 16, 2021
Revised: November 24, 2021
Accepted: April 24, 2022
Article in press: April 24, 2022
Published online: May 28, 2022

Hai-Yang Chen, Peng Ge, Jia-Yue Liu, Jia-Lin Qu, Fang Bao, Cai-Ming Xu, Hai-Long Chen, Dong Shang, Gui-Xin Zhang, Laboratory of Integrative Medicine, The First Affiliated Hospital of Dalian Medical University, Dalian 116011, Liaoning Province, China

Hai-Yang Chen, Peng Ge, Jia-Yue Liu, Fang Bao, Cai-Ming Xu, Hai-Long Chen, Dong Shang, Gui-Xin Zhang, Department of General Surgery, Pancreatic-Biliary Center, The First Affiliated Hospital of Dalian Medical University, Dalian 116011, Liaoning Province, China

Jia-Lin Qu, Cai-Ming Xu, Hai-Long Chen, Dong Shang, Gui-Xin Zhang, Institute (College) of Integrative Medicine, Dalian Medical University, Dalian 116044, Liaoning Province, China

Corresponding author: Gui-Xin Zhang, PhD, Professor, Director, Department of General Surgery, Pancreatic-Biliary Center, The First Affiliated Hospital of Dalian Medical University, No. 222 Zhongshan Road, Dalian 116011, Liaoning Province, China. zgx0109@126.com

Abstract

Given the breakthroughs in key technologies, such as image recognition, deep learning and neural networks, artificial intelligence (AI) continues to be increasingly developed, leading to closer and deeper integration with an increasingly data-, knowledge- and brain labor-intensive medical industry. As society continues to advance and individuals become more aware of their health needs, the problems associated with the aging of the population are receiving increasing attention, and there is an urgent demand for improving medical technology, prolonging human life and enhancing health. Digestive system diseases are the most common clinical diseases and are characterized by complex clinical manifestations and a general lack of obvious symptoms in the early stage. Such diseases are very difficult to diagnose and treat. In recent years, the incidence of diseases of the digestive system has increased. As AI applications in the field of health care continue to be developed, AI has begun playing an important role in the diagnosis and treatment of diseases of the digestive system. In this paper, the application of AI in assisted diagnosis and the application and prospects of AI in malignant and benign digestive system diseases are reviewed.

Key Words: Artificial intelligence; Digestive disease; Convolutional neural network; Deep learning; Review

Core Tip: With the continuous development of artificial intelligence, its integration in the field of medical and health care has received increasing attention, allowing the development and application of medical expert systems and artificial neural networks in the medical field. The development of artificial intelligence has resulted in not only more accurate diagnoses of digestive system diseases but also new treatments. Further research on the progress of artificial intelligence in digestive system diseases is needed to better serve patients.

Citation: Chen HY, Ge P, Liu JY, Qu JL, Bao F, Xu CM, Chen HL, Shang D, Zhang GX. Artificial intelligence: Emerging player in the diagnosis and treatment of digestive disease. *World J Gastroenterol* 2022; 28(20): 2152-2162
URL: https://www.wjgnet.com/1007-9327/full/v28/i20/2152.htm
DOI: https://dx.doi.org/10.3748/wjg.v28.i20.2152

INTRODUCTION

Artificial intelligence (AI) is a branch of computer science[1] inspired by human intelligence that operates in a different way. AI can be considered a set of computing techniques that allow machines to sense, learn, reason, act, *etc.* AI was first used at the Dartmouth AI Conference in the summer of 1956, which is considered the official birth of AI. In the 1990s, as technology continued to improve, hardware became more affordable, performance became more reliable, computing power, storage capacity and the ability to process data were greatly improved, and AI returned to life. In recent years, the application of AI in the medical field has reached an unprecedented height and scale. To date, great progress has been achieve in the use of AI in medicine and health, including speech recognition, medical imaging, wearable devices, risk management, pathology, *etc*[2].

The digestive system contains the largest number of organs in the human body and can be divided into the digestive tract and digestive glands. The digestive tract includes the oral cavity, pharynx, esophagus, stomach, duodenum, small intestine, large intestine, colon, *etc*. The digestive glands comprise the salivary glands, liver, pancreas, *etc.* The digestive system digests food, takes up nutrients and eliminates waste. The coordination of gastrointestinal physiological activities depends on the completion of the normal physiological function of the digestive system. Digestive system diseases, which are the most common clinical diseases, have complicated clinical manifestations, are interrelated with each other, and form a hot spot in the medical field[3]. The incidence of digestive system diseases is high, and often, there are no obvious symptoms in the early stage. Consequently, most digestive diseases are first noted in the middle and late stages; at this point, the prognosis is poor. As AI technology has continued to be developed, its strong computing power and learning ability have been gradually applied to solve complex medical problems. In the field of digestive diseases, such as gastric, liver, and pancreatic cancer and ulcerative colitis, AI can help improve the accuracy and sensitivity of the diagnosis and provide treatment options (Figure 1). AI not only improves the diagnostic accuracy of the disease but also provides a plan for clinical treatment.

In this review, we discuss AI and related technologies, their applications in digestive diseases and their future developments. We used PubMed and Google to search for relevant articles by using the keywords “digestive system diseases”, “artificial intelligence”, “machine learning”, “deep learning”, “computer-aided diagnosis”, “convolutional neural network”, and “endoscopy and endoscope images” for this review.

AI AUXILIARY DIAGNOSIS

In China, the development of AI has received considerable attention, particularly in the application of AI in the medical field. The development of AI has laid a solid foundation for precision medicine. In 2017, the China State Council announced that AI application should be promoted in the health care system. Subsequently, hundreds of new companies dedicated to the application of medical AI have emerged in China, promoting the development of AI in the medical field[4]. AI effectively improves the uneven allocation of medical resources, reduces medical costs and enhances medical efficiency. AI algorithms improve the ease of medical work and lead to not only technological innovations but also a transformation of the medical service mode. AI is applied in all fields of medicine and health, especially in the auxiliary diagnosis of diseases, and includes the following three aspects: intelligent guidance, electronic health records and risk monitoring of diagnosis and treatment.

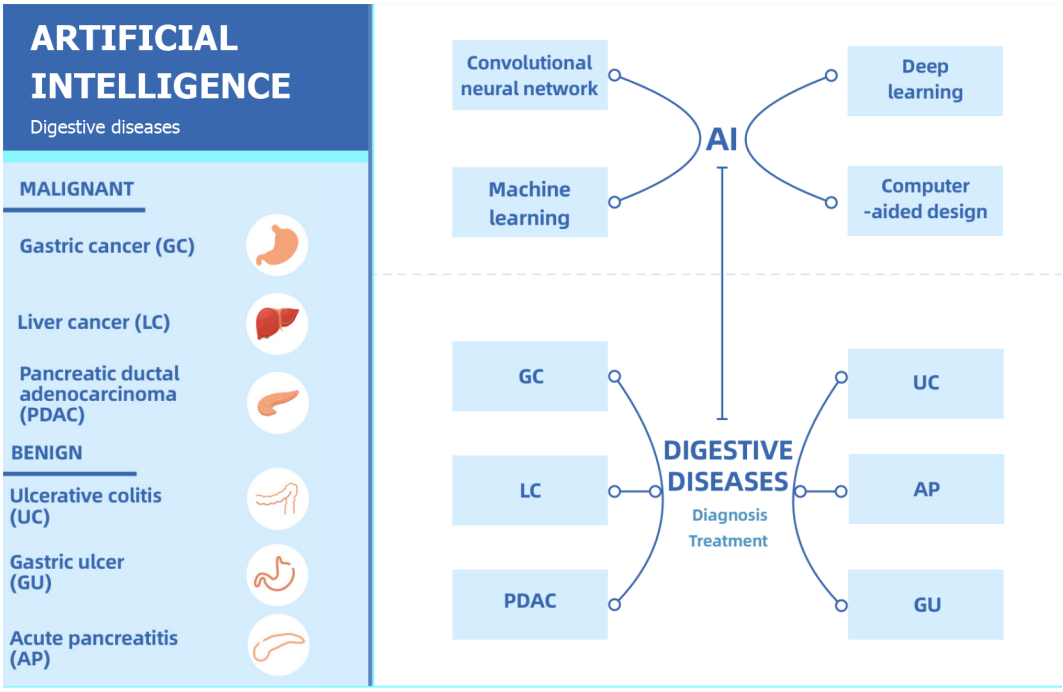

DOI: 10.3748/wjg.v28.i20.2152

Figure 1 Artificial intelligence and digestive diseases. AI: Artificial intelligence; GC: Gastric cancer; LC: Liver cancer; PDAC: Pancreatic ductal adenocarcinoma; UC: Ulcerative colitis; AP: Acute pancreatitis; GU: Gastric ulcer.

Intelligent guidance

Outpatient triage has gradually transitioned from a traditional manual system to an internet- and intelligence-based system. Most admitted patients lack an understanding of their disease and the hospital. To improve the efficiency and experience of the patients, intelligent guidance systems have been developed. Patients enter the Mini Program through screens on official hospital accounts to describe symptoms or diseases, and guidance assistants intelligently follow up and guide the patients to provide symptoms to accurately match departments, recommend doctors with the most consistent professional direction, and perform online guidance registration in one step. The research and development leading to intelligent guidance systems has led to a reduction in not only the workload of outpatient staff but also the human resource needs and costs of hospitals. These systems can guide patients to seek medical treatment quickly and accurately, improve the accuracy of patient registration and the efficiency of the physician response, increase efficiency at all steps of the patient stay, and effectively provide accurate medical treatment (Figure 2).

Electronic health record

Traditional health records are typically kept on paper, which tend to be scattered in hospital archives, limiting their value. The widespread use of the internet has facilitated the creation of electronic health records (EHRs), which are currently widely used worldwide[5]. EHRs can improve management processes, overcome problems with paper documentation, and ensure the quality of treatment. Both theoretically and practically, EHRs have guiding and economic value, while their applicative value continues to improve. In addition, EHRs can improve clinical decision-making, collaboration between health care teams, and medical efficiency.

Risk monitoring of diagnosis and treatment

Diagnostic risk monitoring systems can improve the diagnostic accuracy and greatly reduce the risk of misdiagnosis, and in this regard, AI has significant advantages over clinical experience. Compared with the United States, domestic equipment is used much more frequently under the same resource allocation[6]. This is the main point of medical care in China. Additionally, the large associated workload and high repeatability result in a cumbersome manual analysis and diagnosis. An accurate diagnosis rate is important for ensuring that radiologists can provide high-quality care to patients. A report in 1999 showed that 98000 people die of misdiagnosis each year, and diagnostic errors by radiologists are a key contributor[7]. Under a heavy workload, the diagnosis results can only be judged and analyzed by subjective individual experience, leading to high misdiagnosis and missed diagnosis rates. The large market demand for pathologists and diagnostic efficiency have also led to new challenges in the medical service industry. However, digestive system diseases increasingly depend on auxiliary diagnoses based on medical images while continuing to demonstrate a yearly increase in

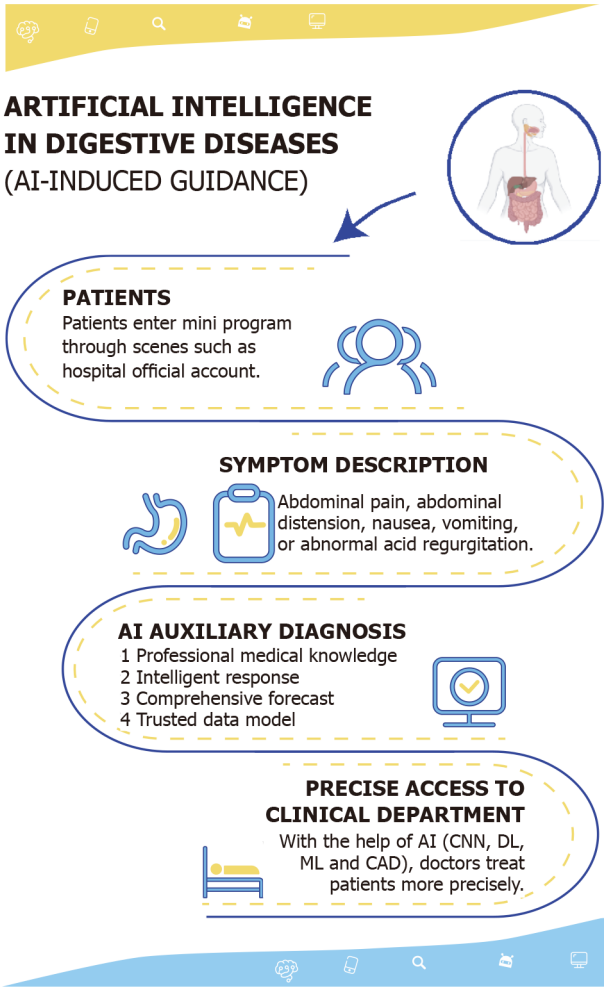

DOI: 10.3748/wjg.v28.i20.2152

Figure 2 Artificial intelligence and Intelligent guidance. CNN: Convolutional neural network; DL: Deep learning; ML: machine learning; CAD: Computer-aided design.

incidence.

The emergence of AI has led to its gradual use in digestive diseases. Machine learning (ML) is a branch of AI that aims to predict results by analyzing existing data and performing calculations based on an understanding of these data. Deep learning (DL) is a relatively new branch of ML that imitates learning through machine algorithms and provides a set of possible and reasonable solutions[8,9]. In esophageal cancer, van der Sommen *et al*[10] developed an automatic algorithm to distinguish early neoplastic lesions. Huang *et al*[11] used 84 images from 30 patients to train an AI-based neural network model to predict Helicobacter pylori infection. DL can be used to share more comprehensive medical diagnosis and treatment information with doctors with lightweight methods. At a higher level, we can comprehensively manage and guide the overall diagnosis and treatment level of the physician team to build a more scientific, accurate and friendly diagnosis and treatment risk monitoring system.

MALIGNANT DIGESTIVE DISEASES

The digestive system is a common site for malignant tumors, particularly gastric cancer, liver cancer, colorectal cancer and pancreatic cancer. Given the changes in lifestyle, diet and disease spectrum of the population, the incidence of malignant tumors of the digestive system continues to rise[12]. The early diagnosis of malignant tumors is critical for treatment, but patients with malignant tumors often have no obvious symptoms at the early stage, leading to difficulties in early diagnosis. This section summarizes the application of AI in the following three types of malignant tumors with high morbidity and mortality: gastric, liver and pancreatic cancer. The latest clinical studies concerning AI, gastric cancer, liver cancer, and pancreatic ductal adenocarcinoma are summarized in Table 1.

Table 1 Recent researches on artificial intelligence in malignant digestive system diseases

Ref.	Study design	Study population	Year	Disease	Country/Region	Number of cases	Methods	Results
Tang *et al*[48]	Retrospective	Hospital	2020	GC	China	45240 Images	DCNN	Accuracy: 85.1%-91.2%; Sensitivity: 85.9%-95.5%; Specificity: 81.7%-90.3%; AUC: 0.887-0.940
Zhang *et al*[49]	Retrospective	Hospital	2020	GC	China	21,217 Images	CNN	Accuracy: 78.7%
Nagao *et al*[50]	Retrospective	Hospital	2020	GC	Japan	16557 images	CNN	Accuracy: WLI (94.5%); Accuracy: NBI (94.3%); Accuracy: Indigo (95.5%)
Song *et al*[51]	Retrospective	Hospital	2020	GC	China	3212 Images	DL	Accuracy: 0.873; Sensitivity: 0.996; Specificity: 0.843; AUC: 0.986
Ma *et al*[52]	Retrospective	Hospital	2020	GC	China	763 Images	CNN	Accuracy: 98.4%; Specificity: 98.9%; Sensitivity: 98.0%;
Zhen *et al*[17]	Retrospective	Hospital	2020	LC	China	31608 Images	CNN	AUC: 0.946
Giordano *et al*[53]	Retrospective	Hospital	2020	LC	Italy	167 Cases	SVM, RF	Accuracy: Exceeded 94%
Jeong *et al*[54]	Retrospective	Cancer Institute	2020	LC	China	1421 Cases	DL	AUC: 0.84
Appelbaum *et al*[31]	Retrospective	Hospital	2020	PDAC	America	594 Cases	LR	AUC: 0.71
Marya *et al*[44]	Retrospective	Hospital	2020	PDAC	America	1174461 EUS Images	EUS-CNN	Sensitivity: 99%; Specificity: 98%
Tonozuka *et al*[55]	Retrospective	Hospital	2020	PDAC	Japan	920 Cases	EUS-CAD	AUC: 0.94

GC: Gastric cancer; LC: Liver cancer; PDAC: Pancreatic ductal adenocarcinoma; DCNN: Deep convolutional neural network; CNN: Convolutional neural network; DL: Deep learning; SVM: Support vector machine; RF: Random forest; LR: Logistic regression; EUS-CNN: Endoscopic ultrasound convolutional neural network; EUS-CAD: Computer-assisted diagnosis system using deep learning analysis of EUS images; AUC: area under the curve; WLI: White-light imaging; NBI: Nonmagnifying narrow-band imaging.

AI and gastric cancer

Gastric cancer (GC) is the fifth most common cancer and ranks third in cancer mortality worldwide, with more than 1 million new cases and 780000 deaths each year[13]. The stage at which GC is diagnosed can greatly affect the prognosis, with a poor prognosis typical in the late stage and a 5-year survival rate of early GC (EGC) exceeding 90%[14]. There are two difficulties in the early diagnosis of GC. First, EGC is difficult to detect, often presenting with slight reddish bulges or depressions under endoscopy that are not easily distinguished from inflammatory lesions. The second difficulty lies in judging the depth of the invasion of GC. In general, intramucosal GC or GC invading the superficial submucosal layer should be resected endoscopically, while GC invading the deep submucosal layer should be resected with open surgery; otherwise, there could be a risk of lymph node and distant metastasis. However, it is difficult to distinguish among these three forms of GC. The rapid development of DL and ML has led to great progress in AI, whose image recognition has transcended that of humans. By reviewing the published literature, this section discusses the diagnosis, treatment and prognosis of GC with AI.

Hirasawa *et al*[15] constructed a diagnostic system based on a convolutional neural network (CNN). The authors used 13584 endoscopic images to train the web-based learning model and 2296 GC images from 69 patients to evaluate its performance. The model took 47 s to analyze 2296 images and correctly diagnosed 77 GC lesions with a total sensitivity of 92%. This web-based learning model for the detection of EGC processes a large number of stored endoscopic images with clinical-related diagnostic capabilities in a very short time and may play a role in real-time gastroscopy[15].

Kubota *et al*[16] used a back propagation neural network algorithm to analyze the depth of gastric wall infiltration in endoscopic images of 344 GC patients and developed a computer-aided design (CAD) system. The cross-validation results revealed that the diagnostic accuracy of T1, T2, T3 and T4 GC was 77%, 49%, 51% and 55%, respectively. The accuracy in detecting intramucosal carcinoma (T1a) and submucosal invasive carcinoma (T1b) is 69%[16]. This study may be used to screen for EGC in the near future.

AI and liver cancer

Liver cancer (LC) is the second leading cause of death worldwide, and its incidence continues to increase[17]. In recent years, AI has been used in various aspects of LC diagnosis and treatment, especially in the field of imaging. However, individual differences in liver morphology and the internal anatomy and the highly heterogeneous molecular and pathological features of LC lead to great challenges in the implementation of AI, ML and DL for the diagnosis and treatment of this disease[18].

The following two modes of AI application are commonly used in the diagnosis of LC: DL and radiomics. Imaging plays a key role in the identification and diagnosis of hepatobiliary diseases and the establishment of surgical treatment plans. Radiologists and surgeons demarcate organs and diagnose diseases based on their experience and judgment, which can be subjective, time consuming and unreproducible; AI can address these limitations. DL is mainly used for the diagnosis of LC *via* traditional machine learning (TML) and CNNs. In TML, a well-developed anatomical model must be established in advance and manually corrected in the later stages[19], while the application of CNNs allows images to be directly used in the learning process, allowing the extraction and utilization of all information contained in the image for DL[20]. Shaw Hospital of Zhejiang University developed a DL system for liver tumor diagnosis through a CNN. In addition to learning more than 30000 magnetic resonance (MR) images, the system incorporates patient clinical data (medical records, examination results, etc.) and demonstrates excellent diagnostic performance with a coincidence rate with a final pathological result of 92%[17].

The application of AI in the treatment of LC has led to new opportunities and challenges, promoting the standardization and intelligence of LC management. Hu *et al*[21] used 3D visualization to evaluate the spatial relationship between tumors and surrounding blood vessels before hepatectomy, which serves as a suitable guide for surgical resection. In the treatment of LC by radiofrequency ablation, fusion imaging can integrate enhanced computed tomography (CT)/MR images with real-time ultrasound imaging by electromagnetic tracking to accurately locate the target lesions[22-24]. AI has been applied to all aspects of LC treatment and auxiliary diagnosis, but further prospective research is needed.

AI and pancreatic ductal adenocarcinoma

Pancreatic ductal adenocarcinoma (PDAC) is a rapidly progressive and highly malignant tumor of the digestive tract[25]. Although many methods have been developed for the diagnosis and treatment of PDAC in recent years, the effective rate of treatment and prognosis remain poor (the 5-year survival rate is only 9%[26]). The early detection and accurate treatment of PDAC are important directions requiring urgent solutions.

Recently, rapid developments have been achieved in the AI-based screening and diagnosis of PDAC, leading to acceptable effects. Ansari *et al*[27] applied artificial neural networks (ANNs) to a long-term survival prediction of patients after radical surgery for PDAC for the first time and achieved a consistency index of 0.79, indicating that their ANN could predict the survival rate of PDAC patients after radical surgery. Fine needle aspiration (FNA) biopsy is an elaborate approach used to diagnose solid masses of the pancreas. Due to the small number of cases, its development is limited. Momeni-Boroujeni *et al*[28] used a multilayer-perceptron neural network (MNN) to evaluate 277 cell mass images from 75 pancreatic FNA patients and achieved an accuracy of 100% in the classification of benign and malignant tumors. In particular, the sensitivity and specificity of MNN in identifying atypical cases were 80% and 75%, respectively. Intraductal papillary mucinous neoplasm (IPMN), a papillary mucinous tumor with many subtypes, has particular malignant potential. Endoscopic ultrasonography (EUS) can reveal the structure of the pancreas and the dilation of the pancreatic duct and can be used to evaluate the degree of malignancy of IPMN. Indeed, Kuwahara *et al*[29] used AI to build a system to perform this function. The authors uploaded 3970 EUS images of 50 patients to the system for DL analysis. The endpoint of their system was the accuracy in diagnosing the malignancy degree of IPMNs by AI. The results showed that the AI system had significantly better value in diagnosing malignant IPMNs than benign IPMNs, with an area under the receiver operating characteristic curve of 0.91 in diagnosing malignant IPMNs. In addition, a three-dimensional depth supervised segmentation network has been developed to classify CT images from PDAC patients and control groups. Chu *et al*[30] standardized the number of cases, the sizes of the segmented images, and the selection of organs and then segmented the boundaries of the abdominal organs and pancreatic tumors in 575 control subjects and 750 patients with PDAC. The results showed that the sensitivity and specificity of the algorithm in detecting PDAC in patients were 94.1% and 98.5%, respectively. The early diagnosis of PDAC is a problem that many physicians find difficult. Appelbaum *et al*[31] developed a risk model for the prediction of PDAC based on patient EHRs that could identify high-risk groups one year in advance,

suggesting that their risk scores could also be used as an initial filter for PDAC.

BENIGN DIGESTIVE DISEASES

In addition to gastric cancer, liver cancer and other malignant tumors, other digestive system diseases include ulcerative colitis, pancreatitis, gastric ulcer, gastritis, intestinal polyp and other benign digestive system diseases. We summarize the application of AI for the benign digestive system diseases discussed below. The latest applications of AI in ulcerative colitis, severe acute pancreatitis, gastric ulcers, gastritis and intestinal polyps are summarized in Table 2.

AI and ulcerative colitis

Ulcerative colitis (UC) is a common chronic intestinal disease; however, there is no single gold standard for the diagnosis of this disease. Combining clinical, laboratory, imaging, endoscopic and histopathological findings, the diagnosis is made by excluding infectious and other noninfectious forms of colitis [32]. Endoscopy is essential, but the accuracy and precision of the diagnosis are limited by doctors' subjectivity. Yao *et al*[33] established a fully automatic endoscopic disease grading video analysis system through AI. These authors used a CNN to train models to predict the amount of information in still images and, thus, determine the severity of the disease. Then, the authors examined 51 and 264 videos from developed high-resolution and multicenter clinical trial test sets, respectively. The results showed that the static image information classification system had good performance, with a sensitivity of 0.902 and specificity of 0.870. For the high-resolution videos, the fully automated methods correctly predicted the Mayo endoscopic score (MES) in 78%. The automated MES grading of the clinical trial videos (often low resolution) correctly distinguished remitted *vs* active disease in 83.7%. To analyze endoscopic images of UC more accurately, Takenaka *et al*[34] developed a deep neural network system and tested 40758 colonoscopy images and 6885 biopsy results from 2012 UC patients. The results identified endoscopic remission with 90.1% accuracy and histologic remission with 92.9% accuracy. In addition, Maeda *et al*[35] developed a CAD system to predict persistent histologic inflammation using endocytoscopy and evaluated its accuracy using 12900 endocytoscopy images. The results showed that the CAD system provided a diagnostic sensitivity, specificity, and accuracy of 74%, 97% and 91%, respectively. In recent years, great progress has been achieved in the treatment of UC, but surgery remains important [36]. These results show that AI has great potential in the diagnosis and treatment of UC.

AI and pancreatitis

Acute pancreatitis (AP) is a common clinical acute abdomen disease with a complex and variable presentation. Severe AP (SAP) is often life threatening, with multiple organ dysfunction induced by SAP being a particularly difficult clinical problem[37]. Qiu *et al*[38] developed three ML algorithms to predict the risk of organ failure in moderate SAP (MSAP) and SAP. These authors inputted 16 parameters from 263 patients with MSAP and SAP into a support vector machine (SVM), logical regression analysis (LRA) and ANN models. The results showed that the SVM, LRA and ANN models could effectively predict the risk of multiorgan failure in MSAP and SAP. Respiratory failure is the main cause of early death in SAP. The early prediction of acute lung injury (ALI) is beneficial for reducing mortality from SAP. The ANN model established by Fei *et al*[39] can effectively predict the occurrence of ALI induced by SAP, with the accuracy of predicting severe acute respiratory distress syndrome reaching 82.8%. Abdominal infection is an important risk factor for organ failure induced by SAP. Compared with logistic regression analyses, the ANN model developed by Qiu *et al*[40] can more accurately predict abdominal infection in MSAP and SAP, with a sensitivity and specificity of 80.99% and 89.44%, respectively. Fei *et al*[41] constructed and verified an ANN model based on clinical and laboratory data from 72 patients with AP. Notably, the sensitivity, specificity, positive predictive value and negative predictive value of the ANN model for portosplenomesenteric venous thrombosis (PSMVT) were 80%, 85.7%, 77.6% and 90.7%, respectively. Thus, this model provides a good reference for the clinical prediction of the occurrence of PSMVT. The recurrence rate after the first attack of AP is approximately 22%, but few indicators can predict this recurrence. Chen *et al*[42] developed a quantitative radiology model based on contrast-enhanced CT. The results of the verification analysis showed that the model can predict the recurrence of AP well in the main and verification populations, with accuracies of 87.1% and 89.0%, respectively. This finding suggests that their model may be a good quantitative method for the prediction of recurrence in patients with AP. Chronic pancreatitis (CP), which is another common clinical digestive system disease, is an important factor in inducing pancreatic cancer. Although traditional pancreaticoduodenectomy, distal pancreatectomy, and the Frey and Beger procedures have achieved considerable success in relieving CP pain, the approaches are often accompanied by serious complications. Therefore, minimally invasive surgery and robot platforms are gradually being applied in the surgical treatment of CP. A retrospective study based on 812 cases of robotic pancreatectomy and reconstruction showed that the robotic platform is safe and feasible in performing complex pancreatectomy to alleviate the sequelae of CP[43]. Autoimmune pancreatitis (AIP) is a rare and special type of chronic pancreatitis, and its diagnosis is clinically challenging. Marya *et al*

Table 2 Recent researches on artificial intelligence in benign digestive system diseases

Ref.	Study design	Study population	Year	Disease	Country/Region	Number of cases	Methods	Results
Maeda *et al*[35]	Retrospective	Hospital	2019	UC	Japan	12900 Images	CAD	Sensitivity: 74%; Specificity: 97%; Accuracy: 91%
Popa *et al*[56]	Retrospective	Hospital	2020	UC	Romania	55 Cases	ML	Accuracy: 90%; AUC: 0.92
Tong *et al*[57]	Retrospective	Hospital	2020	UC	China	6399 Cases	RF, CNN	Sensitivity: RF (0.89); Sensitivity: CNN (0.90)
Qiu *et al*[38]	Retrospective	Hospital	2019	SAP	China	263 Cases	ANN	Sensitivity: 80.99%; Specificity: 89.44%
Chen *et al*[42]	Retrospective	Hospital	2019	SAP	China	389 Cases	LR	Accuracy: 87.1%
Namikawa *et al*[45]	Retrospective	Hospital	2020	Gastric ulcer	Japan	720 Images	A-CNN	Sensitivity: 93.3%; Specificity: 99.0%; PPV: 99.1%
Steinbuss *et al*[46]	Retrospective	Hospital	2020	Gastritis	Germany	1230 Images	CNN	Accuracy: 84%; Sensitivity: 100%; Specificity: 93%
Ozawa *et al*[47]	Retrospective	Hospital	2020	Colorectal polyps	Japan	16418 Images	CNN	Sensitivity: 92%; PPV: 86%

UC: Ulcerative colitis; SAP: Severe acute pancreatitis; CAD: Computer-aided diagnosis; ML: Machine learning; RF: Random forest; CNN: Convolutional neural network; ANN: Artificial neural networks; LR: Logistic regression; A-CNN: Advanced convolutional neural network; AUC: Area under the curve; PPV: Positive predictive value.

[44] developed and validated a CNN model based on a database containing 174461 EUS images and videos from 583 patients. After training, the model could accurately distinguish AIP from PDAC and other benign pancreatic diseases with a sensitivity and specificity of 90% and 85%, respectively.

AI and other diseases

AI has been used in numerous applications for other diseases, such as gastric ulcers, gastritis and colorectal polyps. Namikawa *et al*[45] developed an advanced CNN (A-CNN) based on the original convolutional neural network and evaluated its applicability in the classification of gastric ulcers. These authors used 720 images from 120 patients with gastric ulcers to evaluate the diagnostic performance of the A-CNN. The results showed that the sensitivity, specificity, and positive predictive value of the A-CNN in classifying gastric ulcers were 93.3%, 99.0%, and 99.1%, respectively. There are several subtypes of gastritis, including autoimmune, bacterial, and chemical. Steinbuss *et al*[46] evaluated the ability of a CNN to classify the common gastritis subtypes using a small data set of 1230 gastric antrum and corpus biopsy images. The results showed that the overall accuracy in the test set was 84%, and the sensitivity and specificity for bacterial gastritis were 100% and 93%, respectively. Ozawa *et al*[47] constructed a deep CNN architecture and trained the CNN using 16418 images from 4752 colorectal polyps and 4013 normal colorectal images. Then, the performance of the trained CNN was verified with 7077 additional colonoscopy images. The results showed that the sensitivity of the CNN was 92%, and the positive predictive value was 86%, proving that it has excellent potential as a colonoscopy CP-diagnosis support system based on AI.

CONCLUSION

With the steady development of AI and its heavy integration in the medical industry, AI has received increasing attention in the fields of medicine and health. Digestive system AI technology differs from other AI technologies because of the nonstandard nature of most digestive endoscopic images and the large number of influencing factors, resulting in difficulty in developing such technology. Currently, AI plays an important role in digestive system diseases, particularly in its gradual application in diagnosis and treatment in the clinic. AI has broad prospects in the field of medicine and health, but the cooperation of medical workers and computer experts is needed to develop more intelligent applications and higher-quality services for patients. In summary, as an emerging player, AI will continue to play an increasingly important role in future development. The close combination of AI and medicine can address problems, such as the insufficient supply and uneven distribution of medical resources and

low degree of medical efficiency. More in-depth research should be performed to investigate the application of AI in digestive system diseases from various perspectives to obtain additional diagnosis and treatment measures, promote diagnosis, optimize treatment, improve patient prognosis, and gradually achieve intelligent and accurate medical treatment.

FOOTNOTES

Author contributions: Chen HY, Ge P, Liu JY contributed equally to the manuscript; Chen HY conceived this review and drafted the manuscript; Ge P, Liu JY, Bao F and Qu JL are responsible for the figure drawing and literature collation; Xu CM, Chen HL and Shang D edited and finalized the manuscript for submission; Zhang GX reviewed and approved the submitted manuscript.

Supported by Key Discipline of Liaoning Traditional Chinese Medicine Clinical Ability Promote Construction Project, No. LNZYXZY201903; and Development Guidance Plan Projects in Liaoning Province, No. 2019JH-8/10300028.

Conflict-of-interest statement: There is no conflict of interest associated with any of the senior author or other coauthors contributed their efforts in this manuscript.

Country/Territory of origin: China

ORCID number: Hai-Yang Chen 0000-0002-6705-2249; Peng Ge 0000-0002-2647-2474; Jia-Yue Liu 0000-0001-9294-7493; Jia-Lin Qu 0000-0003-2020-4783; Fang Bao 0000-0002-1609-2953; Cai-Ming Xu 0000-0001-7794-2301; Hai-Long Chen 0000-0001-5247-7343; Dong Shang 0000-0002-4300-359X; Gui-Xin Zhang 0000-0002-6171-394X.

S-Editor: Wang JL
L-Editor: A
P-Editor: Wang JL

REFERENCES

1 **Parasher G**, Wong M, Rawat M. Evolving role of artificial intelligence in gastrointestinal endoscopy. *World J Gastroenterol* 2020; **26**: 7287-7298 [PMID: 33362384 DOI: 10.3748/wjg.v26.i46.7287]
2 **Sensakovic WF**, Mahesh M. Role of the Medical Physicist in the Health Care Artificial Intelligence Revolution. *J Am Coll Radiol* 2019; **16**: 393-394 [PMID: 30446397 DOI: 10.1016/j.jacr.2018.09.022]
3 **Togashi K**. Applications of artificial intelligence to endoscopy practice: The view from Japan Digestive Disease Week 2018. *Dig Endosc* 2019; **31**: 270-272 [PMID: 30681203 DOI: 10.1111/den.13354]
4 **He J**, Baxter SL, Xu J, Zhou X, Zhang K. The practical implementation of artificial intelligence technologies in medicine. *Nat Med* 2019; **25**: 30-36 [PMID: 30617336 DOI: 10.1038/s41591-018-0307-0]
5 **Rudin RS**, Friedberg MW, Shekelle P, Shah N, Bates DW. Getting Value From Electronic Health Records: Research Needed to Improve Practice. *Ann Intern Med* 2020; **172**: S130-S136 [PMID: 32479182 DOI: 10.7326/M19-0878]
6 **Hershberger AG**. Review of 'Delivering Health Care in America: A Systems Approach, 3rd edition'. 2005
7 **Kohn LT**, Corrigan JM, Donaldson MS; Institute of Medicine (US) Committee on Quality of Health Care in America. To err is human: building a safer health system. Washington: National Academies Press (US), 2000: 245-246 [PMID: 25077248 DOI: 10.17226/9728]
8 **Schmidhuber J**. Deep learning in neural networks: an overview. *Neural Netw* 2015; **61**: 85-117 [PMID: 25462637 DOI: 10.1016/j.neunet.2014.09.003]
9 **Deo RC**. Machine Learning in Medicine. *Circulation* 2015; **132**: 1920-1930 [PMID: 26572668 DOI: 10.1161/CIRCULATIONAHA.115.001593]
10 **van der Sommen F**, Zinger S, Curvers WL, Bisschops R, Pech O, Weusten BL, Bergman JJ, de With PH, Schoon EJ. Computer-aided detection of early neoplastic lesions in Barrett's esophagus. *Endoscopy* 2016; **48**: 617-624 [PMID: 27100718 DOI: 10.1055/s-0042-105284]
11 **Huang CR**, Sheu BS, Chung PC, Yang HB. Computerized diagnosis of Helicobacter pylori infection and associated gastric inflammation from endoscopic images by refined feature selection using a neural network. *Endoscopy* 2004; **36**: 601-608 [PMID: 15243882 DOI: 10.1055/s-2004-814519]
12 **Bray F**, Ferlay J, Soerjomataram I, Siegel RL, Torre LA, Jemal A. Global cancer statistics 2018: GLOBOCAN estimates of incidence and mortality worldwide for 36 cancers in 185 countries. *CA Cancer J Clin* 2018; **68**: 394-424 [PMID: 30207593 DOI: 10.3322/caac.21492]
13 **Hirasawa T**, Ikenoyama Y, Ishioka M, Namikawa K, Horiuchi Y, Nakashima H, Fujisaki J. Current status and future

perspective of artificial intelligence applications in endoscopic diagnosis and management of gastric cancer. *Dig Endosc* 2021; **33**: 263-272 [PMID: 33159692 DOI: 10.1111/den.13890]

14 **Sano T**, Coit DG, Kim HH, Roviello F, Kassab P, Wittekind C, Yamamoto Y, Ohashi Y. Proposal of a new stage grouping of gastric cancer for TNM classification: International Gastric Cancer Association staging project. *Gastric Cancer* 2017; **20**: 217-225 [PMID: 26897166 DOI: 10.1007/s10120-016-0601-9]

15 **Hirasawa T**, Aoyama K, Tanimoto T, Ishihara S, Shichijo S, Ozawa T, Ohnishi T, Fujishiro M, Matsuo K, Fujisaki J, Tada T. Application of artificial intelligence using a convolutional neural network for detecting gastric cancer in endoscopic images. *Gastric Cancer* 2018; **21**: 653-660 [PMID: 29335825 DOI: 10.1007/s10120-018-0793-2]

16 **Kubota K**, Kuroda J, Yoshida M, Ohta K, Kitajima M. Medical image analysis: computer-aided diagnosis of gastric cancer invasion on endoscopic images. *Surg Endosc* 2012; **26**: 1485-1489 [PMID: 22083334 DOI: 10.1007/s00464-011-2036-z]

17 **Zhen SH**, Cheng M, Tao YB, Wang YF, Juengpanich S, Jiang ZY, Jiang YK, Yan YY, Lu W, Lue JM, Qian JH, Wu ZY, Sun JH, Lin H, Cai XJ. Deep Learning for Accurate Diagnosis of Liver Tumor Based on Magnetic Resonance Imaging and Clinical Data. *Front Oncol* 2020; **10**: 680 [PMID: 32547939 DOI: 10.3389/fonc.2020.00680]

18 **Calderaro J**, Ziol M, Paradis V, Zucman-Rossi J. Molecular and histological correlations in liver cancer. *J Hepatol* 2019; **71**: 616-630 [PMID: 31195064 DOI: 10.1016/j.jhep.2019.06.001]

19 **Wang CJ**, Hamm CA, Savic LJ, Ferrante M, Schobert I, Schlachter T, Lin M, Weinreb JC, Duncan JS, Chapiro J, Letzen B. Deep learning for liver tumor diagnosis part II: convolutional neural network interpretation using radiologic imaging features. *Eur Radiol* 2019; **29**: 3348-3357 [PMID: 31093705 DOI: 10.1007/s00330-019-06214-8]

20 **Hamm CA**, Wang CJ, Savic LJ, Ferrante M, Schobert I, Schlachter T, Lin M, Duncan JS, Weinreb JC, Chapiro J, Letzen B. Deep learning for liver tumor diagnosis part I: development of a convolutional neural network classifier for multi-phasic MRI. *Eur Radiol* 2019; **29**: 3338-3347 [PMID: 31016442 DOI: 10.1007/s00330-019-06205-9]

21 **Hu M**, Hu H, Cai W, Mo Z, Xiang N, Yang J, Fang C. The Safety and Feasibility of Three-Dimensional Visualization Technology Assisted Right Posterior Lobe Allied with Part of V and VIII Sectionectomy for Right Hepatic Malignancy Therapy. *J Laparoendosc Adv Surg Tech A* 2018; **28**: 586-594 [PMID: 29172950 DOI: 10.1089/lap.2017.0479]

22 **Citone M**, Fanelli F, Falcone G, Mondaini F, Cozzi D, Miele V. A closer look to the new frontier of artificial intelligence in the percutaneous treatment of primary lesions of the liver. *Med Oncol* 2020; **37**: 55 [PMID: 32424627 DOI: 10.1007/s12032-020-01380-y]

23 **Ahn SJ**, Lee JM, Lee DH, Lee SM, Yoon JH, Kim YJ, Lee JH, Yu SJ, Han JK. Real-time US-CT/MR fusion imaging for percutaneous radiofrequency ablation of hepatocellular carcinoma. *J Hepatol* 2017; **66**: 347-354 [PMID: 27650284 DOI: 10.1016/j.jhep.2016.09.003]

24 **Huang Q**, Zeng Q, Long Y, Tan L, Zheng R, Xu E, Li K. Fusion imaging techniques and contrast-enhanced ultrasound for thermal ablation of hepatocellular carcinoma - A prospective randomized controlled trial. *Int J Hyperthermia* 2019; **36**: 1207-1215 [PMID: 31813295 DOI: 10.1080/02656736.2019.1687945]

25 **Iovanna J**. Implementing biological markers as a tool to guide clinical care of patients with pancreatic cancer. *Transl Oncol* 2021; **14**: 100965 [PMID: 33248412 DOI: 10.1016/j.tranon.2020.100965]

26 **Siegel RL**, Miller KD, Jemal A. Cancer statistics, 2020. *CA Cancer J Clin* 2020; **70**: 7-30 [PMID: 31912902 DOI: 10.3322/caac.21590]

27 **Ansari D**, Nilsson J, Andersson R, Regnér S, Tingstedt B, Andersson B. Artificial neural networks predict survival from pancreatic cancer after radical surgery. *Am J Surg* 2013; **205**: 1-7 [PMID: 23245432 DOI: 10.1016/j.amjsurg.2012.05.032]

28 **Momeni-Boroujeni A**, Yousefi E, Somma J. Computer-assisted cytologic diagnosis in pancreatic FNA: An application of neural networks to image analysis. *Cancer Cytopathol* 2017; **125**: 926-933 [PMID: 28885766 DOI: 10.1002/cncy.21915]

29 **Kuwahara T**, Hara K, Mizuno N, Okuno N, Matsumoto S, Obata M, Kurita Y, Koda H, Toriyama K, Onishi S, Ishihara M, Tanaka T, Tajika M, Niwa Y. Usefulness of Deep Learning Analysis for the Diagnosis of Malignancy in Intraductal Papillary Mucinous Neoplasms of the Pancreas. *Clin Transl Gastroenterol* 2019; **10**: 1-8 [PMID: 31117111 DOI: 10.14309/ctg.0000000000000045]

30 **Chu LC**, Park S, Kawamoto S, Wang Y, Zhou Y, Shen W, Zhu Z, Xia Y, Xie L, Liu F, Yu Q, Fouladi DF, Shayesteh S, Zinreich E, Graves JS, Horton KM, Yuille AL, Hruban RH, Kinzler KW, Vogelstein B, Fishman EK. Application of Deep Learning to Pancreatic Cancer Detection: Lessons Learned From Our Initial Experience. *J Am Coll Radiol* 2019; **16**: 1338-1342 [PMID: 31492412 DOI: 10.1016/j.jacr.2019.05.034]

31 **Appelbaum L**, Cambronero JP, Stevens JP, Horng S, Pollick K, Silva G, Haneuse S, Piatkowski G, Benhaga N, Duey S, Stevenson MA, Mamon H, Kaplan ID, Rinard MC. Development and validation of a pancreatic cancer risk model for the general population using electronic health records: An observational study. *Eur J Cancer* 2021; **143**: 19-30 [PMID: 33278770 DOI: 10.1016/j.ejca.2020.10.019]

32 **Ooi CJ**, Fock KM, Makharia GK, Goh KL, Ling KL, Hilmi I, Lim WC, Kelvin T, Gibson PR, Gearry RB, Ouyang Q, Sollano J, Manatsathit S, Rerknimitr R, Wei SC, Leung WK, de Silva HJ, Leong RW; Asia Pacific Association of Gastroenterology Working Group on Inflammatory Bowel Disease. The Asia-Pacific consensus on ulcerative colitis. *J Gastroenterol Hepatol* 2010; **25**: 453-468 [PMID: 20370724 DOI: 10.1111/j.1440-1746.2010.06241.x]

33 **Yao H**, Najarian K, Gryak J, Bishu S, Rice MD, Waljee AK, Wilkins HJ, Stidham RW. Fully automated endoscopic disease activity assessment in ulcerative colitis. *Gastrointest Endosc* 2021; **93**: 728-736.e1 [PMID: 32810479 DOI: 10.1016/j.gie.2020.08.011]

34 **Takenaka K**, Ohtsuka K, Fujii T, Negi M, Suzuki K, Shimizu H, Oshima S, Akiyama S, Motobayashi M, Nagahori M, Saito E, Matsuoka K, Watanabe M. Development and Validation of a Deep Neural Network for Accurate Evaluation of Endoscopic Images From Patients With Ulcerative Colitis. *Gastroenterology* 2020; **158**: 2150-2157 [PMID: 32060000 DOI: 10.1053/j.gastro.2020.02.012]

35 **Maeda Y**, Kudo SE, Mori Y, Misawa M, Ogata N, Sasanuma S, Wakamura K, Oda M, Mori K, Ohtsuka K. Fully automated diagnostic system with artificial intelligence using endocytoscopy to identify the presence of histologic inflammation associated with ulcerative colitis (with video). *Gastrointest Endosc* 2019; **89**: 408-415 [PMID: 30268542 DOI: 10.1016/j.gie.2018.09.024]

36 **Crippa J**, Carvello M, Kotze PG, Spinelli A. Robotic Surgery in Inflammatory Bowel Disease. *Curr Drug Targets* 2021;

22: 112-116 [PMID: 33109059 DOI: 10.2174/1389450121999200820125918]
37 **Ge P**, Luo Y, Okoye CS, Chen H, Liu J, Zhang G, Xu C. Intestinal barrier damage, systemic inflammatory response syndrome, and acute lung injury: A troublesome trio for acute pancreatitis. *Biomed Pharmacother* 2020; **132**: 110770 [PMID: 33011613 DOI: 10.1016/j.biopha.2020.110770]
38 **Qiu Q**, Nian YJ, Guo Y, Tang L, Lu N, Wen LZ, Wang B, Chen DF, Liu KJ. Development and validation of three machine-learning models for predicting multiple organ failure in moderately severe and severe acute pancreatitis. *BMC Gastroenterol* 2019; **19**: 118 [PMID: 31272385 DOI: 10.1186/s12876-019-1016-y]
39 **Fei Y**, Gao K, Li WQ. Artificial neural network algorithm model as powerful tool to predict acute lung injury following to severe acute pancreatitis. *Pancreatology* 2018; **18**: 892-899 [PMID: 30268673 DOI: 10.1016/j.pan.2018.09.007]
40 **Qiu Q**, Nian YJ, Tang L, Guo Y, Wen LZ, Wang B, Chen DF, Liu KJ. Artificial neural networks accurately predict intra-abdominal infection in moderately severe and severe acute pancreatitis. *J Dig Dis* 2019; **20**: 486-494 [PMID: 31328389 DOI: 10.1111/1751-2980.12796]
41 **Fei Y**, Hu J, Li WQ, Wang W, Zong GQ. Artificial neural networks predict the incidence of portosplenomesenteric venous thrombosis in patients with acute pancreatitis. *J Thromb Haemost* 2017; **15**: 439-445 [PMID: 27960048 DOI: 10.1111/jth.13588]
42 **Chen Y**, Chen TW, Wu CQ, Lin Q, Hu R, Xie CL, Zuo HD, Wu JL, Mu QW, Fu QS, Yang GQ, Zhang XM. Radiomics model of contrast-enhanced computed tomography for predicting the recurrence of acute pancreatitis. *Eur Radiol* 2019; **29**: 4408-4417 [PMID: 30413966 DOI: 10.1007/s00330-018-5824-1]
43 **Hamad A**, Zenati MS, Nguyen TK, Hogg ME, Zeh HJ 3rd, Zureikat AH. Safety and feasibility of the robotic platform in the management of surgical sequelae of chronic pancreatitis. *Surg Endosc* 2018; **32**: 1056-1065 [PMID: 29273874 DOI: 10.1007/s00464-017-6010-2]
44 **Marya NB**, Powers PD, Chari ST, Gleeson FC, Leggett CL, Abu Dayyeh BK, Chandrasekhara V, Iyer PG, Majumder S, Pearson RK, Petersen BT, Rajan E, Sawas T, Storm AC, Vege SS, Chen S, Long Z, Hough DM, Mara K, Levy MJ. Utilisation of artificial intelligence for the development of an EUS-convolutional neural network model trained to enhance the diagnosis of autoimmune pancreatitis. *Gut* 2021; **70**: 1335-1344 [PMID: 33028668 DOI: 10.1136/gutjnl-2020-322821]
45 **Namikawa K**, Hirasawa T, Nakano K, Ikenoyama Y, Ishioka M, Shiroma S, Tokai Y, Yoshimizu S, Horiuchi Y, Ishiyama A, Yoshio T, Tsuchida T, Fujisaki J, Tada T. Artificial intelligence-based diagnostic system classifying gastric cancers and ulcers: comparison between the original and newly developed systems. *Endoscopy* 2020; **52**: 1077-1083 [PMID: 32503056 DOI: 10.1055/a-1194-8771]
46 **Steinbuss G**, Kriegsmann K, Kriegsmann M. Identification of Gastritis Subtypes by Convolutional Neuronal Networks on Histological Images of Antrum and Corpus Biopsies. *Int J Mol Sci* 2020; **21** [PMID: 32932860 DOI: 10.3390/ijms21186652]
47 **Ozawa T**, Ishihara S, Fujishiro M, Kumagai Y, Shichijo S, Tada T. Automated endoscopic detection and classification of colorectal polyps using convolutional neural networks. *Therap Adv Gastroenterol* 2020; **13**: 1756284820910659 [PMID: 32231710 DOI: 10.1177/1756284820910659]
48 **Tang D**, Wang L, Ling T, Lv Y, Ni M, Zhan Q, Fu Y, Zhuang D, Guo H, Dou X, Zhang W, Xu G, Zou X. Development and validation of a real-time artificial intelligence-assisted system for detecting early gastric cancer: A multicentre retrospective diagnostic study. *EBioMedicine* 2020; **62**: 103146 [PMID: 33254026 DOI: 10.1016/j.ebiom.2020.103146]
49 **Zhang L**, Zhang Y, Wang L, Wang J, Liu Y. Diagnosis of gastric lesions through a deep convolutional neural network. *Dig Endosc* 2021; **33**: 788-796 [PMID: 32961597 DOI: 10.1111/den.13844]
50 **Nagao S**, Tsuji Y, Sakaguchi Y, Takahashi Y, Minatsuki C, Niimi K, Yamashita H, Yamamichi N, Seto Y, Tada T, Koike K. Highly accurate artificial intelligence systems to predict the invasion depth of gastric cancer: efficacy of conventional white-light imaging, nonmagnifying narrow-band imaging, and indigo-carmine dye contrast imaging. *Gastrointest Endosc* 2020; **92**: 866-873.e1 [PMID: 32592776 DOI: 10.1016/j.gie.2020.06.047]
51 **Song Z**, Zou S, Zhou W, Huang Y, Shao L, Yuan J, Gou X, Jin W, Wang Z, Chen X, Ding X, Liu J, Yu C, Ku C, Liu C, Sun Z, Xu G, Wang Y, Zhang X, Wang D, Wang S, Xu W, Davis RC, Shi H. Clinically applicable histopathological diagnosis system for gastric cancer detection using deep learning. *Nat Commun* 2020; **11**: 4294 [PMID: 32855423 DOI: 10.1038/s41467-020-18147-8]
52 **Ma B**, Guo Y, Hu W, Yuan F, Zhu Z, Yu Y, Zou H. Artificial Intelligence-Based Multiclass Classification of Benign or Malignant Mucosal Lesions of the Stomach. *Front Pharmacol* 2020; **11**: 572372 [PMID: 33132910 DOI: 10.3389/fphar.2020.572372]
53 **Giordano S**, Takeda S, Donadon M, Saiki H, Brunelli L, Pastorelli R, Cimino M, Soldani C, Franceschini B, Di Tommaso L, Lleo A, Yoshimura K, Nakajima H, Torzilli G, Davoli E. Rapid automated diagnosis of primary hepatic tumour by mass spectrometry and artificial intelligence. *Liver Int* 2020; **40**: 3117-3124 [PMID: 32662575 DOI: 10.1111/liv.14604]
54 **Jeong S**, Ge Y, Chen J, Gao Q, Luo G, Zheng B, Sha M, Shen F, Cheng Q, Sui C, Liu J, Wang H, Xia Q, Chen L. Latent Risk Intrahepatic Cholangiocarcinoma Susceptible to Adjuvant Treatment After Resection: A Clinical Deep Learning Approach. *Front Oncol* 2020; **10**: 143 [PMID: 32140448 DOI: 10.3389/fonc.2020.00143]
55 **Tonozuka R**, Itoi T, Nagata N, Kojima H, Sofuni A, Tsuchiya T, Ishii K, Tanaka R, Nagakawa Y, Mukai S. Deep learning analysis for the detection of pancreatic cancer on endosonographic images: a pilot study. *J Hepatobiliary Pancreat Sci* 2021; **28**: 95-104 [PMID: 32910528 DOI: 10.1002/jhbp.825]
56 **Popa IV**, Burlacu A, Mihai C, Prelipcean CC. A Machine Learning Model Accurately Predicts Ulcerative Colitis Activity at One Year in Patients Treated with Anti-Tumour Necrosis Factor α Agents. *Medicina (Kaunas)* 2020; **56** [PMID: 33233514 DOI: 10.3390/medicina56110628]
57 **Tong Y**, Lu K, Yang Y, Li J, Lin Y, Wu D, Yang A, Li Y, Yu S, Qian J. Can natural language processing help differentiate inflammatory intestinal diseases in China? *BMC Med Inform Decis Mak* 2020; **20**: 248 [PMID: 32993636 DOI: 10.1186/s12911-020-01277-w]

World Journal of Gastroenterology

Submit a Manuscript: https://www.f6publishing.com

World J Gastroenterol 2022 May 28; 28(20): 2163-2175

DOI: 10.3748/wjg.v28.i20.2163

ISSN 1007-9327 (print) ISSN 2219-2840 (online)

MINIREVIEWS

Advances in medical treatment for pancreatic neuroendocrine neoplasms

Yuan-Liang Li, Zi-Xuan Cheng, Fu-Huan Yu, Chao Tian, Huang-Ying Tan

Specialty type: Oncology

Provenance and peer review: Invited article; Externally peer reviewed.

Peer-review model: Single blind

Peer-review report's scientific quality classification

Grade A (Excellent): A
Grade B (Very good): 0
Grade C (Good): C
Grade D (Fair): 0
Grade E (Poor): 0

P-Reviewer: Fujimori N, Japan; Maurea S, Italy

Received: October 27, 2021
Peer-review started: October 27, 2021
First decision: December 27, 2021
Revised: December 31, 2021
Accepted: April 15, 2022
Article in press: April 15, 2022
Published online: May 28, 2022

Yuan-Liang Li, Zi-Xuan Cheng, Fu-Huan Yu, Chao Tian, Huang-Ying Tan, Department of Integrative Oncology, China-Japan Friendship Hospital, Beijing 100029, China

Yuan-Liang Li, Zi-Xuan Cheng, Fu-Huan Yu, Chao Tian, Graduate School, Beijing University of Chinese Medicine, Beijing 100029, China

Corresponding author: Huang-Ying Tan, MD, PhD, Professor, Department of Integrative Oncology, China-Japan Friendship Hospital, No. 2 Yinghuayuan East Street, Chaoyang District, Beijing 100029, China. tanhuangying@263.net

Abstract

Pancreatic neuroendocrine neoplasms (PanNENs) are rare neoplasms with strong heterogeneity that have experienced an increasing incidence rate in recent years. For patients with locally advanced or distant metastatic PanNENs, systemic treatment options vary due to the different differentiations, grades and stages. The available options for systemic therapy include somatostatin analogs, molecularly targeted agents, cytotoxic chemotherapeutic agents, immune checkpoint inhibitors, and peptide receptor radionuclide therapy. In addition, the development of novel molecularly targeted agents is currently in progress. The sequence of selection between different chemotherapy regimens has been of great interest, and resistance to chemotherapeutic agents is the major limitation in their clinical application. Novel agents and high-level clinical evidence continue to emerge in the field of antiangiogenic agents. Peptide receptor radionuclide therapy is increasingly employed for the treatment of advanced neuroendocrine tumors, and greater therapeutic efficacy may be achieved by emerging radiolabeled peptides. Since immune checkpoint inhibitor monotherapies for PanNENs appear to have limited antitumor activity, dual immune checkpoint inhibitor therapies or combinations of antiangiogenic therapies and immune checkpoint inhibitors have been applied in the clinic to improve clinical efficacy. Combining the use of a variety of agents with different mechanisms of action provides new possibilities for clinical treatments. In the future, the study of systemic therapies will continue to focus on the screening of the optimal benefit population and the selection of the best treatment sequence strategy with the aim of truly achieving individualized precise treatment of PanNENs.

Key Words: Pancreatic neuroendocrine neoplasms; Advanced neuroendocrine tumors; Medical treatment; Peptide receptor radionuclide therapy; Advances

Core Tip: Pancreatic neuroendocrine neoplasms (PanNENs) are rare neoplasms with strong heterogeneity. The systemic treatment options of advanced PanNENs vary due to the different differentiations, grades and stages and include somatostatin analogs, molecularly targeted agents, cytotoxic chemotherapeutic agents, immune checkpoint inhibitors, and peptide receptor radionuclide therapy. Despite the multiple systemic therapeutic options for PanNENs, problems such as drug resistance, adverse side effects and limited scope of application still exist. Thus, we review the clinical development of medical treatment options, focusing on ongoing clinical studies and the development of novel targeted drugs, to provide a reference for clinicians and researchers.

Citation: Li YL, Cheng ZX, Yu FH, Tian C, Tan HY. Advances in medical treatment for pancreatic neuroendocrine neoplasms. *World J Gastroenterol* 2022; 28(20): 2163-2175
URL: https://www.wjgnet.com/1007-9327/full/v28/i20/2163.htm
DOI: https://dx.doi.org/10.3748/wjg.v28.i20.2163

INTRODUCTION

Neuroendocrine neoplasms (NENs) are a group of rare neoplasms originating from neuroendocrine cells. However, with the development of diagnostic techniques and improvements in the clinical understanding of these tumors, the incidence is increasing yearly. Based on the United States Surveillance, Epidemiology, and End Results database, the age-adjusted incidence of NENs has increased nearly 6.4-fold from 1.09 per 100000 persons in 1973 to 6.98 per 100000 in 2012. The pancreas (0.84 per 100000 persons) is one of the most common primary sites of NENs, ranked after the lung, small intestine, and rectum[1]. In countries such as China and India, pancreatic NENs (PanNETs) are the most common gastroenteropancreatic neuroendocrine tumors (GEP-NETs) and have the highest morbidity [2].

PanNENs are highly heterogeneous neoplasms that appear as various clinical manifestations and biological behaviors. PanNENs can be classified as nonfunctional PanNENs (60%-90%) or functional PanNETs based on the absence or presence of symptoms associated with the overproduction of specific hormones, respectively[3]. The most common functional PanNETs are gastrinomas and insulinomas; less frequent are glucagonomas, somatostatinomas, vasoactive intestinal polypeptide-secreting tumors, and adrenocorticotropic hormone-secreting tumors[4-7]. The majority of PanNETs are sporadic, although PanNETs can occur as part of hereditary multiple tumor syndromes, such as multiple endocrine neoplasia type 1 and von Hippel-Lindau (VHL) disease[8]. PanNENs are classified into three main histological categories according to the 2019 World Health Organization Classification of Tumors of the Digestive System (5th edition): well-differentiated neuroendocrine tumors (NETs), poorly differentiated neuroendocrine carcinomas (NECs), and mixed neuroendocrine-non-neuroendocrine neoplasms. NETs are further classified into three grades (G1, G2, and G3) according to their mitotic rate (mitoses/2 mm^2) and Ki-67 proliferation index[9]. PanNENs clinical staging is currently based on the eighth edition of the American Joint Committee on Cancer tumor node metastasis (TNM) staging system. Well-differentiated PanNETs are staged by PanNENs TNMs, whereas poorly differentiated PanNECs are staged according to the TNM staging of pancreatic cancer[10].

Therapeutic strategies vary due to the different grades and stages of PanNENs. Radical surgery is the primary treatment option for patients with locally resectable PanNENs; however, 40%-50% of NENs present with distant metastases at the time of initial diagnosis, limiting the opportunity for surgical resection. Moreover, many patients with resected PanNENs will develop recurrence with distant metastases[11,12]. Systemic therapeutic options for patients with locally advanced or distant metastatic PanNENs involve somatostatin analogs (SSAs), molecularly targeted agents, cytotoxic chemotherapeutic agents, immune checkpoint inhibitors, and peptide receptor radionuclide therapy (PRRT) (Figure 1).

The therapeutic goals for patients with locally unresectable and metastatic PanNENs include both hormone control and anti-tumor therapy. The scope of this article does not include medical treatments for the control of functional PanNENs hormone-related symptoms, but rather focuses on anti-tumor therapy. Despite the multiple systemic therapeutic options for PanNENs, problems such as drug resistance, adverse side effects and limited scope of application still exist, and clinical needs have not been met. Thus, conquering drug resistance, expanding the scope of application and developing new clinical drugs have been the main focus of researchers in recent decades. This article reviews the clinical development of existing drugs, focusing on ongoing clinical studies and the development of novel targeted drugs, to provide a reference for addressing the current clinical treatment dilemma and the future direction of PanNENs drug research.

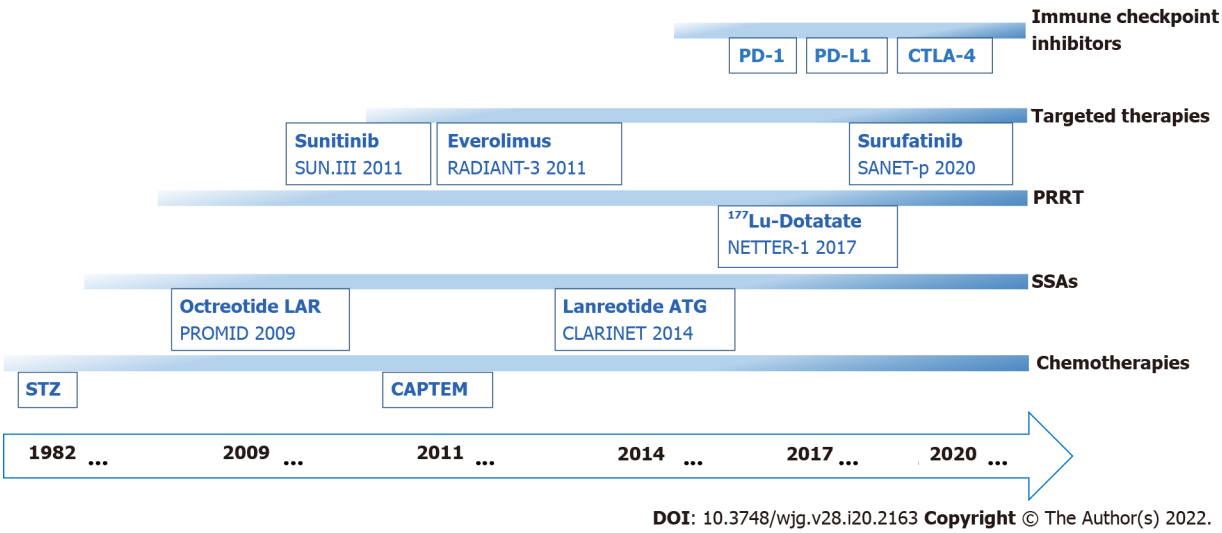

DOI: 10.3748/wjg.v28.i20.2163

Figure 1 History and key events in the development of pancreatic neuroendocrine neoplasms systemic therapy. PRRT: Peptide receptor radionuclide therapy; SSAs: Somatostatin analogs; PD-L1: Programmed cell death-ligand 1 inhibitor; PD-1: Programmed cell death-1 inhibitor; CTLA-4: Cytotoxic T-lymphocyte antigen 4 inhibitor; STZ: Streptozotocin; CAPTEM: Capecitabine and temozolomide regimen; PROMID[13], NCT00171873; CLARINET[14], NCT00353496; SUN.III[15], NCT00428597; RADIANT-3[16], NCT00510068; SANET-P[17], NCT02589821; NETTER-1[18], NCT01578239.

ADVANCES IN CHEMOTHERAPY

Systemic treatment with chemotherapy is one of the main therapies for advanced PanNENs. Appropriate chemotherapy regimens are delivered according to pathological classification and grades, mainly including temozolomide-based combination regimens and platinum-based regimens. Among them, temozolomide-based combination chemotherapy (CAPTEM and STEM) regimens can be used for the first-line treatment of patients with advanced PanNETs G2/G3[19-21] and for the second-line treatment of patients with PanNECs[22,23]. The synergistic effect of capecitabine in combination with temozolomide chemotherapy may be due to its ability to deplete O6-methylguanine DNA methyltransferase (MGMT) levels in tumor cells, thereby enhancing the alkylating effect of temozolomide[24]. The association between MGMT expression status and temozolomide efficacy has been demonstrated in other tumor types, and several studies in NENs have suggested that MGMT promoter methylation or low protein expression correlates better with a favorable therapeutic response to temozolomide and that MGMT status can be used as a biological indicator of the response to alkylating agent treatment in NENs[25,26]. However, because most of the current studies on the relationship between MGMT status and temozolomide efficacy are small-sample, retrospective studies, there is some controversy. A prospective study (NCT03217097) of the relationship between MGMT status and temozolomide efficacy in NETs is underway in which patients with advanced NETs have been divided into two groups according to whether they have MGMT methylation and are receiving temozolomide or oxaliplatin-based chemotherapy at a 1:1 (unmethylated group) and 2:1 (methylated group) ratio, respectively. ORR was used as the primary outcome indicator[27]. Additional prospective studies (NCT02698410, NCT01824875, NCT01525082) have evaluated MGMT status as a secondary outcome.

In clinical practice, drug resistance is one of the major obstacles to the effective treatment of temozolomide-based chemotherapy in PanNENs. Current studies on temozolomide resistance mechanisms are mainly conducted in the field of glioma. In addition to the overexpression of MGMT, the overexpression of the base excision repair (BER) pathway, alteration of autophagy, and activation of the phosphoinositide 3-kinase/protein kinase B/mammalian target of rapamycin (PI3K/AKT/mTOR) pathway contribute to acquired temozolomide resistance[28]. Wu *et al*[29] found enhanced temozolomide sensitivity in a preclinical study of glioblastoma multiforme (GBM) that poly (ADP-ribose) polymerase (PARP) inhibitors, particularly in MGMT-unmethylated GBM, and this effect may be mediated by inhibition of MGMT-mediated repair by abolishing MGMT function and inhibition of BER-mediated repair (Figure 2). Therefore, the combination of PARP inhibitors and temozolomide may be one solution for overcoming temozolomide resistance, and clinical trials applying this combination regimen in patients with small-cell lung cancer have yielded good clinical results[30]. A phase II clinical trial (NCT04394858) is currently evaluating the efficacy of single-agent temozolomide *vs* the combination of temozolomide and olaparib in patients with advanced pheochromocytoma and paraganglioma; however, no clinical trials of temozolomide in combination with PARP inhibitors for PanNENs have been conducted. Temozolomide resistance has also been observed to be associated with activation of the PI3K/AKT/mTOR pathway, and inhibition of the PI3K/AKT/mTOR pathway sensitizes tumor cells to apoptosis upon temozolomide treatment[31]. In a prospective phase II clinical trial, temozolomide in combination with everolimus as second-line therapy for advanced PanNETs resulted in an ORR of 40%

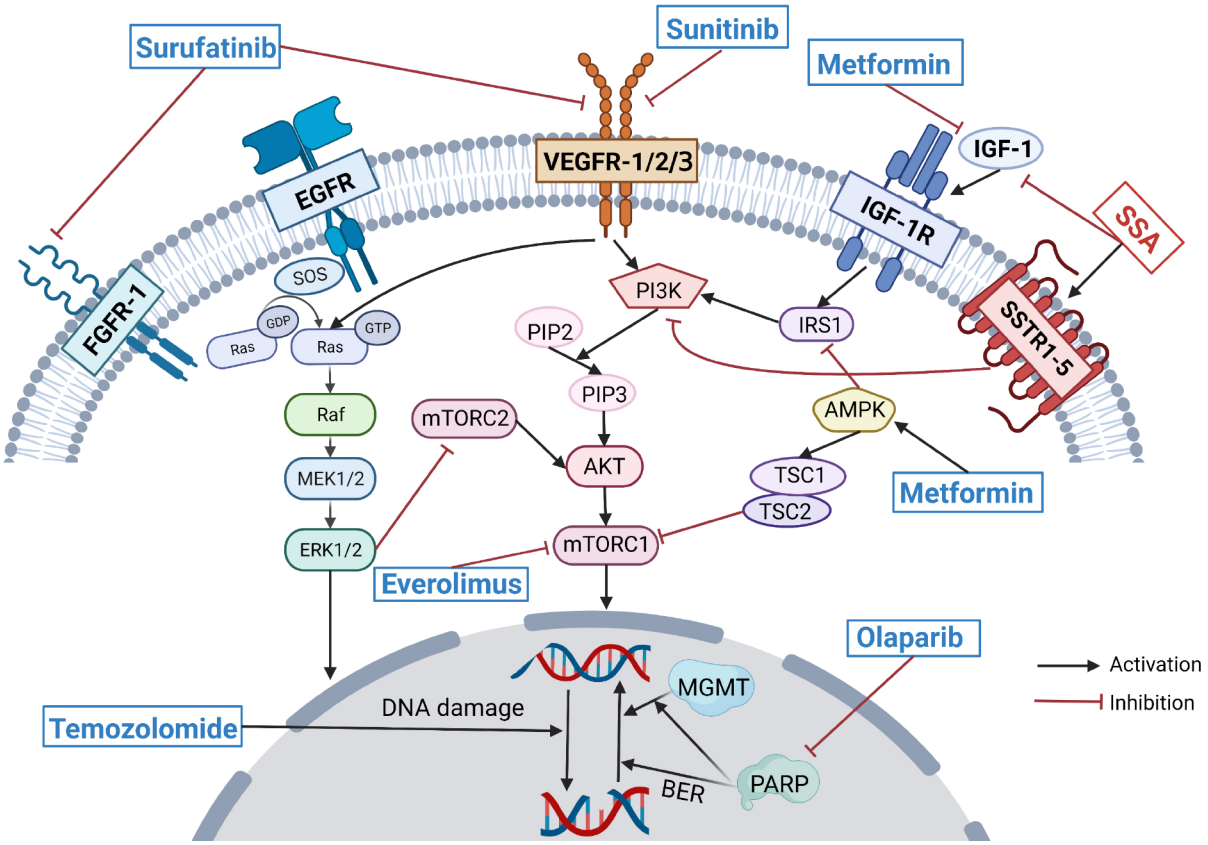

Figure 2 Molecular mechanisms of the action of somatostatin analog, antiangiogenic agents, everolimus, temozolomide, olaparib, and metformin on pancreatic neuroendocrine neoplasms and interactions. FGFR: Fibroblast growth factor receptor; EGFR: Epidermal growth factor receptor; VEGFR: Vascular endothelial growth factor receptor; IGF-1: Type 1 insulin-like growth factor; IGF-1R: Type 1 insulin-like growth factor receptor; SSTR: Somatostatin receptor; PI3K: Phosphoinositide 3-kinase; PIP2: Phosphatidylinositol-4,5-bisphosphate; PIP3: Phosphatidylinositol-3,4,5-triphosphate; AKT: Protein kinase B; mTORC1: Mechanistic target of rapamycin complex 1; mTORC2: Mechanistic target of rapamycin complex 2; IRS1: Insulin receptor substrate 1; AMPK: Adenosine 5'-monophosphate-activated protein kinase; TSC1: Tuberous sclerosis complex 1; TSC2: Tuberous sclerosis complex 2; SOS: Son of sevenless; RAS: Rat sarcoma virus; RAF: Rapidly accelerated fibrosarcoma; MEK: Methyl ethyl ketone; ERK: Extracellular signal-regulated kinase; BER: Base-excision repair; MGMT: O6-methylguanine DNA methyltransferase; PARP: Poly (ADP-ribose) polymerase. Citation: Created with BioRender.com.

and a median PFS of 15.4 mo, with no synergistic toxicity observed[32].

The most frequent chemotherapy schemes in advanced PanNECs are platinum-based (EP, EC) regimens for first-line therapy and FOLFOX, FOLFIRI, or CAPTEM regimens for second-line therapy [19,33,34]. For other options of first-line treatment regimens for PanNECs, a prospective study (NCT04325425) is evaluating the mFOLFIRINOX regimen *vs* the EP/EC regimen for advanced gastroenteropancreatic neuroendocrine carcinomas (GEP-NECs) as first-line therapy. Another study (NCT03387592) is evaluating the efficiency of the CAPTEM regimen *vs* the FOLFIRI regimen as second-line therapy for advanced NECs. These prospective clinical studies provide additional treatment options for patients with advanced PanNECs and high-level evidence for clinical decision-making.

ADVANCES IN SOMATOSTATIN ANALOGS

SSAs, with their antisecretory and antiproliferative effects, are some of the most common first-line treatments for patients with advanced PanNENs and can be used to control hormonal symptoms in patients with functional PanNETs[35] and for patients with advanced nonfunctional PanNENs to play an antiproliferative role. SSAs are primary treatment options for patients with PanNETs-G1/G2, Ki-67 < 10%, SSTR-positive, and slow-growing tumors[11-14,19,36]. The most widely used clinical SSAs include octreotide LAR and lanreotide autogel, both of which bind primarily to SSTR2 and SSTR5.

Several investigators have also evaluated the efficacy of SSAs in exerting antitumor effects in PanNENs with Ki-67 ≥ 10%. A multicenter retrospective study included advanced, well-differentiated PanNETs with Ki-67 of 10%-35% receiving first-line, long-acting SSAs and observed that SSAs still exert antiproliferative activity against PanNETs with Ki-67 ≥ 10% but have limited effect in PanNETs with high grade (G3) and hepatic tumor load > 25%[37].

In clinical practice, using SSAs at nonconventional high doses (increased administered dose or reduced administration interval) is a common empirical option in patients with progression PanNETs on a standard SSA first-line treatment[38]. A multicenter retrospective study of nonconventional doses of SSAs for GEP-NETs showed that in well-differentiated G1/G2 GEP-NETs, the overall median PFS was 31 mo with high-dose SSA (HD-SSA) therapy after progression on a standard SSA therapy, suggesting that HD-SSAs are active and safe treatment options in patients with progressive well-differentiated GEP-NETs[39]. A prospective single-arm phase II study (NCT02651987) assessed the efficacy of increasing the dose frequency of 120 mg lanreotide autogel (LAN) in 48 patients with progressive G1/G2 PanNETs and showed that 120 mg LAN every 14 d in PanNETs (progressive on standard 120 mg LAN every 28 d) produced promising PFS and DCR, especially in patients with Ki-67 ≤ 10%[40].

In addition, SSAs in combination with other agents (chemotherapy agents, antiangiogenic therapies, everolimus, immune checkpoint inhibitors, *etc.*) are also frequent second-line treatment options in real-world studies[41]. SSA combination therapy may have better efficacy in well-differentiated PanNETs with Ki-67 > 10% or high tumor burden, and a prospective multicenter phase II clinical study (NCT02231762) evaluating the efficacy of the combination of LAN and temozolomide in patients with advanced GEP-NETs is being conducted.

The efficacy of SSAs is correlated with the expression of somatostatin receptors on the tumor cell surface[38]. DNA methyltransferase inhibitors and histone deacetylase inhibitors were observed to upregulate SSTR2 expression in NET cell lines in some preclinical studies and could potentially be an option for overcoming SSA resistance, but the lack of progress in clinical studies requires further validation[42,43]. In clinical management, it is essential to identify the population favorable for SSA therapy, and SSAs in combination with other agents are expected to be synergistic in patients with higher grade, higher tumor load, and SSTR-positive PanNETs.

ADVANCES IN TARGETED THERAPIES

The targeted therapies currently used in PanNETs mainly include mammalian target of rapamycin (mTOR) inhibitors and antiangiogenic agents. FDA-approved target agents for the treatment of PanNENs include everolimus (mTOR inhibitor) and sunitinib (tyrosine kinase inhibitor)[12,19], and the recommendation of surufatinib (tyrosine kinase inhibitor) has been added to the Chinese guidelines for the diagnosis and treatment of pancreatic neuroendocrine neoplasms (2020)[36].

Everolimus, a mTOR inhibitor, has been shown to inhibit tumor cell growth through suppression of the PI3K/AKT/mTOR pathway. The primary results of the RADIANT-3 trial reported that patients with advanced PanNETs in the everolimus group had a median PFS of 11 mo, with a 6.4-mo increase *vs* the placebo group, and the safety profile of everolimus was good[16]. Everolimus resistance is thought to be related to its ability to inhibit only partial mTORC1 but not mTORC2, thus causing over-activation of upstream signaling, including PI3K/AKT[44]. Thus, both the dual PI3K/mTOR inhibitor BEZ235 and the dual inhibitor of mTORC1 and mTORC2, CC-223, are thought to have the potential to overcome everolimus resistance, but the phase II clinical trial of BEZ235 failed due to severe adverse effects[45]. The results of a phase II clinical trial of CC-233 in nonpancreatic NETs patients who failed first-line therapy suggested a DCR of 90% (95%CI: 76.9-97.3%) and a median PFS of 19.5 mo (95%CI: 10.4-28.5 mo), with a safety profile comparable with that of everolimus, but its use in PanNET patients still needs to be prospectively explored[46].

Several preclinical studies suggest that SSAs can inhibit insulin-like growth factor-1 (IGF-1), an upstream signal of the PI3K/AKT/mTOR pathway (Figure 2), and LAN was observed to reduce the survival rate of everolimus-resistant cell lines. SSAs may be able to overcome resistance to everolimus [38,47]. Unfortunately, in the COOPERATE-2 study of everolimus in combination with pasireotide LAR *vs* everolimus monotherapy in patients with advanced PanNETs, no prolongation of PFS was observed in the combination group *vs* the monotherapy group[48]. However, the trial extension results of the LUNA study of everolimus in combination with pasireotide LAR for advanced pulmonary and thymic NETs suggested that the everolimus combined with pasireotide group had a significantly longer median PFS than the pasireotide monotherapy group and the everolimus monotherapy group (8.51 mo *vs* 12.48 mo *vs* 16.53 mo)[49]. The Japan Clinical Oncology Group is also conducting a multicenter, randomized, controlled, phase III trial (jRCT1031200023) to confirm the superiority of combined everolimus plus lanreotide therapy over everolimus monotherapy for advanced GEP-NETs[50].

Resistance to everolimus may also be overcome by combined metformin therapy. Pusceddu *et al*[51] conducted a retrospective analysis of 445 patients with advanced PanNETs treated with everolimus and/or SSAs in 24 medical centers in Italy and observed that the median PFS of 44.2 mo was significantly longer in patients treated with metformin glucose-lowering therapy than in nondiabetic patients (15.1 mo) and longer than that in diabetic patients receiving other glucose-lowering treatments (20.8 mo). Metformin is associated with increased PFS in patients treated with SSA and in patients treated with everolimus (with or without SSAs). A preclinical study showed that metformin may induce more effective mTOR blockade through its effects on IGF-1 and adenosine 5'-monophosphate-activated protein kinase and may counteract the resistance mechanism triggered by everolimus (Figure 2)[52].

Because both metformin and SSA were observed to have the potential to overcome everolimus resistance in preclinical studies, a prospective study evaluating the efficacy of the triple-drug combination of everolimus, octreotide, and metformin for the treatment of advanced PanNENs (NCT02294006) is underway.

Antiangiogenic agents include tyrosine kinase inhibitors (TKIs) and non-TKI agents such as bevacizumab [anti-vascular endothelial growth factor (VEGF) monoclonal antibody]. PanNETs are highly vascularized with overexpression of proangiogenic factors such as VEGF, so antitumor angiogenesis is an effective therapeutic approach[53]. Antiangiogenic agents have evolved rapidly in the field of PanNET therapy in recent years, with new agents and high-grade clinical evidence emerging. Sunitinib, a polytyrosine kinase inhibitor, became the first antiangiogenic agent approved by the FDA for the treatment of patients with advanced PanNETs based on favorable results from a randomized double-blind phase III clinical trial[15]. Surufatinib is a new multitargeted TKI that blocks tumor angiogenesis by inhibiting both vascular endothelial growth factor receptor-1/2/3 (VEGFR-1/2/3) and fibroblast growth factor receptor-1 (FGFR-1) (Figure 2) and regulates tumor-associated macrophages to promote the immune response of the body to tumor cells by inhibiting colony-stimulating factor-1 receptor[54]. The SANET-p study, a phase III clinical trial of surufatinib in patients with advanced PanNETs, suggested a significant prolongation of median PFS (10.9 mo *vs* 3.7 mo) and improvement of ORR (19% *vs* 2%) in the surufatinib group compared with the placebo group[17]. The results from the PanNET cohort of the phase II cohort study (NCT01466036) of cabozantinib, a multitargeted tyrosine kinase inhibitor targeting VEGFR2 and cellular-mesenchymal epithelial transition factor, suggested a median PFS of 21.8 mo (95%CI: 8.5-32.0 mo) and an ORR of 15% (95%CI: 5%-36%)[55]. This result has raised expectations for the publication of the results of the ongoing randomized, double-blind phase III clinical trial of cabozantinib (NCT03375320). The TALENT study (GETNE1509) is a phase II clinical study of the VEGFR1-3 and FGFR1-4 inhibitors lenvatinib in which good clinical efficacy was observed in the PanNET cohort with a tolerable safety profile[56]. In addition, the TALENT study quantified a series of proangiogenic factors, such as VEGF-A, angiopoietin-2 (Ang2), and VEGFR-2. The results suggested that high Ang2 Levels and low FGF2 Levels were significantly associated with ORR, and Ang2 and VEGFR-2 Levels in patients treated with sunitinib could predict the efficacy of lenvatinib, confirming that biomarkers can not only predict drug efficacy but also provide a reference for patient sequential therapy selection[57]. Axitinib[58] and pazopanib[59] have also demonstrated efficacy in phase II clinical trials for the treatment of NETs. Clinical advances in antiangiogenic agents have brought more new options for the treatment of advanced PanNETs.

ADVANCES IN IMMUNOTHERAPY

With the advent of the immunotherapy era, phase I/II clinical trials of various immune checkpoint inhibitors such as programmed cell death-ligand 1 (PD-L1) inhibitors, programmed cell death-1 (PD-1) inhibitors and cytotoxic T-lymphocyte antigen 4 inhibitors have been widely conducted and rapidly developed in the PanNEN field. The results of a phase Ib study of toripalimab as a second-line regimen for the treatment of patients with advanced NENs suggested an ORR of 22.2% and a DCR of 55.5% in the PanNEN subgroup and observed that patients with positive PD-L1 expression, TMB-H (top 10%) and/or MSI-H positivity may preferentially benefit from the treatment[60]. The results of some current clinical trials have shown no significant benefit observed in patients with NENs treated with immune checkpoint inhibitors alone[61,62], and dual immunotherapy with PD-L1/PD-1 inhibitors in combination with CLTA-4 inhibitors is starting to gain interest. The DUNE study (GETNE 1601) is a phase II multicohort clinical study assessing the efficacy of durvalumab in combination with tremelimumab for the treatment of advanced GEP-NENs and pulmonary NETs, with recent results suggesting an ORR of 6.3% for the G1/G2 grade PanNET cohort, 9.1% for the G3 grade GEP-NEN cohort, and 7.4% and 0% for the pulmonary NET and giNET cohorts respectively[63]. A multicohort phase II clinical trial (NCT02923934) assessed the efficacy of ipilimumab in combination with nivolumab in NETs, with the latest results suggesting an ORR of 25% for the NET cohort (20 pts), and the study is still ongoing[64]. Clinical trials of immune checkpoint inhibitors in combination with other agents (antiangiogenic agents, chemotherapy, PRRT, and SSAs) continue to emerge, and some current clinical studies of immunotherapy in combination with antiangiogenic agents suggest better efficacy. An ORR of 20% and a median PFS of 3.94 mo were observed in a phase II clinical trial of toripalimab in combination with surufatinib in patients with advanced NECs after the failure of first-line chemotherapy. Surufatinib in combination with toripalimab has been suggested as a second-line treatment option for patients with advanced NECs[65], and a phase III clinical trial (NCT05015621) is evaluating the efficacy of the combination of surufatinib and toripalimab versus FOLFIRI regimen as a second-line treatment option for patients with advanced NECs. Clinical trials of immunotherapy in combination with other therapies being conducted in patients with NENs are shown in Table 1.

Table 1 Ongoing clinical trials of immune checkpoint inhibitors in combination with other therapies for the treatment of neuroendocrine neoplasms

Drugs	Population	*n*	Phase	Primary outcomes	NCT number
Surufatinib + toripalimab *vs* FOLFIRI	NEC	194	III	OS	NCT05015621
Penpulimab + anlotinib	NET	150	II	ORR	NCT04207463
Pembrolizumab + liver-directed/PRRT	NET	32		ORR	NCT03457948
Nivolumab + chemotherapy	NEN G3	38	II	OS	NCT03980925
Toripalimab + FOLFSIM *vs* EP/EC	Advanced NEC	336	II/III	OS	NCT03992911
Nivolumab + ipilimumab + cabozantinib	PD-NET	30	II	ORR	NCT04079712
Pembrolizumab + lanreotide depot	GEP-NET	22	Ib/II	ORR	NCT03043664

FOLFIRI: Folinic acid, fluorouracil and irinotecan regimen; FOLFSIM: Simmtecan and 5-FU/LV regimen; EP: Etoposide and cisplatin regimen; EC: Etoposide and carboplatin regimen; PD-NET: Poorly differentiated neuroendocrine tumor; ORR: Objective response rate; OS: Overall survival.

ADVANCES IN PEPTIDE RECEPTOR RADIONUCLIDE THERAPY

PRRT has been widely used in the treatment of NETs in Europe, the USA and Asia[66]. ^{177}Lu-DOTATATE has been used for more than a decade, but clinical studies of PRRT are still dominated by phase I/II clinical trials, and there is a lack of phase III clinical trials with large samples for NETs. The NETTER-1 study, a pivotal phase III clinical study of PRRT, treated two groups of midgut NETs with ^{177}Lu-DOTATATE combined with long-acting octreotide (30 mg every 28 d) and high-dose long-acting octreotide (60 mg every 28 d) and observed that ^{177}Lu-DOTATATE significantly increased the ORR (18% *vs* 3%) and prolonged the median OS of patients (48 *vs* 36.3 mo)[18,67]. Unfortunately, the NETTER-1 study, while suggesting good efficacy of PRRT, did not involve PanNETs, and the subsequent NETTER-2 study (NCT03972488), which is still ongoing enrolled SSTR+ G2/G3 GEP-NETs to evaluate the efficacy of ^{177}Lu-DOTATATE in combination with long-acting octreotide (30 mg every 28 days) compared with a high dose of long-acting octreotide (60 mg every 28 d). Prior to the results of the NETTER-2 study, the results of the multicenter retrospective NETTER-R study, which provided evidence for the use of PRRT in PanNETs, suggested that ^{177}Lu-DOTATATE had a median PFS of 24.8 (95%CI: 17.5-34.5) months and an ORR of 40.3% (95%CI: 28.1-53.6) in patients with advanced SSTR-positive PanNETs[68]. ^{177}Lu-DOTA-JR11 is a novel radiolabeled SSTR2 antagonist, and its application in SSTR-positive NETs in phase I/II clinical trials resulted in a DCR (12 mo) of 90% and an acceptable safety profile, suggesting that ^{177}Lu-DOTA-JR11 has good research potential[69]. Among emerging α-emitters, ^{225}Ac-DOTATATE, ^{213}Bi-DOTATOC and ^{212}Pb-DOTAMTATE have also shown good results in small samples of NETs, and clinical trials are underway[70].

NEW TARGETED AGENTS

In addition to common targets such as SSTR2, mTOR, and VEGFR, researchers are actively exploring new targeted agents for clinical application in the field of PanNENs. Cyclin-dependent kinases (CDKs), which regulate cell cycle progression, have been considered promising new targets for tumor therapy. Palbociclib, a small molecule compound that specifically inhibits CDK4 and CDK6, induced G1 phase blockade in Rb-positive CDK4-overexpressing PanNET cell lines in an *in vitro* assay, blocking and inhibiting the growth of PanNET cell lines[71,72]. However, the results of a phase II clinical trial of palbociclib for G1/G2 grade PanNETs suggested a median PFS of only 2.6 mo (95%CI: 0-14.4)[71]. ONC201, an agent with specific targeting of the dopamine-like DRD2 receptor and the mitochondrial protease ClpP, inhibits the growth of PanNET cell lines by TRAIL/DR5 upregulation, dual AKT/ERK pathway inhibition and promotion of a comprehensive stress response to exerting anticancer effects. The phase II study of ONC201 for NETs (NCT03034200) included 10 patients with metastatic PC-PGs (Group A) and 12 patients with other neuroendocrine tumors (Group B), and the latest results of this study suggested 5 PRs and 2 SDs in Group A and 1 PR and 2 SDs in Group B. A full outcome report is still pending[73]. Antibody-coupled drugs developed against SSTR targets have received much attention. PEN-221, an antibody-drug conjugate (ADC) targeting SSTR2, connects the cytotoxic microtubule protein inhibitor DM1 to Tyr3-octreotate and can rapidly internalize DM1 into SSTR2-expressing cells and exert cytotoxic effects after binding to SSTR2[74]. A phase II clinical study of PEN221 in SSTR2-positive gastrointestinal NETs is ongoing, and the latest results suggested that 23

Table 2 Ongoing clinical trials of new targeted agents

Drugs	Targets	Population	*n*	Phase	Primary outcomes	NCT number
Ribociclib + Everolimus	CDK4/6 Inhibitor	Advanced NET	21	II	PFS	NCT03070301
Abemaciclib	CDK4/6 Inhibitor	Advanced GEP-NET	37	II	ORR	NCT03891784
BAY 1895344	ATR Kinase Inhibitor	SCLC/PD-NEC/PDA	87	I	MTD, AEs	NCT04514497
Lurbinectedin, berzosertib	ATR Kinase Inhibitor	SCLC/HGNEC	75	I/II	MTD, ORR	NCT04802174
BI 764532	DLL3 Inhibitor	SCLC/NEN Expressing DLL3	110	I	MTD	NCT04429087
Entinostat	HDAC Inhibitor	Abdominal NET	40	II	ORR	NCT03211988
Niraparib + dostarlimab	PARP Inhibitor	SCLC/HGNEC	48		PFS, ORR	NCT04701307

SCLC: Small-cell lung carcinoma; PD-NEC: Poorly differentiated neuroendocrine carcinoma; PDA: Pancreatic adenocarcinoma; HGNEC: High-grade neuroendocrine cancer; CDK: Cyclin-dependent kinase; ATR kinase: Ataxia telangiectasia and RAD3-related kinase; DLL3: Delta-like protein 3; HDAC: Histone deacetylase; PARP: Poly (ADP-ribose) polymerase; PFS: Progression-free survival; MTD: Maximum tolerated dose; ORR: Objective response rate; AEs: Adverse events.

(88.5%) of 26 evaluable patients were assessed as SD, with a median PFS of 9 mo[75]. Belzutifan is a second-generation small-molecule hypoxia-inducible factor (HIF)-2α inhibitor, which is recommended in the latest NCCN guidelines for advanced PanNET patients with germline VHL alteration[19]. In a phase II, open-label, single-group trial of belzutifan in patients with renal cell carcinoma associated with VHL disease, 22 patients with PanNETs were included, among them 20 patients (91%) had a confirmed response (including 3 patients (14%) who had a complete response)[76]. Phase I/II clinical trials of new targeted agents such as ATR inhibitors, DLL3 inhibitors, HDAC inhibitors, and PARP inhibitors applied to NETs are currently underway (Table 2), but there is still a long way to go before clinical application.

CONCLUSION

Although there are various treatments for PanNENs, choosing appropriate therapeutic schemes for different patients in terms of pathological classification, grades and stages is still difficult. The selection of a cytotoxic chemotherapy regimen is a concern of researchers, and the results of prospective studies may help to address it. First, the problem of drug resistance facing CAPTEM regimen, the most widely used plan, will probably be solved by the combination of PARP inhibitors and mTOR inhibitors, although more evidence is needed. Due to the limited effect of SSAs on inhibiting cancer cell proliferation, progress has mainly been made in the selection of appropriate patients and the synergistic effect of combination therapy. Many new antiangiogenic agents and high-level clinical evidence have emerged, and the reversal of drug resistance to everolimus has also advanced. The use of PRRT in the treatment of NETs is increasingly common, and new radiolabeled peptides appear to be more effective. Immunotherapy faces challenges, and the better curative effect of dual immune checkpoint inhibitor therapies and the combinations of immune checkpoint inhibitors plus other agents need further investigation. Although there are limited choices in the treatment of PanNENs, the combination of common medicines such as SSAs, cytotoxic chemotherapy, everolimus, sunitinib and immune checkpoint inhibitors can have synergistic effects or alleviate drug resistance, thus bringing new vitality to the treatment of PanNENs. The development of biomarkers in clinical research provides a reference for the prediction of curative effects and the selection of sequential therapy, and biomarker-directed therapy helps in choosing appropriate medicines for different people. Advances in the search for new targets and the use of new medicines on common targets will provide more choices for the treatment of PanNENs, but applying them in clinical practice will still take time. Further investigation of PRRT and immunotherapy and the development of new targeted agents will be the focus of future research, and the progress made in the reversal of drug resistance will help clinical practice. In addition, the selection of appropriate therapeutic schemes for different patients and the execution of individualized and precise therapy will be a continuous concern for researchers.

FOOTNOTES

Author contributions: Li YL and Cheng ZX made equal contributions to this paper and should be regarded as a co-

first author; Li YL and Cheng ZX searched the literature and wrote the manuscript; Yu FH and Tian C translated the manuscript; Tan HY revised the manuscript.

Supported by National Key R&D Program of China, No. 2019YFB1309704.

Conflict-of-interest statement: Authors declare no conflict of interests for this article.

Country/Territory of origin: China

ORCID number: Yuan-Liang Li 0000-0003-0774-614X; Zi-Xuan Cheng 0000-0002-5183-3198; Fu-Huan Yu 0000-0003-2634-3530; Chao Tian 0000-0002-6635-1079; Huang-Ying Tan 0000-0002-6165-5196.

S-Editor: Wang JL
L-Editor: A
P-Editor: Wang JL

REFERENCES

1 **Dasari A**, Shen C, Halperin D, Zhao B, Zhou S, Xu Y, Shih T, Yao JC. Trends in the Incidence, Prevalence, and Survival Outcomes in Patients With Neuroendocrine Tumors in the United States. *JAMA Oncol* 2017; **3**: 1335-1342 [PMID: 28448665 DOI: 10.1001/jamaoncol.2017.0589]
2 **Das S**, Dasari A. Epidemiology, Incidence, and Prevalence of Neuroendocrine Neoplasms: Are There Global Differences? *Curr Oncol Rep* 2021; **23**: 43 [PMID: 33719003 DOI: 10.1007/s11912-021-01029-7]
3 **Falconi M**, Eriksson B, Kaltsas G, Bartsch DK, Capdevila J, Caplin M, Kos-Kudla B, Kwekkeboom D, Rindi G, Klöppel G, Reed N, Kianmanesh R, Jensen RT; Vienna Consensus Conference participants. ENETS Consensus Guidelines Update for the Management of Patients with Functional Pancreatic Neuroendocrine Tumors and Non-Functional Pancreatic Neuroendocrine Tumors. *Neuroendocrinology* 2016; **103**: 153-171 [PMID: 26742109 DOI: 10.1159/000443171]
4 **Wu W**, Jin G, Li H, Miao Y, Wang C, Liang T, Ou J, Zhao Y, Yuan C, Li Y, Lou W, Wu Z, Qin R, Wang H, Hao J, Yu X, Huang H, Tan G, Liu X, Xu K, Wang L, Yang Y, Hao C, Wang W, Guo K, Wei J, Wang Y, Peng C, Wang X, Cai S, Jiang J, Wu X, Li F, Pancreatic SSGO. The current surgical treatment of pancreatic neuroendocrine neoplasms in China: a national wide cross-sectional study. *J Pancreatol* 2019; **2**: 35-42 [DOI: 10.1097/JP9.0000000000000019]
5 **Ito T**, Igarashi H, Nakamura K, Sasano H, Okusaka T, Takano K, Komoto I, Tanaka M, Imamura M, Jensen RT, Takayanagi R, Shimatsu A. Epidemiological trends of pancreatic and gastrointestinal neuroendocrine tumors in Japan: a nationwide survey analysis. *J Gastroenterol* 2015; **50**: 58-64 [PMID: 24499825 DOI: 10.1007/s00535-014-0934-2]
6 **Halfdanarson TR**, Rabe KG, Rubin J, Petersen GM. Pancreatic neuroendocrine tumors (PNETs): incidence, prognosis and recent trend toward improved survival. *Ann Oncol* 2008; **19**: 1727-1733 [PMID: 18515795 DOI: 10.1093/annonc/mdn351]
7 **Garcia-Carbonero R**, Capdevila J, Crespo-Herrero G, Díaz-Pérez JA, Martínez Del Prado MP, Alonso Orduña V, Sevilla-García I, Villabona-Artero C, Beguiristain-Gómez A, Llanos-Muñoz M, Marazuela M, Alvarez-Escola C, Castellano D, Vilar E, Jiménez-Fonseca P, Teulé A, Sastre-Valera J, Benavent-Viñuelas M, Monleon A, Salazar R. Incidence, patterns of care and prognostic factors for outcome of gastroenteropancreatic neuroendocrine tumors (GEP-NETs): results from the National Cancer Registry of Spain (RGETNE). *Ann Oncol* 2010; **21**: 1794-1803 [PMID: 20139156 DOI: 10.1093/annonc/mdq022]
8 **Jensen RT**, Berna MJ, Bingham DB, Norton JA. Inherited pancreatic endocrine tumor syndromes: advances in molecular pathogenesis, diagnosis, management, and controversies. *Cancer* 2008; **113**: 1807-1843 [PMID: 18798544 DOI: 10.1002/cncr.23648]
9 **Nagtegaal ID**, Odze RD, Klimstra D, Paradis V, Rugge M, Schirmacher P, Washington KM, Carneiro F, Cree IA; WHO Classification of Tumours Editorial Board. The 2019 WHO classification of tumours of the digestive system. *Histopathology* 2020; **76**: 182-188 [PMID: 31433515 DOI: 10.1111/his.13975]
10 **Doescher J**, Veit JA, Hoffmann TK. [The 8th edition of the AJCC Cancer Staging Manual: Updates in otorhinolaryngology, head and neck surgery]. *HNO* 2017; **65**: 956-961 [PMID: 28717958 DOI: 10.1007/s00106-017-0391-3]
11 **Halfdanarson TR**, Strosberg JR, Tang L, Bellizzi AM, Bergsland EK, O'Dorisio TM, Halperin DM, Fishbein L, Eads J, Hope TA, Singh S, Salem R, Metz DC, Naraev BG, Reidy-Lagunes DL, Howe JR, Pommier RF, Menda Y, Chan JA. The North American Neuroendocrine Tumor Society Consensus Guidelines for Surveillance and Medical Management of Pancreatic Neuroendocrine Tumors. *Pancreas* 2020; **49**: 863-881 [PMID: 32675783 DOI: 10.1097/MPA.0000000000001597]
12 **Pavel M**, O'Toole D, Costa F, Capdevila J, Gross D, Kianmanesh R, Krenning E, Knigge U, Salazar R, Pape UF, Öberg K; Vienna Consensus Conference participants. ENETS Consensus Guidelines Update for the Management of Distant Metastatic Disease of Intestinal, Pancreatic, Bronchial Neuroendocrine Neoplasms (NEN) and NEN of Unknown Primary Site. *Neuroendocrinology* 2016; **103**: 172-185 [PMID: 26731013 DOI: 10.1159/000443167]
13 **Rinke A**, Müller HH, Schade-Brittinger C, Klose KJ, Barth P, Wied M, Mayer C, Aminossadati B, Pape UF, Bläker M,

Harder J, Arnold C, Gress T, Arnold R; PROMID Study Group. Placebo-controlled, double-blind, prospective, randomized study on the effect of octreotide LAR in the control of tumor growth in patients with metastatic neuroendocrine midgut tumors: a report from the PROMID Study Group. *J Clin Oncol* 2009; **27**: 4656-4663 [PMID: 19704057 DOI: 10.1200/JCO.2009.22.8510]

14 **Caplin ME**, Pavel M, Ćwikła JB, Phan AT, Raderer M, Sedláčková E, Cadiot G, Wolin EM, Capdevila J, Wall L, Rindi G, Langley A, Martinez S, Blumberg J, Ruszniewski P; CLARINET Investigators. Lanreotide in metastatic enteropancreatic neuroendocrine tumors. *N Engl J Med* 2014; **371**: 224-233 [PMID: 25014687 DOI: 10.1056/NEJMoa1316158]

15 **Raymond E**, Dahan L, Raoul JL, Bang YJ, Borbath I, Lombard-Bohas C, Valle J, Metrakos P, Smith D, Vinik A, Chen JS, Hörsch D, Hammel P, Wiedenmann B, Van Cutsem E, Patyna S, Lu DR, Blanckmeister C, Chao R, Ruszniewski P. Sunitinib malate for the treatment of pancreatic neuroendocrine tumors. *N Engl J Med* 2011; **364**: 501-513 [PMID: 21306237 DOI: 10.1056/NEJMoa1003825]

16 **Yao JC**, Shah MH, Ito T, Bohas CL, Wolin EM, Van Cutsem E, Hobday TJ, Okusaka T, Capdevila J, de Vries EG, Tomassetti P, Pavel ME, Hoosen S, Haas T, Lincy J, Lebwohl D, Öberg K; RAD001 in Advanced Neuroendocrine Tumors, Third Trial (RADIANT-3) Study Group. Everolimus for advanced pancreatic neuroendocrine tumors. *N Engl J Med* 2011; **364**: 514-523 [PMID: 21306238 DOI: 10.1056/NEJMoa1009290]

17 **Xu J**, Shen L, Bai C, Wang W, Li J, Yu X, Li Z, Li E, Yuan X, Chi Y, Yin Y, Lou W, Xu N, Bai Y, Zhang T, Xiu D, Wang X, Yuan Y, Chen J, Qin S, Jia R, Lu M, Cheng Y, Zhou Z, He J, Su W. Surufatinib in advanced pancreatic neuroendocrine tumours (SANET-p): a randomised, double-blind, placebo-controlled, phase 3 study. *Lancet Oncol* 2020; **21**: 1489-1499 [PMID: 32966810 DOI: 10.1016/S1470-2045(20)30493-9]

18 **Strosberg J**, El-Haddad G, Wolin E, Hendifar A, Yao J, Chasen B, Mittra E, Kunz PL, Kulke MH, Jacene H, Bushnell D, O'Dorisio TM, Baum RP, Kulkarni HR, Caplin M, Lebtahi R, Hobday T, Delpassand E, Van Cutsem E, Benson A, Srirajaskanthan R, Pavel M, Mora J, Berlin J, Grande E, Reed N, Seregni E, Öberg K, Lopera Sierra M, Santoro P, Thevenet T, Erion JL, Ruszniewski P, Kwekkeboom D, Krenning E; NETTER-1 Trial Investigators. Phase 3 Trial of ^{177}Lu-Dotatate for Midgut Neuroendocrine Tumors. *N Engl J Med* 2017; **376**: 125-135 [PMID: 28076709 DOI: 10.1056/NEJMoa1607427]

19 **Shah MH**, Goldner WS, Benson AB, Bergsland E, Blaszkowsky LS, Brock P, Chan J, Das S, Dickson PV, Fanta P, Giordano T, Halfdanarson TR, Halperin D, He J, Heaney A, Heslin M J, Kandeel F, Kardan A, Khan SA, Kuvshinoff BW, Lieu C, Miller K, Pillarisetty VG, Reidy D, Salgado SA, Shaheen S, Soares HP, Soulen MC, Strosberg JR, Sussman CR, Trikalinos NA, Uboha NA, Vijayvergia N, Wong T, Lynn B, Hochstetler C. National Comprehensive Cancer Network Clinical Practice Guidelines in Oncology: Neuroendocrine and Adrenal Tumors Version 4; 2021. Available from: https://www.nccn.org/Login?ReturnURL=https://www.nccn.org/professionals/physician_gls/pdf/neuroendocrine.pdf

20 **Zhao J**, Zhao H, Chi Y. Safety and Efficacy of the S-1/Temozolomide Regimen in Patients with Metastatic Neuroendocrine Tumors. *Neuroendocrinology* 2018; **106**: 318-323 [PMID: 28817826 DOI: 10.1159/000480402]

21 **Strosberg JR**, Fine RL, Choi J, Nasir A, Coppola D, Chen DT, Helm J, Kvols L. First-line chemotherapy with capecitabine and temozolomide in patients with metastatic pancreatic endocrine carcinomas. *Cancer* 2011; **117**: 268-275 [PMID: 20824724 DOI: 10.1002/cncr.25425]

22 **Pavel M**, Öberg K, Falconi M, Krenning EP, Sundin A, Perren A, Berruti A; ESMO Guidelines Committee. Electronic address: clinicalguidelines@esmo.org. Gastroenteropancreatic neuroendocrine neoplasms: ESMO Clinical Practice Guidelines for diagnosis, treatment and follow-up. *Ann Oncol* 2020; **31**: 844-860 [PMID: 32272208 DOI: 10.1016/j.annonc.2020.03.304]

23 **Rogowski W**, Wachuła E, Gorzelak A, Lebiedzińska A, Sulżyc-Bielicka V, Iżycka-Świeszewska E, Żołnierek J, Kos-Kudła B. Capecitabine and temozolomide combination for treatment of high-grade, well-differentiated neuroendocrine tumour and poorly-differentiated neuroendocrine carcinoma - retrospective analysis. *Endokrynol Pol* 2019; **70**: 313-317 [PMID: 30843182 DOI: 10.5603/EP.a2019.0010]

24 **Chatzellis E**, Angelousi A, Daskalakis K, Tsoli M, Alexandraki KI, Wachuła E, Meirovitz A, Maimon O, Grozinsky-Glasberg S, Gross D, Kos-Kudła B, Koumarianou A, Kaltsas G. Activity and Safety of Standard and Prolonged Capecitabine/Temozolomide Administration in Patients with Advanced Neuroendocrine Neoplasms. *Neuroendocrinology* 2019; **109**: 333-345 [PMID: 31167197 DOI: 10.1159/000500135]

25 **Trillo Aliaga P**, Spada F, Peveri G, Bagnardi V, Fumagalli C, Laffi A, Rubino M, Gervaso L, Guerini Rocco E, Pisa E, Curigliano G, Fazio N. Should temozolomide be used on the basis of O^6-methylguanine DNA methyltransferase status in patients with advanced neuroendocrine tumors? *Cancer Treat Rev* 2021; **99**: 102261 [PMID: 34332293 DOI: 10.1016/j.ctrv.2021.102261]

26 **Qi Z**, Tan H. Association between MGMT status and response to alkylating agents in patients with neuroendocrine neoplasms: a systematic review and meta-analysis. *Biosci Rep* 2020; **40** [PMID: 32141507 DOI: 10.1042/BSR20194127]

27 **Lemelin A**, Barritault M, Hervieu V, Payen L, Péron J, Couvelard A, Cros J, Scoazec JY, Bin S, Villeneuve L, Lombard-Bohas C, Walter T; MGMT-NET investigators. O6-methylguanine-DNA methyltransferase (MGMT) status in neuroendocrine tumors: a randomized phase II study (MGMT-NET). *Dig Liver Dis* 2019; **51**: 595-599 [PMID: 30824408 DOI: 10.1016/j.dld.2019.02.001]

28 **Yan Y**, Xu Z, Dai S, Qian L, Sun L, Gong Z. Targeting autophagy to sensitive glioma to temozolomide treatment. *J Exp Clin Cancer Res* 2016; **35**: 23 [PMID: 26830677 DOI: 10.1186/s13046-016-0303-5]

29 **Wu S**, Li X, Gao F, de Groot JF, Koul D, Yung WKA. PARP-mediated PARylation of MGMT is critical to promote repair of temozolomide-induced O6-methylguanine DNA damage in glioblastoma. *Neuro Oncol* 2021; **23**: 920-931 [PMID: 33433610 DOI: 10.1093/neuonc/noab003]

30 **Farago AF**, Yeap BY, Stanzione M, Hung YP, Heist RS, Marcoux JP, Zhong J, Rangachari D, Barbie DA, Phat S, Myers DT, Morris R, Kem M, Dubash TD, Kennedy EA, Digumarthy SR, Sequist LV, Hata AN, Maheswaran S, Haber DA, Lawrence MS, Shaw AT, Mino-Kenudson M, Dyson NJ, Drapkin BJ. Combination Olaparib and Temozolomide in Relapsed Small-Cell Lung Cancer. *Cancer Discov* 2019; **9**: 1372-1387 [PMID: 31416802 DOI: 10.1158/2159-8290.CD-19-0582]

31 **Zając A**, Sumorek-Wiadro J, Langner E, Wertel I, Maciejczyk A, Pawlikowska-Pawlęga B, Pawelec J, Wasiak M, Hułas-

Stasiak M, Bądziul D, Rzeski W, Reichert M, Jakubowicz-Gil J. Involvement of PI3K Pathway in Glioma Cell Resistance to Temozolomide Treatment. *Int J Mol Sci* 2021; **22** [PMID: 34068110 DOI: 10.3390/ijms22105155]

32 **Chan JA**, Blaszkowsky L, Stuart K, Zhu AX, Allen J, Wadlow R, Ryan DP, Meyerhardt J, Gonzalez M, Regan E, Zheng H, Kulke MH. A prospective, phase 1/2 study of everolimus and temozolomide in patients with advanced pancreatic neuroendocrine tumor. *Cancer* 2013; **119**: 3212-3218 [PMID: 23733618 DOI: 10.1002/cncr.28142]

33 **Bardasi C**, Spallanzani A, Benatti S, Spada F, Laffi A, Antonuzzo L, Lavacchi D, Marconcini R, Ferrari M, Rimini M, Caputo F, Santini C, Cerma K, Casadei-Gardini A, Andrikou K, Salati M, Bertolini F, Fontana A, Dominici M, Luppi G, Gelsomino F. Irinotecan-based chemotherapy in extrapulmonary neuroendocrine carcinomas: survival and safety data from a multicentric Italian experience. *Endocrine* 2021; **74**: 707-713 [PMID: 34231124 DOI: 10.1007/s12020-021-02813-y]

34 **Hadoux J**, Malka D, Planchard D, Scoazec JY, Caramella C, Guigay J, Boige V, Leboulleux S, Burtin P, Berdelou A, Loriot Y, Duvillard P, Chougnet CN, Déandréis D, Schlumberger M, Borget I, Ducreux M, Baudin E. Post-first-line FOLFOX chemotherapy for grade 3 neuroendocrine carcinoma. *Endocr Relat Cancer* 2015; **22**: 289-298 [PMID: 25770151 DOI: 10.1530/ERC-15-0075]

35 **Stueven AK**, Kayser A, Wetz C, Amthauer H, Wree A, Tacke F, Wiedenmann B, Roderburg C, Jann H. Somatostatin Analogues in the Treatment of Neuroendocrine Tumors: Past, Present and Future. *Int J Mol Sci* 2019; **20** [PMID: 31234481 DOI: 10.3390/ijms20123049]

36 **Wu WM**, Chen J, Bai CM, Chi Y, Du YQ, Feng ST, Huo L, Jiang YX, Li JN, Lou WH, Luo J, Shao CH, Shen L, Wang F, Wang LW, Wang O, Wang Y, Wu HW, Xing XP, Xu JM, Xue HD, Xue L, Yang Y, Yu XJ, Yuan CH, Zhao H, Zhu XZ, Zhao YP; Chinese Pancreatic Surgery Association, Chinese Society of Surgery, Chinese Medical Association. [The Chinese guidelines for the diagnosis and treatment of pancreatic neuroendocrine neoplasms (2020)]. *Zhonghua Wai Ke Za Zhi* 2021; **59**: 401-421 [PMID: 34102722 DOI: 10.3760/cma.j.cn112139-20210319-00135]

37 **Merola E**, Alonso Gordoa T, Zhang P, Al-Toubah T, Pellè E, Kolasińska-Ćwikła A, Zandee W, Laskaratos F, de Mestier L, Lamarca A, Hernando J, Cwikla J, Strosberg J, de Herder W, Caplin M, Cives M, van Leeuwaarde R. Somatostatin Analogs for Pancreatic Neuroendocrine Tumors: Any Benefit When Ki-67 Is ≥10%? *Oncologist* 2021; **26**: 294-301 [PMID: 33301235 DOI: 10.1002/onco.13633]

38 **Carmona-Bayonas A**, Jiménez-Fonseca P, Custodio A, Grande E, Capdevila J, López C, Teule A, Garcia-Carbonero R; Spanish Neuroendocrine Tumor Group (GETNE). Optimizing Somatostatin Analog Use in Well or Moderately Differentiated Gastroenteropancreatic Neuroendocrine Tumors. *Curr Oncol Rep* 2017; **19**: 72 [PMID: 28920153 DOI: 10.1007/s11912-017-0633-2]

39 **Lamberti G**, Faggiano A, Brighi N, Tafuto S, Ibrahim T, Brizzi MP, Pusceddu S, Albertelli M, Massironi S, Panzuto F, Badalamenti G, Riccardi F, Butturini G, Gelsomino F, De Divitiis C, Modica R, Bongiovanni A, La Salvia A, Torchio M, Colao A, Ferone D, Campana D. Nonconventional Doses of Somatostatin Analogs in Patients With Progressing Well-Differentiated Neuroendocrine Tumor. *J Clin Endocrinol Metab* 2020; **105** [PMID: 31545377 DOI: 10.1210/clinem/dgz035]

40 **Pavel M**, Ćwikła JB, Lombard-Bohas C, Borbath I, Shah T, Pape UF, Capdevila J, Panzuto F, Truong Thanh XM, Houchard A, Ruszniewski P. Efficacy and safety of high-dose lanreotide autogel in patients with progressive pancreatic or midgut neuroendocrine tumours: CLARINET FORTE phase 2 study results. *Eur J Cancer* 2021; **157**: 403-414 [PMID: 34597974 DOI: 10.1016/j.ejca.2021.06.056]

41 **Jalbert JJ**, Casciano R, Meng J, Brais LK, Pulgar SJ, Berthon A, Dinet J, Kulke MH. Treatment Patterns and Health Resource Use Among Patients with Metastatic Gastroenteropancreatic Neuroendocrine Tumors Treated at a Tertiary Referral Center. *Oncologist* 2020; **25**: e644-e650 [PMID: 31999024 DOI: 10.1634/theoncologist.2019-0691]

42 **Guenter RE**, Aweda T, Carmona Matos DM, Whitt J, Chang AW, Cheng EY, Liu XM, Chen H, Lapi SE, Jaskula-Sztul R. Pulmonary Carcinoid Surface Receptor Modulation Using Histone Deacetylase Inhibitors. *Cancers (Basel)* 2019; **11** [PMID: 31163616 DOI: 10.3390/cancers11060767]

43 **Jin XF**, Auernhammer CJ, Ilhan H, Lindner S, Nölting S, Maurer J, Spöttl G, Orth M. Combination of 5-Fluorouracil with Epigenetic Modifiers Induces Radiosensitization, Somatostatin Receptor 2 Expression, and Radioligand Binding in Neuroendocrine Tumor Cells In Vitro. *J Nucl Med* 2019; **60**: 1240-1246 [PMID: 30796167 DOI: 10.2967/jnumed.118.224048]

44 **Lee L**, Ito T, Jensen RT. Everolimus in the treatment of neuroendocrine tumors: efficacy, side-effects, resistance, and factors affecting its place in the treatment sequence. *Expert Opin Pharmacother* 2018; **19**: 909-928 [PMID: 29757017 DOI: 10.1080/14656566.2018.1476492]

45 **Fazio N**, Buzzoni R, Baudin E, Antonuzzo L, Hubner RA, Lahner H, DE Herder WW, Raderer M, Teulé A, Capdevila J, Libutti SK, Kulke MH, Shah M, Dey D, Turri S, Aimone P, Massacesi C, Verslype C. A Phase II Study of BEZ235 in Patients with Everolimus-resistant, Advanced Pancreatic Neuroendocrine Tumours. *Anticancer Res* 2016; **36**: 713-719 [PMID: 26851029]

46 **Wolin E**, Mita A, Mahipal A, Meyer T, Bendell J, Nemunaitis J, Munster PN, Paz-Ares L, Filvaroff EH, Li S, Hege K, de Haan H, Mita M. A phase 2 study of an oral mTORC1/mTORC2 kinase inhibitor (CC-223) for non-pancreatic neuroendocrine tumors with or without carcinoid symptoms. *PLoS One* 2019; **14**: e0221994 [PMID: 31527867 DOI: 10.1371/journal.pone.0221994]

47 **Sciammarella C**, Luce A, Riccardi F, Mocerino C, Modica R, Berretta M, Misso G, Cossu AM, Colao A, Vitale G, Necas A, Fedacko J, Galdiero M, Correale P, Faggiano A, Caraglia M, Capasso A, Grimaldi A. Lanreotide Induces Cytokine Modulation in Intestinal Neuroendocrine Tumors and Overcomes Resistance to Everolimus. *Front Oncol* 2020; **10**: 1047 [PMID: 32766136 DOI: 10.3389/fonc.2020.01047]

48 **Kulke MH**, Ruszniewski P, Van Cutsem E, Lombard-Bohas C, Valle JW, De Herder WW, Pavel M, Degtyarev E, Brase JC, Bubuteishvili-Pacaud L, Voi M, Salazar R, Borbath I, Fazio N, Smith D, Capdevila J, Riechelmann RP, Yao JC. A randomized, open-label, phase 2 study of everolimus in combination with pasireotide LAR or everolimus alone in advanced, well-differentiated, progressive pancreatic neuroendocrine tumors: COOPERATE-2 trial. *Ann Oncol* 2019; **30**: 1846 [PMID: 31407000 DOI: 10.1093/annonc/mdz219]

49 **Baudin E**, Berruti A, Giuliano M, Mansoor W, Bobirca C, Houtsma E, Fagan N, Oberg K E, Ferolla P. First long-term

results on efficacy and safety of long-acting pasireotide in combination with everolimus in patients with advanced carcinoids (NET) of the lung/thymus: Phase II LUNA trial. *J Clin Oncol* 2021; **39**: 8574-8574 [DOI: 10.1200/JCO.2021.39.15_suppl.8574]

50 **Hijioka S**, Morizane C, Ikeda M, Ishii H, Okusaka T, Furuse J. Current status of medical treatment for gastroenteropancreatic neuroendocrine neoplasms and future perspectives. *Jpn J Clin Oncol* 2021; **51**: 1185-1196 [PMID: 34038547 DOI: 10.1093/jjco/hyab076]

51 **Pusceddu S**, Vernieri C, Di Maio M, Marconcini R, Spada F, Massironi S, Ibrahim T, Brizzi MP, Campana D, Faggiano A, Giuffrida D, Rinzivillo M, Cingarlini S, Aroldi F, Antonuzzo L, Berardi R, Catena L, De Divitiis C, Ermacora P, Perfetti V, Fontana A, Razzore P, Carnaghi C, Davì MV, Cauchi C, Duro M, Ricci S, Fazio N, Cavalcoli F, Bongiovanni A, La Salvia A, Brighi N, Colao A, Puliafito I, Panzuto F, Ortolani S, Zaniboni A, Di Costanzo F, Torniai M, Bajetta E, Tafuto S, Garattini SK, Femia D, Prinzi N, Concas L, Lo Russo G, Milione M, Giacomelli L, Buzzoni R, Delle Fave G, Mazzaferro V, de Braud F. Metformin Use Is Associated With Longer Progression-Free Survival of Patients With Diabetes and Pancreatic Neuroendocrine Tumors Receiving Everolimus and/or Somatostatin Analogues. *Gastroenterology* 2018; **155**: 479-489.e7 [PMID: 29655834 DOI: 10.1053/j.gastro.2018.04.010]

52 **Vitali E**, Boemi I, Tarantola G, Piccini S, Zerbi A, Veronesi G, Baldelli R, Mazziotti G, Smiroldo V, Lavezzi E, Spada A, Mantovani G, Lania AG. Metformin and Everolimus: A Promising Combination for Neuroendocrine Tumors Treatment. *Cancers (Basel)* 2020; **12** [PMID: 32748870 DOI: 10.3390/cancers12082143]

53 **Couvelard A**, O'Toole D, Turley H, Leek R, Sauvanet A, Degott C, Ruszniewski P, Belghiti J, Harris AL, Gatter K, Pezzella F. Microvascular density and hypoxia-inducible factor pathway in pancreatic endocrine tumours: negative correlation of microvascular density and VEGF expression with tumour progression. *Br J Cancer* 2005; **92**: 94-101 [PMID: 15558070 DOI: 10.1038/sj.bjc.6602245]

54 **Xu JM**, Wang Y, Chen YL, Jia R, Li J, Gong JF, Qi C, Hua Y, Tan CR, Wang J, Li K, Sai Y, Zhou F, Ren YX, Qing WG, Jia H, Su WG, Shen L. Sulfatinib, a novel kinase inhibitor, in patients with advanced solid tumors: results from a phase I study. *Oncotarget* 2017; **8**: 42076-42086 [PMID: 28159938 DOI: 10.18632/oncotarget.14942]

55 **Chan JA**, Faris JE, Murphy JE, Blaszkowsky LS, Kwak EL, McCleary NJ, Fuchs CS, Meyerhardt JA, Ng K, Zhu AX, Abrams TA, Wolpin BM, Zhang S, Reardon A, Fitzpatrick B, Kulke MH, Ryan DP. Phase II trial of cabozantinib in patients with carcinoid and pancreatic neuroendocrine tumors (pNET). *J Clin Oncol* 2017; **35**: 228-228 [DOI: 10.1200/JCO.2017.35.4_suppl.228]

56 **Capdevila J**, Fazio N, Lopez Lopez C, Teule A, Valle J W, Tafuto S, Custodio A B, Reed N, Raderer M, Grande E, Garcia-Carbonero R, Jiménez-Fonseca P, Alonso V, Antonuzzo L, Spallanzani A, Berruti A, Sevilla I, La Casta Munoa A, Hernando-Cubero J, Ibrahim T. Final results of the TALENT trial (GETNE1509): a prospective multicohort phase II study of lenvatinib in patients (pts) with G1/G2 advanced pancreatic (panNETs) and gastrointestinal (giNETs) neuroendocrine tumors (NETs). *J Clin Oncol* 2019; **37**: 4106-4106 [DOI: 10.1200/JCO.2019.37.15_suppl.4106]

57 **Capdevila J**, Jimenez-Valerio G, Martinez A, Hernando J, Ibrahim T, Fazio N, Lopez C, Teule A, Valle W, Tafuto S, Custodio B, Reed NS, Raderer M, Grande E, Garcia-Carbonero R, Jiménez-Fonseca P, Alonso V, Casanovas O. Plasma biomarker study of lenvatinib in gastroenteropancreatic neuroendocrine tumors reveals Ang2 and FGF2 as predictors of treatment response: Results from the international phase II TALENT trial (GETNE 1509). *J Clin Oncol* 2021; **39**: 4113-4113 [DOI: 10.1200/JCO.2021.39.15_suppl.4113]

58 **Strosberg JR**, Cives M, Hwang J, Weber T, Nickerson M, Atreya CE, Venook A, Kelley RK, Valone T, Morse B, Coppola D, Bergsland EK. A phase II study of axitinib in advanced neuroendocrine tumors. *Endocr Relat Cancer* 2016; **23**: 411-418 [PMID: 27080472 DOI: 10.1530/ERC-16-0008]

59 **Grande E**, Capdevila J, Castellano D, Teulé A, Durán I, Fuster J, Sevilla I, Escudero P, Sastre J, García-Donas J, Casanovas O, Earl J, Ortega L, Apellaniz-Ruiz M, Rodriguez-Antona C, Alonso-Gordoa T, Díez JJ, Carrato A, García-Carbonero R. Pazopanib in pretreated advanced neuroendocrine tumors: a phase II, open-label trial of the Spanish Task Force Group for Neuroendocrine Tumors (GETNE). *Ann Oncol* 2015; **26**: 1987-1993 [PMID: 26063633 DOI: 10.1093/annonc/mdv252]

60 **Lu M**, Zhang P, Zhang Y, Li Z, Gong J, Li J, Li Y, Zhang X, Lu Z, Wang X, Zhou J, Peng Z, Wang W, Feng H, Wu H, Yao S, Shen L. Efficacy, Safety, and Biomarkers of Toripalimab in Patients with Recurrent or Metastatic Neuroendocrine Neoplasms: A Multiple-Center Phase Ib Trial. *Clin Cancer Res* 2020; **26**: 2337-2345 [PMID: 32086343 DOI: 10.1158/1078-0432.CCR-19-4000]

61 **Strosberg J**, Mizuno N, Doi T, Grande E, Delord JP, Shapira-Frommer R, Bergsland E, Shah M, Fakih M, Takahashi S, Piha-Paul SA, O'Neil B, Thomas S, Lolkema MP, Chen M, Ibrahim N, Norwood K, Hadoux J. Efficacy and Safety of Pembrolizumab in Previously Treated Advanced Neuroendocrine Tumors: Results From the Phase II KEYNOTE-158 Study. *Clin Cancer Res* 2020; **26**: 2124-2130 [PMID: 31980466 DOI: 10.1158/1078-0432.CCR-19-3014]

62 **Mulvey C**, Raj NP, Chan JA, Aggarwal RR, Cinar P, Hope T A, Kolli K, Zhang L, Calabrese S, Grabowsky JA, Modarresi L, Kelly V, Stonely D, Munster PN, Reidy DL, Fong L, Bergsland EK. Phase II study of pembrolizumab-based therapy in previously treated extrapulmonary poorly differentiated neuroendocrine carcinomas: Results of Part A (pembrolizumab alone). *J Clin Oncol* 2019; **37**: 363-363 [DOI: 10.1200/JCO.2019.37.4_suppl.363]

63 **Matos Garcia I**, Grande E, Garcia-Carbonero R, Lopez C, Teule A, Capdevila J. A multicohort phase II study of durvalumab plus tremelimumab for the treatment of patients (PTS) with advanced neuroendocrine neoplasms (NENs) of gastroenteropancreatic (GEP) or lung origin (the DUNE trial-GETNE1601-). *J Clin Oncol* 2017; **35**: TPS4146-TPS4146 [DOI: 10.1200/JCO.2017.35.15_suppl.TPS4146]

64 **Klein O**, Kee D, Markman B, Chang Lee R, Michael M, Mileshkin LR, Scott CL, Linklater R, Menon S, Tebbutt NC, Palmer J, Behren A, Cebon JS. A phase II clinical trial of ipilimumab/nivolumab combination immunotherapy in patients with rare upper gastrointestinal, neuroendocrine, and gynecological malignancies. *J Clin Oncol* 2019; **37**: 2570-2570 [DOI: 10.1200/JCO.2019.37.15_suppl.2570]

65 **Shen L**, Yu X, Lu M, Zhang X, Cheng Y, Zhang Y, Li Z, Xu J, Weng D, Wu C, Ma Y, Cheng K, WANG W, Gao H, Li Y, Zhou J, Shi H, Tan P, Su W. Surufatinib in combination with toripalimab in patients with advanced neuroendocrine carcinoma: Results from a multicenter, open-label, single-arm, phase II trial. *J Clin Oncol* 2021; **39**: e16199-e16199 [DOI:

10.1200/JCO.2021.39.15_suppl.e16199]

66 **Ito T**, Masui T, Komoto I, Doi R, Osamura RY, Sakurai A, Ikeda M, Takano K, Igarashi H, Shimatsu A, Nakamura K, Nakamoto Y, Hijioka S, Morita K, Ishikawa Y, Ohike N, Kasajima A, Kushima R, Kojima M, Sasano H, Hirano S, Mizuno N, Aoki T, Ohtsuka T, Okumura T, Kimura Y, Kudo A, Konishi T, Matsumoto I, Kobayashi N, Fujimori N, Honma Y, Morizane C, Uchino S, Horiuchi K, Yamasaki M, Matsubayashi J, Sato Y, Sekiguchi M, Abe S, Okusaka T, Kida M, Kimura W, Tanaka M, Majima Y, Jensen RT, Hirata K, Imamura M, Uemoto S. JNETS clinical practice guidelines for gastroenteropancreatic neuroendocrine neoplasms: diagnosis, treatment, and follow-up: a synopsis. *J Gastroenterol* 2021; **56**: 1033-1044 [PMID: 34586495 DOI: 10.1007/s00535-021-01827-7]

67 **Strosberg JR**, Caplin ME, Kunz PL, Ruszniewski PB, Bodei L, Hendifar AE, Mittra E, Wolin E M, Yao JC, Pavel ME, Grande E, Van Cutsem E, Seregni E, Duarte H, Gericke G, Bartalotta A, Demange A, Mutevelic S, Krenning E. Final overall survival in the phase 3 NETTER-1 study of lutetium-177-DOTATATE in patients with midgut neuroendocrine tumors. *J Clin Oncol* 2021; **39**: 4112-4112 [DOI: 10.1200/JCO.2021.39.15_suppl.4112]

68 **Clement D**, Navalkissoor S, Srirajaskanthan R, Courbon F, Dierickx L, Eccles A, Lewington V, Mitjavila M, Percovich J C, Lequoy B, He B, Folitar I, Ramage J. Efficacy and safety of 177Lu-DOTATATE in patients (pts) with advanced pancreatic neuroendocrine tumors (PanNETs): Data from the NETTER-R international, retrospective registry. *J Clin Oncol* 2021; **39**: 4116-4116 [DOI: 10.1200/JCO.2021.39.15_suppl.4116]

69 **Nicolas GP**, Ansquer C, Lenzo NP, Grønbæk H, Haug A, Navalkissoor S, Beauregard J, Germann N, McEwan S, Wild D, Hicks RJ. An international open-label study on safety and efficacy of 177Lu-satoreotide tetraxetan in somatostatin receptor positive neuroendocrine tumours (NETs): An interim analysis. *Ann Oncol* 2020; **31**: S711-S724 [DOI: 10.1016/j.annonc.2020.08.1373]

70 **Cives M**, Pelle' E, Strosberg J. Emerging Treatment Options for Gastroenteropancreatic Neuroendocrine Tumors. *J Clin Med* 2020; **9** [PMID: 33202931 DOI: 10.3390/jcm9113655]

71 **Grande E**, Teulé A, Alonso-Gordoa T, Jiménez-Fonseca P, Benavent M, Capdevila J, Custodio A, Vera R, Munarriz J, La Casta A, Díez JJ, Gajate P, Molina-Cerrillo J, Matos I, Cristóbal EM, Ruffinelli JC, Palacios J, García-Carbonero R. The PALBONET Trial: A Phase II Study of Palbociclib in Metastatic Grade 1 and 2 Pancreatic Neuroendocrine Tumors (GETNE-1407). *Oncologist* 2020; **25**: 745-e1265 [PMID: 32045050 DOI: 10.1634/theoncologist.2020-0033]

72 **Tang LH**, Contractor T, Clausen R, Klimstra DS, Du YC, Allen PJ, Brennan MF, Levine AJ, Harris CR. Attenuation of the retinoblastoma pathway in pancreatic neuroendocrine tumors due to increased cdk4/cdk6. *Clin Cancer Res* 2012; **18**: 4612-4620 [PMID: 22761470 DOI: 10.1158/1078-0432.CCR-11-3264]

73 **Anderson PM**, Gortz J. Phase 2 study of DRD2 antagonist/ClpP agonist ONC201 in neuroendocrine tumors. *J Clin Oncol* 2021; **39**: 3002-3002 [DOI: 10.1200/JCO.2021.39.15_suppl.3002]

74 **White BH**, Whalen K, Kriksciukaite K, Alargova R, Au Yeung T, Bazinet P, Brockman A, DuPont M, Oller H, Lemelin CA, Lim Soo P, Moreau B, Perino S, Quinn JM, Sharma G, Shinde R, Sweryda-Krawiec B, Wooster R, Bilodeau MT. Discovery of an SSTR2-Targeting Maytansinoid Conjugate (PEN-221) with Potent Activity in Vitro and in Vivo. *J Med Chem* 2019; **62**: 2708-2719 [PMID: 30735385 DOI: 10.1021/acs.jmedchem.8b02036]

75 **Halperin DM**, Johnson ML, Chan JA, Hart LL, Cook N, Patel VM, Schlechter BL, Cave J, Dowlati A, Blaszkowsky LS, Meyer T, Eads JR, Culp D, Kriksciukaite K, Mei L, Bilodeau M, Bloss J, Kulke MH. The safety and efficacy of PEN-221 somatostatin analog (SSA)-DM1 conjugate in patients (PTS) with advanced GI mid-gut neuroendocrine tumor (NET): Phase 2 results. *J Clin Oncol* 2021; **39**: 4110-4110 [DOI: 10.1200/JCO.2021.39.15_suppl.4110]

76 **Jonasch E**, Donskov F, Iliopoulos O, Rathmell WK, Narayan VK, Maughan BL, Oudard S, Else T, Maranchie JK, Welsh SJ, Thamake S, Park EK, Perini RF, Linehan WM, Srinivasan R; MK-6482-004 Investigators. Belzutifan for Renal Cell Carcinoma in von Hippel-Lindau Disease. *N Engl J Med* 2021; **385**: 2036-2046 [PMID: 34818478 DOI: 10.1056/NEJMoa2103425]

World Journal of Gastroenterology

Submit a Manuscript: https://www.f6publishing.com

World J Gastroenterol 2022 May 28; 28(20): 2176-2183

DOI: 10.3748/wjg.v28.i20.2176

ISSN 1007-9327 (print) ISSN 2219-2840 (online)

MINIREVIEWS

Radiomics for the detection of microvascular invasion in hepatocellular carcinoma

Kun Lv, Xin Cao, Peng Du, Jun-Yan Fu, Dao-Ying Geng, Jun Zhang

Specialty type: Gastroenterology and hepatology

Provenance and peer review: Invited article; Externally peer reviewed.

Peer-review model: Single blind

Peer-review report's scientific quality classification

Grade A (Excellent): A
Grade B (Very good): B
Grade C (Good): 0
Grade D (Fair): 0
Grade E (Poor): 0

P-Reviewer: Granito A, Italy; Zhou X, China

Received: November 16, 2021
Peer-review started: November 16, 2021
First decision: December 26, 2021
Revised: January 9, 2022
Accepted: April 22, 2022
Article in press: April 22, 2022
Published online: May 28, 2022

Kun Lv, Xin Cao, Peng Du, Jun-Yan Fu, Dao-Ying Geng, Jun Zhang, Department of Radiology, Huashan Hospital, Fudan University, Shanghai 200040, China

Xin Cao, Dao-Ying Geng, Jun Zhang, Institute of Functional and Molecular Medical Imaging, Fudan University, Shanghai 200040, China

Xin Cao, Dao-Ying Geng, Jun Zhang, Center for Shanghai Intelligent Imaging for Critical Brain Diseases Engineering and Technology Research, Science and Technology Commission of Shanghai Municipality, Shanghai 200040, China

Xin Cao, Dao-Ying Geng, Jun Zhang, Institute of Intelligent Imaging Phenomics, International Human Phenome Institutes (Shanghai), Shanghai 200040, China

Corresponding author: Dao-Ying Geng, MD, PhD, Dean, Doctor, Department of Radiology, Huashan Hospital, Fudan University, No. 12 Wulumuqi Road (Middle), Shanghai 200040, China. gdy_2019@163.com

Abstract

Hepatocellular carcinoma (HCC) is the most common primary liver cancer, accounting for about 90% of liver cancer cases. It is currently the fifth most common cancer in the world and the third leading cause of cancer-related mortality. Moreover, recurrence of HCC is common. Microvascular invasion (MVI) is a major factor associated with recurrence in postoperative HCC. It is difficult to evaluate MVI using traditional imaging modalities. Currently, MVI is assessed primarily through pathological and immunohistochemical analyses of postoperative tissue samples. Needle biopsy is the primary method used to confirm MVI diagnosis before surgery. As the puncture specimens represent just a small part of the tumor, and given the heterogeneity of HCC, biopsy samples may yield false-negative results. Radiomics, an emerging, powerful, and non-invasive tool based on various imaging modalities, such as computed tomography, magnetic resonance imaging, ultrasound, and positron emission tomography, can predict the HCC-MVI status preoperatively by delineating the tumor and/or the regions at a certain distance from the surface of the tumor to extract the image features. Although positive results have been reported for radiomics, its drawbacks have limited its clinical translation. This article reviews the application of radiomics, based on various imaging modalities, in preoperative evaluation of HCC-MVI and explores future research directions that facilitate its clinical translation.

Key Words: Microvascular invasion; Hepatocellular carcinoma; Radiomics; Texture analysis; Diagnostic imaging; Liver

Core Tip: Hepatocellular carcinoma-microvascular invasion (HCC-MVI) is closely related to the prognosis of patients, so accurate and individualized prediction of MVI status before treatment is very important. Radiomics is a non-invasive method for predicting HCC-MVI status preoperatively. The standardization of relevant implementation processes of radiomics, such as the delineation of the region of interest, the improvement of algorithms, and the combination of liver imaging reporting and data system, will all contribute to the accurate prediction of MVI. In addition, the introduction of the biological significance of the disease can make up for the shortcomings of the clinical transformation of radiomics to a certain extent.

Citation: Lv K, Cao X, Du P, Fu JY, Geng DY, Zhang J. Radiomics for the detection of microvascular invasion in hepatocellular carcinoma. *World J Gastroenterol* 2022; 28(20): 2176-2183
URL: https://www.wjgnet.com/1007-9327/full/v28/i20/2176.htm
DOI: https://dx.doi.org/10.3748/wjg.v28.i20.2176

INTRODUCTION

Hepatocellular carcinoma (HCC) is the most common primary liver cancer, accounting for about 90% of liver cancers cases[1]. According to the World Health Organization, HCC is currently the fifth most common cancer in the world and the third leading cause of cancer-related mortality[2]. The rate of HCC occurrence varies with geographic regions. It is more commonly observed in the underdeveloped regions of the world; for example, its annual incidence rate in East Asia and Sub-Saharan Africa is higher, exceeding 15 per 100000 individuals. Nonetheless, the incidence of HCC is rising rapidly in Europe and the United States, and is expected to continue to rise over the next 10 years[3-5]. Although various treatment modalities are available for different stages of HCC, recurrence is common in the following types of HCC patients: patients with single masses with preserved liver function, no portal hypertension, and treated with resection; patients with multiple intrahepatic tumors or poor liver function, no major comorbidities, and listed for transplantation; patients with up to three tumors (each 4 cm or smaller), not eligible for transplantation, and treated with ablation; patients not eligible for ablation and receiving embolization; and some patients subjected to systemic and radiation treatments [6-8]. According to a previous study, about 70% of HCC patients relapse within 5 years after surgical resection and 35% relapse within 5 years after liver transplantation[9]. Microvascular invasion (MVI) is defined as the invasion of tumor cells into the vascular endothelial cell space, including microvessels of the portal vein, hepatic artery, and lymphatic vessels[10]. Previous studies[11,12] demonstrated that MVI is the strongest independent predictor of early HCC recurrence. It is primarily detected through immunohistochemical and pathological analyses of postoperative tissue specimens[13]. The inability to identify MVI preoperatively leads to incomplete surgical resection and increases the risk of postoperative recurrence. This limits the effectiveness of treatment and affects the long-term survival of liver cancer patients. Although conventional imaging examinations, such as computed tomography (CT)-based quantitative image analysis and dynamic contrast enhanced ultrasound (CEUS)[14,15] can predict MVI preoperatively, routine analyses of these images provide insufficient information, such as two-dimensional analysis of lesion morphology, size, *etc* based on conventional images.

Radiomics is an emerging, powerful, and non-invasive tool that uses a series of data mining algorithms and statistical analysis tools for the high-throughput analysis of image features. It can detect delicate features from conventional radiological images that are invisible to the naked eye and has been increasingly adopted to predict MVI. This enables extraction of many features at the whole lesion level. These features may provide information regarding heterogeneity and invasiveness of the disease that can be of predictive or prognostic value, thus leading to the selection of the best possible treatment[16]. HCC shows a large amount of intra- and inter-tumor heterogeneity at the biological level[17-20]. Biopsy, which is the main method for diagnosing HCC, usually involves removal of only a small part of the tumor, thus excluding the possibility of assessing intratumoral heterogeneity. Hence, in recent years, research pertaining to HCC using radiomics has attracted increasing attention[21]. Quantitative radiomics data, along with models or nomograms based on multiple imaging modalities including CT, magnetic resonance imaging (MRI), ultrasound (US), and positron emission tomography (PET), demonstrate high accuracy in predicting HCC-MVI preoperatively. In this review, we discuss the

applications of radiomics based on various imaging modalities in the preoperative detection of HCC-MVI (Table 1). In addition, future research directions are explored.

CT-BASED RADIOMICS

Liver cirrhosis or hepatitis B-related HCC can be diagnosed highly accurately through non-invasive approaches based on multi-phase CT/MRI imaging features, such as hyperenhancement in the arterial phase (AP) and hypoenhancement in the portal venous phase (PVP)[22]. For example, Peng *et al*[23] constructed a radiomics model based on hepatic AP and PVP images to delineate tumor regions and extract radiomic features to predict the preoperative MVI status of HCC related to hepatitis B. They found that radiomics signature, the alpha-fetoprotein (AFP) level, hypoattenuating halo, internal arteries, and non-smooth tumor margins are independent predictors of MVI. This model showed good correction and discrimination capabilities in the training and validation cohorts. The C indices for the training and validation cohorts were 0.846 and 0.844, respectively, and the area under the curve (AUC) of the radiomics nomogram in the MVI risk analysis was 0.845. In a similar study, Ma *et al*[24] found that the radiomics features of PVP were better than those of the AP and delayed phase (DP); the C index and AUC values of the model, combined with radiomic features and clinical factors, were close to those reported by Peng *et al*[23]. In a recent study based on AP and PVP images, Xu *et al*[9] marked the tumor regions and regions 5 mm away from the tumor surface, as regions of interest (ROI) to extract radiomic features to predict the HCC-MVI status and long-term clinical outcomes of patients with HCC. It was found that aspartate aminotransferase (AST) and AFP levels, tumor margin, growth pattern, capsule, peritumoral enhancement, radio-genomic venous invasion (RVI), and the radiomic score (R-score) were all predictors of MVI. The AUC of this model was 0.909, and the progression-free survival and overall survival of the MVI group were significantly lower than those of the non-MVI group. This showed that combining large-scale clinical radiology and radiomics analyses could reliably predict MVI and clinical outcomes.

MRI-BASED RADIOMICS

Although both conventional multi-phase contrast enhanced CT and MRI can be used to obtain the unique image features of HCC, MRI provides many additional imaging sequences that are helpful in diagnosing HCC without radiation damage; the additional sequences include T2-weighted imaging (T2WI), diffusion weighted imaging (DWI), and enhanced scanning by combined use of some extracellular and hepatocyte contrast agents, such as gadoxetic acid, that have the ability to distinguish relatively small and subtle lesions through the hypointensity received in the hepatobiliary phase (HBP)[25]. Moreover, a combination of MRI parameters can facilitate early diagnosis of small HCC. For example, double hypointensity in the portal/venous phase and HBP can be considered an MRI pattern that is highly suggestive of hypovascular HCC[26]. Thus, MRI-based radiomics provides more possibilities for HCC-MVI assessment. Feng *et al*[27], based on a gadolinium-ethoxybenzyl-diethylenetriamine (Gd-EOB-DTPA) MRI HBP image, delineated the tumor and designated a 1-cm area around it as the ROI. The combined intratumoral and peritumoral radiomics model presented in that study predicted the AUC value of MVI to be 0.85. In another study, Yang *et al*[28] used gadoxetic acid-enhanced MRI to delineate the tumor, which was then used as the ROI. They found that the AFP level, non-smooth tumor margins, arterial peritumoral enhancement, and radiomics signatures of HBP T1WI and HBP T1 maps could all be used as predictors of MVI. The prediction model that combined clinical radiation factors and fusion radiomic features from HBP images predicted the AUC of MVI to be 0.943, which was higher than that reported by Feng *et al*[27]. Meanwhile, the C indices of the generated nomograms in the training and validation groups were 0.936 and 0.864, respectively. This may stem from the varied delineation of the ROIs and the construction of models based on different sequences. Recently, Nebbia *et al*[29] devised a method based on radiomics through multi-sequence and traditional Gd-DTPA MRI for preoperative detection of MVI. It was found that the T2 and PVP sequences were superior to other MRI sequences in single-sequence models (*i.e.* T1, DWI, and late AP). The combination of these two sequences obtained the highest AUC value of 0.867 in predicting MVI, indicating that preoperative liver MRI scans are promising for predicting MVI and that the information obtained from a multi-parameter MRI sequence is crucial in identifying MVI.

US-BASED RADIOMICS

Compared with CT/MR, US is radiation-free, easy to implement, and simple to use for liver examinations. If potential predictors can be identified, US/CEUS may become an alternative technique to provide additional information for the detection of MVI. Hu *et al*[30], based on US images, outlined the

Table 1 Based on various imaging modalities radiomics in the application of microvascular invasion

Ref.	Modality/images/patients/ROI	Software	Predictors of MVI
Peng *et al*[23]	CT/AP and PVP CT images/304/tumor	IBEX software package	Radiomics signature, AFP level, hypoattenuating halo, internal arteries, and nonsmooth tumor margin
Ma *et al*[24]	CT/AP, PVP and DP CT images/157/tumor	ITK-Snap	Age, MTD, AFP, Radiomics signature, hepatitis B
Xu *et al*[9]	CT/AP and PVP CT images/495/VOI^{entire}, $VOI^{50\%}$, and $VOI^{penumbra}$	In-house software written in Python 3.6.1	AST, AFP, tumor margin, growth pattern, capsule, peritumoral enhance, RVI, R-score of VOI^{entire} on PP
Feng *et al*[27]	MRI/HBP of Gd-EOB-DTPA/160/tumoural and peritumoural (1cm) regions	ITK-Snap	NA
Yang *et al*[28]	MRI/T1, T2, DWI, Gd-EOB-DTPA MRI AP, PVP, DP, and HBP/208/tumor	ITK-Snap	AFP, nonsmooth tumor margin, arterial peritumoral enhancement, radiomics signatures of HBP T1WI and HBP T1 maps
Nebbia *et al*[29]	MRI/T1, T2, DWI, Gd-DTPA MRI AP and PVP/99/tumoural and peritumoural (1 cm) regions	NA	NA
Hu *et al*[30]	US/Grayscale US/482/tumor	A.K. software	radiomics score, AFP, and tumor size
Dong *et al*[31]	US/Grayscale US/322/tumor and peri-tumor (half of the tumor radius)	MITK	NA
Li *et al*[35]	PET-CT/[^{18}F]FDG PET-CT/80/areas with abnormal uptake	Lifex software	SUV_{max}, TLR, Rad-score

AFP: Alpha-fetoprotein; A.K. software: Artificial Intelligence Kit, version 1.1, GE Healthcare; AP: Artery phase; AST: Aspartate aminotransferase; CT: Computed tomography; DP: Delay phase; DWI: Diffusion weighted imaging; [^{18}F]FDG PET: 18-fluorodeoxyglucose positron emission tomography; Gd-DTPA: Gadopentetic acid; Gd-EOB-DTPA: Gadolinium-ethoxybenzyl-diethylenetriamine; HBP: Hepatobiliary phase; MITK: Medical Imaging Interaction Toolkit; MRI: Magnetic resonance imaging; MTD: Maximum tumour diameter; MVI: Microvascular invasion; NA: Not available; PP: Portal-venous phase imaging; PVP: Portal venous phase; ROI: Region of interest; R-score: Radiomic score; RVI: Radiogenomic venous invasion; SUV_{max}: Maximum standard uptake value; TLR: Maximum SUV of the tumor/mean SUV of the normal liver; US: Ultrasound; VOI^{entire}: Entire-volumetric interest; $VOI^{50\%}$: 50% of the entire tumor volume; $VOI^{penumbra}$: A region with 5 mm distance to tumor surface.

tumor region as the ROI to extract radiomic features and constructed a US-based radiomics score for preoperative prediction of HCC-MVI. The study showed that an AFP level > 400 ng/mL and tumor size > 5 cm were significantly related to MVI. The AFP level, gray-scale US-based tumor size, and radiomics score were identified to be independent predictors of MVI. The radiomics-based nomogram (AUC: 0.731) showed better performance in MVI detection than the clinical nomogram (AUC: 0.634). However, there was no significant difference between the MVI-positive and -negative groups in terms of other clinical and pathological features, as well as CEUS features. Similarly, Dong *et al*[31] envisaged that radiomic algorithms based on US images might have potential predictive value in the detection of MVI in patients with HCC. Unlike Hu *et al*[30], Dong *et al*[31] delineated the gross-tumor region (GTR) and the peri-tumoral region (PTR, the uniform dilated half of the tumor radius) and showed that the AUC of the radiomic nomogram, combined with the AFP level, characteristics of the tumor, and the area around the tumor, was 0.744, which was slightly higher than that reported by Hu *et al*[30]. This also supports the idea that the peritumoral area is an onset area of MVI. It is thought to be the main blood transmission route of portal vein thrombosis and the main route for intra- and extra-hepatic metastases [32]. This signifies that, when evaluating HCC-MVI based on radiomics, the area around the tumor also needs to be evaluated.

PET-BASED RADIOMICS

High glucose consumption by the tumor cell microenvironment, including that in HCC, can be reflected in 18-fluorodeoxyglucose PET (^{18}FDG-PET). Although the tumor detection efficiency is affected by liver cirrhosis and a high background signal, studies have confirmed that the maximum standard uptake value (SUVmax) of ^{18}FDG-PET is related to the recurrence rate of HCC and patient survival, and that the combination of MRI and ^{18}FDG-PET can improve the accuracy of HCC histopathological grading[33,34]. In a recent study[35], the PET/CT model, after integrating the radiomic features composed of five PET- and six CT-derived texture features, showed an AUC of 0.891 in the training cohort. The prediction of disease-free survival (DFS) was also more accurate (C index of 0.831). This study indicated that the newly developed [^{18}F]FDG PET/CT radiomics feature is an independent biomarker for evaluating MVI

and DFS in patients with ultra-early and early HCC.

LIMITATIONS

Although radiomics has achieved some exciting results in evaluating the HCC-MVI status, many limitations still exist. The current lack of standardization in image acquisition schemes, segmentation methods, and radiomics tools used for analysis may lead to differences in the measurement of radiomic features that do not stem from biological differences[16]. Existing studies[36] have shown varied reproducibility in extracting quantitative imaging features from tumor regions segmented by different methods. Fortunately, the radiomics quality score (RQS) has been proposed to assess whether radiomics research meets best practices[37]. In addition, there are huge challenges in interpreting the correlation between radiomics features and their biological significance, especially that of the texture features obtained from high-level analysis. This leads to restrictions on the use of radiomics in clinical applications[38].

FUTURE DIRECTIONS

Every step involved in radiomics-based analyses needs to be optimized and standardized, including the adjustment of imaging schemes and parameters, development of (semi-) automated segmentation methods, and refinement of algorithms and high-throughput analysis modeling methods. In addition, in the process of establishing a radiomics model, potential independent variables should be included in the multivariate analysis (such as protein induced by vitamin K absence or antagonist-II), which will help improve the sensitivity, specificity, and predictive ability of the model[39]. In addition, the imaging characteristics of certain liver nodules in patients with chronic liver disease are complex and diverse. For example, the imaging manifestations of primary and recurrent cirrhosis nodules are different[40], and tuberculosis nodules are easily misdiagnosed as HCC[41]. Through targeted collection of a large number of these different liver nodules, corresponding predictions can also be made using radiomics. Furthermore, due to the complexity and similarity in imaging characteristics of certain hepatic nodules in high-risk HCC, the American College of Radiology (ACR) has issued a diagnostic program, namely the liver imaging reporting and data system (LI-RADS, https://www.acr.org). Several studies[42-44] have indicated that ACR CT/MRI LI-RADS and CEUS LI-RADS possess high application value in identifying primary hepatic nodules in patients with high-risk HCC, and especially display high diagnostic performance with LR-5 and LR-M nodules. In a recent study, Zhou *et al*[45] observed that the model incorporating CEUS LR-M and clinical features was able to predict the MVI status of HCC. Therefore, undoubtedly, LI-RADS combined with radiomics using various imaging modalities shows promise in the prediction of HCC-MVI.

Although radiomics can predict MVI and determine related predictors, there are differences between groups. With the exponential growth of interest in the development of artificial intelligence (AI)-based applications, there is now an opportunity to apply AI in radiomics analyses. Deep learning, especially convolutional neural networks (CNNs), can capture texture information in the initial convolution layer. CNNs may replace several current radiomics-based analysis methods[46]. Recently, a new concept of "deep radiomics" was proposed. This technique combines radiomics and deep learning analysis by creating feature images based on texture features and then using them as input for CNNs to classify the images. Therefore, along with the prediction of MVI, the use of AI-based technology is also expected to identify individual MVI.

Data-driven radiomics is inherently unable to provide insights into the biological basis of the observed relationship. It is important to note that HCC shows large intra- and inter-tumor heterogeneity at the biological level. With the rapid development and popularization of machine learning, researchers are paying increasing attention to the improvement of prediction ability; however, they are far from understanding the biological significance of the observed research results. This disconnect between the predictive models and their biological significance inherently limits their widespread clinical translation. Therefore, it is necessary to introduce biological significance into the radiomics field through various available biological methods, such as genome association, immunohistochemical analyses, local microscopic pathological image texture analyses, and evaluation of macroscopic histopathological marker expression (Figure 1)[47].

CONCLUSION

Radiomics based on multiple imaging modalities has performed remarkably well in predicting the HCC-MVI status. In future, researchers need to focus on standardizing image segmentation and radiomics processing processes and the optimization of algorithms to further improve the accuracy of

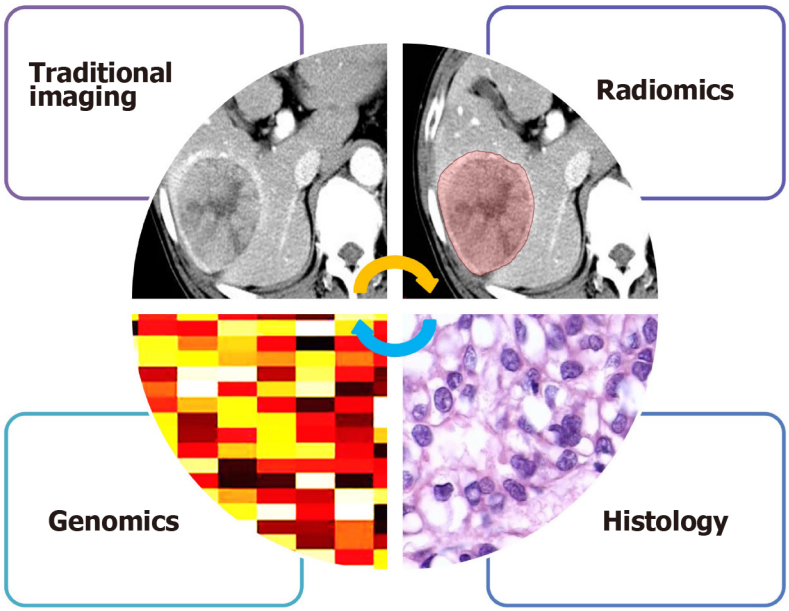

DOI: 10.3748/wjg.v28.i20.2176

Figure 1 Histology and genomic analysis can provide specific small-scale insights and help validate radiomic results.

individualized prediction. Importantly, it may be possible to provide some new insights through combining deep learning and LI-RADS with radiomics and introducing biological significance.

FOOTNOTES

Author contributions: All authors contributed to this paper; Geng DY and Zhang J designed the outline for the review; Lv K wrote the review; Cao X, Du P, and Fu JY offered assistance for correct the syntax errors of the paper; Zhang J and Lv K revised and edited the final version.

Supported by the Shanghai Municipal Commission of Science and Technology, No. 19411951200; Clinical Research Plan of SHDC, No. SHDC2020CR3020A; and the Research Startup Fund of Huashan Hospital Fudan University, No. 2021QD035.

Conflict-of-interest statement: There is no conflict of interest associated with any of the senior author or other coauthors contributed their efforts in this manuscript.

Country/Territory of origin: China

ORCID number: Kun Lv 0000-0003-4967-3727; Xin Cao 0000-0003-3839-3076; Peng Du 0000-0002-6970-1329; Jun-Yan Fu 0000-0002-1000-2507; Dao-Ying Geng 0000-0002-3585-6883; Jun Zhang 0000-0003-1849-9199.

S-Editor: Yan JP
L-Editor: Filipodia
P-Editor: Yan JP

REFERENCES

1 **Omata M**, Cheng AL, Kokudo N, Kudo M, Lee JM, Jia J, Tateishi R, Han KH, Chawla YK, Shiina S, Jafri W, Payawal DA, Ohki T, Ogasawara S, Chen PJ, Lesmana CRA, Lesmana LA, Gani RA, Obi S, Dokmeci AK, Sarin SK. Asia-Pacific clinical practice guidelines on the management of hepatocellular carcinoma: a 2017 update. *Hepatol Int* 2017; **11**: 317-370 [PMID: 28620797 DOI: 10.1007/s12072-017-9799-9]

2 **Marrero JA**, Kulik LM, Sirlin CB, Zhu AX, Finn RS, Abecassis MM, Roberts LR, Heimbach JK. Diagnosis, Staging, and Management of Hepatocellular Carcinoma: 2018 Practice Guidance by the American Association for the Study of Liver Diseases. *Hepatology* 2018; **68**: 723-750 [PMID: 29624699 DOI: 10.1002/hep.29913]

3 **European Association for the Study of the Liver**. EASL Clinical Practice Guidelines: Management of hepatocellular carcinoma. *J Hepatol* 2018; **69**: 182-236 [PMID: 29628281 DOI: 10.1016/j.jhep.2018.03.019]

4 **Petrick JL**, Braunlin M, Laversanne M, Valery PC, Bray F, McGlynn KA. International trends in liver cancer incidence, overall and by histologic subtype, 1978-2007. *Int J Cancer* 2016; **139**: 1534-1545 [PMID: 27244487 DOI: 10.1002/ijc.30211]

5 **Petrick JL**, Kelly SP, Altekruse SF, McGlynn KA, Rosenberg PS. Future of Hepatocellular Carcinoma Incidence in the United States Forecast Through 2030. *J Clin Oncol* 2016; **34**: 1787-1794 [PMID: 27044939 DOI: 10.1200/JCO.2015.64.7412]

6 **Tabrizian P**, Jibara G, Shrager B, Schwartz M, Roayaie S. Recurrence of hepatocellular cancer after resection: patterns, treatments, and prognosis. *Ann Surg* 2015; **261**: 947-955 [PMID: 25010665 DOI: 10.1097/SLA.0000000000000710]

7 **Grandhi MS**, Kim AK, Ronnekleiv-Kelly SM, Kamel IR, Ghasebeh MA, Pawlik TM. Hepatocellular carcinoma: From diagnosis to treatment. *Surg Oncol* 2016; **25**: 74-85 [PMID: 27312032 DOI: 10.1016/j.suronc.2016.03.002]

8 **Witt JS**, Rosenberg SA, Bassetti MF. MRI-guided adaptive radiotherapy for liver tumours: visualising the future. *Lancet Oncol* 2020; **21**: e74-e82 [PMID: 32007208 DOI: 10.1016/S1470-2045(20)30034-6]

9 **Xu X**, Zhang HL, Liu QP, Sun SW, Zhang J, Zhu FP, Yang G, Yan X, Zhang YD, Liu XS. Radiomic analysis of contrast-enhanced CT predicts microvascular invasion and outcome in hepatocellular carcinoma. *J Hepatol* 2019; **70**: 1133-1144 [PMID: 30876945 DOI: 10.1016/j.jhep.2019.02.023]

10 **Gouw AS**, Balabaud C, Kusano H, Todo S, Ichida T, Kojiro M. Markers for microvascular invasion in hepatocellular carcinoma: where do we stand? *Liver Transpl* 2011; **17** Suppl 2: S72-S80 [PMID: 21714066 DOI: 10.1002/lt.22368]

11 **Roayaie S**, Blume IN, Thung SN, Guido M, Fiel MI, Hiotis S, Labow DM, Llovet JM, Schwartz ME. A system of classifying microvascular invasion to predict outcome after resection in patients with hepatocellular carcinoma. *Gastroenterology* 2009; **137**: 850-855 [PMID: 19524573 DOI: 10.1053/j.gastro.2009.06.003]

12 **Lim KC**, Chow PK, Allen JC, Chia GS, Lim M, Cheow PC, Chung AY, Ooi LL, Tan SB. Microvascular invasion is a better predictor of tumor recurrence and overall survival following surgical resection for hepatocellular carcinoma compared to the Milan criteria. *Ann Surg* 2011; **254**: 108-113 [PMID: 21527845 DOI: 10.1097/SLA.0b013e31821ad884]

13 **Rodríguez-Perálvarez M**, Luong TV, Andreana L, Meyer T, Dhillon AP, Burroughs AK. A systematic review of microvascular invasion in hepatocellular carcinoma: diagnostic and prognostic variability. *Ann Surg Oncol* 2013; **20**: 325-339 [PMID: 23149850 DOI: 10.1245/s10434-012-2513-1]

14 **Zheng J**, Chakraborty J, Chapman WC, Gerst S, Gonen M, Pak LM, Jarnagin WR, DeMatteo RP, Do RKG, Simpson AL; Hepatopancreatobiliary Service in the Department of Surgery of the Memorial Sloan Kettering Cancer Center; Research Staff in the Department of Surgery at Washington University School of Medicine. Preoperative Prediction of Microvascular Invasion in Hepatocellular Carcinoma Using Quantitative Image Analysis. *J Am Coll Surg* 2017; **225**: 778-788.e1 [PMID: 28941728 DOI: 10.1016/j.jamcollsurg.2017.09.003]

15 **Dong Y**, Qiu Y, Yang D, Yu L, Zuo D, Zhang Q, Tian X, Wang WP, Jung EM. Potential application of dynamic contrast enhanced ultrasound in predicting microvascular invasion of hepatocellular carcinoma. *Clin Hemorheol Microcirc* 2021; **77**: 461-469 [PMID: 33459703 DOI: 10.3233/CH-201085]

16 **Gillies RJ**, Kinahan PE, Hricak H. Radiomics: Images Are More than Pictures, They Are Data. *Radiology* 2016; **278**: 563-577 [PMID: 26579733 DOI: 10.1148/radiol.2015151169]

17 **Fransvea E**, Paradiso A, Antonaci S, Giannelli G. HCC heterogeneity: molecular pathogenesis and clinical implications. *Cell Oncol* 2009; **31**: 227-233 [PMID: 19478390 DOI: 10.3233/CLO-2009-0473]

18 **Friemel J**, Rechsteiner M, Frick L, Böhm F, Struckmann K, Egger M, Moch H, Heikenwalder M, Weber A. Intratumor heterogeneity in hepatocellular carcinoma. *Clin Cancer Res* 2015; **21**: 1951-1961 [PMID: 25248380 DOI: 10.1158/1078-0432.CCR-14-0122]

19 **Lin DC**, Mayakonda A, Dinh HQ, Huang P, Lin L, Liu X, Ding LW, Wang J, Berman BP, Song EW, Yin D, Koeffler HP. Genomic and Epigenomic Heterogeneity of Hepatocellular Carcinoma. *Cancer Res* 2017; **77**: 2255-2265 [PMID: 28302680 DOI: 10.1158/0008-5472.CAN-16-2822]

20 **Zhu S**, Hoshida Y. Molecular heterogeneity in hepatocellular carcinoma. *Hepat Oncol* 2018; **5**: HEP10 [PMID: 30302198 DOI: 10.2217/hep-2018-0005]

21 **Yip SS**, Aerts HJ. Applications and limitations of radiomics. *Phys Med Biol* 2016; **61**: R150-R166 [PMID: 27269645 DOI: 10.1088/0031-9155/61/13/R150]

22 **Heimbach JK**, Kulik LM, Finn RS, Sirlin CB, Abecassis MM, Roberts LR, Zhu AX, Murad MH, Marrero JA. AASLD guidelines for the treatment of hepatocellular carcinoma. *Hepatology* 2018; **67**: 358-380 [PMID: 28130846 DOI: 10.1002/hep.29086]

23 **Peng J**, Zhang J, Zhang Q, Xu Y, Zhou J, Liu L. A radiomics nomogram for preoperative prediction of microvascular invasion risk in hepatitis B virus-related hepatocellular carcinoma. *Diagn Interv Radiol* 2018; **24**: 121-127 [PMID: 29770763 DOI: 10.5152/dir.2018.17467]

24 **Ma X**, Wei J, Gu D, Zhu Y, Feng B, Liang M, Wang S, Zhao X, Tian J. Preoperative radiomics nomogram for microvascular invasion prediction in hepatocellular carcinoma using contrast-enhanced CT. *Eur Radiol* 2019; **29**: 3595-3605 [PMID: 30770969 DOI: 10.1007/s00330-018-5985-y]

25 **Roberts LR**, Sirlin CB, Zaiem F, Almasri J, Prokop LJ, Heimbach JK, Murad MH, Mohammed K. Imaging for the diagnosis of hepatocellular carcinoma: A systematic review and meta-analysis. *Hepatology* 2018; **67**: 401-421 [PMID: 28859233 DOI: 10.1002/hep.29487]

26 **Granito A**, Galassi M, Piscaglia F, Romanini L, Lucidi V, Renzulli M, Borghi A, Grazioli L, Golfieri R, Bolondi L. Impact of gadoxetic acid (Gd-EOB-DTPA)-enhanced magnetic resonance on the non-invasive diagnosis of small hepatocellular carcinoma: a prospective study. *Aliment Pharmacol Ther* 2013; **37**: 355-363 [PMID: 23199022 DOI: 10.1111/apt.12166]

27 **Feng ST**, Jia Y, Liao B, Huang B, Zhou Q, Li X, Wei K, Chen L, Li B, Wang W, Chen S, He X, Wang H, Peng S, Chen

ZB, Tang M, Chen Z, Hou Y, Peng Z, Kuang M. Preoperative prediction of microvascular invasion in hepatocellular cancer: a radiomics model using Gd-EOB-DTPA-enhanced MRI. *Eur Radiol* 2019; **29**: 4648-4659 [PMID: 30689032 DOI: 10.1007/s00330-018-5935-8]

28 **Yang L**, Gu D, Wei J, Yang C, Rao S, Wang W, Chen C, Ding Y, Tian J, Zeng M. A Radiomics Nomogram for Preoperative Prediction of Microvascular Invasion in Hepatocellular Carcinoma. *Liver Cancer* 2019; **8**: 373-386 [PMID: 31768346 DOI: 10.1159/000494099]

29 **Nebbia G**, Zhang Q, Arefan D, Zhao X, Wu S. Pre-operative Microvascular Invasion Prediction Using Multi-parametric Liver MRI Radiomics. *J Digit Imaging* 2020; **33**: 1376-1386 [PMID: 32495126 DOI: 10.1007/s10278-020-00353-x]

30 **Hu HT**, Wang Z, Huang XW, Chen SL, Zheng X, Ruan SM, Xie XY, Lu MD, Yu J, Tian J, Liang P, Wang W, Kuang M. Ultrasound-based radiomics score: a potential biomarker for the prediction of microvascular invasion in hepatocellular carcinoma. *Eur Radiol* 2019; **29**: 2890-2901 [PMID: 30421015 DOI: 10.1007/s00330-018-5797-0]

31 **Dong Y**, Zhou L, Xia W, Zhao XY, Zhang Q, Jian JM, Gao X, Wang WP. Preoperative Prediction of Microvascular Invasion in Hepatocellular Carcinoma: Initial Application of a Radiomic Algorithm Based on Grayscale Ultrasound Images. *Front Oncol* 2020; **10**: 353 [PMID: 32266138 DOI: 10.3389/fonc.2020.00353]

32 **Hu HT**, Shen SL, Wang Z, Shan QY, Huang XW, Zheng Q, Xie XY, Lu MD, Wang W, Kuang M. Peritumoral tissue on preoperative imaging reveals microvascular invasion in hepatocellular carcinoma: a systematic review and meta-analysis. *Abdom Radiol (NY)* 2018; **43**: 3324-3330 [PMID: 29845312 DOI: 10.1007/s00261-018-1646-5]

33 **Cho KJ**, Choi NK, Shin MH, Chong AR. Clinical usefulness of FDG-PET in patients with hepatocellular carcinoma undergoing surgical resection. *Ann Hepatobiliary Pancreat Surg* 2017; **21**: 194-198 [PMID: 29264581 DOI: 10.14701/ahbps.2017.21.4.194]

34 **Kaissis GA**, Lohöfer FK, Hörl M, Heid I, Steiger K, Munoz-Alvarez KA, Schwaiger M, Rummeny EJ, Weichert W, Paprottka P, Braren R. Combined DCE-MRI- and FDG-PET enable histopathological grading prediction in a rat model of hepatocellular carcinoma. *Eur J Radiol* 2020; **124**: 108848 [PMID: 32006931 DOI: 10.1016/j.ejrad.2020.108848]

35 **Li Y**, Zhang Y, Fang Q, Zhang X, Hou P, Wu H, Wang X. Radiomics analysis of [^{18}F]FDG PET/CT for microvascular invasion and prognosis prediction in very-early- and early-stage hepatocellular carcinoma. *Eur J Nucl Med Mol Imaging* 2021; **48**: 2599-2614 [PMID: 33416951 DOI: 10.1007/s00259-020-05119-9]

36 **Qiu Q**, Duan J, Duan Z, Meng X, Ma C, Zhu J, Lu J, Liu T, Yin Y. Reproducibility and non-redundancy of radiomic features extracted from arterial phase CT scans in hepatocellular carcinoma patients: impact of tumor segmentation variability. *Quant Imaging Med Surg* 2019; **9**: 453-464 [PMID: 31032192 DOI: 10.21037/qims.2019.03.02]

37 **Lambin P**, Leijenaar RTH, Deist TM, Peerlings J, de Jong EEC, van Timmeren J, Sanduleanu S, Larue RTHM, Even AJG, Jochems A, van Wijk Y, Woodruff H, van Soest J, Lustberg T, Roelofs E, van Elmpt W, Dekker A, Mottaghy FM, Wildberger JE, Walsh S. Radiomics: the bridge between medical imaging and personalized medicine. *Nat Rev Clin Oncol* 2017; **14**: 749-762 [PMID: 28975929 DOI: 10.1038/nrclinonc.2017.141]

38 **Lewis S**, Hectors S, Taouli B. Radiomics of hepatocellular carcinoma. *Abdom Radiol (NY)* 2021; **46**: 111-123 [PMID: 31925492 DOI: 10.1007/s00261-019-02378-5]

39 **Xu XF**, Yu JJ, Xing H, Shen F, Yang T. How to better predict microvascular invasion and recurrence of hepatocellular carcinoma. *J Hepatol* 2017; **67**: 1119-1120 [PMID: 28736140 DOI: 10.1016/j.jhep.2017.06.034]

40 **Leoni S**, Piscaglia F, Granito A, Borghi A, Galassi M, Marinelli S, Terzi E, Bolondi L. Characterization of primary and recurrent nodules in liver cirrhosis using contrast-enhanced ultrasound: which vascular criteria should be adopted? *Ultraschall Med* 2013; **34**: 280-287 [PMID: 23616066 DOI: 10.1055/s-0033-1335024]

41 **Yang C**, Liu X, Ling W, Song B, Liu F. Primary isolated hepatic tuberculosis mimicking small hepatocellular carcinoma: A case report. *Medicine (Baltimore)* 2020; **99**: e22580 [PMID: 33031307 DOI: 10.1097/MD.0000000000022580]

42 **Lee SM**, Lee JM, Ahn SJ, Kang HJ, Yang HK, Yoon JH. LI-RADS Version 2017 *vs* Version 2018: Diagnosis of Hepatocellular Carcinoma on Gadoxetate Disodium-enhanced MRI. *Radiology* 2019; **292**: 655-663 [PMID: 31310175 DOI: 10.1148/radiol.2019182867]

43 **Lv K**, Cao X, Dong Y, Geng D, Zhang J. CT/MRI LI-RADS version 2018 *vs* CEUS LI-RADS version 2017 in the diagnosis of primary hepatic nodules in patients with high-risk hepatocellular carcinoma. *Ann Transl Med* 2021; **9**: 1076 [PMID: 34422988 DOI: 10.21037/atm-21-1035]

44 **Zhang T**, Huang ZX, Wei Y, Jiang HY, Chen J, Liu XJ, Cao LK, Duan T, He XP, Xia CC, Song B. Hepatocellular carcinoma: Can LI-RADS v2017 with gadoxetic-acid enhancement magnetic resonance and diffusion-weighted imaging improve diagnostic accuracy? *World J Gastroenterol* 2019; **25**: 622-631 [PMID: 30774276 DOI: 10.3748/wjg.v25.i5.622]

45 **Zhou H**, Sun J, Jiang T, Wu J, Li Q, Zhang C, Zhang Y, Cao J, Sun Y, Jiang Y, Liu Y, Zhou X, Huang P. A Nomogram Based on Combining Clinical Features and Contrast Enhanced Ultrasound LI-RADS Improves Prediction of Microvascular Invasion in Hepatocellular Carcinoma. *Front Oncol* 2021; **11**: 699290 [PMID: 34307168 DOI: 10.3389/fonc.2021.699290]

46 **Parekh VS**, Jacobs MA. Deep learning and radiomics in precision medicine. *Expert Rev Precis Med Drug Dev* 2019; **4**: 59-72 [PMID: 31080889 DOI: 10.1080/23808993.2019.1585805]

47 **Tomaszewski MR**, Gillies RJ. The Biological Meaning of Radiomic Features. *Radiology* 2021; **298**: 505-516 [PMID: 33399513 DOI: 10.1148/radiol.2021202553]

World Journal of Gastroenterology

Submit a Manuscript: https://www.f6publishing.com

World J Gastroenterol 2022 May 28; 28(20): 2184-2200

DOI: 10.3748/wjg.v28.i20.2184

ISSN 1007-9327 (print) ISSN 2219-2840 (online)

ORIGINAL ARTICLE

Basic Study

Long noncoding RNA TNFRSF10A-AS1 promotes colorectal cancer through upregulation of HuR

Dan-Dan Wang, Dong-Lei Sun, Shao-Peng Yang, Jia Song, Meng-Yao Wu, Wei-Wei Niu, Mei Song, Xiao-Lan Zhang

Specialty type: Gastroenterology and hepatology

Provenance and peer review: Unsolicited article; Externally peer reviewed.

Peer-review model: Single blind

Peer-review report's scientific quality classification

Grade A (Excellent): 0
Grade B (Very good): B, B
Grade C (Good): 0
Grade D (Fair): 0
Grade E (Poor): 0

P-Reviewer: Kołat D, Poland; Yoshimatsu K, Japan

Received: October 26, 2021
Peer-review started: October 26, 2021
First decision: December 27, 2021
Revised: January 10, 2022
Accepted: April 20, 2022
Article in press: April 20, 2022
Published online: May 28, 2022

Dan-Dan Wang, Dong-Lei Sun, Shao-Peng Yang, Jia Song, Meng-Yao Wu, Wei-Wei Niu, Mei Song, Xiao-Lan Zhang, Department of Gastroenterology, The Second Hospital of Hebei Medical University, Shijiazhuang 050000, Hebei Province, China

Corresponding author: Xiao-Lan Zhang, MD, PhD, Chief Physician, Department of Gastroenterology, The Second Hospital of Hebei Medical University, No. 215 Heping West Road, Shijiazhuang 050000, Hebei Province, China. xiaolanzh@126.com

Abstract

BACKGROUND

Recent studies have emphasized the emerging importance of long noncoding RNAs (lncRNAs) in colorectal cancer (CRC). However, the functions and regulatory mechanisms of numerous lncRNAs in CRC have not been fully elucidated.

AIM

To explore the functional role and underlying molecular mechanisms of lncRNA TNFRSF10A-AS1 in CRC.

METHODS

TNFRSF10A-AS1 expression was measured by quantitative real-time polymerase chain reaction in CRC, and the relationship between TNFRSF10A-AS1 levels and the clinicopathological features of CRC patients was analyzed. The effect of TNFRSF10A-AS1 expression on CRC proliferation and metastasis was examined *in vitro* and *in vivo*. Mechanistically, we investigated how TNFRSF10A-AS1 is involved in CRC as a competitive endogenous RNA.

RESULTS

TNFRSF10A-AS1 was expressed at a high level in CRC and the upregulation of TNFRSF10A-AS1 was associated with advanced T grade and tumor size in CRC patients. A functional investigation revealed that TNFRSF10A-AS1 enhanced the proliferation, migration ability and invasion ability of colon cancer cells *in vitro* and *in vivo*. A mechanistic analysis demonstrated that TNFRSF10A-AS1 acted as a miR-3121-3p molecular sponge to regulate HuR expression, ultimately promoting colorectal tumorigenesis and progression.

CONCLUSION

TNFRSF10A-AS1 exerts a tumor-promoting function through the miR-3121-3p/HuR axis in CRC, indicating that it may be a novel target for CRC therapy.

Key Words: Colorectal cancer; Long noncoding RNA; TNFRSF10A-AS1; miR-3121-3p; HuR

Core Tip: TNFRSF10A-AS1 was upregulated in colorectal cancer (CRC) tumor tissues and cell lines, and it was positively correlated with tumor grade and size in patients with CRC. In addition, TNFRSF10A-AS1 facilitated CRC growth and metastasis. Mechanistically, TNFRSF10A-AS1 was predominantly found in the cytoplasm of CRC cell lines and upregulated the level of the downstream target, HuR, by sponging miR-3121-3p, thereby further promoting colorectal tumorigenesis and progression.

Citation: Wang DD, Sun DL, Yang SP, Song J, Wu MY, Niu WW, Song M, Zhang XL. Long noncoding RNA TNFRSF10A-AS1 promotes colorectal cancer through upregulation of HuR. *World J Gastroenterol* 2022; 28(20): 2184-2200
URL: https://www.wjgnet.com/1007-9327/full/v28/i20/2184.htm
DOI: https://dx.doi.org/10.3748/wjg.v28.i20.2184

INTRODUCTION

Colorectal cancer (CRC) is one of the most commonly diagnosed cancers and the third leading cause of cancer-related deaths around the world[1]. Despite marked advances in CRC diagnosis and therapy in recent years, the prognosis remains poor for many patients due to a lack of timely diagnosis and individualized disease management measures. The 5-year survival rate for CRC patients with distant metastases is approximately 14%[2]. Notably, CRC incidence and mortality rates are rising rapidly in developing countries[3]. In addition, epidemiological studies have shown an increasing incidence in adolescents and adults less than 50 years of age[4]. Genetic factors and poor lifestyle habits are the main predisposing factors for CRC, but the exact pathogenesis is unknown. Therefore, in-depth studies of the pathogenesis of CRC are of great clinical importance.

Recent evidence from studies of CRC-related pathogenesis has suggested that tumor-specific long noncoding RNAs (lncRNAs) may contribute to early diagnosis and prognostic assessment as well as improve disease treatment outcomes. LncRNAs are long (over 200 nucleotides) RNAs[5] that can interact with DNA, RNA and proteins. The function of lncRNAs mainly depends on their subcellular localization. Nuclear lncRNAs tend to bind DNA and proteins to regulate chromatin interactions, transcription and RNA processing, while cytoplasmic lncRNAs modulate mRNA stability or translation to influence cellular signaling cascades and can also act as competing endogenous RNAs (ceRNAs). CeRNAs competitively bind microRNA response elements (MREs) to regulate downstream gene expression[6,7]. In cells, ceRNAs containing the same MREs can competitively bind to the same microRNA (miRNA) and play posttranscriptional regulatory roles. Recent studies have shown that lncRNA/miRNA/mRNA mechanisms are involved in several aspects of CRC, including tumorigenesis, epithelial-mesenchymal transition (EMT), inflammatory processes and chemo-/radio-resistance[8]. For example, lncRNA SNHG6 serves as a ceRNA of miR-26a/b and miR-214, thereby regulating their common target, EZH2, to promote CRC growth and metastasis[9]. However, the functions and mechanisms of a vast majority of CRC-associated lncRNAs remain unclear.

LncRNA TNFRSF10A-AS1 is a novel lncRNA that has been demonstrated to be associated with the mechanism of autophagy in CRC, and Kaplan-Meier survival analysis has indicated that patients with high expression of TNFRSF10A-AS1 have a better prognosis. However, TNFRSF10A-AS1 expression in CRC cell lines is relatively high, which is inconsistent with the above findings[10]. Another study has identified five lncRNAs, including TNFRSF10A-AS1, by the expression of genome-wide lncRNAs in high-throughput RNA sequencing data, which may be useful to predict gastric cancer prognosis[11]. The current evidence on TNFRSF10A-AS1 is all based on The Cancer Genome Atlas (TCGA) data analysis, and the role of TNFRSF10A-AS1 in tumors is inconsistent. Moreover, the exact mechanism of TNFRSF10A-AS1 is unclear. Therefore, clinical and biological studies are needed to validate these findings. Our work is aimed to study the expression, functional roles and exact mechanisms of TNFRSF10A-AS1 in CRC. In the present study, our findings suggested that TNFRSF10A-AS1 was a novel oncogenic lncRNA that promoted CRC progression and might provide new ideas for CRC therapy.

MATERIALS AND METHODS

Database search

The expression of lncRNA TNFRSF10A-AS1 in colon adenocarcinoma (COAD) and rectum adenocarcinoma (READ) was analyzed using Gene Expression Profiling Interactive Analysis (GEPIA). GEPIA is an online analysis tool that is available to provide fast and customizable analysis based on TCGA data. We compared the expression of TNFRSF10A-AS1 between CRC tumor and nontumor tissues by box plots, which used $\log_2$(TPM + 1) for log-scale ($P < 0.05$ compared to control).

Patient tissue samples

We collected 40 pairs of surgically resected CRC tumor tissues and matched adjacent non-tumor tissue samples. These samples were obtained from patients with pathologically diagnosed CRC at the Second Hospital of Hebei Medical University. Patients were required to be free of radiotherapy, chemotherapy and other antitumor treatments prior to surgery, as well as free of any other malignant disease other than CRC. After isolation, some specimens were immediately placed in liquid nitrogen and stored at -80 °C for RNA and protein analysis, and other specimens were fixed in 4% paraformaldehyde for histological examination. All patients who met the above criteria signed informed consent forms. The study was approved by the Ethics Committee of the Second Hospital of Hebei Medical University (2021-R241).

Cell lines

Six human colon cancer cell lines (Caco-2, DLD1, HCT116, HCT15, HT29 and SW480) and one normal colonic epithelial cell line (FHC) were obtained from American Type Culture Collection (ATCC; Manassas, VA, United States). All cell lines were routinely cultured in Dulbecco's modified Eagle's medium (DMEM; Gibco BRL, Grand Island, NY, United States), containing 10% fetal bovine serum (FBS; Gibco BRL).

We conducted cell transfection using Lipofectamine 2000 (Invitrogen, Carlsbad, CA, United States), including small interfering RNA (siRNA), miRNA mimics, miRNA inhibitor and negative control oligonucleotides (Shanghai GenePharma Co., Ltd., Shanghai, China). The stable TNFRSF10A-AS1 overexpression lentiviral vector, TNFRSF10A-AS1 knockdown vector and empty vector were designed and synthesized by GenePharma. And finally, cell lines were screened according to the resistance carried by the lentivirus.

RNA extraction and quantitative real-time polymerase chain reaction

Total RNA was isolated from CRC tissue and cell samples, and then reverse transcribed into complementary DNA (cDNA), and finally quantitative real-time polymerase chain reaction (qRT-PCR) was conducted with cDNA and specific primers. Gene expression was calculated using GAPDH or U6 as internal reference genes. Table 1 lists all the qRT-PCR primer sequences involved in the study.

Cell counting kit-8 proliferation assay

Seeded colon cancer cells into 96-well cell culture plates at 1000 cells/100 μL per well according to the experimental grouping. At 24, 48, 72, 96 and 120 h, 10 μL of Cell Counting Kit-8 (CCK-8) reagent (Shanghai Share-bio Biotechnology Co., Shanghai, China) was added directly to each well. After incubation for 2 h at 37 °C, the optical density (OD) value (450 nm) was estimated.

Colony formation assay

Colon cancer cells were plated in 6-well cell culture plates at 1000 cells per well according to the experimental grouping and routinely cultured in a cell incubator. Cell culture was terminated once colonies were visible. Cells were then washed, fixed, stained, photographed and counted.

Cell cycle and apoptosis assays

Cell cycle analysis was performed using a Cell Cycle and Apoptosis Analysis Kit (Beyotime Biotechnology Co., Shanghai, China) following the manufacturer's protocol. Cells were fixed with ethanol, washed and stained with PI staining solution. Cell apoptosis was assayed using an Annexin V-FITC Apoptosis Detection Kit (Beyotime Biotechnology Co.), in which early and late apoptotic/dead cells were labeled using Annexin-V and PI, respectively.

Transwell assay

The upper chamber of Transwells (Corning, Kennebunk, ME, United States) was seeded with cells in 200 μL of culture medium without serum. The bottom chamber of Transwells was filled with medium supplemented with 10% FBS. The invasion and migration characteristics assay were distinguished by the presence or absence of Matrigel in the upper chamber. Cells in the bottom chambers of Transwells were fixed, stained and photographed following twenty-four hours of routine culture.

Table 1 Primers for real-time polymerase chain reaction

Primer name	Forward (5'-3')	Reverse (5'-3')
TNFRSF10A-AS1	TCTCAGATCACGTGACCTTGA	GTGGGCAGCTCTCATCCTAA
U2 snRNA	CATCGCTTCTCGGCCTTTTG	TGGAGGTACTGCAATACCAGG
S14	GGCAGACCGAGATGAATCCTC	CAGGTCCAGGGGTCTTGGTCC
GAPDH	CAGGGGGGAGCCAAAAGGGTCA	TGGGTGGCAGTGATGGCATGGA
HuR	CCAAAUCUUUGCAUAGGUATT	UACCUAUGCAAAGAUUUGGTTA
miR-3121-3p	TAAATAGAGTAGGCAAAGGACA	
miR-663a	AGGCGGGGCGCCGCGGGACCGC	
miR-4529-3p	ATTGGACTGCTGATGGCCCGT	
miR-505-3p	CGTCAACACTTGCTGGTTTCCT	
miR-5002-5p	AATTTGGTTTCTGAGGCACTTAGT	
miR-934	TGTCTACTACTGGAGACACTGG	
miR-1263	ATGGTACCCTGGCATTACTGAGT	
miR-5009-5p	TTGGACTTTTTCAGATTTGGGGAT	
miR-2115-5p	AGCTTCCATGACTCCTGATGGA	
miR-377-3p	ATCACACAAAGGCAACTTTTGT	
miR-3144-3p	ATATACCTGTTCGGTCTCTTTA	
miR-548av-5p	AAAAGTACTTGCGGATTT	
miR-4426	GAAGATGGACGTACTTT	
miR-224-5p	CAAGTCACTAGTGGTTCCGTT	
miR-548k	AAAAGTACTTGCGGATTTTGCT	
U6	TCGTCCCGTAGACAAAATGG	

Western blot assay

Total protein from tissue and cell samples was extracted and the protein concentrations were tested. Different concentrations of polyacrylamide gels were prepared according to the molecular weight of the protein to be detected. Proteins were then electrophoresed and transferred to polyvinylidene fluoride (PVDF) membranes. Finally, the membranes were first incubated with primary antibodies against cyclin D1, proliferating cell nuclear antigen (PCNA), cleaved caspase-3, cleaved PARP, HuR as well as GAPDH (Cell Signaling Technology, Danvers, MA, United States) at 4 °C overnight and then the proteins were incubated with secondary antibodies (Cell Signaling Technology) for 1 h.

Immunohistochemistry

Tissue samples were fixed in paraformaldehyde, dehydrated in alcohol, embedded in paraffin as well as sectioned. In addition, immunohistochemical staining of tissue sections was carried out according to the experimental steps. Finally, staining of the sections was observed under a microscope.

Luciferase reporter assay

TNFRSF10A-AS1 containing wild-type (WT) or mutant (MUT) miR-3121-3p-binding sequences was designed, synthesized and sub-cloned into the pmiRGLO vector (Shanghai GenePharma Co., Ltd.). DLD1 cells were cotransfected with reporter plasmid, miR-3121-3p mimics or mimics NC. After cotransfection under routine culture conditions for 48 h, the Dual-Luciferase Reporter Assay System (Promega, Madison, WI, United States) was used to evaluate the luciferase activity of all the above reporter vectors.

Subcutaneous xenograft models

We performed animal experiments for *in vivo* validation. BALB/c nude mice at four- to six-week-old were subcutaneously injected with DLD1 cells stably transfected with sh-TNFRSF10A-AS1 (sh-lnc) or sh-negative control vector (sh-NC) (1×10^7, 200 μL) and HCT116 cells stably overexpressing TNFRSF10A-AS1 (oe-lnc) or empty vector (control) (1×10^7, 200 μL) into the right and left dorsal flanks of the nude mice, respectively. After implantation, the tumor volume was observed and measured every 2 d. The tumor volume was calculated using the measured length and width of the tumor according to

Table 2 Associations between TNFRSF10A-AS1 levels and clinicopathological features in colorectal cancer patients

Characteristics	Case	TNFRSF10A-AS1 expression		*P* value
		Low	High	
Age (yr)				0.751
< 60	18	10	8	
≥ 60	22	10	12	
Gender				0.751
Male	22	12	10	
Female	18	8	10	
Tumor location				1.000
Colon	19	9	10	
Rectum	21	11	10	
Tumor size (cm)				0.001[a]
≥ 5	21	5	16	
< 5	19	15	4	
T grade				0.014[a]
T1 + T2	12	10	2	
T3 + T4	28	10	18	
TNM stage				1.000
I-II	30	15	15	
III-IV	10	5	5	
Histological grade				0.661
Low	6	2	4	
Middle-High	34	18	16	

[a]$P < 0.05$.

the formula: Tumor volume = (length × width^2)/2. At the end of the animal study, subcutaneous tumors were removed and used to assess tumor volume and weight as well as to perform qRT-PCR, Western blot and histological analyses.

Statistical analysis

Statistical analyses were performed using GraphPad Prism 9 software or SPSS 22.0 software. Data were presented as the mean ± SD. TNFRSF10A-AS1 and miR-3121-3p expression levels in CRC patients were compared using the paired-sample *t* test. Statistical significance between groups was analyzed using the χ^2 test, Fisher's exact probability, Student's *t* test or one-way Analysis of Variance (ANOVA). $P < 0.05$ was considered statistically significant.

RESULTS

TNFRSF10A-AS1 is upregulated in CRC

To identify whether lncRNA TNFRSF10A-AS1 is differentially expressed in CRC, we first analyzed TNFRSF10A-AS1 expression in TCGA database. We used the GEPIA online database to analyze TNFRSF10A-AS1 expression of CRC tissues, and results showed that TNFRSF10A-AS1 was expressed higher in both colon and rectal carcinoma tissues than that of corresponding adjacent normal tissues (Figure 1A). We then examined TNFRSF10A-AS1 expression in 40 pairs of CRC tissue samples. TNFRSF10A-AS1 expression was significantly increased in 34 of 40 (75%) tumor samples compared to the adjacent normal mucosa tissues (Figure 1B). Next, TNFRSF10A-AS1 expression was verified in multiple colon cancer cell lines, namely, DLD1, HCT15, HT29, HCT116, SW480 and Caco-2, and human colon mucosal epithelial FHC cells. TNFRSF10A-AS1 was significantly upregulated in the colon cancer

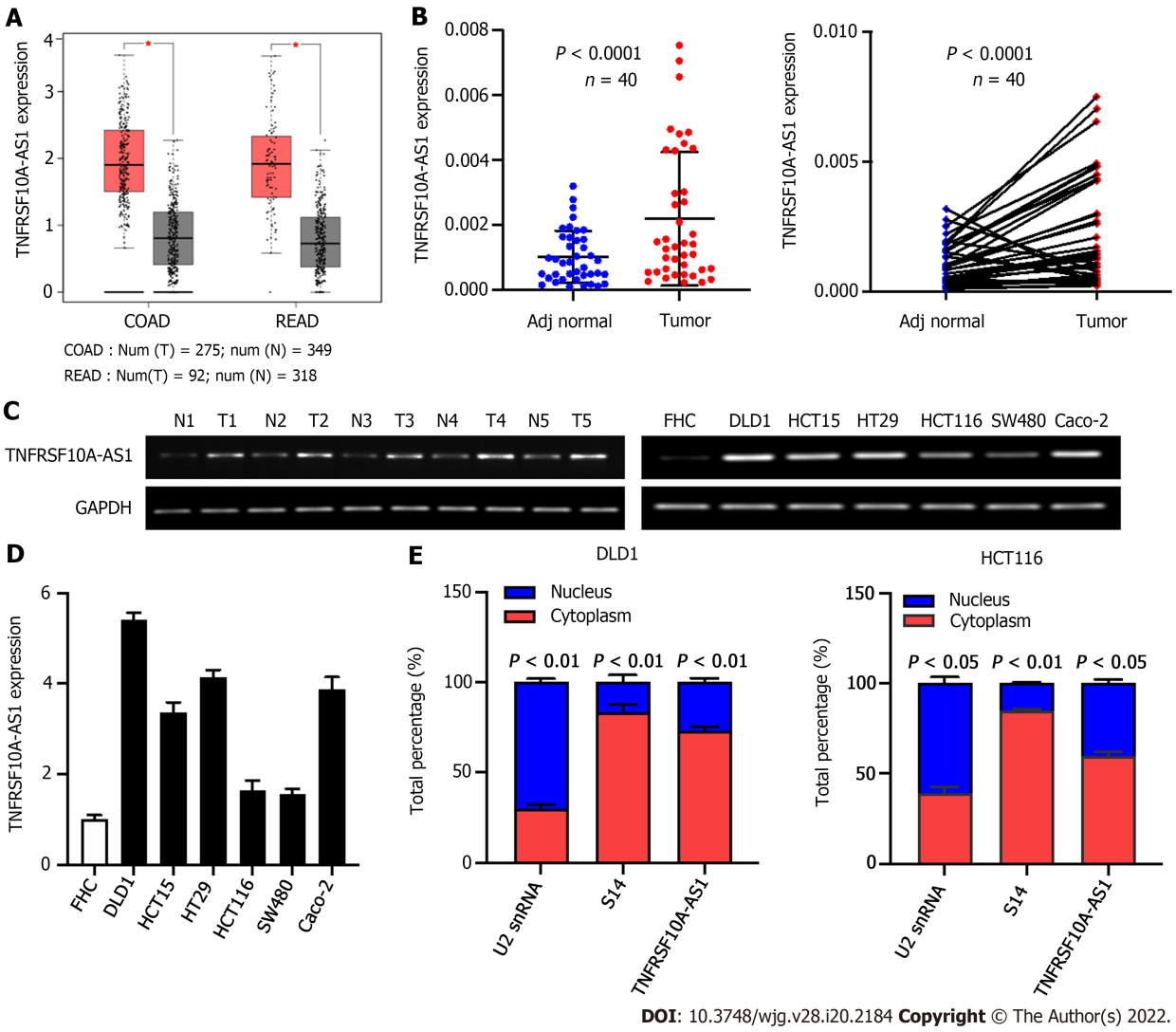

DOI: 10.3748/wjg.v28.i20.2184

Figure 1 TNFRSF10A-AS1 is upregulated in colorectal cancer. A: TNFRSF10A-AS1 was upregulated in tumor tissues compared to normal tissues in TCGA colorectal cancer (CRC) database; B: TNFRSF10A-AS1 was overexpressed in CRC tumor tissues compared to matched adjacent nontumor tissues (n = 40); C: Levels of TNFRSF10A-AS1 in CRC were measured by reverse transcription-polymerase chain reaction (RT-PCR); D: TNFRSF10A-AS1 was higher in colon cancer cell lines than in colon mucosal epithelial FHC cells; E: The expression levels of TNFRSF10A-AS1 in the cytoplasm and nucleus of DLD1 and HCT116 cells were detected by quantitative real-time polymerase chain reaction (qRT-PCR). U2 snRNA was used as the internal reference for genes expressed in the nucleus, and S14 was used as the internal reference for genes expressed in the cytoplasm. COAD: Colon adenocarcinoma; READ: Rectum adenocarcinoma.

cell lines compared to FHC cells (Figure 1D). RT-PCR also confirmed that TNFRSF10A-AS1 was upregulated in CRC tissues and cells (Figure 1C). We further explored the cellular localization of TNFRSF10A-AS1 in DLD1 and HCT116 cells. qRT-PCR results showed that TNFRSF10A-AS1 was predominantly found in the cytoplasm (Figure 1E), which indicated that TNFRSF10A-AS1 might function in the cytoplasm. In addition, we analyzed associations between TNFRSF10A-AS1 and clinicopathological features of CRC patients and found that the upregulation of TNFRSF10A-AS1 was associated with advanced T grade and tumor size (Table 2). Collectively, the above findings indicated that TNFRSF10A-AS1 was increased in CRC and might be involved in colorectal carcinogenesis as an oncogene.

TNFRSF10A-AS1 promotes colon cancer cell proliferation, migration and invasion as well as inhibits cell apoptosis

To explore the biological function of TNFRSF10A-AS1 in colon cancer cells, we first designed a siRNA against TNFRSF10A-AS1, a short hairpin RNA (shRNA) against TNFRSF10A-AS1 and a lentiviral overexpression vector for TNFRSF10A-AS1. Silencing TNFRSF10A-AS1 in DLD1 and HT29 cells significantly inhibited cell viability and clonogenicity, whereas ectopic expression of TNFRSF10A-AS1 in HCT116 and SW480 cells significantly promoted cell viability and clonogenicity (Figure 2A and B). We also conducted flow cytometry to clarify the role of TNFRSF10A-AS1 in cell cycle distribution. Knockdown of TNFRSF10A-AS1 led to a significant increase in G1 phase cells and a decrease in S-phase cells in both DLD1 and HT29 cells. In contrast, the opposite results were exhibited in both HCT116 and

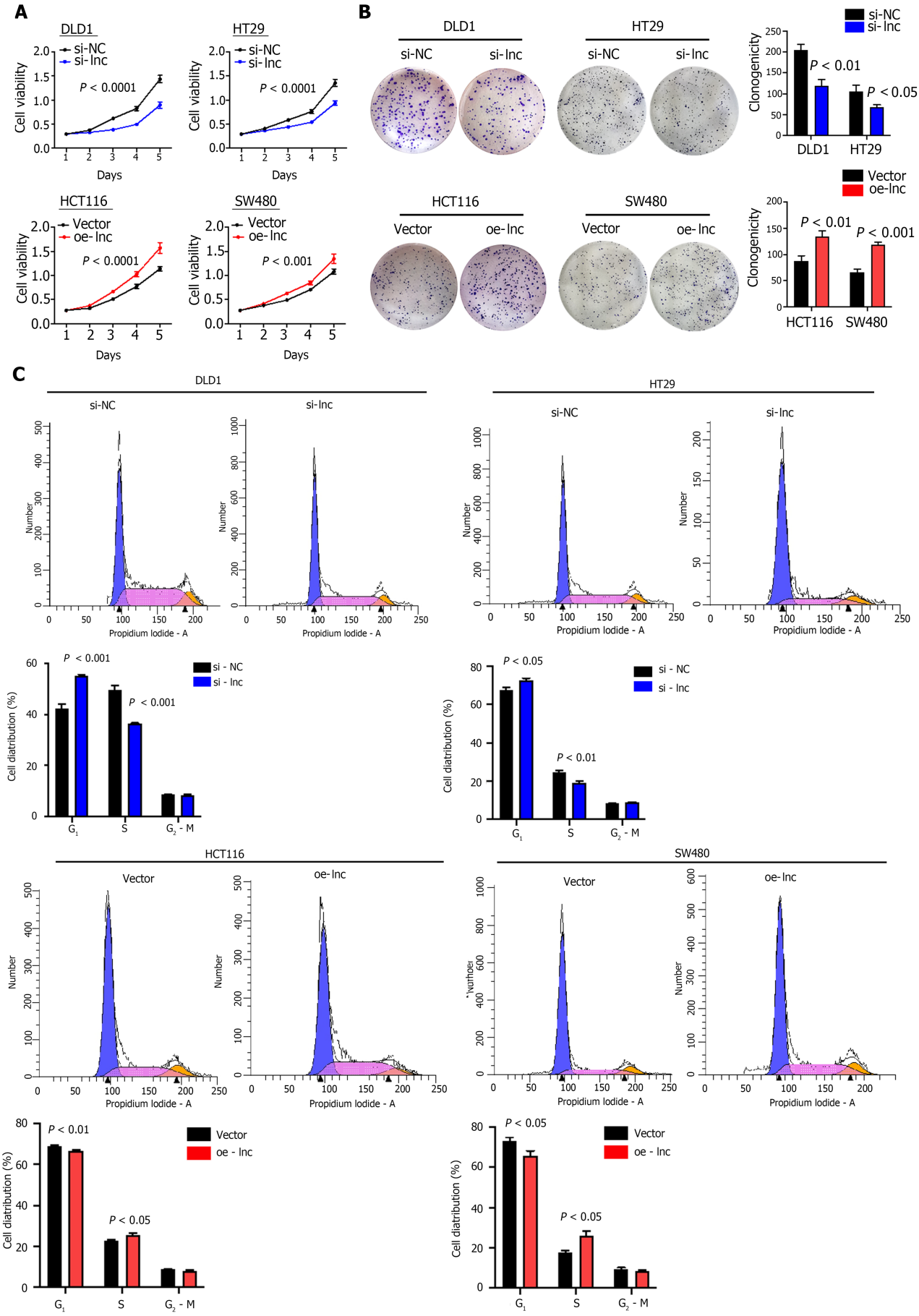
A
DLD1
HT29
HCT116
SW480
si-NC
si-lnc
Vector
oe-lnc
Cell viability
Days
P < 0.0001
P < 0.001
B
DLD1
HT29
HCT116
SW480
si-NC
si-lnc
Vector
oe-lnc
Clonogenicity
P < 0.01
P < 0.05
P < 0.001
C
Number
Propidium Iodide - A
Cell diatribution (%)
si - NC
si - lnc
Vector
oe - lnc
P < 0.001
P < 0.05
P < 0.01
G1
S
G2 - M

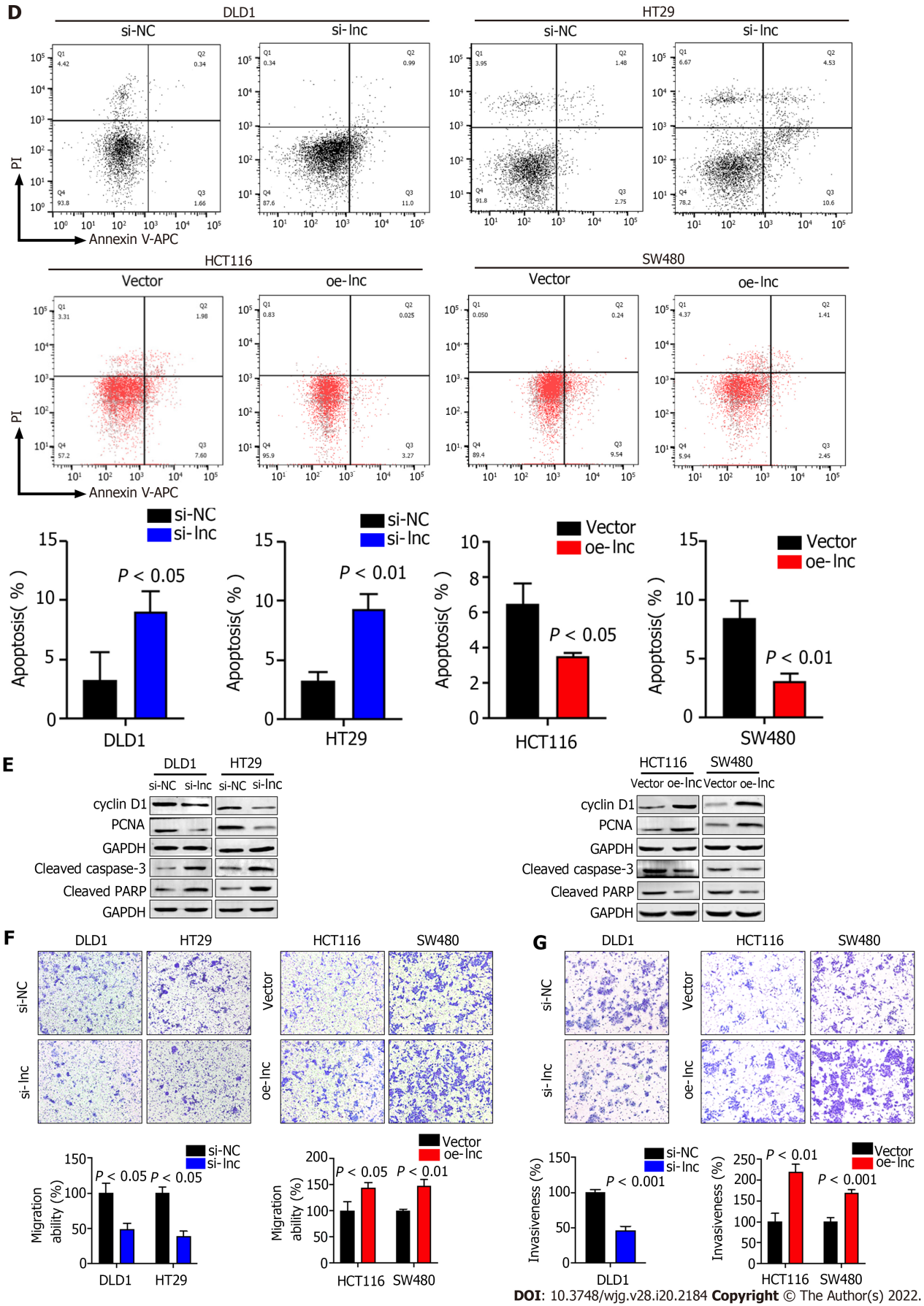

DOI: 10.3748/wjg.v28.i20.2184

Figure 2 TNFRSF10A-AS1 promotes colon cancer cell proliferation, migration and invasion as well as inhibits cell apoptosis *in vitro*. A and B: Downregulation of TNFRSF10A-AS1 decreased cell viability and clonogenicity in DLD1 and HT29 cells, whereas upregulation of TNFRSF10A-AS1 greatly

increased cell viability and clonogenicity in HCT116 and SW480 cells; C: Silencing TNFRSF10A-AS1 arrested cells at the G1/S transition, whereas overexpressing TNFRSF10A-AS1 facilitated this transition; D: Downregulation of TNFRSF10A-AS1 enhanced cell apoptosis, whereas upregulation of TNFRSF10A-AS1 inhibited cell apoptosis; E: Western blot analysis showed that TNFRSF10A-AS1 knockdown decreased the expression of cyclin D1 and PCNA but increased the activation of caspase-3 and PARP, whereas TNFRSF10A-AS1 overexpression had the opposite effect; F and G: Silencing TNFRSF10A-AS1 suppressed DLD1 and HT29 cell migration and invasion abilities, whereas these abilities were significantly enhanced by overexpressing TNFRSF10A-AS1 in HCT116 and SW480 cells.

SW480 cells with overexpression of TNFRSF10A-AS1 (Figure 2C). Moreover, Western blot analysis revealed that downregulation of TNFRSF10A-AS1 decreased cyclin D1 and PCNA expression, while the upregulation of TNFRSF10A-AS1 increased cyclin D1 and PCNA expression (Figure 2E). In general, genes that promote proliferation can suppress cell apoptosis. Therefore, we conducted Annexin V-APC/PI staining and Western blot analysis to test the impact of TNFRSF10A-AS1 on the apoptosis of colon cancer cells. The results showed that downregulation of TNFRSF10A-AS1 increased the apoptosis rate and the expression of the cleaved forms of caspase-3 and PARP, which are markers of cell apoptosis, whereas upregulation of TNFRSF10A-AS1 led to the opposite effects (Figure 2D and E).

In addition to malignant proliferation, tumor cells also exhibit migration and invasion abilities. Therefore, we performed Transwell assays with or without Matrigel to explore the impact of TNFRSF10A-AS1 on the migration and invasion properties of colon cancer cells. Downregulation of TNFRSF10A-AS1 markedly suppressed the migration and invasion abilities of DLD1 and HT29 cells, whereas overexpressing TNFRSF10A-AS1 significantly enhanced the abilities of HCT116 and SW480 cells (Figure 2F and G). Therefore, these findings demonstrated that TNFRSF10A-AS1 exerted a cancer-promoting role in CRC, prompting further investigations of its potential regulatory mechanisms.

miR-3121-3p is downregulated in CRC

The above findings suggested that TNFRSF10A-AS1 might play a tumor-promoting role in the cytoplasm. Thus, we explored the potential molecular mechanism of TNFRSF10A-AS1 based on the ceRNA mechanism. We first predicted potential target miRNAs of TNFRSF10A-AS1 by using miRNA target prediction tools, including miRDB, DIANA and LncRNAMAP. The prediction results of the three databases yielded 15 candidate miRNAs (Figure 3A). Among them, miR-3121-3p expression was upregulated in TNFRSF10A-AS1-deficient cells and downregulated in TNFRSF10A-AS1-overexpressing cells, consistent with the ceRNA mechanism theory (Figure 3B). Subsequently, we performed qRT-PCR to evaluate miR-3121-3p expression in CRC tissues, which indicated significant downregulation of miR-3121-3p in colorectal tumor tissues compared to matched nontumor tissues (Figure 3C). We further confirmed the interaction between TNFRSF10A-AS1 and miR-3121-3p using a dual-luciferase reporter assay (Figure 3E). Luciferase activity was reduced in cells cotransfected with TNFRSF10A-AS1-WT and the miR-3121-3p mimics, whereas there was no difference between cells cotransfected with TNFRSF10A-AS1-MUT and the miR-3121-3p mimics and cells cotransfected with TNFRSF10A-AS1-MUT and mimics NC (Figure 3F). Finally, we analyzed the correlation between miR-3121-3p levels and the clinicopathological features of CRC patients and discovered that downregulation of miR-3121-3p was associated with large tumor size (Table 3). These results suggested that miR-3121-3p might be a tumor suppressor and exert an inhibitory effect on CRC.

miR-3121-3p inhibits the proliferation, migration and invasion of colon cancer cells by silencing HuR

Because there are few studies related to miR-3121-3p and no relevant studies in CRC, we set out to investigate the function and mechanism of miR-3121-3p in CRC. We first predicted the downstream proteins of miR-3121-3p using four online databases, *i.e.*, miRDB, TargetScan, miRTarBase and RNA22, and then obtained 3 candidate genes (ELAVL1, PLEKHA6 and ATL3) after taking the intersection (Figure 4A). Of the three candidate genes, ELAVL1 (HuR) has been demonstrated to be involved in CRC progression and may act as an oncogene in CRC. qRT-PCR showed that the expression of miR-3121-3p was relatively lower in DLD1 cells and higher in HCT116 cells (Figure 3D). Thus, we selected DLD1 cells and HCT116 cells for transfection with miR-3121-3p mimics and inhibitor, respectively, to further identify the effects of miR-3121-3p on the malignant phenotype of CRC. Experimental results at both the mRNA and protein levels indicated that upregulation of miR-3121-3p decreased HuR expression, whereas downregulation of miR-3121-3p increased HuR expression (Figure 4B), suggesting that HuR might be a downstream target protein of miR-3121-3p.

We next studied the impacts of miR-3121-3p on the biological function of colon cancer cells. Growth curves based on the CCK-8 assay displayed that upregulation of miR-3121-3p suppressed the proliferation and viability of DLD1 cells, whereas downregulation of miR-3121-3p enhanced the proliferation and viability of HCT116 cells (Figure 4C). The colony number of DLD1 cells transfected with the miR-3121-3p mimics was significantly lower than that of the control group, whereas the colony number of HCT116 cells transfected with the miR-3121-3p inhibitor was significantly higher than the control group (Figure 4D). In addition, Transwell assays indicated that upregulation of miR-3121-3p in DLD1 cells significantly impaired the migration and invasion abilities, whereas downregulation of miR-3121-3p in HCT116 cells significantly enhanced these abilities (Figure 4E). In summary, the above results confirmed

Table 3 Associations between miR-3121-3p levels and clinicopathological features in colorectal cancer patients

Characteristics	Case	miR-3121-3p expression		*P* value
		Low	High	
Age (yr)				0.751
< 60	18	10	8	
≥ 60	22	10	12	
Gender				0.751
Male	22	12	10	
Female	18	8	10	
Tumor location				1.000
Colon	19	10	9	
Rectum	21	10	11	
Tumor size (cm)				0.010[a]
≥ 5	21	15	6	
< 5	19	5	14	
T grade				0.082
T1 + T2	12	9	3	
T3 + T4	28	11	17	
TNM stage				0.716
I-II	30	14	16	
III-IV	10	6	4	
Histological grade				1.000
Low	6	3	3	
Middle-High	34	17	17	

[a]$P < 0.05$.

that miR-3121-3p played a suppressive effect in the malignant phenotype of CRC, including aberrant proliferation and metastasis.

TNFRSF10A-AS1 accelerates the proliferation, migration and invasion of colon cancer cells via the miR-3121-3p/HuR axis

We performed rescue experiments using miR-3121-3p mimics and inhibitor with the aim of verifying whether TNFRSF10A-AS1 exerts a tumor-promoting effect through the miR-3121-3p/HuR axis. We first examined HuR expression at the mRNA and protein levels. Silencing TNFRSF10A-AS1 decreased the mRNA and protein levels of HuR in DLD1 cells, whereas overexpressing TNFRSF10A-AS1 in HCT116 cells enhanced HuR expression. In addition, the miR-3121-3p inhibitor and mimics reversed the regulatory effects on HuR expression caused by TNFRSF10A-AS1 silencing and overexpression, respectively (Figure 5A). Furthermore, we sought to clarify whether the miR-3121-3p mimics and inhibitor reverse the impacts of TNFRSF10A-AS1 on CRC biological functions. All the experiments results, including CCK-8, colony formation as well as Transwell assays, indicated that the suppressive impacts on DLD1 cells caused by TNFRSF10A-AS1 knockdown could be balanced by miR-3121-3p inhibitor, while miR-3121-3p mimics could counteract the promoting effect of TNFRSF10A-AS1 overexpression on HCT116 cells (Figure 5B-E). The above results indicated that the miR-3121-3p/HuR regulatory axis might be one of the mechanisms by which TNFRSF10A-AS1 promoted CRC proliferation, migration and invasion.

TNFRSF10A-AS1 promotes CRC growth in vivo

Given that the above *in vitro* experimental results suggested that TNFRSF10A-AS1 had a tumor-promoting effect on colon cancer cells, we selected TNFRSF10A-AS1-deficient DLD1 cells and TNFRSF10A-AS1-overexpressing HCT116 cells for tumor xenograft experiments to verify the effect of TNFRSF10A-AS1 *in vivo*. Consistent with the results of *in vitro* experiments, we found that the downreg-

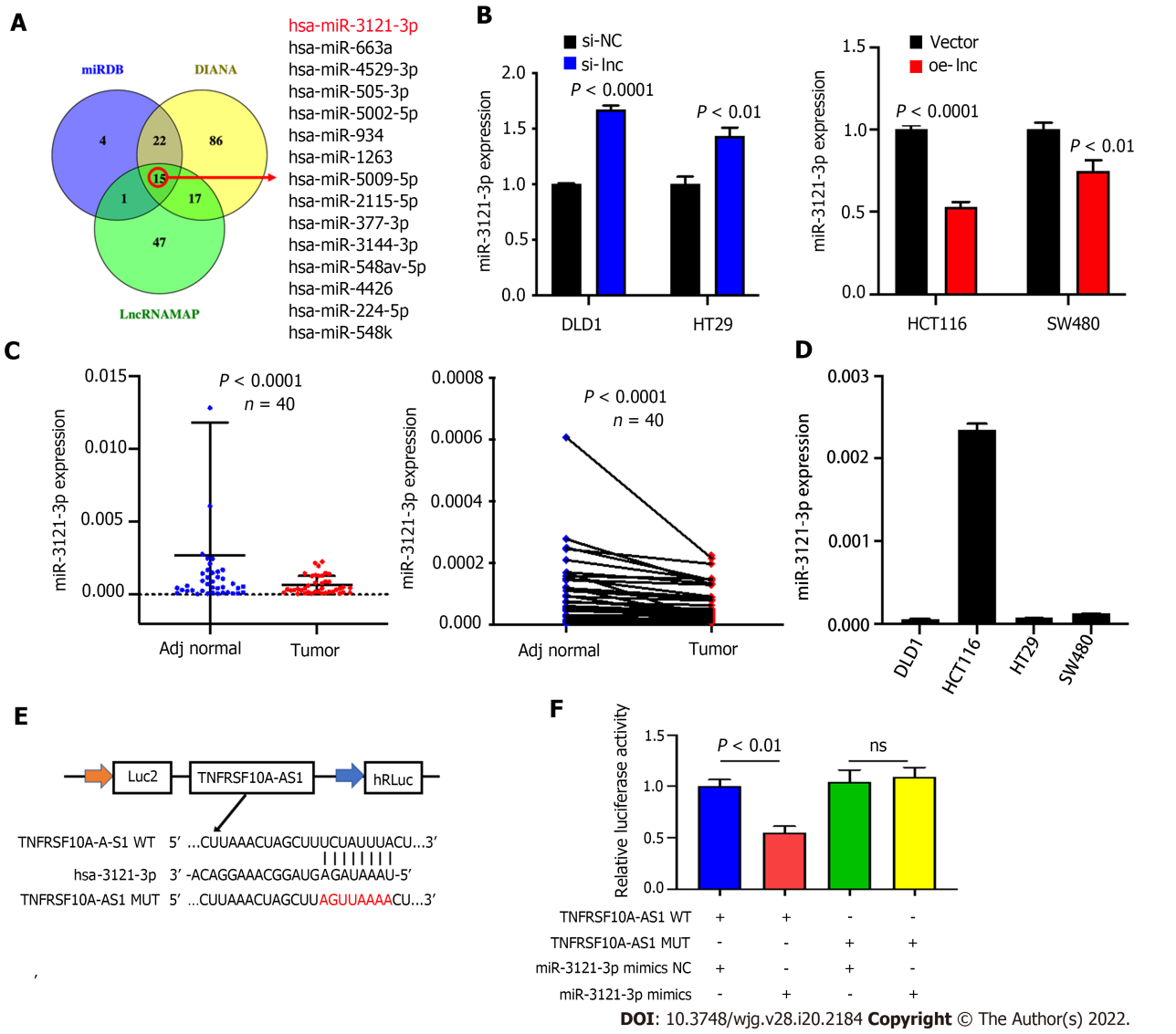

DOI: 10.3748/wjg.v28.i20.2184 **Copyright** © The Author(s) 2022.

Figure 3 miR-3121-3p is downregulated in colorectal cancer. A: We used three websites (miRDB, DIANA and LncRNAMAP) to predict 15 microRNAs with binding sites for TNFRSF10A-AS1; B: miR-3121-3p expression was increased in cells transfected with si-lnc and decreased in cells transfected with oe-lnc; C: miR-3121-3p was downregulated in colorectal cancer tumor tissues compared to matched nontumor tissues (n = 40); D: Levels of miR-3121-3p in colon cancer cell lines were detected by quantitative real-time polymerase chain reaction; E: Schematic illustration of the predicted binding sites of miR-3121-3p in the TNFRSF10A-AS1 sequence; F: Relative luciferase activities after cotransfection with TNFRSF10A-AS1-WT, TNFRSF10A-AS1-MUT, miR-3121-3p mimics or NC in DLD1 cells. WT: Wild-type; MUT: Mutant.

ulation of TNFRSF10A-AS1 significantly reduced the tumor size and weight of DLD1 xenografts (Figure 6A), whereas upregulation of TNFRSF10A-AS1 markedly promoted HCT116 xenograft growth (Figure 6B). Moreover, IHC assays demonstrated that downregulation of TNFRSF10A-AS1 reduced the expression of the Ki-67 proliferation marker in xenograft tumor tissues, whereas upregulation of TNFRSF10A-AS1 produced the opposite effect (Figure 6C). qRT-PCR, Western blot and IHC analyses all revealed that HuR expression was downregulated in TNFRSF10A-AS1-deficient xenograft tumor tissues but upregulated in TNFRSF10A-AS1-overexpressing xenograft tumor tissues (Figure 6C-E). Western blot analysis of tissue samples from CRC patients also showed that HuR was increased in tumor tissues compared to paired nontumor tissues (Figure 6F). Therefore, these *in vivo* results further supported the tumor-promoting role of TNFRSF10A-AS1 in CRC, which functioned at least in part as a molecular sponge of miR-3121-3p to upregulate HuR expression.

DISCUSSION

In this study, we first uncovered TNFRSF10A-AS1 as an oncogene that participated in colorectal carcinogenesis and progression. Although the available findings have demonstrated that TNFRSF10A-AS1 is involved in the autophagic mechanism of CRC as well as gastric cancer prognosis, the current

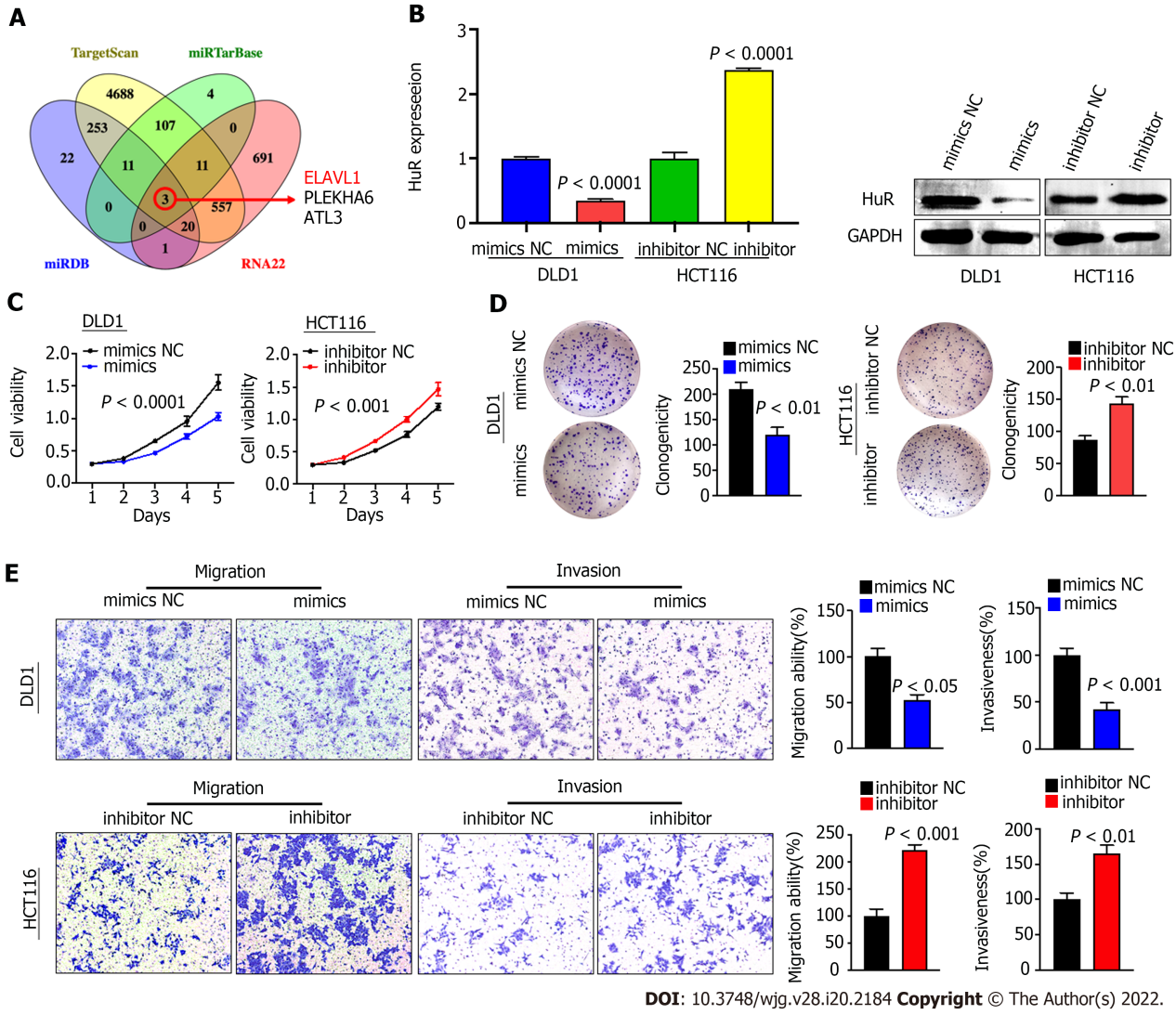

DOI: 10.3748/wjg.v28.i20.2184

Figure 4 miR-3121-3p suppresses colon cancer cell proliferation, migration and invasion *in vitro*. A: Four websites (miRDB, TargetScan, miRTarBase and RNA22) were used to predict 3 downstream target mRNAs with binding sites for miR-3121-3p; B: HuR expression was assessed in DLD1 and HCT116 cells transfected with miR-3121-3p mimics, miR-3121-3p inhibitor or NC using quantitative real-time polymerase chain reaction and Western blot assays; C and D: miR-3121-3p mimics inhibited cell viability and clonogenicity, but miR-3121-3p inhibitor enhanced cell viability and clonogenicity; E: Upregulation of miR-3121-3p inhibited cell migration and invasion capabilities, whereas downregulation of miR-3121-3p enhanced these capabilities.

evidence is all based on the analysis of TCGA data, and its functional roles and detailed mechanisms in CRC cannot be determined. Our study showed that TNFRSF10A-AS1 was upregulated in CRC and the upregulation of TNFRSF10A-AS1 was associated with advanced tumor size and T grade. In functional experiments both *in vitro* and *in vivo*, we found that TNFRSF10A-AS1 enhanced the malignant phenotype of colon cancer cells. Regarding the molecular mechanism of TNFRSF10A-AS1, we identified miR-3121-3p by bioinformatics analyses and verified the direct interaction between TNFRSF10A-AS1 and miR-3121-3p by dual-luciferase reporter assays. In contrast to TNFRSF10A-AS1, miR-3121-3p was downregulated in CRC, negatively associated with the tumor size as well as exerted inhibitory effects on the malignant phenotype of colon cancer cells, which is consistent with ceRNA mechanism theory. Mechanistically, one of the ways in which TNFRSF10A-AS1 exerted its pro-cancer effects was through sponging miR-3121-3p. By binding to miR-3121-3p, TNFRSF10A-AS1 attenuated the silencing effect of miR-3121-3p on its downstream target gene, HuR. Taken together, our findings provide evidence for an important role of TNFRSF10A-AS1 and the TNFRSF10A-AS1/miR-3121-3p/HuR axis in CRC progression, thereby providing a theoretical basis for the diagnosis and treatment of CRC.

ceRNA is an important regulatory mode of cytoplasmic lncRNA. Here, after confirming that TNFRSF10A-AS1 was more abundant in the cytoplasm of CRC cell lines, we used online tools to predict potential target miRNAs of TNFRSF10A-AS1. We further validated the expression relationship between TNFRSF10A-AS1 and candidate miRNAs, and we discovered that miR-3121-3p might be a downstream target miRNA of TNFRSF10A-AS1. And the dual-luciferase reporter assay further confirmed that TNFRSF10A-AS1 might function as the molecular sponge of miR-3121-3p. In the lncRNA-miRNA-mRNA network, miRNAs, as intermediate mediators, exert biological effects by modulating

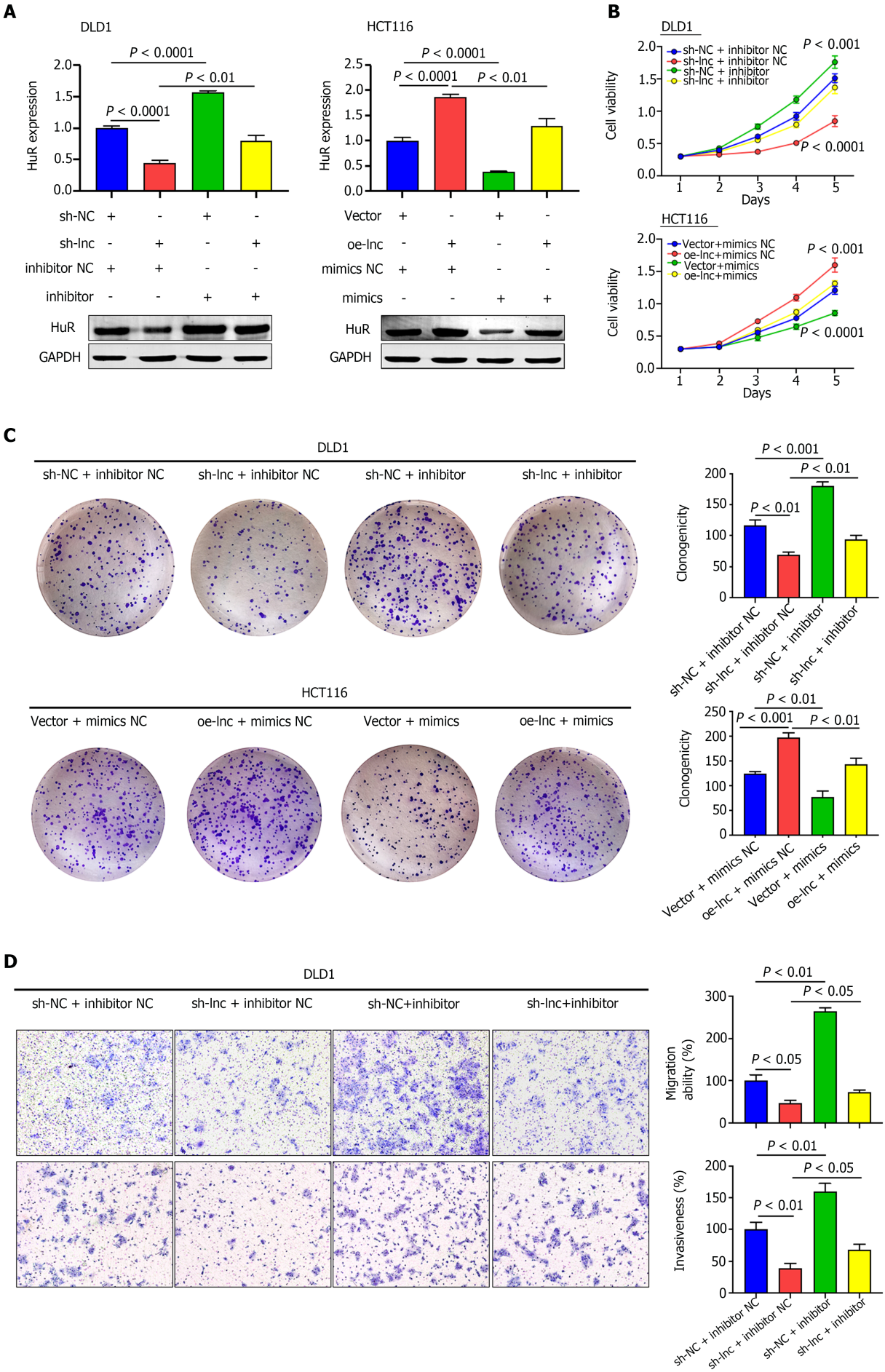
A
DLD1
HCT116
HuR expression
P < 0.0001
P < 0.01
sh-NC
sh-lnc
inhibitor NC
inhibitor
Vector
oe-lnc
mimics NC
mimics
HuR
GAPDH
B
DLD1
HCT116
Cell viability
Days
sh-NC + inhibitor NC
sh-lnc + inhibitor NC
sh-NC + inhibitor
sh-lnc + inhibitor
Vector+mimics NC
oe-lnc+mimics NC
Vector+mimics
oe-lnc+mimics
C
DLD1
HCT116
Clonogenicity
sh-NC + inhibitor NC
sh-lnc + inhibitor NC
sh-NC + inhibitor
sh-lnc + inhibitor
Vector + mimics NC
oe-lnc + mimics NC
Vector + mimics
oe-lnc + mimics
D
DLD1
sh-NC+inhibitor
sh-lnc+inhibitor
Migration ability (%)
Invasiveness (%)

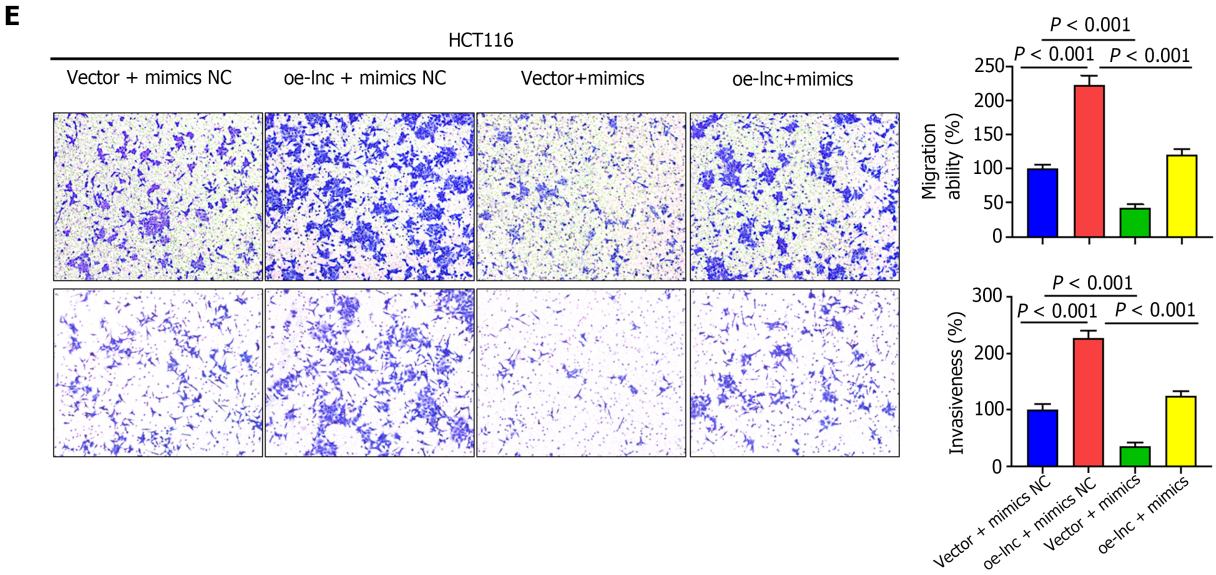

DOI: 10.3748/wjg.v28.i20.2184

Figure 5 TNFRSF10A-AS1 promotes colon cancer cell proliferation, migration and invasion *via* the miR-3121-3p/HuR axis. A: HuR was evaluated in DLD1 and HCT116 cells transfected with miR-3121-3p mimics, miR-3121-3p inhibitor, NC, sh-lnc or oe-lnc; B and C: Cell proliferation abilities were estimated using Counting Kit-8 and colony formation assays in DLD1 and HCT116 cells transfected with miR-3121-3p mimics, miR-3121-3p inhibitor, NC, sh-lnc or oe-lnc; D and E: Transwell assays were performed to analyze cell migration and invasion abilities in DLD1 and HCT116 cells transfected with miR-3121-3p mimics, miR-3121-3p inhibitor, NC, sh-lnc or oe-lnc.

downstream target proteins. After experimental evidence established that TNFRSF10A-AS1 could sponge miR-3121-3p, we explored its effector genes. Among candidate target genes predicted by target prediction software, only HuR has been shown previously to regulate CRC progression, and our results also verified that miR-3121-3p exerted a negative regulatory effect on HuR expression. Rescue experiments also confirmed that miR-3121-3p mimics and inhibitor counteracted the regulatory effects of TNFRSF10A-AS1 overexpression and knockdown, respectively, on HuR expression, cell proliferation, migration ability and invasion ability. Thus, one of the mechanisms by which TNFRSF10A-AS1 acts may be as a molecular sponge for miR-3121-3p, which upregulates HuR expression and ultimately promotes colorectal carcinogenesis and progression.

HuR, a cancer-associated RNA-binding protein (RBP), is a member of the embryonic lethal abnormal vision (ELAV) family, and it increases mRNA stability by binding to conserved AU-rich elements (AREs) within 3′ untranslated regions (UTRs), thereby preventing gene degradation[12]. HuR expression is upregulated in different tumors, including breast cancer, CRC, gastric cancer and prostate cancer, and it is correlated with advanced clinicopathological parameters, expression of tumor-associated proteins, a low survival rate and poor prognosis[13-16]. CRC-related studies show that HuR is upregulated and promotes colon cancer growth by targeting RNA in the cytoplasm[17]. In addition, increased HuR protein in the cytoplasm is correlated with T stage, and importantly, HuR overexpression increases the growth of colon cancer cells in nude mouse models[18]. A recent study has revealed that miR-22, as a tumor suppressive miRNA, directly binds to HuR and downregulates its expression to inhibit proliferation and migration abilities of CRC, as well as xenogeneic tumor growth [19]. Through our experimental research, we found that the upstream lncRNA TNFRSF10A-AS1 sponged an important tumor suppressive miRNA in CRC, miR-3121-3p, which negatively regulated HuR expression. Consistent with previous studies, HuR was highly expressed in CRC. Our study results further suggested that the expression of HuR might be positively regulated by the upstream molecular TNFRSF10A-AS1, which might be one of the mechanisms by which TNFRSF10A-AS1 exerted a pro-cancer effect in CRC.

Based on the results of comprehensive analyses, including bioinformatics analyses, cell functional experiments and clinical research tools, we have sufficient evidence that TNFRSF10A-AS1 is a novel oncogene that promotes tumor malignancy in CRC. Mechanistically, TNFRSF10A-AS1 regulates the expression of the downstream target, HuR, by sponging miR-3121-3p, which further promotes CRC progression. Targeting the TNFRSF10A-AS1/miR-3121-3p/HuR axis may have potential therapeutic implications for CRC.

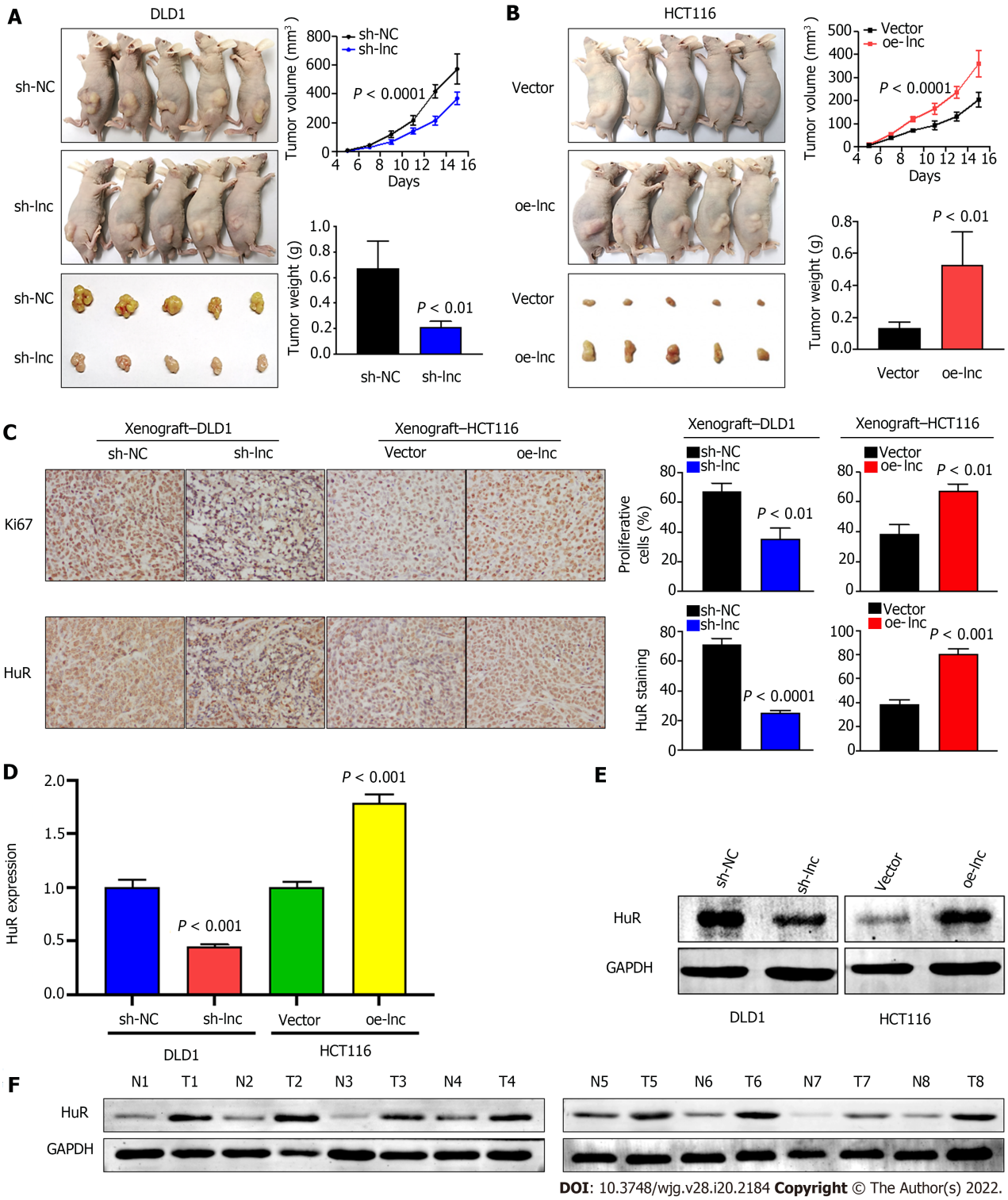

DOI: 10.3748/wjg.v28.i20.2184 **Copyright** © The Author(s) 2022.

Figure 6 TNFRSF10A-AS1 promotes the growth of colorectal cancer *in vivo*. A and B: Tumor volume and weight were significantly decreased in the TNFRSF10A-AS1 knockdown group but markedly increased in the TNFRSF10A-AS1 overexpression group; C-E: TNFRSF10A-AS1 enhanced cell proliferation (as assessed by Ki67 staining) and increased HuR expression (as assessed by HuR staining, quantitative real-time polymerase chain reaction and Western blot) in xenograft tumor tissues; F: HuR was upregulated in colorectal cancer patient tumor tissues compared to matched nontumor tissues by Western blot analysis.

CONCLUSION

TNFRSF10A-AS1 as a ceRNA promotes tumor malignancy of CRC through the miR-3121-3p/HuR axis. TNFRSF10A-AS1/miR-3121-3p/HuR axis may provide more effective targets for CRC therapy.

ARTICLE HIGHLIGHTS

Research background

The critical importance of long noncoding RNAs (lncRNAs) to the onset and exacerbation of colorectal cancer (CRC) has been validated in an increasing number of studies. However, numerous lncRNAs associated with CRC remain unidentified and the detailed mechanisms remain poorly understood. TNFRSF10A-AS1 is a new lncRNA, the function in CRC and gastric cancer is inconsistent and the exact mechanism is unclear.

Research motivation

The present study will clarify the oncogenic pathogenesis of TNFRSF10A-AS1 in CRC progression, leading to new ideas for CRC therapy.

Research objectives

To detect TNFRSF10A-AS1 expression in CRC and investigate the functions and potential mechanisms of TNFRSF10A-AS1 in CRC onset and exacerbation.

Research methods

In this study, the authors detected TNFRSF10A-AS1 expression in CRC and clarified the relationship between TNFRSF10A-AS1 levels and clinicopathological features of CRC patients. Furthermore, a series of functional experiments both *in vitro* and *in vivo* were performed to explore the role of TNFRSF10A-AS1. The mechanism of TNFRSF10A-AS1 mainly focused on its role as a miRNA molecular sponge.

Research results

TNFRSF10A-AS1 expression was increased in CRC and positively associated with advanced tumor size and T grade of CRC patients. TNFRSF10A-AS1 enhanced the malignant phenotype of colon cancer cells by promoting CRC proliferation and metastasis. Mechanistically, TNFRSF10A-AS1 was more abundant in the cytoplasm and upregulated the downstream target, HuR, by sponging miR-3121-3p, ultimately promoting CRC progression.

Research conclusions

TNFRSF10A-AS1 upregulates HuR expression by sponging miR-3121-3p, ultimately promoting colorectal tumorigenesis and progression. Therefore, TNFRSF10A-AS1 and the TNFRSF10A-AS1/miR-3121-3p/HuR axis may play an important role in CRC onset and exacerbation.

Research perspectives

Targeting TNFRSF10A-AS1 and the TNFRSF10A-AS1/miR-3121-3p/HuR axis may have potential novel therapeutic implications for CRC.

ACKNOWLEDGEMENTS

The authors acknowledge the support of Dr. Jun Yu (The Chinese University of Hong Kong) for supervising this study and revising the manuscript.

FOOTNOTES

Author contributions: Wang DD, Sun DL and Zhang XL conceived, designed the study; Wang DD, Sun DL, Yang SP and Song J performed most experiments, analyzed the data, wrote the manuscript and edited the paper; Sun DL and Zhang XL helped to supervise the study; Wu MY, Niu WW and Song M helped to perform the experiments and analyzed the data; Sun DL and Zhang XL helped to edit the paper.

Institutional review board statement: The study was reviewed and approved by the Ethics Committee of the Second Hospital of Hebei Medical University (No. 2021-R241).

Institutional animal care and use committee statement: All procedures involving animals were reviewed and approved by the Ethics Committee of the Second Hospital of Hebei Medical University (No. 2021-AE011).

Conflict-of-interest statement: There are no conflicts of interest to report.

Data sharing statement: No additional data are available.

ARRIVE guidelines statement: The authors have read the ARRIVE Guidelines, and the manuscript was prepared and

revised according to the ARRIVE Guidelines.

Country/Territory of origin: China

ORCID number: Dan-Dan Wang 0000-0001-7809-7429; Dong-Lei Sun 0000-0002-7930-7544; Shao-Peng Yang 0000-0002-1322-1609; Jia Song 0000-0003-4291-6837; Meng-Yao Wu 0000-0003-0510-8654; Wei-Wei Niu 0000-0002-9243-3625; Mei Song 0000-0002-2504-2480; Xiao-Lan Zhang 0000-0003-4951-0952.

S-Editor: Chen YL
L-Editor: A
P-Editor: Cai YX

REFERENCES

1 **Siegel RL**, Miller KD, Jemal A. Cancer statistics, 2020. *CA Cancer J Clin* 2020; **70**: 7-30 [PMID: 31912902 DOI: 10.3322/caac.21590]
2 **Yang KM**, Park IJ, Lee JL, Kim CW, Yoon YS, Lim SB, Yu CS, Kim JC. Benefits of repeated resections for liver and lung metastases from colorectal cancer. *Asian J Surg* 2020; **43**: 102-109 [PMID: 30910376 DOI: 10.1016/j.asjsur.2019.03.002]
3 **Zhou LL**, Zou MD, Li WM. Recent advances in colorectal cancer-specific nucleic acid aptamers for diagnostic and therapeutic applications. *Sci Adv Mater* 2020; **12**: 38-43 [DOI: 10.1166/sam.2020.3727]
4 **The Lancet Oncology**. Colorectal cancer: a disease of the young? *Lancet Oncol* 2017; **18**: 413 [PMID: 28368245 DOI: 10.1016/S1470-2045(17)30202-4]
5 **Fang Y**, Fullwood MJ. Roles, Functions, and Mechanisms of Long Non-coding RNAs in Cancer. *Genomics Proteomics Bioinformatics* 2016; **14**: 42-54 [PMID: 26883671 DOI: 10.1016/j.gpb.2015.09.006]
6 **Schmitt AM**, Chang HY. Long Noncoding RNAs in Cancer Pathways. *Cancer Cell* 2016; **29**: 452-463 [PMID: 27070700 DOI: 10.1016/j.ccell.2016.03.010]
7 **Tsagakis I**, Douka K, Birds I, Aspden JL. Long non-coding RNAs in development and disease: conservation to mechanisms. *J Pathol* 2020; **250**: 480-495 [PMID: 32100288 DOI: 10.1002/path.5405]
8 **Wang L**, Cho KB, Li Y, Tao G, Xie Z, Guo B. Long Noncoding RNA (lncRNA)-Mediated Competing Endogenous RNA Networks Provide Novel Potential Biomarkers and Therapeutic Targets for Colorectal Cancer. *Int J Mol Sci* 2019; **20** [PMID: 31744051 DOI: 10.3390/ijms20225758]
9 **Xu M**, Chen X, Lin K, Zeng K, Liu X, Xu X, Pan B, Xu T, Sun L, He B, Pan Y, Sun H, Wang S. lncRNA SNHG6 regulates EZH2 expression by sponging miR-26a/b and miR-214 in colorectal cancer. *J Hematol Oncol* 2019; **12**: 3 [PMID: 30626446 DOI: 10.1186/s13045-018-0690-5]
10 **Wei J**, Ge X, Tang Y, Qian Y, Lu W, Jiang K, Fang Y, Hwang M, Fu D, Xiao Q, Ding K. An Autophagy-Related Long Noncoding RNA Signature Contributes to Poor Prognosis in Colorectal Cancer. *J Oncol* 2020; **2020**: 4728947 [PMID: 33149738 DOI: 10.1155/2020/4728947]
11 **Ren W**, Zhang J, Li W, Li Z, Hu S, Suo J, Ying X. A Tumor-Specific Prognostic Long Non-Coding RNA Signature in Gastric Cancer. *Med Sci Monit* 2016; **22**: 3647-3657 [PMID: 27727196 DOI: 10.12659/msm.901190]
12 **Brennan CM**, Steitz JA. HuR and mRNA stability. *Cell Mol Life Sci* 2001; **58**: 266-277 [PMID: 11289308 DOI: 10.1007/PL00000854]
13 **Kotta-Loizou I**, Giaginis C, Theocharis S. Clinical significance of HuR expression in human malignancy. *Med Oncol* 2014; **31**: 161 [PMID: 25112469 DOI: 10.1007/s12032-014-0161-y]
14 **Heinonen M**, Bono P, Narko K, Chang SH, Lundin J, Joensuu H, Furneaux H, Hla T, Haglund C, Ristimäki A. Cytoplasmic HuR expression is a prognostic factor in invasive ductal breast carcinoma. *Cancer Res* 2005; **65**: 2157-2161 [PMID: 15781626 DOI: 10.1158/0008-5472.CAN-04-3765]
15 **Denkert C**, Koch I, von Keyserlingk N, Noske A, Niesporek S, Dietel M, Weichert W. Expression of the ELAV-like protein HuR in human colon cancer: association with tumor stage and cyclooxygenase-2. *Mod Pathol* 2006; **19**: 1261-1269 [PMID: 16799479 DOI: 10.1038/modpathol.3800645]
16 **Mrena J**, Wiksten JP, Thiel A, Kokkola A, Pohjola L, Lundin J, Nordling S, Ristimäki A, Haglund C. Cyclooxygenase-2 is an independent prognostic factor in gastric cancer and its expression is regulated by the messenger RNA stability factor HuR. *Clin Cancer Res* 2005; **11**: 7362-7368 [PMID: 16243808 DOI: 10.1158/1078-0432.CCR-05-0764]
17 **Al-Haidari A**, Algaber A, Madhi R, Syk I, Thorlacius H. MiR-155-5p controls colon cancer cell migration *via* post-transcriptional regulation of Human Antigen R (HuR). *Cancer Lett* 2018; **421**: 145-151 [PMID: 29471005 DOI: 10.1016/j.canlet.2018.02.026]
18 **López de Silanes I**, Fan J, Yang X, Zonderman AB, Potapova O, Pizer ES, Gorospe M. Role of the RNA-binding protein HuR in colon carcinogenesis. *Oncogene* 2003; **22**: 7146-7154 [PMID: 14562043 DOI: 10.1038/sj.onc.1206862]
19 **Liu Y**, Chen X, Cheng R, Yang F, Yu M, Wang C, Cui S, Hong Y, Liang H, Liu M, Zhao C, Ding M, Sun W, Liu Z, Sun F, Zhang C, Zhou Z, Jiang X. The Jun/miR-22/HuR regulatory axis contributes to tumourigenesis in colorectal cancer. *Mol Cancer* 2018; **17**: 11 [PMID: 29351796 DOI: 10.1186/s12943-017-0751-3]

World Journal of Gastroenterology

Submit a Manuscript: https://www.f6publishing.com

World J Gastroenterol 2022 May 28; 28(20): 2201-2213

DOI: 10.3748/wjg.v28.i20.2201

ISSN 1007-9327 (print) ISSN 2219-2840 (online)

ORIGINAL ARTICLE

Retrospective Cohort Study

Digital single-operator video cholangioscopy improves endoscopic management in patients with primary sclerosing cholangitis-a retrospective observational study

Arne Bokemeyer, Frank Lenze, Viorelia Stoica, Timur Selcuk Sensoy, Iyad Kabar, Hartmut Schmidt, Hansjoerg Ullerich

Specialty type: Gastroenterology and hepatology

Provenance and peer review: Invited article; Externally peer reviewed.

Peer-review model: Single blind

Peer-review report's scientific quality classification

Grade A (Excellent): 0
Grade B (Very good): B
Grade C (Good): C, C
Grade D (Fair): D
Grade E (Poor): 0

P-Reviewer: Fujimori N, Japan; Gerussi A, Italy; Kitamura K, Japan

Received: January 2, 2022
Peer-review started: January 2, 2022
First decision: March 10, 2022
Revised: March 18, 2022
Accepted: April 20, 2022
Article in press: April 20, 2022
Published online: May 28, 2022

Arne Bokemeyer, Frank Lenze, Viorelia Stoica, Iyad Kabar, Hansjoerg Ullerich, Department of Medicine B (Gastroenterology, Hepatology, Endocrinology, Clinical Infectiology), University Hospital Muenster, Muenster 48149, Germany

Arne Bokemeyer, Timur Selcuk Sensoy, Hartmut Schmidt, Department of Gastroenterology, Hepatology and Transplant Medicine, University Hospital Essen, Essen 45147, Germany

Corresponding author: Arne Bokemeyer, MD, Academic Research, Doctor, Postdoc, Research Scientist, Department of Gastroenterology, Hepatology and Transplant Medicine, University Hospital Essen, Hufelandstraße 55, Essen 45147, Germany. arne.bokemeyer@googlemail.com

Abstract

BACKGROUND

Patients with primary sclerosing cholangitis (PSC) are at a high risk of developing cholestatic liver disease and biliary cancer, and endoscopy is crucial for the complex management of these patients.

AIM

To clarify the utility of recently introduced digital single-operator video cholangioscopy (SOVC) for the endoscopic management of PSC patients.

METHODS

In this observational study, all patients with a history of PSC and in whom digital SOVC (using the SpyGlass DS System) was performed between 2015 and 2019 were included and retrospectively analysed. Examinations were performed at a tertiary referral centre in Germany. In total, 46 SOVCs performed in 38 patients with a history of PSC were identified. The primary endpoint was the evaluation of dominant biliary strictures using digital SOVC, and the secondary endpoints were the performance of selective guidewire passage across biliary strictures and the diagnosis and treatment of biliary stone disease in PSC patients.

RESULTS

The 22 of 38 patients had a dominant biliary stricture (57.9%). In 4 of these 22 patients, a cholangiocellular carcinoma was diagnosed within the stricture (18.2%). Diagnostic evaluation of dominant biliary strictures using optical signs

showed a sensitivity of 75% and a specificity of 94.4% to detect malignant strictures, whereas SOVC-guided biopsies to gain tissue for histopathological analysis showed a sensitivity of 50% and a specificity of 100%. In 13% of examinations, SOVC was helpful for guidewire passage across biliary strictures that could not be passed by conventional methods (technical success rate 100%). Biliary stone disease was observed in 17.4% of examinations; of these, in 37.5% of examinations, biliary stones could only be visualized by SOVC and not by standard fluoroscopy. Biliary stone treatment was successful in all cases (100%); 25% required SOVC-assisted electrohydraulic lithotripsy. Complications, such as postinterventional cholangitis and pancreatitis, occurred in 13% of examinations; however, no procedure-associated mortality occurred.

CONCLUSION

Digital SOVC is effective and safe for the endoscopic management of PSC patients and may be regularly considered an additive tool for the complex endoscopic management of these patients.

Key Words: Cholangitis; Sclerosing; Biliary tract diseases; Biliary strictures; Endoscopy; Gastrointestinal; Cholangioscopy; Digital single-operator video cholangioscopy

Core Tip: Endoscopic management of patients with primary sclerosing cholangitis (PSC) is complex; our study is the first to evaluate the utility of single-operator video cholangioscopy (SOVC) with digital imaging quality in these patients. Our data indicate that the use of digital SOVC in PSC patients substantially improves the evaluation of biliary strictures and that SOVC effectively supports interventions, such as stricture dilation and biliary stone treatment, in PSC patients; mild to moderate complications occurred in a minority of cases. Concluding digital SOVC may be effective and safe as an additive tool for the complex endoscopic management of PSC patients.

Citation: Bokemeyer A, Lenze F, Stoica V, Sensoy TS, Kabar I, Schmidt H, Ullerich H. Digital single-operator video cholangioscopy improves endoscopic management in patients with primary sclerosing cholangitis-a retrospective observational study. *World J Gastroenterol* 2022; 28(20): 2201-2213
URL: https://www.wjgnet.com/1007-9327/full/v28/i20/2201.htm
DOI: https://dx.doi.org/10.3748/wjg.v28.i20.2201

INTRODUCTION

Primary sclerosing cholangitis (PSC) is an immune-mediated chronic liver disease characterized by inflammatory, fibrotic, and destructive changes of the bile ducts, leading to cholestasis, biliary stricture development and hepatic fibrosis. Because of the chronic disease course, PSC patients are at a high risk of developing liver cirrhosis and cholangiocellular carcinoma (CCC)[1,2]. Although PSC patients do not regularly show clinical symptoms in early disease, those with advanced disease often develop typical clinical symptoms including right upper quadrant pain (20%), pruritus (10%), jaundice (6%) and fatigue (6%)[1]. Endoscopy is crucial for the diagnostic and therapeutic management of PSC patients, as documented by recent guidelines[2,3]. Standard endoscopic management of PSC patients includes endoscopic retrograde cholangiography (ERC) and is often challenging. In particular, standard endoscopic management is required in patients with biliary strictures: Diagnostic assessment of strictures may become necessary to exclude malignancy, and therapeutic interventions, including stricture dilation to improve cholestatic disease, may be needed[2,3]. Despite endoscopic treatment, PSC patients may develop advanced liver cirrhosis requiring organ transplantation[4], revealing the unmet need for additional therapeutic options.

Cholangioscopic techniques have progressed in recent years. In 2015, the first digital single-operator video cholangioscope (SpyGlass™ DS System, Boston Scientific, Marlborough, MA, United States) was released[5]. Compared with the previous fibre-optic system, this digital single-operator video cholangioscopy (SOVC) instrument is armed with digital imaging, enabling up to four-times higher resolution, a 60% wider field of view, improved manoeuvrability, and irrigation capacities to clean the field of view [5-9]. Furthermore, forceps biopsies are available, allowing SOVC-guided tissue sampling[5,6,8,9], guidewires can be selectively passed across biliary strictures to allow subsequent interventions[8], and SOVC-assisted lithotripsy devices are ready to treat biliary stone disease[10]. Recently, digital SOVC was technically updated, leading to further advances in lighting and image resolution (SpyGlassDS 2.0; Boston Scientific, Marlborough, MA, United States).

The latest guidelines state that intraductal cholangioscopy can help to diagnose indeterminate biliary strictures in PSC patients and that cholangioscopy may be useful for tissue sampling[2,3]. However, the data are rare, and no study thus far has reported the use of newly introduced digital SOVC in PSC patients. Considering the superior imaging quality and manoeuvrability of digital SOVC instruments, further research is required to address the question of whether digital SOVC may offer an effective additive endoscopic treatment in these patients.

Therefore, this study aimed to evaluate the efficacy and safety of digital SOVC for the diagnostic and interventional endoscopic management of patients with PSC.

MATERIALS AND METHODS

Study design and inclusion criteria

This retrospective, monocentre study was performed at the Department of Medicine B for Gastroenterology, Hepatology, Endocrinology and Clinical Infectiology of the University Hospital Muenster, Germany. The data from all patients ≥ 18 years of age and with a previously diagnosed PSC who had undergone digital SOVC using the SpyGlass DS System (Boston Scientific, Marlborough, MA, United States) between December 2015 and November 2019 were retrieved from the clinical data systems. PSC diagnosis was previously known and not initially established during performed SOVC examinations. Biliary tract cancer was not previously diagnosed in these patients; likewise, IgG4-related sclerosing cholangitis was not known in our patient cohort. The study conformed to the ethical guidelines of the 1975 Declaration of Helsinki and was approved by the Ethics Board of the Westphalian Wilhelms-University of Muenster and Medical Council of Westphalia-Lippe, Germany. To minimize known sources of bias, this trial was reported according to the STROBE statement, wherever appropriate and applicable[11].

Technical aspects of digital single-operator video cholangioscopy

Cholangioscopies were performed by highly experienced endoscopists according to the generally accepted guidelines using an ERC case volume exceeding 200/year and performing ERC procedures for at least five years[12]. Before examination, all the patients received prophylactic antibiotic treatment; nonsteroidal anti-inflammatory drugs (NSAIDs; *e.g.*, indomethacin) were not regularly administered before the procedure. CO_2 insufflation was used during all examinations. Before cholangioscopy, an endoscopic papillotomy was performed, or one had been previously performed. The cholangioscope (digital SOVC; Boston Scientific, Marlborough, MA, United States) was inserted into the biliary duct in a guidewire-assisted method; targeted biopsies were acquired using SpyBite forceps (Boston Scientific, Marlborough, MA, United States). For biliary stone treatment, electrohydraulic lithotripsy (EHL) was performed using a bipolar lithotripsy 2.4 F catheter probe (Walz Elektrotechnik GmbH, Rohrdorf, Germany) with saline solution irrigation (SSI) controlled over a dedicated irrigation pump. The probe produces high-frequency hydraulic pressure waves, resulting in the fragmentation of biliary stones[10,13].

The primary endpoint of this study was to evaluate the efficacy and safety of digital SOVC to detect malignancy in dominant biliary strictures in patients with PSC, depending on the visual inspection and histological evaluation of SOVC-acquired biopsies. According to the European guidelines, strictures were defined as dominant if they had a diameter smaller than 1.5 mm in the common bile duct and smaller than 1 mm in the right and left hepatic ducts[14]. Visual signs suggesting malignancy were documented if the performing endoscopists classified visual findings as suspicious for malignancy in the presence of irregular vessels, easy bleeding, irregular surfaces and elevated masses protruding into the duct lumen[15,16]. Acquired biopsy material was analysed by an experienced pathologist and classified as suspicious for malignancy if cancer cells or high-grade cell dysplasia were detected. The final diagnosis (reference standard) of biliary stricture dignity was based on a detailed evaluation of all the available data, including clinical information, cross-sectional imaging reports and histopathological analyses, which could be found in the electronic patient chart. The median follow-up time was 12 mo [interquartile range (IQR) 7-27 mo]; during this time, the patients were followed up by repeated checks of the available electronic medical records.

For secondary endpoint analysis, the use of digital SOVC for the diagnosis and treatment of biliary stone disease in PSC patients was documented. Furthermore, the use of digital SOVC for selective guidewire insertion across biliary strictures in cases that were solely performed because of a previous failure of conventional endoscopic methods to treat a biliary stricture *via* selective guidewire placement was evaluated.

Safety analysis

Adverse events following examination were documented as follows: (1) Postinterventional pancreatitis was defined if patients developed abdominal pain and a threefold increase in the serum lipase levels within 48 h of the examination[17]; (2) Postinterventional cholangitis was documented as the presence of new fever (> 38.0 °C) and newly or significantly higher cholestatic and inflammatory markers

requiring antibiotics within three days of the examination[17]; and (3) Severe bleeding was diagnosed if bleeding was observed during intervention that required immediate endoscopic therapy or if haemoglobin level decreased by two points or more[17]. Adverse events were graded as mild, moderate, or severe, depending on the length of additional hospital stay (mild = 1-3 d, moderate = 4-10 d, severe = > 10 d)[17].

Statistical analysis

The data were analysed using IBM SPSS Statistics 27.0 (IBM Corp., Armonk, United States). Additionally, contingency table-derived data were determined using StatPages[18]. Frequencies and percentages were recorded for categorical variables; means and standard errors (SEs) were reported for continuous variables. Missing data are indicated and reported in the text and tables. The statistical methods of this study were reviewed by Arne Bokemeyer.

RESULTS

Study population

During the study period, 151 ERCs were performed in 72 patients with PSC, and in 30.5% of these ERCs, digital SOVC was additionally carried out (46/151). These 46 cholangioscopies, conducted in 38 PSC patients, were included in the final dataset (Figures 1 and 2). The main indication for SOVC use was the assessment of biliary strictures (80.4%), followed by selective guidewire placement across biliary strictures (13%) and treatment of biliary stone disease (4.3%). A total of 68.4% of the patients were male, whereas 31.6% of the patients were female. The mean age was 44.8 years (SE: ± 2.1 years). Considering all patients, the mean period from the initial ERC performed for PSC diagnosis to the performance of the first SOVC was 99.9 mo (SE ± 16.6). A total of 52.6% of the patients had liver cirrhosis, and 29% were enrolled for liver transplantation. In 10.5% of patients, a final diagnosis of a malignant biliary tumour was established (Table 1). In these patients, the mean time from initial ERC performed for PSC diagnosis to the digital SOVC, which was sufficient to establish bile duct cancer diagnosis, was 71.3 mo (standard error: ± 16.6) with a range of at least 11 mo up to 150 mo.

Of the cholangioscopies, 38 examinations were initial, and 8 were repeated examinations (Table 2). All the examinations were ERC-based (100%). The median total examination time was 73 min (± 5.2 min; missing data in 6/46 examinations). In one case, the digital SOVC system technically failed during examination and could not be relaunched (2.2%; Table 2).

During SOVC, the main procedures were selective SOVC-assisted guidewire insertions to support diagnostic assessment and therapeutic interventions of the biliary tract in 84.7% of examinations, SOVC-assisted forceps biopsy acquisition in 54.3% of examinations, and the performance of SOVC-assisted EHL for refractory biliary stone disease in 4.3% of examinations. Biliary strictures were dilated in 76.1% of examinations, and endoprostheses were placed in 10.9% of examinations (Table 2).

Diagnostic efficacy of stricture assessment in PSC using SOVC

Dominant biliary strictures were present in 22 of 38 patients (57.9%; Table 3). Dominant strictures were mainly localized intrahepatically (59.1%), followed by strictures at the intra- and extrahepatic passages (27.3%) and extrahepatic strictures (13.6%). In 4 of 22 patients, dominant strictures were of a malignant entity (18.2%). The malignant strictures were localized at the intra- and extrahepatic crossing in three patients, and in one patient the stricture was localized intrahepatically at the left hepatic duct. Using SOVC, visual signs of malignancy could be observed in 18.2% of patients. In 13 of 22 patients, SOVC-assisted forceps biopsies were obtained (59.1%; Figure 1). In 2 of 13 biopsies, histopathological analysis revealed signs of malignancy (carcinoma or high-grade dysplasia; 15.4%). In 1 of 13 patients, insufficient tissue was obtained using forceps biopsies, making an accurate histopathological analysis impossible (7.7%; Table 3). The visual examination of dominant strictures had an accuracy of 90.9% (CI: 72.8%-99.2%), a sensitivity of 75% (CI: 25.2%-97.8%), a specificity of 94.4% (83.4%-99.5%), a positive predictive value of 75% (25.2%-97.8%), and a negative predictive value of 94.4% (83.4%-99.5%; Table 4). Histopathological analysis of SOVC-assisted biopsy acquisition had an accuracy of 83.3% (CI: 57.2%-83.3%), a sensitivity of 50% (10.8%-50%), a specificity of 100% (80.4%-100%), a positive predictive value of 100% (21.7%-100%), and a negative predictive value of 80% (64.3%-80%) (Table 4).

Use of SOVC for biliary stone treatment in patients with PSC

In 8 of 46 examinations (17.3%), biliary stones were found (Table 5). Stones were localized intrahepatically (37.5%), extrahepatically (37.5%) and both intra- and extrahepatically (25%). The stone size ranged between 3 and 20 mm, and the number of stones ranged between 1 and 5 *per* examination. In 3 of 8 cases (37.5%), biliary stones were only visualized using SOVC, and standard fluoroscopy failed to detect biliary stones. In all 8 examinations, biliary stone treatment was finally successful; however, in 2 of 8 examinations (25%), biliary stone disease was refractory to standard ERC methods, including stone extraction with baskets and/or balloon catheters, which was why EHL was applied for stone

Table 1 Characteristics of patients with primary sclerosing cholangitis undergoing digital single-operator video cholangioscopy

Variable	Patients (*n* = 38)
Primary sclerosing cholangitis, *n* (%)	38 (100)
Age (in years)	44.8 (± 2.1)
Male, *n* (%)	26 (68.4)
Female, *n* (%)	12 (31.6)
Liver cirrhosis, *n* (%)	20 (52.6)
Enlisted for liver transplantation, *n* (%)	11 (28.9)
Diagnosis of a cholangiocellular carcinoma, *n* (%)	4 (10.5)

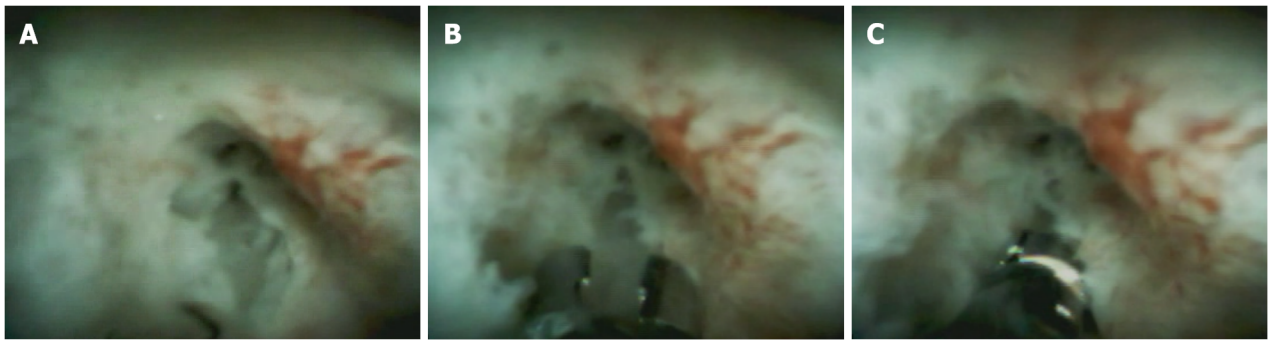

DOI: 10.3748/wjg.v28.i20.2201

Figure 1 Digital single-operator video cholangioscopy-assisted biliary stricture evaluation in a patient with primary sclerosing cholangitis. A: Using digital single-operator video cholangioscopy (SOVC) enabled the direct visualization of a biliary stricture showing typical signs of chronic inflammation in a patient with primary sclerosing cholangitis; B and C: To rule out malignancy, multiple SOVC-guided forceps biopsies of the biliary stricture were obtained.

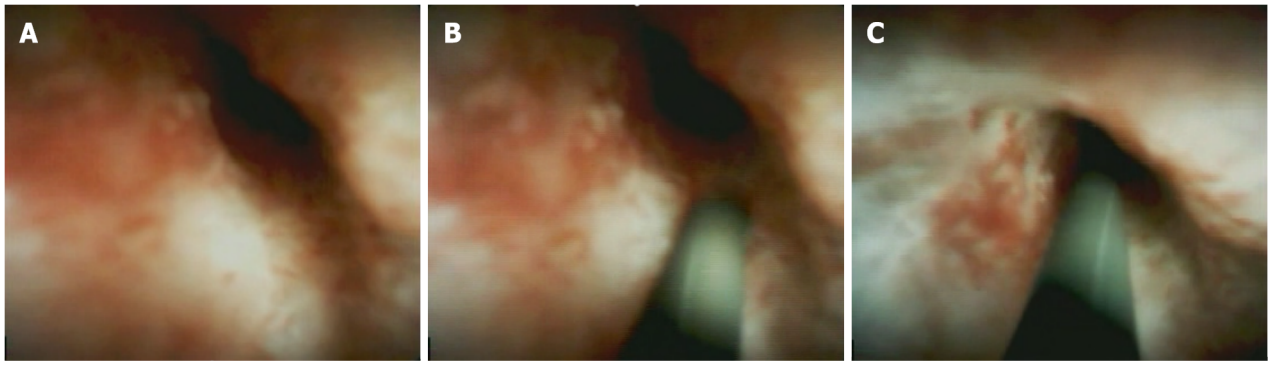

DOI: 10.3748/wjg.v28.i20.2201

Figure 2 Selective guidewire placement across a biliary stricture in a patient with primary sclerosing cholangitis using digital single-operator video cholangioscopy. A: Multiple attempts to pass a biliary stricture in a patient with primary sclerosing cholangitis using conventional selective guidewire insertion failed, which is why digital single-operator video cholangioscopy (SOVC) was used and helped visualize the stricture; B and C: Under SOVC-assisted guidance, a guidewire was successfully placed across the biliary stricture, enabling subsequent endoscopic therapy.

fragmentation. In both cases, EHL successfully led to complete stone fragmentation (100%; Table 5).

SOVC-assisted selective guidewire passage across PSC-associated strictures

The 6 of 46 examinations were solely performed because of a previous failure of conventional endoscopic methods to treat a biliary stricture *via* selective guidewire placement (13%; Figure 2). Of these, 5 were initial SOVC procedures, and one was a repeated procedure. The technical success rate of SOVC-assisted guidewire insertions across biliary strictures was 100%, enabling subsequent dilation of the stricture (Table 5).

Table 2 Basic analysis of digital single-operator video cholangioscopies performed in patients with primary sclerosing cholangitis

Variable	Digital SOVC (*n* = 46)
Type of digital SOVC	
Initial examinations, *n* (%)	38 (82.6)
Repeated examinations, *n* (%)	8 (17.4)
Main indication for using SOVC	
Stricture assessment, *n* (%)	37 (80.4)
Selective guidewire placement, *n* (%)	6 (13)
Cholangiolithiasis, *n* (%)	2 (4.3)
Others, *n* (%)	1 (2.2)
Clinical patient data before SOVC (multiple items permitted)	
Prior papillotomy, *n* (%)	41 (89.1)
Elevated serum bilirubin level (> 1.2 mg/dl), *n* (%)	30 (65.2)
Prior post-ERC-pancreatitis, *n* (%)	10 (21.7)
Type of digital SOVC	
ERC-based digital SOVC, *n* (%)	46 (100)
Total examination time (ERC + digital SOVC; min)	73 (± 5.2); *n* = 40/46
Dysfunction of the SOVC-system, *n* (%)	1 (2.2)
Procedures during SOVC-examination (multiple items permitted)	
SOVC-assisted guidewire insertion, *n* (%)	39 (84.7)
SOVC-assisted forceps biopsies, *n* (%)	25 (54.3)
SOVC-assisted EHL, *n* (%)	2 (4.3)
Additive procedures during ERC-examination (multiple items permitted)	
Balloon dilation of the biliary tract, *n* (%)	35 (76.1)
New papillotomy, *n* (%)	7 (15.2)
Conventional transpapillary biopsy, *n* (%)	6 (13.0)
Endoprosthesis placement, *n* (%)	5 (10.9)
Periinterventional application of drugs to prevent AE	
Antibiotics, *n* (%)	46 (100)
NSAID (Diclofenac/Indomethacin), *n* (%)	6 (13)

SOVC: Single-operator video cholangioscopy; EHL: Electrohydraulic lithotripsy; AE: Adverse event; ERC: Endoscopic retrograde cholangiography; NSAID: Nonsteroidal anti-inflammatory drug.

Adverse events

In 13% of the procedures, adverse events were documented (Table 6). More specifically, postinterventional pancreatitis was observed in 6.5% of cases, of which 67% had a moderate and 33% a severe disease course. Postinterventional cholangitis occurred in 6.5% of cases, of which all had a moderate disease course (100%). Other procedure-related adverse events, including severe bleeding or organ perforations, did not occur. All procedure-related complications could be successfully managed by conservative therapeutic approaches. No mortality due to procedure-related adverse events occurred. Because of side effects, patients needed to stay in the hospital for 6.5 more days (SE ± 1.5 d) (Table 6).

DISCUSSION

Although a few previous reports evaluated the utility of cholangioscopy in PSC patients in general[19, 20], our study is the first to evaluate the efficacy and safety of SOVC with digital imaging quality in patients with PSC. Digital SOVC is effective and safe as an additive tool for the complex endoscopic

Table 3 Evaluation of dominant biliary strictures in patients with primary sclerosing cholangitis using digital single-operator video cholangioscopy (*n* = 22)

Variable	Dominant strictures (*n* = 22)
Entity of dominant stricture, *n* (%)	
Benign	18 (81.8)
Malignant	4 (18.2)
Localization of dominant stricture, *n* (%)	
Intrahepatic	13 (59.1)
Extrahepatic	3 (13.6)
Intra- and extrahepatic crossing	6 (27.3)
Visual evaluation of stricture by endoscopists, *n* (%)	
Suspicious for malignancy	4 (18.2)
Suspicious for benignancy	18 (81.8)
SOVC-guided forceps biopsies, *n* (%)	
Carcinoma/high-grade dysplasia	2 (9.1)
Benign findings	10 (45.5)
Inadequate material	1 (4.5)

SOVC: Single-operator video cholangioscopy.

Table 4 Diagnostic efficacy of digital single-operator video cholangioscopy for diagnosing malignancy in dominant biliary strictures in patients with primary sclerosing cholangitis (*n* = 22; cholangioscopic-assisted visual evaluation, *n* = 22 and cholangioscopic-guided biopsies, *n* = 12)

Variable	Accuracy (%)	Sensitivity (%)	Specificity (%)	Pos. pred. value (%)	Neg. pred. value (%)
Visual evaluation (95%CI)	90.9 (72.8-99.2)	75 (25.2-97.8)	94.4 (83.4-99.5)	75 (25.2-97.8)	94.4 (83.4-99.5)
Histological evaluation (95%CI)	83.3 (57.2-83.3)	50 (10.8-50.0)	100 (80.4-100)	100 (21.7-100)	80 (64.3-80)

95%CI: 95% confidence interval; pos.: Positive; neg.: Negative; pred.: Predictive.

management of these patients. In addition to evaluating biliary strictures, digital SOVC facilitates interventions to the biliary tract because of selective guidewire placements across biliary strictures and helps to diagnose and treat biliary stone disease.

Stricture assessment of biliary strictures in PSC patients is critical to excluding malignancy: PSC patients have a lifetime risk of developing CCC of up to 20%[2]. Clinical judgement, laboratory markers, and cross-sectional imaging are insufficient to exclude malignancy, explaining why endoscopic evaluation, including tissue sampling, becomes necessary[2,3,21]. If a standard work-up including ERC with transpapillary tissue sampling fails to determine stricture aetiology, the performance of peroral cholangioscopy is suggested[21]. Visual interpretation of biliary strictures using cholangioscopy may help diagnose indeterminate biliary strictures: A recent meta-analysis including 283 procedures with digital SOVC in unselected patients found a sensitivity of 94% and a specificity of 95% in detecting malignancy in biliary strictures[22]. In addition to optical evaluation, cholangioscopic-guided biopsies can be obtained: Another recent meta-analysis in unselected patients found a sensitivity of 72% and a specificity of 99% in diagnosing biliary malignancy using cholangioscopy-guided biopsies[23]. Despite these promising results in unselected patients, the results in selected PSC patients might be different: A prospective trial using legacy fibreoptic SOVC in 47 patients with PSC evaluated the use of SOVC-assisted forceps biopsies and found a sensitivity of only 33% and a specificity of 100% in detecting malignant biliary strictures[20]. In our study, visual evaluation of indeterminate biliary strictures identified malignancy with a sensitivity of 75% and a specificity of 94% and histopathological analysis of SOVC-guided biopsies showed a sensitivity of 50% and specificity of 100%. In comparison, our study showed a lower sensitivity and specificity of visual and bioptical stricture assessment than those in

Table 5 Diagnosis and treatment of biliary stone disease and performance of selective guidewire placements across biliary strictures (with a previous failure of conventional endoscopic methods to pass a guidewire) using digital single-operator video cholangioscopy in patients with primary sclerosing cholangitis

Variable	Examinations (*n* = 46)
Cholangiolithiasis, *n* (%)	**8/46 (17.3)**
Localization	
Extrahepatic, *n* (%)	3/8 (37.5)
Intrahepatic, *n* (%)	3/8 (37.5)
Intra- and extrahepatic, *n* (%)	2/8 (25)
Stone size (range)	3-20 mm
Stone number (range)	1-5
Treatment	
Complete success (conventional ± EHL), *n* (%)	8/8 (100)
Success only *via* use of EHL, *n* (%)	2/8 (25)
Stone identification only *via* SOVC, *n* (%)	3/8 (37.5)
Selective guidewire insertion across biliary strictures, *n* (%)	**6/46 (13)**
Kind of procedures	
Initial examinations, *n* (%)	5/6 (83.3)
Repeated examinations, *n* (%)	1/6 (16.7)
Technical success, *n* (%)	6/6 (100)

EHL: Electrohydraulic lithotripsy; SOVC: Single-operator video cholangioscopy.

Table 6 Safety data of digital single-operator video cholangioscopies in patients with primary sclerosing cholangitis

Variable	Digital SOVCs (*n* = 46)
Overall complications, *n* (%)	**6 (13)**
Pancreatitis, *n* (%)	3 (6.5)
Grade 1	0 (0)
Grade 2	2 (4.3)
Grade 3	1 (2.2)
Cholangitis, *n* (%)	3 (6.5)
Grade 1	0 (0)
Grade 2	3 (6.5)
Grade 3	0 (0)
Others (bleeding/perforation), *n* (%)	0 (0)
Procedure-related mortality, *n* (%)	0 (0)
Suspected prolonged hospital stay due to complications (in days)	6.5 (± 1.5)

SOVC: Single-operator video cholangioscopy.

previous studies in unselected patients using SOVC. However, comparing our results to previous studies with fibreoptic SOVC including only selected PSC patients, our sensitivity and specificity rates for the diagnostic evaluation of biliary strictures might be improved. As a limitation, digital SOVCs might only be advanced with difficulties to all intrahepatic strictures due to the decreasing lumen of the proximal bile ducts making proximal intrahepatic ducts partially inaccessible for cholangioscopic assessment. To guide cholangioscopy intrahepatically, the use of guidewires can help to advance the

cholangioscope to more proximal localized strictures.

In conclusion, this study shows that using SOVC with digital imaging quality may significantly improve the diagnostic evaluation of indeterminate strictures in PSC patients. However, validated criteria for optical evaluation of strictures are missing and may be particularly needed in stricture evaluation of PSC patients because inflammatory tissue alterations of the bile ducts hinder easy evaluation of biliary stricture aetiology. Furthermore, no consensus exists concerning the number of biopsies that should be obtained to ensure adequate biopsy material[24]. Speculatively, the sensitivity rates of histopathological evaluation may be improved by a higher number of SOVC-guided biopsies [25]; furthermore, larger forceps biopsies for digital SOVC were recently introduced, promising to further improve cholangioscopic diagnostics in the future. Histopathological analysis is essential for excluding differential diagnoses including Ig4-related sclerosing cholangitis, which may mimic a PSC-like disease. In addition to radiologic and serological assessment, tissue acquisition for histopathological analysis is important for diagnostic assessment[26], and SOVCs might help to gain sufficient histopathological material for correct assessment.

Endoscopic interventions, including stricture dilation, can be performed to improve cholestatic disease in PSC patients and are part of current guideline recommendations[2,3]. Technically, biliary dilation should be preferred to inserting biliary stents[2,3]: Notably, in our cohort, stricture dilation was regularly performed in most patients (76%), whereas only a few received biliary stenting (10.9%). To facilitate biliary dilation or stenting, a guidewire must be placed across the biliary stricture[8,27,28]; however, this selective guidewire placement might fail using standard ERC techniques. A previous trial using fiberoptic SOVCs in 15 patients after liver transplantation showed a technical success rate of 60% of placing a guidewire across a stricture[28]. Another study, which was published by our group, using digital SOVC for selective guidewire insertion in 23 unselected patients showed an overall technical success rate of 70%; notably, the technical success rate was significantly higher in benign strictures than in malignant strictures (88% *vs* 46%; $P = 0.02$)[8]. In the current study, in 6 examinations, conventional ERC techniques failed to pass a guidewire across a biliary stricture, and digital SOVC helped in all cases to perform selective guidewire placement, enabling subsequent stricture dilation (technical success rate: 100%). In conclusion, digital SOVC with improved imaging quality is highly successful in facilitating selective guidewire placement across biliary strictures, even in PSC patients in whom previous attempts to pass a stricture with a guidewire failed using standard ERC techniques.

Patients with PSC may have a high incidence of biliary stone disease[29,30]. In two previous studies, PSC patients had an incidence of biliary stone disease of up to 50%[29,30]. In our cohort, we found a slightly lower incidence of biliary stone disease; however, stones were still frequently found in 17.3% of examinations. A previous trial with 41 PSC patients undergoing fibreoptic cholangioscopy using the mother-baby-technique suggested that 30% of biliary stones were missed by standard fluoroscopy and could only be visualized using cholangioscopy[29]. In our cohort, nearly 40% of biliary stones were missed on fluoroscopy and could only be detected using digital SOVC likely confirming that digital SOVC with improved imaging quality substantially helps detect biliary stones in PSC patients. Although the utility of cholangioscopy for stone detection in PSC patients might be superior using digital SOVC, it might be less likely that a routine use of digital SOVCs for stone detection in PSC patients is cost-effective, which might especially be true for MRCP-negative cases. Sometimes the extraction of biliary stones proximal to biliary strictures might be challenging. Dilation of the distal biliary stricture might substantially help extract stones. Furthermore, EHL might be used for stone fragmentation. In 25% of our cases, SOVC-assisted EHL was used for refractory biliary stone disease and showed complete treatment success (100%). This high technical success rate of biliary stone treatment was similar to that in previous trials, varying from 86% to 100%[9,10,15,16,31] supporting the role of digital SOVC as an effective treatment for refractory biliary stone disease, even in PSC patients.

Additionally, we evaluated the safety of using digital SOVC in PSC patients. In ERC, adverse events occurred in approximately 7% of examinations[32]. Concerning digital SOVC, earlier studies observed complication rates ranging from 0 to 16.4%[9,10,15,16,31], and a recent meta-analysis applying digital SOVC to evaluate biliary strictures found a complication rate of 7%[33]. We found a complication rate of 13%, which is in the upper range of previous trials, although only fully trained endoscopists performed procedures in our cohort. Our cholangitis rate (6.5%) was slightly higher than that of unselected patients (4%), likely because of the complexity of our cases: Only PSC patients were included in our cohort; among these, more than 50% had cirrhotic liver disease, and nearly 30% were enlisted for liver transplantation. The risk of cholangioscopy in PSC patients is controversial: Considering that the stricturing disease course hampers adequate biliary drainage post contrast injection, PSC patients may be at special risk of developing post-ERC cholangitis[34]. Furthermore, our pancreatitis rate (6.5%) was slightly higher than the post-ERC pancreatitis rates observed in unselected patients (2%-4%)[32,35]. Fortunately, all cases of pancreatitis could be managed conservatively, and no surgical management was necessary. In our cohort, rectal NSAIDs were not routinely applied at the start of the study; however, considering our results, rectal NSAIDs should be regularly dispensed in all patients with PSC undergoing digital SOVC, which is the current standard of care in our department and part of recent guideline recommendations[17]. In summary, considering this moderate rate of complications, digital SOVC should be performed in selected cases and by experienced endoscopists at tertiary referral centres.

Our study has several limitations. First, our study was retrospective and is limited by a small sample size comprising only 46 procedures; however, it is the first to exclusively evaluate digital SOVC use in PSC patients; furthermore, PSC is a rare disease, making our number of procedures noteworthy. Second, we included cases at only one hospital in our analysis; however, our centre is a large tertiary referral centre offering special endoscopic experience to perform cholangioscopic procedures, and we could ensure that all endoscopists were fully trained, improving the reliability of our results. Nevertheless, our study results are limited by a lack of validation, making future prospective multicentre studies necessary. Third, our endoscopists were not blinded to patient history, likely biasing their visual impression to determine the biliary stricture dignity; however, digital SOVC was performed because strictures were still indeterminate despite previously performed diagnostics. Fourth, in all our patients, a previous traditional cholangiography was performed before the use of digital SOVC, which might have confounded the rate of cholangitis described in our study. However, this setting was our routine clinical practice. Initially, endoscopists performed traditional cholangiography, which revealed findings making further cholangioscopic assessment instantly necessary.

CONCLUSION

In summary, our data indicate that using digital SOVC in patients with PSC is efficient and safe. In addition to evaluating biliary strictures, which may be substantially improved because of superior image quality, SOVC supports interventions due to selective guidewire placements across biliary strictures and helps diagnose and treat biliary stone disease, explaining why digital SOVC might be frequently used as an additive tool for the complex endoscopic management of PSC patients.

ARTICLE HIGHLIGHTS

Research background

Patients with primary sclerosing cholangitis (PSC) have a high risk of developing cholestatic liver disease, biliary strictures, and biliary cancer, which frequently require endoscopy for diagnostic and therapeutic management.

Research motivation

Recently, digital single-operator video cholangioscopy (SOVC) was introduced, offering superior image quality and manoeuvrability. However, no study thus far has reported the use of newly introduced digital SOVC in PSC patients.

Research objectives

To clarify the efficacy and safety of the recently introduced SOVC for the endoscopic management of patients with PSC.

Research methods

This observational study retrospectively included all patients with a known PSC and in whom digital SOVC (with the SpyGlass DS System) was performed between 2015 and 2019 at a tertiary referral centre. In total, 46 SOVCs performed in 38 patients with PSC were identified. The primary endpoint was the evaluation of dominant biliary strictures using digital SOVC.

Research results

The 22 of 38 patients had a dominant biliary stricture (57.9%), and in 18.2% of these cases, a cholangiocellular carcinoma was diagnosed within the stricture. Diagnostic evaluation of dominant biliary strictures using optical signs showed a sensitivity of 75% and a specificity of 94.4% in detecting malignant strictures, whereas SOVC-guided biopsies to obtain tissue for histopathological analysis showed a sensitivity of 50% and a specificity of 100%. In 13% of examinations, SOVC was helpful for guidewire passage across biliary strictures that could not be passed by conventional methods (technical success rate 100%) and furthermore, in 8 examinations, SOVC helped visualize and treat biliary stone disease (100% success rate). Mild to moderate complications occurred in 13% of examinations.

Research conclusions

Digital SOVC is effective and safe for the complex endoscopic management of PSC patients.

Research perspectives

In the future, digital SOVC might be regularly considered as an additive tool for the endoscopic management of patients with PSC.

FOOTNOTES

Author contributions: Bokemeyer A and Ullerich H conceived and designed the study and performed the data analysis, literature review, and manuscript writing; Lenze F, Stoica V, Sensoy T, Kabar I and Schmidt H performed the data collection, data analysis, manuscript writing, and literature review; All the authors have read and approve the final manuscript.

Institutional review board statement: The study was approved by the Ethics Board of the Westphalian Wilhelms-University of Muenster and Medical Council of Westphalia-Lippe, Germany, No. 2017-490-f-S.

Informed consent statement: As approved by the Ethics Board, informed patient consent was not required for this study because of its retrospective design.

Conflict-of-interest statement: The authors declare no potential conflict of interests related to this study.

Data sharing statement: No additional data are available.

STROBE statement: The authors have read the STROBE Statement—checklist of items, and the manuscript was prepared and revised according to the STROBE Statement—checklist of items.

Country/Territory of origin: Germany

ORCID number: Arne Bokemeyer 0000-0002-4238-751X; Frank Lenze 0000-0002-5645-4138; Viorelia Stoica 0000-0001-9736-9573; Timur Selcuk Sensoy 0000-0002-4316-3649; Iyad Kabar 0000-0001-5132-3166; Hartmut Schmidt 0000-0002-2402-7764; Hansjoerg Ullerich 0000-0003-2447-3323.

S-Editor: Fan JR
L-Editor: A
P-Editor: Fan JR

REFERENCES

1 **Lazaridis KN**, LaRusso NF. Primary Sclerosing Cholangitis. *N Engl J Med* 2016; **375**: 2501-2502 [PMID: 28002707 DOI: 10.1056/NEJMc1613273]
2 **Chapman MH**, Thorburn D, Hirschfield GM, Webster GGJ, Rushbrook SM, Alexander G, Collier J, Dyson JK, Jones DE, Patanwala I, Thain C, Walmsley M, Pereira SP. British Society of Gastroenterology and UK-PSC guidelines for the diagnosis and management of primary sclerosing cholangitis. *Gut* 2019; **68**: 1356-1378 [PMID: 31154395 DOI: 10.1136/gutjnl-2018-317993]
3 **Aabakken L**, Karlsen TH, Albert J, Arvanitakis M, Chazouilleres O, Dumonceau JM, Färkkilä M, Fickert P, Hirschfield GM, Laghi A, Marzioni M, Fernandez M, Pereira SP, Pohl J, Poley JW, Ponsioen CY, Schramm C, Swahn F, Tringali A, Hassan C. Role of endoscopy in primary sclerosing cholangitis: European Society of Gastrointestinal Endoscopy (ESGE) and European Association for the Study of the Liver (EASL) Clinical Guideline. *Endoscopy* 2017; **49**: 588-608 [PMID: 28420030 DOI: 10.1055/s-0043-107029]
4 **Bjøro K**, Brandsaeter B, Foss A, Schrumpf E. Liver transplantation in primary sclerosing cholangitis. *Semin Liver Dis* 2006; **26**: 69-79 [PMID: 16496235 DOI: 10.1055/s-2006-933565]
5 **SpyGlass-DS-System-ebrochure**. SpyGlass™ DS II Direct Visualization System. [cited 10 January 2022]. Available from: http://www.bostonscientific.com/content/dam/bostonscientific/endo/portfolio-group/SpyGlass%20DS/SpyGlass-DS-System-ebrochure.pdf
6 **Pereira P**, Peixoto A, Andrade P, Macedo G. Peroral cholangiopancreatoscopy with the SpyGlass® system: what do we know 10 years later. *J Gastrointestin Liver Dis* 2017; **26**: 165-170 [PMID: 28617887 DOI: 10.15403/jgld.2014.1121.262.cho]
7 **Shah RJ**, Neuhaus H, Parsi M, Reddy DN, Pleskow DK. Randomized study of digital single-operator cholangioscope compared to fiberoptic single-operator cholangioscope in a novel cholangioscopy bench model. *Endosc Int Open* 2018; **6**: E851-E856 [PMID: 29978005 DOI: 10.1055/a-0584-6458]
8 **Bokemeyer A**, Gross D, Brückner M, Nowacki T, Bettenworth D, Schmidt H, Heinzow H, Kabar I, Ullerich H, Lenze F. Digital single-operator cholangioscopy: a useful tool for selective guidewire placements across complex biliary strictures. *Surg Endosc* 2019; **33**: 731-737 [PMID: 30006839 DOI: 10.1007/s00464-018-6334-6]
9 **Lenze F**, Bokemeyer A, Gross D, Nowacki T, Bettenworth D, Ullerich H. Safety, diagnostic accuracy and therapeutic efficacy of digital single-operator cholangioscopy. *United European Gastroenterol J* 2018; **6**: 902-909 [PMID: 30023068 DOI: 10.1177/2050640618764943]
10 **Brewer Gutierrez OI**, Bekkali NLH, Raijman I, Sturgess R, Sejpal DV, Aridi HD, Sherman S, Shah RJ, Kwon RS,

Buxbaum JL, Zulli C, Wassef W, Adler DG, Kushnir V, Wang AY, Krishnan K, Kaul V, Tzimas D, DiMaio CJ, Ho S, Petersen B, Moon JH, Elmunzer BJ, Webster GJM, Chen YI, Dwyer LK, Inamdar S, Patrick VB, Attwell A, Hosmer A, Ko C, Maurano A, Sarkar A, Taylor LJ, Gregory MH, Strand DS, Raza A, Kothari S, Harris JP, Kumta NA, Manvar A, Topazian MD, Lee YN, Spiceland CM, Trindade AJ, Bukhari MA, Sanaei O, Ngamruengphong S, Khashab MA. Efficacy and Safety of Digital Single-Operator Cholangioscopy for Difficult Biliary Stones. *Clin Gastroenterol Hepatol* 2018; **16**: 918-926.e1 [PMID: 29074446 DOI: 10.1016/j.cgh.2017.10.017]

11 **STROBE**. What is STROBE? [cited 10 January 2022]. Available from: https://www.strobe-statement.org/

12 **Baron TH**, Petersen BT, Mergener K, Chak A, Cohen J, Deal SE, Hoffinan B, Jacobson BC, Petrini JL, Safdi MA, Faigel DO, Pike IM; ASGE/ACG Taskforce on Quality in Endoscopy. Quality indicators for endoscopic retrograde cholangiopancreatography. *Am J Gastroenterol* 2006; **101**: 892-897 [PMID: 16635233 DOI: 10.1111/j.1572-0241.2006.00675.x]

13 **ASGE Technology Committee**, Watson RR, Parsi MA, Aslanian HR, Goodman AJ, Lichtenstein DR, Melson J, Navaneethan U, Pannala R, Sethi A, Sullivan SA, Thosani NC, Trikudanathan G, Trindade AJ, Maple JT. Biliary and pancreatic lithotripsy devices. *VideoGIE* 2018; **3**: 329-338 [PMID: 30402576 DOI: 10.1016/j.vgie.2018.07.010]

14 **European Society of Gastrointestinal Endoscopy**; European Association for the Study of the Liver. Role of endoscopy in primary sclerosing cholangitis: European Society of Gastrointestinal Endoscopy (ESGE) and European Association for the Study of the Liver (EASL) Clinical Guideline. *J Hepatol* 2017; **66**: 1265-1281 [DOI: 10.1016/j.jhep.2017.02.013]

15 **Navaneethan U**, Hasan MK, Kommaraju K, Zhu X, Hebert-Magee S, Hawes RH, Vargo JJ, Varadarajulu S, Parsi MA. Digital, single-operator cholangiopancreatoscopy in the diagnosis and management of pancreatobiliary disorders: a multicenter clinical experience (with video). *Gastrointest Endosc* 2016; **84**: 649-655 [PMID: 26995690 DOI: 10.1016/j.gie.2016.03.789]

16 **Ogura T**, Imanishi M, Kurisu Y, Onda S, Sano T, Takagi W, Okuda A, Miyano A, Amano M, Nishioka N, Yamada T, Masuda D, Takenaka M, Kitano M, Higuchi K. Prospective evaluation of digital single-operator cholangioscope for diagnostic and therapeutic procedures (with videos). *Dig Endosc* 2017; **29**: 782-789 [PMID: 28349613 DOI: 10.1111/den.12878]

17 **ASGE Standards of Practice Committee**, Chandrasekhara V, Khashab MA, Muthusamy VR, Acosta RD, Agrawal D, Bruining DH, Eloubeidi MA, Fanelli RD, Faulx AL, Gurudu SR, Kothari S, Lightdale JR, Qumseya BJ, Shaukat A, Wang A, Wani SB, Yang J, DeWitt JM. Adverse events associated with ERCP. *Gastrointest Endosc* 2017; **85**: 32-47 [PMID: 27546389 DOI: 10.1016/j.gie.2016.06.051]

18 **2-way Contingency**. 2-way Contingency Table Analysis. 2018. [cited 10 January 2022]. Available from: http://statpages.info/ctab2x2.html

19 **Siiki A**, Rinta-Kiikka I, Koivisto T, Vasama K, Sand J, Laukkarinen J. Spyglass single-operator peroral cholangioscopy seems promising in the evaluation of primary sclerosing cholangitis-related biliary strictures. *Scand J Gastroenterol* 2014; **49**: 1385-1390 [PMID: 25259419 DOI: 10.3109/00365521.2014.940376]

20 **Arnelo U**, von Seth E, Bergquist A. Prospective evaluation of the clinical utility of single-operator peroral cholangioscopy in patients with primary sclerosing cholangitis. *Endoscopy* 2015; **47**: 696-702 [PMID: 25826274 DOI: 10.1055/s-0034-1391845]

21 **Pouw RE**, Barret M, Biermann K, Bisschops R, Czakó L, Gecse KB, de Hertogh G, Hucl T, Iacucci M, Jansen M, Rutter M, Savarino E, Spaander MCW, Schmidt PT, Vieth M, Dinis-Ribeiro M, van Hooft JE. Endoscopic tissue sampling - Part 1: Upper gastrointestinal and hepatopancreatobiliary tracts. European Society of Gastrointestinal Endoscopy (ESGE) Guideline. *Endoscopy* 2021; **53**: 1174-1188 [PMID: 34535035 DOI: 10.1055/a-1611-5091]

22 **de Oliveira PVAG**, de Moura DTH, Ribeiro IB, Bazarbashi AN, Franzini TAP, Dos Santos MEL, Bernardo WM, de Moura EGH. Efficacy of digital single-operator cholangioscopy in the visual interpretation of indeterminate biliary strictures: a systematic review and meta-analysis. *Surg Endosc* 2020; **34**: 3321-3329 [PMID: 32342216 DOI: 10.1007/s00464-020-07583-8]

23 **Badshah MB**, Vanar V, Kandula M, Kalva N, Badshah MB, Revenur V, Bechtold ML, Forcione DG, Donthireddy K, Puli SR. Peroral cholangioscopy with cholangioscopy-directed biopsies in the diagnosis of biliary malignancies: a systemic review and meta-analysis. *Eur J Gastroenterol Hepatol* 2019; **31**: 935-940 [PMID: 30896553 DOI: 10.1097/MEG.0000000000001402]

24 **Martinez NS**, Trindade AJ, Sejpal DV. Determining the Indeterminate Biliary Stricture: Cholangioscopy and Beyond. *Curr Gastroenterol Rep* 2020; **22**: 58 [PMID: 33141356 DOI: 10.1007/s11894-020-00797-9]

25 **Kawashima H**, Itoh A, Ohno E, Goto H, Hirooka Y. Transpapillary biliary forceps biopsy to distinguish benign biliary stricture from malignancy: how many tissue samples should be obtained? *Dig Endosc* 2012; **24** Suppl 1: 22-27 [PMID: 22533747 DOI: 10.1111/j.1443-1661.2012.01253.x]

26 **Kamisawa T**, Nakazawa T, Tazuma S, Zen Y, Tanaka A, Ohara H, Muraki T, Inui K, Inoue D, Nishino T, Naitoh I, Itoi T, Notohara K, Kanno A, Kubota K, Hirano K, Isayama H, Shimizu K, Tsuyuguchi T, Shimosegawa T, Kawa S, Chiba T, Okazaki K, Takikawa H, Kimura W, Unno M, Yoshida M. Clinical practice guidelines for IgG4-related sclerosing cholangitis. *J Hepatobiliary Pancreat Sci* 2019; **26**: 9-42 [PMID: 30575336 DOI: 10.1002/jhbp.596]

27 **Lee YY**, Gwak GY, Lee KH, Lee JK, Lee KT, Kwon CH, Joh JW, Lee SK. Predictors of the feasibility of primary endoscopic management of biliary strictures after adult living donor liver transplantation. *Liver Transpl* 2011; **17**: 1467-1473 [PMID: 21898773 DOI: 10.1002/lt.22432]

28 **Woo YS**, Lee JK, Noh DH, Park JK, Lee KH, Lee KT. SpyGlass cholangioscopy-assisted guidewire placement for post-LDLT biliary strictures: a case series. *Surg Endosc* 2016; **30**: 3897-3903 [PMID: 26684207 DOI: 10.1007/s00464-015-4695-7]

29 **Awadallah NS**, Chen YK, Piraka C, Antillon MR, Shah RJ. Is there a role for cholangioscopy in patients with primary sclerosing cholangitis? *Am J Gastroenterol* 2006; **101**: 284-291 [PMID: 16454832 DOI: 10.1111/j.1572-0241.2006.00383.x]

30 **Gluck M**, Cantone NR, Brandabur JJ, Patterson DJ, Bredfeldt JE, Kozarek RA. A twenty-year experience with endoscopic therapy for symptomatic primary sclerosing cholangitis. *J Clin Gastroenterol* 2008; **42**: 1032-1039 [PMID: 18580600 DOI:

10.1097/MCG.0b013e3181646713]
31 **Imanishi M**, Ogura T, Kurisu Y, Onda S, Takagi W, Okuda A, Miyano A, Amano M, Nishioka N, Masuda D, Higuchi K. A feasibility study of digital single-operator cholangioscopy for diagnostic and therapeutic procedure (with videos). *Medicine (Baltimore)* 2017; **96**: e6619 [PMID: 28403110 DOI: 10.1097/MD.0000000000006619]
32 **Andriulli A**, Loperfido S, Napolitano G, Niro G, Valvano MR, Spirito F, Pilotto A, Forlano R. Incidence rates of post-ERCP complications: a systematic survey of prospective studies. *Am J Gastroenterol* 2007; **102**: 1781-1788 [PMID: 17509029 DOI: 10.1111/j.1572-0241.2007.01279.x]
33 **Wen LJ**, Chen JH, Xu HJ, Yu Q, Liu K. Efficacy and Safety of Digital Single-Operator Cholangioscopy in the Diagnosis of Indeterminate Biliary Strictures by Targeted Biopsies: A Systematic Review and Meta-Analysis. *Diagnostics (Basel)* 2020; **10** [PMID: 32887436 DOI: 10.3390/diagnostics10090666]
34 **Navaneethan U**, Jegadeesan R, Nayak S, Lourdusamy V, Sanaka MR, Vargo JJ, Parsi MA. ERCP-related adverse events in patients with primary sclerosing cholangitis. *Gastrointest Endosc* 2015; **81**: 410-419 [PMID: 25085336 DOI: 10.1016/j.gie.2014.06.030]
35 **Korrapati P**, Ciolino J, Wani S, Shah J, Watson R, Muthusamy VR, Klapman J, Komanduri S. The efficacy of peroral cholangioscopy for difficult bile duct stones and indeterminate strictures: a systematic review and meta-analysis. *Endosc Int Open* 2016; **4**: E263-E275 [PMID: 27004242 DOI: 10.1055/s-0042-100194]

World Journal of Gastroenterology

Submit a Manuscript: https://www.f6publishing.com

World J Gastroenterol 2022 May 28; 28(20): 2214-2226

DOI: 10.3748/wjg.v28.i20.2214

ISSN 1007-9327 (print) ISSN 2219-2840 (online)

ORIGINAL ARTICLE

Retrospective Study

Gadolinium-ethoxybenzyl-diethylenetriamine penta-acetic acid-enhanced magnetic resonance imaging for evaluating fibrosis regression in chronic hepatitis C patients after direct-acting antiviral

Xiao-He Li, Rui Huang, Ming Yang, Jian Wang, Ying-Hui Gao, Qian Jin, Dan-Li Ma, Lai Wei, Hui-Ying Rao

Specialty type: Gastroenterology and hepatology

Provenance and peer review: Unsolicited article; Externally peer reviewed.

Peer-review model: Single blind

Peer-review report's scientific quality classification

Grade A (Excellent): 0
Grade B (Very good): B
Grade C (Good): 0
Grade D (Fair): 0
Grade E (Poor): 0

P-Reviewer: Mogahed EA, Egypt

Received: September 30, 2021
Peer-review started: September 30, 2021
First decision: March 11, 2022
Revised: March 25, 2022
Accepted: April 21, 2022
Article in press: April 21, 2022
Published online: May 28, 2022

Xiao-He Li, Rui Huang, Ming Yang, Jian Wang, Ying-Hui Gao, Qian Jin, Dan-Li Ma, Lai Wei, Hui-Ying Rao, Peking University Hepatology Institute, Beijing Key Laboratory of Hepatitis C and Immunotherapy for Liver Diseases, Beijing International Cooperation Base for Science and Technology on NAFLD Diagnosis, Peking University People's Hospital, Beijing 100044, China

Ming Yang, Lai Wei, Hepatopancreatobiliary Center, Beijing Tsinghua Changgung Hospital, Tsinghua University, Beijing 100044, China

Corresponding author: Hui-Ying Rao, MD, Chief Doctor, Professor, Peking University Hepatology Institute, Beijing Key Laboratory of Hepatitis C and Immunotherapy for Liver Diseases, Beijing International Cooperation Base for Science and Technology on NAFLD Diagnosis, Peking University People's Hospital, No.11 Xizhimen South Street, Xicheng District, Beijing 100044, China. rao.huiying@163.com

Abstract

BACKGROUND

Direct acting antiviral (DAA) therapy has enabled hepatitis C virus infection to become curable, while histological changes remain uncontained. Few valid non-invasive methods can be confirmed for use in surveillance. Gadolinium-ethoxy-benzyl-diethylenetriamine penta-acetic acid (Gd-EOB-DTPA) is a liver-specific magnetic resonance imaging (MRI) contrast, related to liver function in the hepatobiliary phase (HBP). Whether Gd-EOB-DTPA-enhanced MRI can be used in the diagnosis and follow up of hepatic fibrosis in patients with chronic hepatitis C (CHC) has not been investigated.

AIM

To investigate the diagnostic and follow-up values of Gd-EOB-DTPA-enhanced MRI for hepatic histology in patients with CHC.

METHODS

Patients with CHC were invited to undergo Gd-EOB-DTPA-enhanced MRI and liver biopsy before treatment, and those with paired qualified MRI and liver biopsy specimens were included. Transient elastography (TE) and blood tests were also arranged. Patients treated with DAAs who achieved 24-wk sustained

virological response (SVR) underwent Gd-EOB-DTPA-enhanced MRI and liver biopsy again. The signal intensity (SI) of the liver and muscle were measured in the unenhanced phase (UEP) ($SI_{UEP\text{-}liver}$, $SI_{UEP\text{-}muscle}$) and HBP ($SI_{HBP\text{-}liver}$, $SI_{HBP\text{-}muscle}$) *via* MRI. The contrast enhancement index (CEI) was calculated as $[(SI_{HBP\text{-}liver}/SI_{HBP\text{-}muscle})]/[(SI_{UEP\text{-}liver}/SI_{UEP\text{-}muscle})]$. Liver stiffness measurement (LSM) was confirmed with TE. Serologic markers, aspartate aminotransferase-to-platelet ratio index (APRI) and Fibrosis-4 (FIB-4), were also calculated according to blood tests. The grade of inflammation and stage of fibrosis were evaluated with the modified histology activity index (mHAI) and Ishak fibrosis score, respectively. Fibrosis regression was defined as a ≥ 1-point decrease in the Ishak fibrosis score. The correlation between the CEI and liver pathology was evaluated. The diagnostic and follow-up values of the CEI, LSM, and serologic markers were compared.

RESULTS

Thirty-nine patients with CHC were enrolled [average age, 42.3 ± 14.4 years; 20/39 (51.3%) male]. Twenty-one enrolled patients had eligible paired Gd-EOB-DTPA-enhanced MRI and liver tissues after achieving SVR. The mHAI median significantly decreased after SVR [baseline 6.0 (4.5-13.5) *vs* SVR 2.0 (1.5-5.5), $Z = 3.322$, $P = 0.017$], but the median stage of fibrosis did not notably change ($P > 0.05$). Sixty pairs of qualified MRI and liver tissue samples were available for use to analyze the relationship between the CEI and hepatic pathology. The CEI was negatively correlated with the mHAI ($r = -0.56$, $P < 0.001$) and Ishak score ($r = -0.69$, $P < 0.001$). Further stratified analysis showed that the value of the CEI decreased with the progression of the stage of fibrosis rather than with the grade of necroinflammation. For patients with Ishak score ≥ 5, the areas under receiver operating characteristics curve of the CEI, LSM, APRI, and FIB-4 were approximately at baseline, 0.87–0.93, and after achieving SVR, 0.83–0.91. The CEI cut-off value was stable (baseline 1.58 and SVR 1.59), but those of the APRI (from 1.05 to 0.24), FIB-4 (from 1.78 to 1.28), and LSM (from 10.8 kpa to 7.1 kpa) decreased dramatically. The APRI and FIB-4 cannot be used as diagnostic means for SVR in patients with Ishak score ≥ 3 ($P > 0.05$). Seven patients achieved fibrosis regression after achieving SVR. In these patients, the CEI median increased (from 1.71 to 1.83, $Z = -1.981$, $P = 0.048$) and those of the APRI (from 1.71 to 1.83, $Z = -2.878$, $P = 0.004$) and LSM (from 6.6 to 4.8, $Z = -2.366$, $P = 0.018$) decreased. However, in patients without fibrosis regression, the medians of the APRI, FIB-4, and LSM also changed significantly ($P < 0.05$).

CONCLUSION

Gd-EOB-DTPA-enhanced MRI has good diagnostic value for staging fibrosis in patients with CHC. It can be used for fibrotic-change monitoring post SVR in patients with CHC treated with DAAs.

Key Words: Gadolinium-ethoxybenzyl-diethylenetriamine penta-acetic acid-enhanced magnetic resonance imaging; Contrast enhancement index; Hepatitis C virus; Direct acting antiviral; Sustained virological response; Fibrosis regression

Core Tip: In this prospective, comparative study, the correlation between the contrast enhancement index (CEI) in the hepatobiliary phase of gadolinium-ethoxybenzyl-diethylenetriamine penta-acetic acid enhanced magnetic resonance imaging and liver pathology measures was analyzed in patients with chronic hepatitis C. It was determined that the CEI has good diagnostic performance and is more useful than serological markers and transient elastography for hepatic-fibrosis monitoring in patients achieving sustained virological response.

Citation: Li XH, Huang R, Yang M, Wang J, Gao YH, Jin Q, Ma DL, Wei L, Rao HY. Gadolinium-ethoxybenzyl-diethylenetriamine penta-acetic acid-enhanced magnetic resonance imaging for evaluating fibrosis regression in chronic hepatitis C patients after direct-acting antiviral. *World J Gastroenterol* 2022; 28(20): 2214-2226
URL: https://www.wjgnet.com/1007-9327/full/v28/i20/2214.htm
DOI: https://dx.doi.org/10.3748/wjg.v28.i20.2214

INTRODUCTION

Chronic hepatitis C (CHC) remains one of the major etiologies of chronic liver disease, causing

substantial morbidity and mortality globally[1,2]. Remarkably well-tolerated, effective, and short-time direct acting antiviral (DAA) regimens have revolutionized therapy for hepatitis C virus (HCV) infection, achieving a high rate of sustained virological response (SVR). However, it has also been reported that despite achieving SVR, patients may still experience disease progression[3,4]. It is critical to follow up pathological changes in the liver after DAA therapy. A growing number of studies have focused on the use of non-invasive tests to substitute liver biopsy[5-7]. However, there are few validated thresholds for longitudinal assessment that correspond to histologic changes in fibrosis, and there is no definite non-invasive method for diagnosing the stage changes in fibrosis after SVR.

Gadolinium-ethoxybenzyl-diethylenetriamine penta-acetic acid (Gd-EOB-DTPA; Promovist® in Europe and Eovist® in the United States, Bayer Healthcare, Berlin, Germany) is a liver-specific magnetic resonance imaging (MRI) contrast agent[8]. The hepatocyte uptake and biliary excretion of Gd-EOB-DTPA mainly take place *via* organic anion transporting polypeptides OATP1B1/3 on the sinusoidal membrane and multidrug resistance-associated proteins MRP2 on the canalicular membrane. Therefore, after intravenous injection, Gd-EOB-DTPA shows extracellular distribution in the dynamic phase and hepatocyte-specific transportation in the hepatobiliary phase (HBP). Decrease in the number of normal hepatocytes and impaired hepatocyte function may reduce the hepatic enhancement of the HBP[9]. It has been reported using Gd-EOB-DTPA-enhanced MRI to identify hepatocellular carcinoma[10], evaluate liver function[11,12], stage liver fibrosis[13,14], and predict liver failure after hepatectomy[15].

To the best of our knowledge, no studies have used Gd-EOB-DTPA-enhanced MRI to evaluate changes in fibrosis after SVR with paired liver biopsy. The primary aim of our study was to evaluate the diagnostic performance of Gd-EOB-DTPA-enhanced MRI in staging liver fibrosis. The secondary aim was to confirm whether this diagnostic test can be used for longitudinal assessment of liver fibrosis in patients with CHC after achieving SVR treated by DAA regimens.

MATERIALS AND METHODS

Study design

Patients with chronic HCV infection treated with DAAs in our hepatology center between January 2014 and December 2016 were prospectively invited to undergo Gd-EOB-DTPA-enhanced MRI and liver biopsy. Patients with qualified Gd-EOB-DTPA-enhanced MRI data and liver biopsy samples were enrolled. The selection of DAA regimens was based on the genotype and state of liver disease. The patients who achieved SVR after DAA therapy underwent the examinations a second time. Exclusion criterias were: (1) Non-HCV etiology-related chronic liver disease (such as chronic hepatitis B, drug-or alcohol-related liver disease, non-alcoholic steatohepatitis, *etc.*); (2) Clinical hepatic decompensation; (3) Solid organ transplantation; (4) Malignancy; (5) Combined with other systemic disease (immune system disease, blood system disease, *etc.*) and (6) Contraindications for MRI and liver biopsy. SVR was defined as undetectable HCV RNA 24 wk after the end of treatment.

Liver biopsy was performed within 1 mo before treatment and 3 mo after SVR. MRI was performed prior to liver biopsy within 1 mo. MRI with marked motion artifacts and specimens of liver tissue with lengths < 10 mm or < six portal areas under the microscope were regarded as inappropriate[16]. Demographic information, virologic data, and laboratory findings were collected.

MRI protocol

All liver MRI examinations were performed with a Discover 750 3.0 T MR scanner (GE Healthcare, Milwaukee, WI, United States) using a 32-channel torso array coil. Patients were in the supine position during horizontal axis scanning and had received prior training on how to breathe. Gd-EOB-DTPA (Promovist®, Bayer Healthcare) was injected intravenously as a contrast agent at a dose of 0.1 mL/kg body weight with a flow rate of 2 mL/s, followed by a 20-mL 0.09% NaCl flush. Three-dimensional T1-weighted contrast-enhanced MRI was conducted in the unenhanced phase (UEP), arterial phase (AP, 25 s), portal phase (60 s), and HBP (20 min).

Image analysis

The signal intensities (SIs) of the liver parenchyma and paraspinal muscle in the UEP ($SI_{UEP\text{-}liver}$ and $SI_{UEP\text{-}muscle}$) and HBP ($SI_{HBP\text{-}liver}$ and $SI_{HBP\text{-}muscle}$) were independently measured by two professional radiologists with nearly 4 and 6 years of experience in interpreting abdominal MRIs, using regions of interests (ROIs). The radiologists were blinded to the patients' clinical data and pathological changes.

Four ROIs were manually circled (size: 100–150 mm^2) in the posterior and anterior segments of the right hepatic lobe and inner and lateral segments of the left hepatic lobe at the hepatic hilar level. The location of the ROIs had to be at the center of each segment, far from the abdominal wall, and avoiding visible blood vessels, bile ducts, and lesions. The ROI of the paraspinal muscle was mainly circled on the left side.

The contrast enhancement index (CEI) was calculated using the following formula[17]:

$CEI = (SI_{HBP\text{-}liver}/SI_{HBP\text{-}muscle})/(SI_{UEP\text{-}liver}/SI_{UEP\text{-}muscle})$

The change rate in the CEI (Δ CEI%) between pre-treatment (CEI_{pre}) and post-SVR (CEI_{post}) was calculated as ($CEI_{post}/CEI_{pre} \times 100\%$).

Histopathological analysis

Specimens were fixed in formalin immediately after liver biopsy and embedded in paraffin; 4-μm-thick sections were cut and stained with hematoxylin and eosin and Masson's trichrome. Two professional hepato-pathologists, both with nearly 30 years of working experience, assessed the degree and stage of necroinflammation and fibrosis of the specimens using the Ishak scoring system [modified histological activity index (mHAI) and Ishak score][18]. The pathologists were blinded to the imaging results and patient clinical data. The stages of liver fibrosis were divided into three groups according to the Ishak score, 0-2, 3-4, and 5-6, respectively. Necro-inflammatory severity was graded according to the mHAI score as 0-4, 5-8, 9-12, and 13-18[19]. Fibrosis regression was defined as a decrease of at least one point in the Ishak score after SVR[20].

Non-invasive fibrosis measurements

Experienced technicians conducted liver stiffness measurements (LSMs) with FibroScan (Echosens, Paris, France). An effective result should have a successful rate > 60% and interquartile range/median ratio ≤ 30%.

With respect to serologic biomarkers of fibrosis, the aspartate aminotransferase (AST)-to-platelet ratio (APRI) and Fibrosis-4 (FIB-4) were calculated as following:

APRI = [(AST/ULN)/platelet count ($\times 10^9$/L)] × 100[21]; FIB-4 = (age × AST)/[(platelet count) ($\times 10^9$/L) × ALT1/2][22]

The change rates in APRI, FIB-4, and LSM between pre-SVR ($value_{pre}$) and post-SVR ($value_{post}$) were calculated similarly with the CEI calculation.

Statistical analyses

Descriptive analyses were performed for sociodemographic characteristics (age, sex), clinical data [alanine aminotransferase (ALT), AST, total bilirubin (TB), albumin (Alb), platelet (PLT) count, HCV RNA, genotype, FIB-4, APRI, LSM, and CEI], histological grading, and staging.

Descriptive analyses were performed for sociodemographic characteristics, clinical data, histological characteristics, and the CEI. The value of HCV RNA was logarithmically transformed with 10 as the base. Continuous variables are expressed as median (interquartile range) (ALT, AST, TB, PLT, APRI, FIB-4, and LSM) or mean ± SD [age, Alb, international normalized ratio (INR), HCV RNA, mHAI, and CEI]. Categorical variables (sex, numbers of patients in the different mHAI and Ishak score groups) are presented as counts and percentages. The absolute values of the interclass correlation coefficients (ICC) were measured for SIs to confirm the interobserver reliability between reviewers. Student's t-test (age, Alb, INR, HCV RNA, mHAI, and CEI) and Mann-Whitney U test (ALT, AST, TB, and PLT) were used to compare continuous variables, and the chi-square test was used for classified variables (sex, HCV genotype). The comparison between pre-and post-SVR was performed with the Wilcoxon sign rank test (ALT, AST, TB, PLT, FIB-4, APRI, and LSM) and paired sample t-test (Alb, INR, and CEI). Spearman's correlation coefficient was calculated for the CEI, mHAI, and Ishak score. The predictive value of the CEI, APRI, FIB-4, and LSM for liver fibrosis was assessed using the area under the receiver operating characteristic curve (AUROC). Sensitivity, specificity, positive predictive value, and negative predictive value were also calculated. An optimal cut-off value was chosen to maximize the Youden index, which is defined as (sensitivity + specificity-1). P values < 0.05 were considered statistically significant. Statistical analyses were performed using IBM SPSS version 26.0 (IBM Corp., Armonk, NY, United States).

RESULTS

Forty-five patients underwent Gd-EOB-DTPA-enhanced MRI and liver biopsy at baseline and six with unqualified samples were excluded. Among the enrolled patients (n = 39), six were recommended to receive treatment with DAA plus Peg-IFN, and three had virological breakthrough. Twenty-five patients underwent MRI and liver biopsy again after achieving SVR, and 21 pairs of data were eligible. Therefore, there were 60 qualified and pairable MRI images and liver tissue samples available for analyzing correlation between CEI and liver pathology. The study flow chart is shown in Figure 1.

Intraclass correlation coefficients

Two radiologists interpreted the Gd-EOB-DTPA-enhanced MRI images. The ICC for the measured SI values were excellent (greater than 0.9) for before and after achieving SVR. The ICC of the CEI was 0.729 (0.481, 0.858) and 0.886 (0.744, 0.952) pre and post SVR, respectively. Details of the inter-observer agreements of the ROI measurements and CEI are presented in Supplementary Table 1.

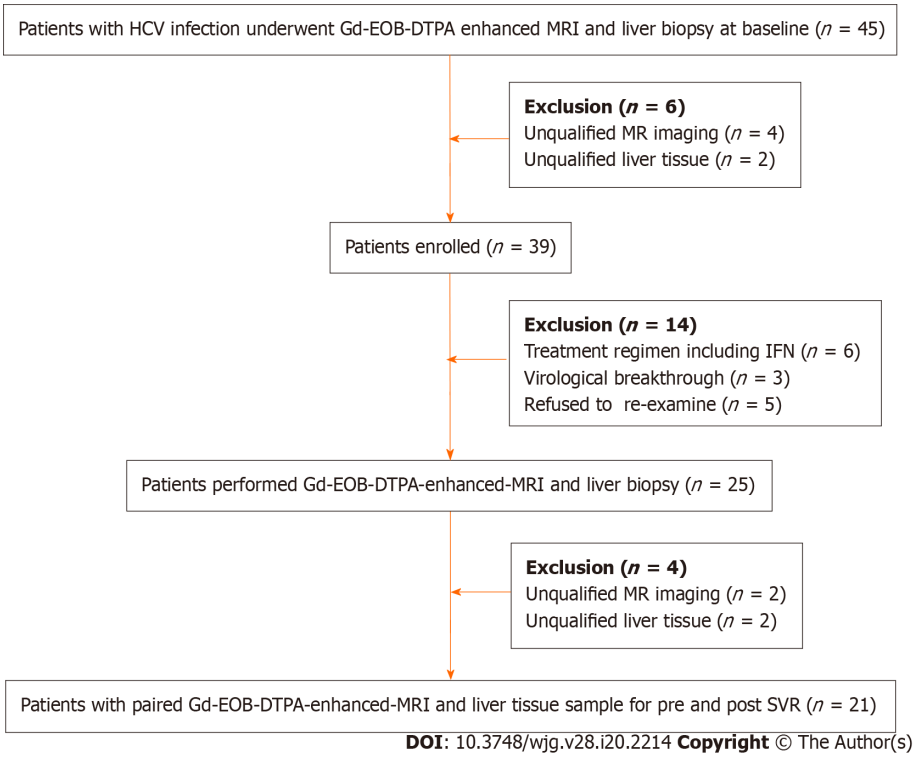

DOI: 10.3748/wjg.v28.i20.2214

Figure 1 The study flow chart. HCV: Hepatitis C virus; Gd-EOD-DTPA: Gadolinium ethoxybenzyl diethylenetriamine penta-acetic acid; MRI: Magnetic resonance imaging; IFN: Interferon; SVR: Sustained virological response.

Patient characteristics

The 39 patients enrolled had a mean age of (42.3 ± 14.4) years, mean HCV RNA of (6.4 ± 0.7) $\log_{10}$ IU/mL, and 20 (51.3%) were male. The distribution of HCV genotypes (GT) was 1, 2, 3, and 6 in 19 (48.7%), 4 (10.3%), 13 (33.3%), and 3 (7.7%) patients, respectively. Patients with Ishak score of 5-6 were elder, had higher ALT and lower PLT levels than those with Ishak scores of 0–2 ($P < 0.05$) (Table 1).

Of the 21 patients who achieved SVR and had paired MRI and liver tissue samples, 13 (62%) received sofosbuvir/ribavirin therapy, and the other eight (38%) received daclatasvir/asunaprevir regimens. As expected, the values of ALT, AST ($P < 0.001$), and necroinflammation grade ($P = 0.023$) significantly decreased post SVR (Table 2). No significant change in fibrosis stage was observed. Among the noninvasive measurements, the median of LSM, FIB-4, and APRI decreased significantly, the mean of the CEI increased slightly without statistically significant ($P = 0.29$) (Table 2). After achieving SVR, 7 (33%) patients achieved fibrosis regression. No patient with Ishak 5-6 ($n = 7$) achieved fibrosis regression.

The CEI decreased with the progression of liver fibrosis

In patients with CHC, the CEI was negatively correlated with the grade of inflammation ($r = -0.56$, $P < 0.001$) and stage of fibrosis ($r = -0.69$, $P < 0.001$). The CEI decreased significantly among patients with Ishak scores 0–2, 3–4, and 5–6 (1.78 ± 0.11, 1.64 ± 0.11, and 1.50 ± 0.09, respectively, $P < 0.001$) (Figure 2A). To further analyze the relationship between the CEI and liver pathology, we stratified the patients according to the mHAI (0–4, 5–8, 9–12, and 13–18) and Ishak score (0–2, 3–4, and 5–6; the numbers of patients in each subgroup are shown in Table 3).

In patients with a mHAI of 0–4, the CEI in Group 2 ($n = 11$) was significantly lower than that in Group 1 ($n = 14$) [(1.67 ± 0.11) *vs* (1.79 ± 0.11), $P = 0.021$] and the CEI of the only patient in Group 3 was 1.52 (Figure 2B). When the mHAI was 5–8, the CEI decreased in the order of fibrosis Group 1 ($n = 3$), 2 ($n = 13$), and 3 ($n = 9$) at 1.75 ± 0.06, 1.62 ± 0.11, and 1.49 ± 0.12, respectively ($P = 0.032$) (Figure 2C). All patients with an mHAI of 13–18 had liver cirrhosis ($n = 9$), and they were not grouped. In contrast, after subgrouping the patients based on the fibrosis grade, there were no significant differences in the CEI among the inflammation groups (all $P > 0.05$) (Figure 2D–F). Therefore, we believe that decrease in the CEI is mainly associated with the progression of fibrosis.

The CEI is more useful for liver fibrosis diagnosis than the LSM, APRI, and FIB-4

Table 4 shows a comparison of the predictive values between the CEI and other non-invasive methods. According to the AUROCs and cut-off values, we found that the diagnostic efficacy of the CEI, LSM, APRI, and FIB-4 before and after DAA treatment was similar for liver cirrhosis (Ishak score ≥ 5), while

Table 1 Comparison of demographic and clinical data of patients

Parameters	Ishak 0-2 (*n* = 9)	Ishak 3-4 (*n* = 18)	Ishak 5-6 (*n* = 12)
Age (yr)	36.3 ± 15.5	37.9 ± 12.4	53.1 ± 11.0[b]
Male, *n* (%)	2 (22.2)	11 (61.1)	7 (58.3)
ALT (U/L)	44 (22.5)	52.5 (35.5)	75.5 (98.7)[a]
TB (μmol/L)	11 (7.5)	14 (3.5)	12.5 (7.5)
Alb (g/L)	46.78 ± 3.77	45.72 ± 3.75	44.17 ± 3.35
INR	0.99 ± 0.07	1.00 ± 0.09	1.09 ± 0.16
PLT (× 10^9/L)	171 (62.5)	177.5 (64.7)	114 (67.5)[b]
HCV RNA (log_{10} IU/mL)	6.43 ± 0.96	6.50 ± 0.71	6.33 ± 0.64
mHAI score	3.4 ± 1.7	5.3 ± 1.6[a]	11.3 ± 4.0[c]

[a]$P < 0.05$ compared with patients with Ishak 0-2.
[b]$P < 0.01$ compared with patients with Ishak 0-2.
[c]$P < 0.001$ compared with patients with Ishak 0-2.
ALT: Alanine aminotransferase; TB: Total bilirubin; INR: International normalized ratio; HCV: Hepatitis C virus; mHAI: Modified histology activity index.

Table 2 Clinical characteristics of patients for pre and post sustained virological response

	Pre SVR	Post SVR	*Z/t* value	*P* value
ALT (U/L)	55 (29.5)	17 (11)	-4.015	< 0.001
AST (U/L)	40 (29.5)	20 (10.5)	-4.016	< 0.001
TB (μmol/L)	14 (6.5)	15.5 (11.3)	-0.541	0.588
Alb (g/L)	44.90 ± 3.40	47.43 ± 3.06	-3.919	0.001
Platelet (× 10^9/L)	165 (87)	199 (130)	-2.576	0.01
INR	1.04 ± 0.14	1.02 ± 0.07	0.425	0.675
mHAI score, *n* (%)			-2.362	0.023
0-4	5 (24)	15 (71)		
5-8	10 (48)	4 (9)		
13-18	6 (28)	2 (10)		
Ishak score, *n* (%)			-0.370	0.713
0-2	5 (24)	7 (33)		
3-4	9 (43)	7 (33)		
5-6	7 (33)	7 (33)		
APRI	0.58 (1.32)	0.25 (0.40)	-4.015	< 0.001
FIB-4	1.34 (3.61)	0.99 (1.81)	-3.007	0.003
LSM (kpa)	6.6 (7.5)	5.8 (4.0)	-2.746	0.006
CEI	1.65 ± 0.11	1.68 ± 0.16	-1.087	0.29

ALT: Alanine aminotransferase; AST: Aspartate aminotransferase; APRI: AST-to platelet ratio index; CEI: Contrast enhancement index; HCV: Hepatitis C virus; INR: International normalized ratio; mHAI: Modified histology activity index; LSM: Liver stiffness measurement; SVR: Sustained virological response; TB: Total bilirubin.

the cut-off values of serological markers such as the APRI and FIB-4 significantly decreased post SVR. The cut-off value of the LSM also showed a similar trend. For significant fibrosis (Ishak score ≥ 3), post SVR, the diagnostic efficacy of the LSM decreased, and the APRI and FIB-4 showed no diagnostic value.

Table 3 Distribution of patients in stratified analysis

Stratified analysis	Group 1	Group 2	Group 3
mHAI score	**Ishak score**		
	0-2	3-4	5-6
0-4	14	11	1
5-8	3	13	9
13-18	0	0	9
Ishak score	**mHAI score**		
	0-4	5-8	13-18
0-4	14	2	0
3-4	10	15	0
5-6	1	9	9

mHAI: Modified histology activity index.

Table 4 The area under receiver operating curve and cut-off value for liver cirrhosis and significant liver fibrosis at pre-sustained virological response and post-sustained virological response with contrast enhancement index, aspartate aminotransferase-to-platelet ratio index, Fibrosis-4 and liver stiffness measurement

	Ishak score ≥ 5		Ishak score ≥ 3	
	Pre SVR	Post SVR	Pre SVR	Post SVR
CEI				
AUROC (95%CI)	0.93 (0.74, 0.97)	0.87 (0.65, 0.97)	0.88 (0.79, 1.00)	0.87 (0.71, 1.00)
Cut-off value	1.58	1.59	1.71	1.68
LSM				
AUROC (95%CI)	0.87(0.71, 1.00)	0.87(0.79, 1.00)	0.91(0.78, 1.00)	0.80(0.60,0.98)
Cut-off value	10.8	7.1	6.2	5.95
APRI				
AUROC (95%CI)	0.89(0.72, 1.00)	0.89(0.74, 1.00)	0.83(0.64, 1.00)	N[2]
Cut-off value	1.05	0.24[1]	0.39	N[2]
FIB-4				
AUROC (95%CI)	0.92(0.80, 1.00)	0.92(0.79, 1.00)	0.80(0.58, 1.00)	N[2]
Cut-off value	1.78	1.28[1]	0.87	N[2]

[1]The cutoff values of aspartate aminotransferase-to-platelet ratio index (APRI) and Fibrosis-4 (FIB-4) or the diagnosis of liver cirrhosis decreased dramatically after sustained virological response (SVR).
[2]N: No diagnosis value of APRI or FIB-4 in patients with significant fibrosis after achieving SVR.
APRI: Aspartate aminotransferase-to-platelet ratio index; AUROC: Area under receiver operating curve; CEI: Contrast enhancement index; CI: Confidence interval; FIB-4: Fibrosis-4; LSM: Liver stiffness measurement; SVR: Sustained virological response.

Only dynamic change in the CEI can be used to evaluate fibrosis regression after achieving SVR

Figure 3 shows the change of the CEI and other non-invasive methods in patients with (red column) and without (black column) fibrosis regression. Among the patients with fibrosis regression (n = 7), the CEI increased significantly (from 1.68 ± 0.09 to 1.83 ± 0.18, P = 0.043) after DAA treatment; similarly, the LSM [from 6.6 (2.6) to 4.8 (1.2), P = 0.018] and APRI [from 0.37 (0.22) to 0.20 (0.08), P = 0.018] values decreased significantly. For patients who did not achieve fibrosis regression (n = 14), only the CEI remained stable (P > 0.05), while the LSM, APRI, and FIB-4 decreased significantly (P < 0.05). It is suggested that the decrease in the latter three noninvasive measurements after treatment may not be related to fibrosis regression. By comparing the change ratios of the four noninvasive indexes before and after treatment, only CEI% changed significantly, and CEI% was moderately positively correlated with

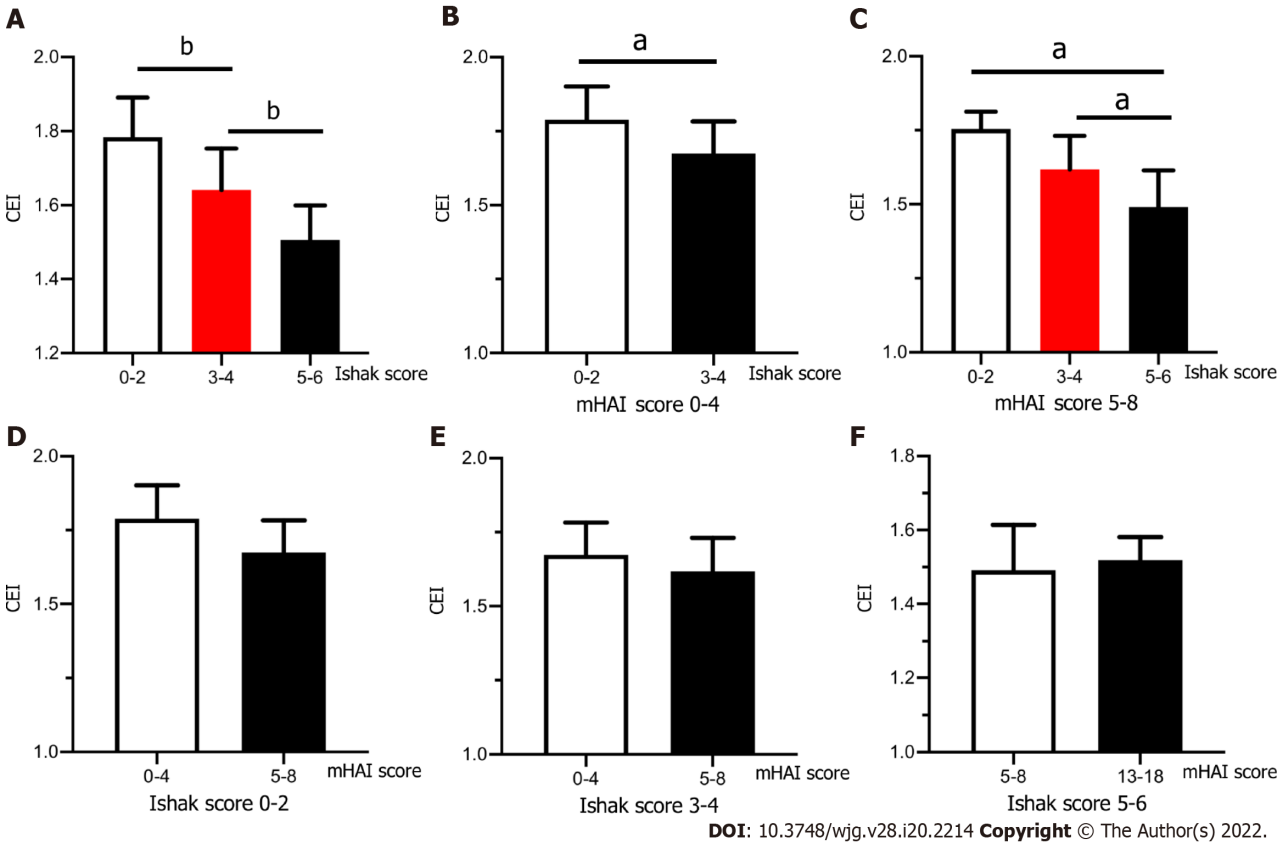

DOI: 10.3748/wjg.v28.i20.2214

Figure 2 Contrast enhancement index decreased with the progression of liver fibrosis. A: Contrast enhancement index (CEI) decreased with the progression of fibrosis, and there was significant difference between patients with Ishak score 0-2, 3-4 and 5-6; B: In patients with modified histology activity index (mHAI) score of 0-4, CEI was lower in patients with Ishak score of 3-4 compared with 0-2; C: In patients with mHAI score of 5-8, CEI decreased with the progression of fibrosis stage; D-F: When the Ishak scores was fixed as 0-2, 3-4 and 5-6 respectively, the value of CEI was not related to the progression of inflammation. $^{a}P < 0.05$; $^{b}P < 0.001$. CEI: Contrast enhancement index; mHAI: Modified histology activity index.

fibrosis regression ($r = 0.50$, $P = 0.021$) (Table 5).

DISCUSSION

In this study, paired liver biopsy and Gd-EOB-DTPA-enhanced MRI data of patients with CHC before and after SVR were reported for the first time. This study concluded that the CEI of Gd-EOB-DTPA-enhanced MRI in the HBP decreased with the progression of liver fibrosis. For patients with CHC, the CEI can be used to distinguish among the different stages of liver fibrosis at baseline and after achieving SVR more effectively than the APRI, FIB-4, and LSM. The change in the CEI between pre and post SVR was related to fibrosis regression. This result increased the options for dynamic assessment of liver fibrosis after achieving SVR.

In our study, patients treated with DAA plus interferon were excluded. Although the combination therapy may have no effect on the evaluation of liver pathology, based on the current situation of CHC treatment, majority of patients can be cured by simple DAAs. So, we pay more attention on correlation between CEI and pathology changes in patients cured by simple DAAs. It is worth mentioning that, HCV RNA was both detected at 12- and 24-wk after the end of treatment. The value of HCV RNA at 12-wk were also undetectable in patients achieving SVR24. Since patients were enrolled between 2014-2016, SVR12 and SVR24 both could be used at that time, while the 24-wk SVR last longer, it was used in our article. We specially agree that the current definition of SVR as an undetectable HCV RNA at 12 wk after the end of treatment.

In the correlation analysis, we found that the CEI was mild negative related to both grade of inflammation and stage of fibrosis. Further hierarchical analysis showed that the CEI mainly decreased with the progression of liver fibrosis, which was consistent with the results of a previous multiple regression analysis[23]. As mentioned above, after achieving SVR, the overall liver fibrosis status was not notably improved, and the CEI also did not change significantly. Therefore, we combined 60 pairs of CEI and liver pathology data before and after treatment for analysis. It should be mentioned that the overall mHAI decreased after treatment, which may have affected the results. However, in our pre-analysis, we

Table 5 Relationship between the changes of contrast enhancement index, aminotransferase-to-platelet ratio index, Fibrosis-4, liver stiffness measurement and fibrosis regression

	Fibrosis regression		*P* value
	Yes (*n* = 7)	No (*n* = 14)	
CEI%[1]	107.36 ± 6.33	99.23 ± 7.14	0.020
LSM%	72.06 ± 20.32	81.31 ± 27.44	0.441
APRI%	45.40 ± 13.16	42.51 ± 16.41	0.702
FIB-4%	90.39 ± 24.09	75.69 ± 23.66	0.936

[1]Value% = $Value_{post}/Value_{pre}$ × 100%.
CEI: Contrast enhancement index; SVR: Sustained virological response; LSM: Liver stiffness measurement; APRI: Aspartate aminotransferase-to-platelet ratio index; FIB-4: Fibrosis-4.

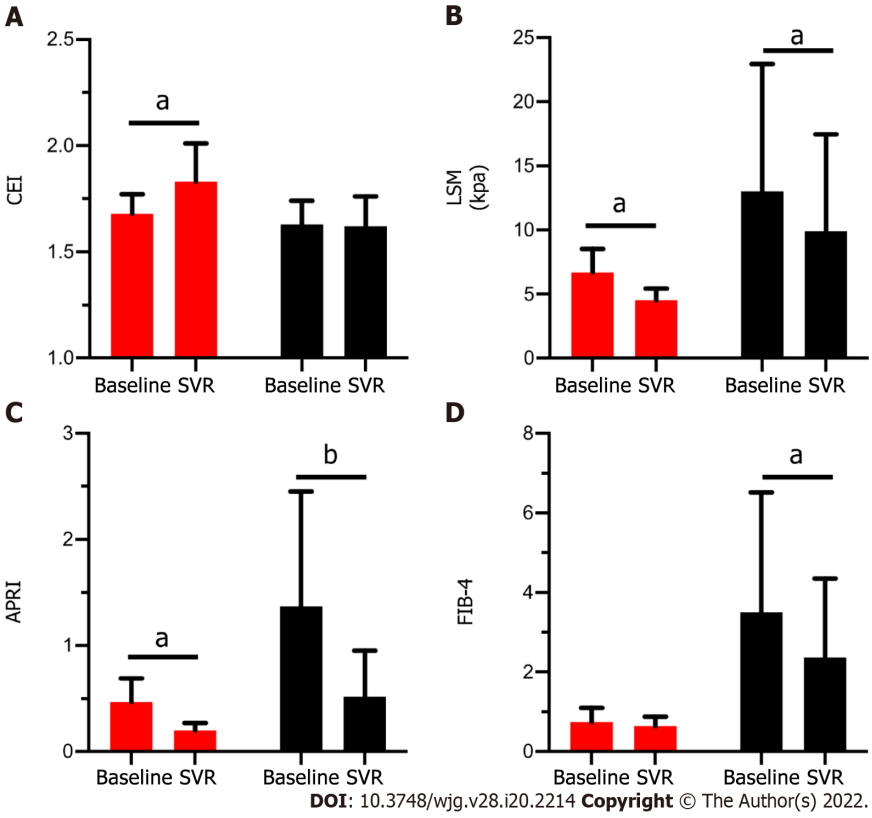

DOI: 10.3748/wjg.v28.i20.2214

Figure 3 Comparison of four noninvasive methods before and after sustained virological response between patients with fibrosis regression or not. A: Value of contrast enhancement index; B: Value of liver stiffness measurement; C: Value of aspartate aminotransferase-to-platelet ratio index; D: Value or Fibrosis-4 in patients with (Red column) and without (Black column) fibrosis regression at baseline and after achieving sustained virological response (SVR). Red column: Patients had fibrosis regression after achieving SVR (*n* = 7). Black column: Patients didn't have fibrosis regression after achieving SVR (*n* = 14). $^{a}P < 0.05$; $^{b}P < 0.001$. CEI: Contrast enhancement index; SVR: Sustained virological response; LSM: Liver stiffness measurement; APRI: Aspartate aminotransferase-to-platelet ratio index; FIB-4: Fibrosis-4.

found that in the 21 paired MRI and liver biopsy samples after treatment, the correlation between the mHAI and Ishak score ($r = 0.74$, $P < 0.001$) remained significant. This may be because the patients with a mHAI > 13 at baseline had liver cirrhosis. After achieving SVR, there was no significant improvement in fibrosis or in the inflammation status. It was also shown that the correlation between the CEI and fibrosis stage remained relatively stable and was not related to the treatment state.

In patients with liver cirrhosis (Ishak score 5-6), the diagnostic values of the CEI and of the other non-invasive methods were similar, which was also partly previously reported by a cross-sectional comparative analysis[23]. As the inflammatory status improved with antiviral treatment, the cut-off values of the APRI (from 1.05 to 0.24) and FIB-4 (from 1.78 to 1.28) both substantially decreased for the same fibrosis status. The serological biomarkers had no diagnostic value for significant fibrosis after HCV eradication, mainly because with the rapid regression of liver necroinflammation, the ALT and

AST levels returned to normal, reducing the diagnostic accuracy of serological biomarkers. Although accessible and common, the APRI and FIB-4 may not be suitable for the surveillance of patients with CHC post SVR[21,24].

Other than the serological biomarkers, the LSM obtained with TE is currently considered useful for fibrosis monitoring[25-27]. However, several studies have reported a rapid decrease in the LSM mainly related to inflammation regression, and its cut-off values are influenced by liver morphometry. Hence, the decrease in the LSM may be misinterpreted as change in the liver fibrosis stage[6,28]. A longitudinal study of 2 years showed that following SVR attainment, the improvements in the LSM were overstated compared to histologic staging[28]. Therefore, the follow-up value of liver fibrosis regression in patients with HCV SVR needs to be further verified. Our findings strengthened this notion in a relative short follow-up time (median of 6.2 mo). The cut-off value of the LSM decreased slightly in patients with liver cirrhosis (from 10.8 kPa to 7.1 kPa), wherein an LSM value of 7.1 kPa obtained with TE was defined as the threshold for absence of or minimal fibrosis in patients with CHC[29]. The comparative analysis also showed significant decrease in the LSM value in patients without fibrosis regression.

Apart from the CEI, several studies have reported multiple hepatobiliary liver enhancement indexes of Gd-EOB-DTPA-enhanced MRI, including RE (calculated as $[SI_{HBP}-SI_{UEP}]/SI_{UEP}$ of the liver parenchyma), liver-to-portal vein contrast ratio (calculated by dividing the liver parenchyma SI by the portal vein SI on HBP images), and liver-to-spleen contrast ratio (calculated by dividing the liver parenchyma SI by the spleen SI on HBP images)[30-32]. In previous reports, the signals of the portal vein and spleen were integrated with plasma or extracellular extravascular space exposure to the contrast agent, thus showing that the liver-to-portal vein contrast ratio and liver-to-spleen contrast ratio were more strongly related to liver function than to liver fibrosis[12,33]. Adjustment of the signal of the paraspinal muscle for SI_{liver} on the same slice was performed to normalize the shimming influences and correct for technical bias. Compared with other organs, SI_{muscle} was more stable and less influenced by age and liver function. Jang *et al*[23] also validated this view. A few articles have shown similar diagnostic accuracies for RE and the CEI. In our study, RE was mildly negatively associated with liver inflammation (r = -0.57, P = 0.007) and fibrosis (r = -0.44, P = 0.043) (unreported), possibly because the SI of the liver after injecting Gd-EOB-DTPA changes, as the window level and width differ in the images [34].

There were several limitations in our study. First, limited by the inclusion criteria, the sample size was small, and the CEI% of patients with fibrosis regression was close to 1. We will explore further by expanding the sample size. Second, we did not use MR elastography (MRE) or T1-mapping to predict liver fibrosis, which have a superior diagnostic value in predicting liver fibrosis than Gd-EOB-DTPA-enhanced MRI[35,36]. However, except for the influence of body mass index and ascites on TE, the sequencing method in MRE is not unified, and the threshold value changes across different methods [26]. In recent years, MR relaxometry in the form of T1 mapping has been considered promising as a non-invasive method for characterizing hepatic fibrosis using the look-locker technique for measurement. Our patients were enrolled between 2014 and 2016, when T1 mapping was not in use. Third, although histology is a gold standard procedure, the tissues used in our study were all from liver biopsies rather than from hepatectomy, and there may have been misjudgment regarding the histological changes. Fourth, the mean follow-up duration after achieving SVR was only 6.2 mo, and a longer follow-up period is warranted.

CONCLUSION

In conclusion, the CEI of Gd-EOB-DTPA-enhanced MRI can be used to diagnose liver fibrosis in patients with CHC. The change of the CEI can be used to monitor fibrosis regression post SVR by DAA therapy.

ARTICLE HIGHLIGHTS

Research background

The histological change and non-invasive method surveillance after hepatitis C virus (HCV) eradication by direct acting antiviral (DAA) therapy have not been elucidated. As using a liver-specific magnetic resonance imaging (MRI) contrast, whether Gadolinium-ethoxybenzyl-diethylenetriamine penta-acetic acid (Gd-EOB-DTPA) enhanced MRI can be used to diagnose and follow-up the liver fibrosis in patients with chronic hepatitis C (CHC) has not been investigated.

Research motivation

The key issues are whether Gd-EOB-DTPA enhanced MRI can be used in diagnosing and following-up in patients with CHC. The result will provide important information on non-invasive method selection for dynamic assessment of liver fibrosis in patients with CHC and histology change after achieving SVR treated by DAAs.

Research objectives

To investigated the diagnostic and follow-up values of Gd-EOB-DTPA-enhanced MRI for hepatic histology in patients with CHC. We further explore the value of Gd-EOB-DTPA enhanced MRI in evaluating fibrosis regression in patients with CHC after achieving sustained virological response (SVR) treated by DAAs.

Research methods

Chronic HCV infected patients with paired liver biopsy and Gd-EOB-DTPA enhanced MRI before and after DAA treated was included. Contrast enhancement index (CEI) was calculated according with signal intensity *via* MRI, and the correlation between CEI and histology change was evaluated. Fibrosis regression was defined as a ≥ 1-point decrease in the Ishak fibrosis score. The diagnostic and follow-up values of the CEI, liver stiffness measurements (LSM), aminotransferase (AST)-to-platelet ratio (APRI) and Fibrosis-4 (FIB-4) were compared.

Research results

Thirty-nine patients with CHC were enrolled, with average age of 42.3 ± 14.4 years and 20/39 (51.3%) were male. Twenty-one enrolled patients had eligible paired Gd-EOB-DTPA-enhanced MRI and liver tissues after achieving SVR. According to correlation and the hierarchical analysis, the CEI mainly decreased with the progression of liver fibrosis. Compared with LSM, APRI and FIB-4, the CEI is more useful for liver fibrosis diagnosis, the correlation between the CEI and fibrosis stage was relatively stable and was not related to the treatment state. In paired analysis using liver pathology and CEI before and after treatment, only the dynamic change in the CEI can be used to evaluate fibrosis regression after achieving SVR.

Research conclusions

The CEI of Gd-EOB-DTPA-enhanced MRI can be used as a non-invasive method to diagnose liver fibrosis in patients with CHC. The dynamic change of the CEI can be used to monitor fibrosis regression post SVR in patients with CHC after DAA therapy.

Research perspectives

Larger and longer-term prospective studies in patients with CHC should be performed in future studies.

ACKNOWLEDGEMENTS

We are sincerely grateful to the radiologists Dr. Xiao-Xuan Jia and Dr. Xin-Yu Zhang for their involvement in the MRI analysis. We also thank Prof. Aileen Wee and Guang-De Zhou for their involvement in the liver pathology confirmation. We also thank Hui-Xin Liu, MD, for help with the statistical review.

FOOTNOTES

Author contributions: Li XH, Rao HY and Wei L designed the protocol of this study; Li XH, Huang R, Yang M, Wang J, Gao YH, Jin Q and Ma DL collected the data; Li XH analyzed and interpreted the patient data and was major contributors in writing the manuscript; Wei L and Rao HY give advice in study design, statistical analysis and writing the manuscript; All authors read and approved the final manuscript.

Supported by National Natural Science Foundation of China, No. 81870406; and Nature Science Foundation of Beijing Municipality, No. 7182174.

Institutional review board statement: This study was reviewed and approved by the Institutional Review Board of Peking University People's Hospital (2020PHB039-01), and the requirement for patient informed consent was waived.

Informed consent statement: Patients were not required to provide informed consent for this study, as the analysis used anonymous clinical data. The Institutional Review Board of Peking University People's Hospital approved waiving the requirement for patient informed consent.

Conflict-of-interest statement: Prof. Rao reports grants from National Natural Science Foundation of China (NSFC), No. 81870406, and Beijing Natural Science Foundation, No. 7182174 during the conduct of the study.

Data sharing statement: No additional data are available.

Country/Territory of origin: China

ORCID number: Xiao-He Li 0000-0001-6600-6067; Rui Huang 0000-0001-5561-8746; Ming Yang 0000-0001-5765-3844; Jian Wang 0000-0002-9578-8288; Ying-Hui Gao 0000-0003-4532-3412; Qian Jin 0000-0002-5213-8680; Dan-Li Ma 0000-0002-0936-6792; Lai Wei 0000-0003-2326-1257; Hui-Ying Rao 0000-0003-2431-3872.

S-Editor: Fan JR
L-Editor: A
P-Editor: Chen YX

REFERENCES

1 **WHO**. Global hepatitis report, 2017. Geneva: World Health Organization, 2017. [cited 10 October 2021]. Available from: https://www.who.int/
2 **Global Burden of Disease Study 2013 Collaborators**. Global, regional, and national incidence, prevalence, and years lived with disability for 301 acute and chronic diseases and injuries in 188 countries, 1990-2013: a systematic analysis for the Global Burden of Disease Study 2013. *Lancet* 2015; **386**: 743-800 [PMID: 26063472 DOI: 10.1016/S0140-6736(15)60692-4]
3 **Lohmann V**, Bartenschlager R. Indelibly Stamped by Hepatitis C Virus Infection: Persistent Epigenetic Signatures Increasing Liver Cancer Risk. *Gastroenterology* 2019; **156**: 2130-2133 [PMID: 31034828 DOI: 10.1053/j.gastro.2019.04.033]
4 **Ahumada A**, Rayón L, Usón C, Bañares R, Alonso Lopez S. Hepatocellular carcinoma risk after viral response in hepatitis C virus-advanced fibrosis: Who to screen and for how long? *World J Gastroenterol* 2021; **27**: 6737-6749 [PMID: 34790004 DOI: 10.3748/wjg.v27.i40.6737]
5 **Knop V**, Hoppe D, Welzel T, Vermehren J, Herrmann E, Vermehren A, Friedrich-Rust M, Sarrazin C, Zeuzem S, Welker MW. Regression of fibrosis and portal hypertension in HCV-associated cirrhosis and sustained virologic response after interferon-free antiviral therapy. *J Viral Hepat* 2016; **23**: 994-1002 [PMID: 27500382 DOI: 10.1111/jvh.12578]
6 **Laursen TL**, Siggaard CB, Kazankov K, Sandahl TD, Møller HJ, Tarp B, Kristensen LH, Laursen AL, Leutscher P, Grønbaek H. Time-dependent improvement of liver inflammation, fibrosis and metabolic liver function after successful direct-acting antiviral therapy of chronic hepatitis C. *J Viral Hepat* 2020; **27**: 28-35 [PMID: 31502741 DOI: 10.1111/jvh.13204]
7 **Jayaswal ANA**, Levick C, Collier J, Tunnicliffe EM, Kelly MD, Neubauer S, Barnes E, Pavlides M. Liver cT_1 decreases following direct-acting antiviral therapy in patients with chronic hepatitis C virus. *Abdom Radiol (NY)* 2021; **46**: 1947-1957 [PMID: 33247768 DOI: 10.1007/s00261-020-02860-5]
8 **Bluemke DA**, Sahani D, Amendola M, Balzer T, Breuer J, Brown JJ, Casalino DD, Davis PL, Francis IR, Krinsky G, Lee FT Jr, Lu D, Paulson EK, Schwartz LH, Siegelman ES, Small WC, Weber TM, Welber A, Shamsi K. Efficacy and safety of MR imaging with liver-specific contrast agent: U.S. multicenter phase III study. *Radiology* 2005; **237**: 89-98 [PMID: 16126918 DOI: 10.1148/radiol.2371031842]
9 **Kim T**, Murakami T, Hasuike Y, Gotoh M, Kato N, Takahashi M, Miyazawa T, Narumi Y, Monden M, Nakamura H. Experimental hepatic dysfunction: evaluation by MRI with Gd-EOB-DTPA. *J Magn Reson Imaging* 1997; **7**: 683-688 [PMID: 9243389 DOI: 10.1002/jmri.1880070413]
10 **Kitao A**, Matsui O, Yoneda N, Kozaka K, Kobayashi S, Koda W, Inoue D, Ogi T, Yoshida K, Gabata T. Gadoxetic acid-enhanced MR imaging for hepatocellular carcinoma: molecular and genetic background. *Eur Radiol* 2020; **30**: 3438-3447 [PMID: 32064560 DOI: 10.1007/s00330-020-06687-y]
11 **Schulze J**, Lenzen H, Hinrichs JB, Ringe B, Manns MP, Wacker F, Ringe KI. An Imaging Biomarker for Assessing Hepatic Function in Patients With Primary Sclerosing Cholangitis. *Clin Gastroenterol Hepatol* 2019; **17**: 192-199.e3 [PMID: 29775791 DOI: 10.1016/j.cgh.2018.05.011]
12 **Yang M**, Zhang Y, Zhao W, Cheng W, Wang H, Guo S. Evaluation of liver function using liver parenchyma, spleen and portal vein signal intensities during the hepatobiliary phase in Gd-EOB-D TPA-enhanced MRI. *BMC Med Imaging* 2020; **20**: 119 [PMID: 33081713 DOI: 10.1186/s12880-020-00519-7]
13 **Kim SW**, Kim YR, Choi KH, Cho EY, Song JS, Kim JE, Kim TH, Lee YH, Yoon KH. Staging of Liver Fibrosis by Means of Semiautomatic Measurement of Liver Surface Nodularity in MRI. *AJR Am J Roentgenol* 2020; **215**: 624-630 [PMID: 32755157 DOI: 10.2214/AJR.19.22041]
14 **Verloh N**, Probst U, Utpatel K, Zeman F, Brennfleck F, Werner JM, Fellner C, Stroszczynski C, Evert M, Wiggermann P, Haimerl M. Influence of hepatic fibrosis and inflammation: Correlation between histopathological changes and Gd-EOB-DTPA-enhanced MR imaging. *PLoS One* 2019; **14**: e0215752 [PMID: 31083680 DOI: 10.1371/journal.pone.0215752]
15 **Chuang YH**, Ou HY, Lazo MZ, Chen CL, Chen MH, Weng CC, Cheng YF. Predicting post-hepatectomy liver failure by combined volumetric, functional MR image and laboratory analysis. *Liver Int* 2018; **38**: 868-874 [PMID: 28987012 DOI: 10.1111/liv.13608]
16 **Mauro E**, Crespo G, Montironi C, Londoño MC, Hernández-Gea V, Ruiz P, Sastre L, Lombardo J, Mariño Z, Díaz A,

Colmenero J, Rimola A, Garcia-Pagán JC, Brunet M, Forns X, Navasa M. Portal pressure and liver stiffness measurements in the prediction of fibrosis regression after sustained virological response in recurrent hepatitis C. *Hepatology* 2018; **67**: 1683-1694 [PMID: 28960366 DOI: 10.1002/hep.29557]

17 **Choi YR**, Lee JM, Yoon JH, Han JK, Choi BI. Comparison of magnetic resonance elastography and gadoxetate disodium-enhanced magnetic resonance imaging for the evaluation of hepatic fibrosis. *Invest Radiol* 2013; **48**: 607-613 [PMID: 23538889 DOI: 10.1097/RLI.0b013e318289ff8f]

18 **Goodman ZD**. Grading and staging systems for inflammation and fibrosis in chronic liver diseases. *J Hepatol* 2007; **47**: 598-607 [PMID: 17692984 DOI: 10.1016/j.jhep.2007.07.006]

19 **Rozario R**, Ramakrishna B. Histopathological study of chronic hepatitis B and C: a comparison of two scoring systems. *J Hepatol* 2003; **38**: 223-229 [PMID: 12547412 DOI: 10.1016/s0168-8278(02)00357-4]

20 **Huang R**, Rao H, Yang M, Gao Y, Wang J, Jin Q, Ma D, Wei L. Noninvasive Measurements Predict Liver Fibrosis Well in Hepatitis C Virus Patients After Direct-Acting Antiviral Therapy. *Dig Dis Sci* 2020; **65**: 1491-1500 [PMID: 31654313 DOI: 10.1007/s10620-019-05886-y]

21 **Wai CT**, Greenson JK, Fontana RJ, Kalbfleisch JD, Marrero JA, Conjeevaram HS, Lok AS. A simple noninvasive index can predict both significant fibrosis and cirrhosis in patients with chronic hepatitis C. *Hepatology* 2003; **38**: 518-526 [PMID: 12883497 DOI: 10.1053/jhep.2003.50346]

22 **Sterling RK**, Lissen E, Clumeck N, Sola R, Correa MC, Montaner J, S Sulkowski M, Torriani FJ, Dieterich DT, Thomas DL, Messinger D, Nelson M; APRICOT Clinical Investigators. Development of a simple noninvasive index to predict significant fibrosis in patients with HIV/HCV coinfection. *Hepatology* 2006; **43**: 1317-1325 [PMID: 16729309 DOI: 10.1002/hep.21178]

23 **Jang HJ**, Min JH, Lee JE, Shin KS, Kim KH, Choi SY. Assessment of liver fibrosis with gadoxetic acid-enhanced MRI: comparisons with transient elastography, ElastPQ, and serologic fibrosis markers. *Abdom Radiol (NY)* 2019; **44**: 2769-2780 [PMID: 31041497 DOI: 10.1007/s00261-019-02041-z]

24 **Hsu WF**, Lai HC, Su WP, Lin CH, Chuang PH, Chen SH, Chen HY, Wang HW, Huang GT, Peng CY. Rapid decline of noninvasive fibrosis index values in patients with hepatitis C receiving treatment with direct-acting antiviral agents. *BMC Gastroenterol* 2019; **19**: 63 [PMID: 31029101 DOI: 10.1186/s12876-019-0973-5]

25 **Ioannou GN**, Feld JJ. What Are the Benefits of a Sustained Virologic Response to Direct-Acting Antiviral Therapy for Hepatitis C Virus Infection? *Gastroenterology* 2019; **156**: 446-460.e2 [PMID: 30367836 DOI: 10.1053/j.gastro.2018.10.033]

26 **Patel K**, Sebastiani G. Limitations of non-invasive tests for assessment of liver fibrosis. *JHEP Rep* 2020; **2**: 100067 [PMID: 32118201 DOI: 10.1016/j.jhepr.2020.100067]

27 **Loomba R**, Adams LA. Advances in non-invasive assessment of hepatic fibrosis. *Gut* 2020; **69**: 1343-1352 [PMID: 32066623 DOI: 10.1136/gutjnl-2018-317593]

28 **Pan JJ**, Bao F, Du E, Skillin C, Frenette CT, Waalen J, Alaparthi L, Goodman ZD, Pockros PJ. Morphometry Confirms Fibrosis Regression From Sustained Virologic Response to Direct-Acting Antivirals for Hepatitis C. *Hepatol Commun* 2018; **2**: 1320-1330 [PMID: 30411079 DOI: 10.1002/hep4.1228]

29 **Poynard T**, Munteanu M, Colombo M, Bruix J, Schiff E, Terg R, Flamm S, Moreno-Otero R, Carrilho F, Schmidt W, Berg T, McGarrity T, Heathcote EJ, Gonçales F, Diago M, Craxi A, Silva M, Boparai N, Griffel L, Burroughs M, Brass C, Albrecht J. FibroTest is an independent predictor of virologic response in chronic hepatitis C patients retreated with pegylated interferon alfa-2b and ribavirin in the EPIC^3 program. *J Hepatol* 2011; **54**: 227-235 [PMID: 21056496 DOI: 10.1016/j.jhep.2010.06.038]

30 **Watanabe H**, Kanematsu M, Goshima S, Kondo H, Onozuka M, Moriyama N, Bae KT. Staging hepatic fibrosis: comparison of gadoxetate disodium-enhanced and diffusion-weighted MR imaging--preliminary observations. *Radiology* 2011; **259**: 142-150 [PMID: 21248234 DOI: 10.1148/radiol.10100621]

31 **Verloh N**, Utpatel K, Haimerl M, Zeman F, Fellner C, Fichtner-Feigl S, Teufel A, Stroszczynski C, Evert M, Wiggermann P. Liver fibrosis and Gd-EOB-DTPA-enhanced MRI: A histopathologic correlation. *Sci Rep* 2015; **5**: 15408 [PMID: 26478097 DOI: 10.1038/srep15408]

32 **Hako R**, Kristian P, Jarčuška P, Haková I, Hockicková I, Schréter I, Janičko M. Noninvasive Assessment of Liver Fibrosis in Patients with Chronic Hepatitis B or C by Contrast-Enhanced Magnetic Resonance Imaging. *Can J Gastroenterol Hepatol* 2019; **2019**: 3024630 [PMID: 31058108 DOI: 10.1155/2019/3024630]

33 **Dahlqvist Leinhard O**, Dahlström N, Kihlberg J, Sandström P, Brismar TB, Smedby O, Lundberg P. Quantifying differences in hepatic uptake of the liver specific contrast agents Gd-EOB-DTPA and Gd-BOPTA: a pilot study. *Eur Radiol* 2012; **22**: 642-653 [PMID: 21984449 DOI: 10.1007/s00330-011-2302-4]

34 **Katsube T**, Okada M, Kumano S, Imaoka I, Kagawa Y, Hori M, Ishii K, Tanigawa N, Imai Y, Kudo M, Murakami T. Estimation of liver function using T2* mapping on gadolinium ethoxybenzyl diethylenetriamine pentaacetic acid enhanced magnetic resonance imaging. *Eur J Radiol* 2012; **81**: 1460-1464 [PMID: 21514080 DOI: 10.1016/j.ejrad.2011.03.073]

35 **Wu WP**, Hoi CI, Chen RC, Lin CP, Chou CT. Comparison of the efficacy of Gd-EOB-DTPA-enhanced magnetic resonance imaging and magnetic resonance elastography in the detection and staging of hepatic fibrosis. *Medicine (Baltimore)* 2017; **96**: e8339 [PMID: 29049250 DOI: 10.1097/MD.0000000000008339]

36 **Obmann VC**, Berzigotti A, Catucci D, Ebner L, Gräni C, Heverhagen JT, Christe A, Huber AT. T1 mapping of the liver and the spleen in patients with liver fibrosis-does normalization to the blood pool increase the predictive value? *Eur Radiol* 2021; **31**: 4308-4318 [PMID: 33313965 DOI: 10.1007/s00330-020-07447-8]

World Journal of Gastroenterology

Submit a Manuscript: https://www.f6publishing.com

World J Gastroenterol 2022 May 28; 28(20): 2227-2242

DOI: 10.3748/wjg.v28.i20.2227

ISSN 1007-9327 (print) ISSN 2219-2840 (online)

ORIGINAL ARTICLE

Observational Study

First prospective European study for the feasibility and safety of magnetically controlled capsule endoscopy in gastric mucosal abnormalities

Milán Szalai, Krisztina Helle, Barbara Dorottya Lovász, Ádám Finta, András Rosztóczy, László Oczella, László Madácsy

Specialty type: Gastroenterology and hepatology

Provenance and peer review: Unsolicited article; Externally peer reviewed.

Peer-review model: Single blind

Peer-review report's scientific quality classification

Grade A (Excellent): 0
Grade B (Very good): 0
Grade C (Good): C, C, C
Grade D (Fair): D
Grade E (Poor): 0

P-Reviewer: Kawano S, Japan; Nam SJ, South Korea; Nishida T, Japan

Received: January 3, 2022
Peer-review started: January 3, 2022
First decision: January 27, 2022
Revised: February 14, 2022
Accepted: April 27, 2022
Article in press: April 27, 2022
Published online: May 28, 2022

Milán Szalai, Ádám Finta, László Oczella, László Madácsy, Department of Gastroenterology, Endo-Kapszula Health Centre and Endoscopy Unit, Székesfehérvár 8000, Hungary

Krisztina Helle, András Rosztóczy, Department of Internal Medicine, University of Szeged, Szeged 6725, Hungary

Corresponding author: László Madácsy, MD, PhD, Professor, Department of Gastroenterology, Endo-Kapszula Health Centre and Endoscopy Unit, No. 316 Budai Road, Székesfehérvár 8000, Hungary. endomabt1@gmail.com

Abstract

BACKGROUND

While capsule endoscopy (CE) is the gold standard diagnostic method of detecting small bowel (SB) diseases and disorders, a novel magnetically controlled capsule endoscopy (MCCE) system provides non-invasive evaluation of the gastric mucosal surface, which can be performed without sedation or discomfort. During standard SBCE, passive movement of the CE may cause areas of the complex anatomy of the gastric mucosa to remain unexplored, whereas the precision of MCCE capsule movements inside the stomach promises better visualization of the entire mucosa.

AIM

To evaluate the Ankon MCCE system's feasibility, safety, and diagnostic yield in patients with gastric or SB disorders.

METHODS

Of outpatients who were referred for SBCE, 284 (male/female: 149/135) were prospectively enrolled and evaluated by MCCE. The stomach was examined in the supine, left, and right lateral decubitus positions without sedation. Next, all patients underwent a complete SBCE study protocol. The gastric mucosa was explored with the Ankon MCCE system with active magnetic control of the capsule endoscope in the stomach, applying three standardized pre-programmed computerized algorithms in combination with manual control of the magnetic movements.

RESULTS

The urea breath test revealed *Helicobacter pylori* positivity in 32.7% of patients. The mean gastric and SB transit times with MCCE were 0 h 47 min 40 s and 3 h 46 min 22 s, respectively. The average total time of upper gastrointestinal MCCE examination was 5 h 48 min 35 s. Active magnetic movement of the Ankon capsule through the pylorus was successful in 41.9% of patients. Overall diagnostic yield for detecting abnormalities in the stomach and SB was 81.9% (68.6% minor; 13.3% major pathologies); 25.8% of abnormalities were in the SB; 74.2% were in the stomach. The diagnostic yield for stomach/SB was 55.9%/12.7% for minor and 4.9%/8.4% for major pathologies.

CONCLUSION

MCCE is a feasible, safe diagnostic method for evaluating gastric mucosal lesions and is a promising non-invasive screening tool to decrease morbidity and mortality in upper gastrointestinal diseases.

Key Words: Bowel diseases; Capsule endoscopy; Diagnostic techniques; Gastrointestinal diseases; Gastric mucosa; *Helicobacter pylori*

Core Tip: We evaluate the feasibility, safety, and diagnostic yield of magnetically controlled capsule endoscopy (CE) system developed by Ankon and AnX robotics that provides non-invasive evaluation of the gastric mucosal surface, which can be performed without sedation or patient discomfort. During gold-standard small bowel CE, passive movement may cause areas of the complex gastric mucosa to remain unexplored, whereas the precision of magnetically controlled capsule endoscopy (MCCE) capsule movements inside the gastrointestinal tract achieves better visualization of the entire mucosa, including the stomach. The Ankon MCCE system is a promising, non-invasive screening tool that achieved ~90% diagnostic yield of mucosal abnormalities in this study.

Citation: Szalai M, Helle K, Lovász BD, Finta Á, Rosztóczy A, Oczella L, Madácsy L. First prospective European study for the feasibility and safety of magnetically controlled capsule endoscopy in gastric mucosal abnormalities. *World J Gastroenterol* 2022; 28(20): 2227-2242

URL: https://www.wjgnet.com/1007-9327/full/v28/i20/2227.htm

DOI: https://dx.doi.org/10.3748/wjg.v28.i20.2227

INTRODUCTION

Capsule endoscopy (CE) is a non-invasive, painless, patient-friendly, and safe diagnostic method. It is currently the gold standard examination for small bowel (SB) diseases, including inflammatory bowel disease, suspected polyposis syndromes, unexplained abdominal pain, celiac disease, and obscure gastrointestinal bleeding (OGIB). Small bowel capsule endoscopy (SBCE) provides excellent diagnostic yield, which has been proven in many clinical trials since its introduction in the late 1990s. Currently, it has a fundamental role in gastrointestinal (GI) endoscopy, especially in patients with suspected SB diseases[1]. Attempts to expand the diagnostic role of CE to areas that are traditionally explored with standard endoscopic procedures (gastroscopy and colonoscopy), *e.g.*, the esophagus, stomach, and colon. These aims have been challenged by significant drawbacks in the past due to a lack of optimal preparation, standardized procedural design, and ability to visualize the entire mucosal surface[2]. A common perception is that the anatomical structures of the stomach and colon are too complex for adequate visualization with a passive capsule endoscope[3-5].

Although the SB seems to be a simple pipe, the more complex gastric anatomy with passive movements may cause unexplored areas of the gastric mucosa when utilizing standard CE. Magnetically controlled capsule endoscopy (MCCE) systems were developed over the past ten years to precisely control capsule movements inside the GI tract and to achieve better visualization of the entire mucosa, especially in the stomach. Different approaches have been developed and studied over time, which have enabled manual steering or active movement of the capsule systems. The external magnetic field seems to be the most adequate and energetically effective method for steering and holding the capsule within the stomach[6,7].

According to recent, prospective studies that were mainly conducted in China, a methodology developed by Ankon and AnX robotics could be an optimal method for non-invasive screening and

early diagnosis of gastric diseases such as gastric cancer and intramucosal high-grade dysplasia. It has the potential to become a valuable and accepted screening method in a population with high gastric cancer risk[8].

The aim of this study was to evaluate the feasibility, safety, and diagnostic yield of the Ankon MCCE system in patients with gastric and SB disorders who were referred to our endoscopy unit for SBCE examination between September 2017 and December 2020. Our secondary aim was to evaluate the overall gastric examinations, SB transit times (TTs) and efficacy of MCCE to achieve complete gastric and SBCE investigation by utilizing the same upper GI capsule.

MATERIALS AND METHODS

Study design

Our present study prospectively enrolled outpatients who were seen at the Endo-Kapszula Endoscopy Unit, Székesfehérvár, Hungary, between September 2017 and December 2020. A combined investigation of the stomach and SB of patients referred to for SBCE was performed with a robotically MCCE system (NaviCam, Ankon Technologies Co, Ltd, Shanghai, China).

The primary endpoint of the recent study was to investigate the diagnostic yield of MCCE in the evaluation of gastric and SB abnormalities. The secondary endpoints were to evaluate the feasibility of performing complete gastric and SB investigation by utilizing the same diagnostic procedure; to address safety parameters, including adverse and severe adverse events, and to calculate the capsule TTs, such as esophageal, gastric, and SB TTs, and the overall procedure time.

Patients

All patients who were referred to our endoscopy unit for SBCE and who agreed to our gastric study protocol were included in the current study. During the study period, we enrolled 284 consecutive, eligible patients, of which there were 149 males (52.5%) and 135 females (47.5 %), with a mean age of 44 years. Detailed patient characteristics are shown in Table 1. The indications of MCCE were iron deficiency anemia, OGIB, suspected/established SB Crohn's disease, suspected/confirmed celiac disease, suspected SB neoplastic disease, carcinoid syndrome, and SB polyposis syndromes.

This study was approved by the Ethical Committee of the University of Szeged (Registry No. 5/17.04.26) and registered in the ClinicalTrials.gov trial registry (Identifier: NCT03234725). The present study was conducted according to the World Medical Association's Declaration of Helsinki provisions in 1995. Patients agreed to undergo capsule endoscopies and *Helicobacter pylori* (*H. pylori*) urea breath tests (UBTs) by written informed consent.

Patient preparation for MCCE

According to the SBCE guidelines, we applied the following patient preparation and study protocol: Patients followed a liquid diet and consumed 2 L of water with two sacks of polyethylene glycol (PEG) the day before the study. First, *H. pylori* C^{13} UBT was performed on the morning of the study, while the patient was in a fasting condition. The UBT requires an average of 30 min, during which time the patient should not consume any fluids or food. During that visit, the patient's medical history was recorded, and a physical examination was performed. After the UBT, the patient ingested 2 dL water with simethicone suspension (80 mg) to reduce mucus in the stomach. Then, to distend the stomach properly, approximately 8-10 dL of clean water consumed by all patients within 10 min. Water ingestion may be repeated as needed to enhance gastric distension during examination. After complete visualization of the total gastric mucosal surface, active pyloric propulsion of the capsule was attempted in all patients with the external magnetic field. If it was unsuccessful, 10 mg intravenous metoclopramide was applied 60 min after the capsule was swallowed.

Contraindications of MCCE were the same as of those of SBCE and magnetic resonance imaging (MRI) examination. In our study, absolute contraindications were the patients with previous abdominal surgery and/or a previous capsule retention; with implanted MRI-incompatible electronic devices (*e.g.*, implantable cardioverter-defibrillator and pacemakers), or magnetic, metal foreign bodies; and who were not competent or refused the informed consent form; who were under age 18 or above age 70; and those who were pregnant. A patency capsule test was initially performed in all patients to determine those with relative contraindications, including known or suspected GI obstruction due to SB Crohn's disease, neoplasia, or SB surgery.

Technical methods of MCCE

Our system involves a special static magnet with robotic and manual guidance, computer workstation with ESNavi software (Ankon Technologies Co, Ltd) (Figure 1), magnetic capsule endoscope, capsule locator, and data recorder. The capsule endoscope sizes 26.8 × 11.6 mm, weighs 4.8 g, and has a permanent spherical magnet inside (Figure 2). The operator can adjust the frequency of captured pictures from 0.5 to 6 frames per second (fps). Capsule functioning can be stopped temporarily and

Table 1 Indications of small bowel capsule endoscopy (grouped by gender)

	All cases	Male	Female
Patient characteristics			
n	284	149	135
Age (mean ± SD)	44.0 ± 13.3	44.0 ± 13.3	44.0 ± 13.3
BMI	26.5	27.1	25.5
Indications			
OGiV	61 (21.5%)	30 (20.1%)	31 (22.9%)
Celiac disease	80 (28.2%)	40 (26.8%)	40 (29.7%)
Crohn's or susp. Crohn's	47 (16.5%)	31 (20.9%)	16 (11.9%)
Unexplained abdominal pain	92 (32.4%)	47 (31.5%)	45 (33.3%)
Susp. SB tumor	4 (1.4%)	1 (0.7%)	3 (2.2%)
13C urea breath test			
No. of performed tests	110(38.7%)	56 (50.1%)	54 (49.1%)
Positive	36 (32.7%)	16 (44.4%)	20 (55.6%)
Negative	74 (67.3%)	40 (54%)	34 (46%)

BMI: Body mass index; SB: Small bowel.

DOI: 10.3748/wjg.v28.i20.2227

Figure 1 Robotic C-arm, investigation table, and computer workstation for magnetically controlled capsule endoscopy.

restarted by the operator remotely from the workstation. The picture resolution is 480 × 480 pixels, and the field of view is 140°. The illumination can be automatically adjusted by an automatic picture focusing mechanism, which enables the view depth to shift from 0 mm to 60 mm. Depending on the fps, the battery life can be over 10 h, which allows combined gastric and SB capsule investigations with the same capsule.

The magnetic robotic C-arm generates an adjustable magnetic field outside of the body with a maximum strength of 0.2 T, which allows precise controlled movements in three spatial directions. During the process, the physician guides the magnetic capsule by two joysticks in any chosen, spatial direction or along its axis, and therefore, he can rotate or tilt it. Moreover, the capsule can advance forward 360° by a rotational automatism in the direction of the capsule visual axis, which is helpful for transposition of the capsule from the long axis of the stomach.

The capsule locator is a unique device that activates the capsule by infrared light prior to the patient swallowing it. The presence of the capsule can be detected in the case of suspected capsule retention (Figure 3).

The system is capable of real-time digital transmission of images to the operating system. At the same time, it is continuously obtaining information about the gyroscope, which is built into the capsule

DOI: 10.3748/wjg.v28.i20.2227

Figure 2 Magnetic capsule endoscope (NaviCam).

DOI: 10.3748/wjg.v28.i20.2227

Figure 3 Capsule locator device.

[three-dimensional (3D) motion detector]. It also receives data from the actual spatial location of the camera and localizes the capsule inside the body at any time. The data recorder (Figure 4) may receive all motion information and high-quality pictures *via* wireless transmission from the capsule endoscope. In contrast, the connection between the data recorder and the workstation *via* a USB wire makes visible the real-time pictures and gyroscope information.

Magnetic CE can be transferred along five different axes with the controlling magnet: two rotational and three 3D spaces. To achieve this, there are two joysticks on the workstation desktop: the left one controls the capsule in two rotational axes (horizontal and vertical directions) and the right joystick directs it in the three translational axes (forward/backwards, up/down, left/right). Precise magnetic control is achieved by positioning the examining table, modifying the position of the spherical magnet axis along the 3D space, and dynamically adjusting the strength and direction of the vectorial magnetic fields perpendicular to each other. The above-mentioned robotic systems can also automatically run the magnetic field vector and position it by robotically controlled computer-based software (scripts) in default mode, which can achieve a standardized mucosal scanning during the MCCE procedure without the direct intervention of a physician.

MCCE study protocol and gastric stations

To achieve optimal gastric mucosal visualization and standardization of the MCCE protocol in the stomach, we defined eight different stations with different patient positions to visualize the entire inner gastric surface as during upper GI endoscopy. Changing the patient position from the left lateral decubitus to the supine and right lateral position is necessary to combine gravity and magnetic force, which improve capsule maneuvering (Figure 5). The capsule swallowed by the patients in the left lateral decubitus position (Figure 6).

DOI: 10.3748/wjg.v28.i20.2227

Figure 4 Data recorder.

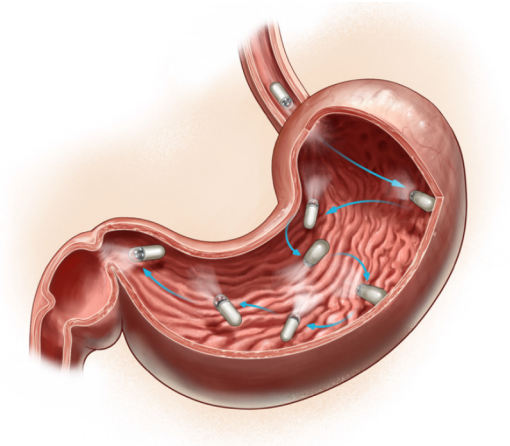

DOI: 10.3748/wjg.v28.i20.2227

Figure 5 Different magnetically controlled capsule endoscopy stations and capsule camera orientations defined to achieve a complete gastric mucosal surface visualization and mapping (created by Zoltán Tóbiás, MD).

Stations at the left lateral decubitus position: Station I. Visualization of the gastric fundus and subcardial region with the cardia (posterior J type retroflexion).

After entering the stomach, the capsule was lowered into the large curvature at the body of the stomach. The magnetic ball was held high up at the level of the patient's right shoulder. The capsule camera was maintained in an obliquely upward orientation of 45° and then horizontally rotated to observe the gastric fundus and the cardia (Figure 7A-C).

Station II. Moving closer to the cardia and the fundus (anterior J type retroflexion).

While using the right joystick, the ball magnet was lowered and fitted closely to the patient's right arm. Due to the proximity of the magnetic field, the capsule rose to the anterior wall and small curvature of the stomach. The capsule was then rotated with the camera oriented vertically upward to observe the cardia up close, with the fundus at a distance (Figure 7D-F).

Station III. Visualization of the gastric body from the fundus.

With the ball magnet in the same position, using the left joystick, the capsule camera was rotated and tilted downwards, enabling visualization of the proximal body of the stomach (corpus) and the gastric folds at the large curvature with a longitudinal view (Figure 7G-I).

Stations in the supine position: Station IV. Visualization of the angular incisure.

Patients were asked to lie on their back, in a supine position. The capsule was moved and located to the distal body into the angular region due to a change of gravity and stepwise magnetic movements. The magnetic ball was moved to the left upper abdomen (hypochondrium) and then lowered, close to the patient abdomen. In this case, the capsule was raised to the anterior wall of the stomach; therefore, the small curvature and the angular incisure were examined as well (Figure 8A-C).

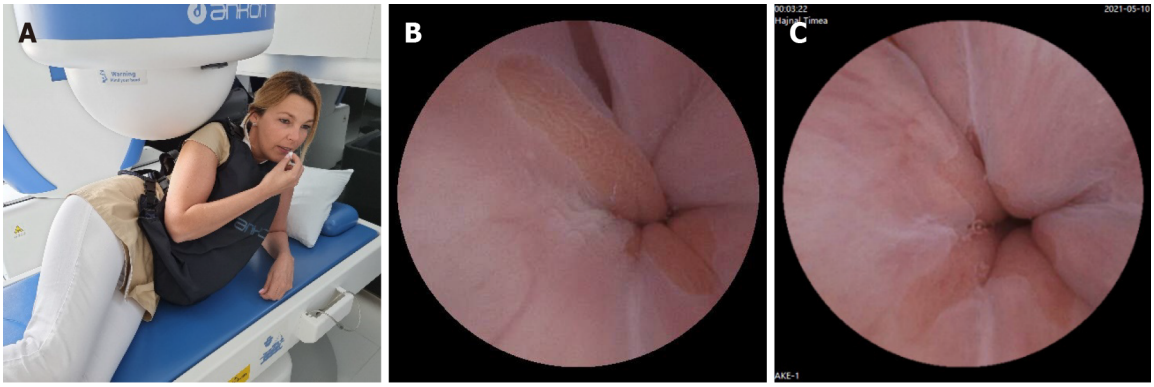

DOI: 10.3748/wjg.v28.i20.2227

Figure 6 The capsule swallowed by the patients in the left lateral decubitus position. A: Patients and ball magnet position; B and C: Pictures of the Z-line by CE from our database.

Station V. Visualization of the larger curvature of the distal body from the angular incisure (U type of retroversion).

The magnetic ball was moved to the epigastric area, close to the abdomen. Then the capsule camera was oriented upward to observe the anterior wall of the gastric body. In this position, the capsule can be turned and rotated (*e.g.*, towards the cardia), enabling visualization of the distal body of the stomach longitudinally, as in the endoscopic view of U-type retroversion (Figure 8D-F).

Stations at the right lateral decubitus patient position: Station VI. Visualization of the antral canal.

In the next phase, patients were asked to turn to the right lateral decubitus position. Due to the gravity force, the capsule sank and moved spontaneously into the antral region. Then, the ball magnet was positioned over the left kidney. The capsule was brought closer to the large curvature with the camera oriented obliquely downward at 45°, which enabled observation of the antrum. Then, the antral canal could be examined with the pylorus, and the angular incisure became visible from the antrum (Figure 9A-C).

Stations in the supine position: Station VII. Prepyloric view and visualization of the pylorus.

After that, each patients were asked to lie on his or her back in the supine position. The ball magnet was positioned close to the body on the right upper abdomen (hypochondrium). The capsule camera was oriented horizontally and laterally toward the pylorus for closer observation. The magnet position ensured that the capsule remained in the antrum. Using both the right and left joysticks, we moved the capsule closer to the pylorus (Figure 10A-C).

Station VIII: Magnetically controlled transpyloric passage of the capsule.

The magnetic ball was placed at the patient's right side at the level of the duodenal bulb. The capsule was then rotated until the camera faced the pylorus. The capsule was dragged close to the pylorus under the guidance of the magnet robot. As the pylorus was opened, peristalsis assisted the capsule into the duodenum. After transpyloric passage, first we depicted the duodenal bulb, then from the descending and inferior horizontal part of the duodenum, we visualized the ampulla of the Vater by tilting the capsule camera upwards to facilitate the retrograde view (Figure 10D-G).

Examining the small intestine

If the capsule entered *via* the small intestine, patients were asked to drink 1 L of PEG solution, and from then on, they were requested to drink clear fluids (*i.e.*, water). The movement of the capsule in the small intestine was then monitored hourly in real-time visualization mode. The examination ended when the capsule arrives at the colon or stops functioning due to the low battery.

RESULTS

An UBT test revealed *H. pylori* positivity in 32.7% of cases. (Table 2). No significant association with HP status and the type (proximal or distal), distribution (diffuse or focal) and severity (minimal or active, erosive) of the gastritis described on MCCE results were depicted.

The mean gastric, SB, and colon TT with MCCE was: 47 h 40 min (M/F: 44 h 15 min/51 h 14 min), 3 h 46 min 22 s (3 h 52 min 44 s/3 h 38 min 21 s) and 1 h 4 min 34 s (1 h 1 min 16 s/1 h 8 min 53 s), respectively. Average total time of MCCE examination: 5 h 48 min 35 s (5 h 46 min 37 s/5 h 50 min 18 s) (Table 3).

Table 2 The results of *Helicobacter pylori* C13 urea breath tests

	n	*H. pylori* positive	%	*H. pylori* negative	%	χ^2	*P* value	
Normal	30	7	23%	23	77%	0.9775	0.3228	NS
Minor proximalgastritis	19	9	47%	10	53%	1.529	0.2163	NS
Minor antralgastritis	19	4	21%	15	79%	1.0322	0.3096	NS
Active, erosive antralgastritis	15	6	40%	9	60%	0.3129	0.5759	NS
Proximal erosivegastritis	22	7	32%	15	68%	0.0069	0.9338	NS
Pangastritis (proximal and antral)	4	3	75%	1	25%	0.5	0.4795	NS
Total HP tested patients	110	36	33%	74	67%	-	-	-

H. pylori: *Helicobacter pylori*.

Table 3 Mean gastric, small bowel, and overall transit times of magnetically controlled capsule endoscopy

Transit time	All cases	SD	Male	Female
Stomach	0 h 47 min 40 s	0 h 43 min 29 s	0 h 44 min 15 s	0 h 51 min 14 s
Small bowel	3 h 46 min 22 s	2 h 1 min 24 s	3 h 52 min 46 s	3 h 38 min 21 s
Total	5 h 48 min 35 s	1 h 50 min 49 s	5 h 46 min 37 s	5 h 50 min 18 s

The diagnostic yields for detecting any abnormalities in the stomach and SB with MCCE were 81.9%: 68.6% for minor pathologies and 13.3% for major pathologies. 25.8% of the abnormalities were found in the SB, and 74.2% were in the stomach. The diagnostic yield for stomach/SB was 4.9%/8.4% for major pathologies and 55.9%/12.7% for minor pathologies (Table 4). In the stomach, ulcers and polyps were considered major, while signs of gastritis were minor pathologies. In the SB signs of Crohn's and celiac disease were the major and non-specific inflammation, diverticula and angiodysplasia the minor pathologies. Based on findings from MCCE examinations, the distribution of pathologies is depicted in Table 5.

The capsule's active magnetic movement through the pylorus was successful using the magnet in 41.9% of all patients (automatized protocol in 56 patients and active manually controlled magnetic activity in 63 patients) (Table 6).

In 18 (M/F: 6/12) patients (6.3%), SB visualization with MCCE was incomplete. There were 13 occurrences of incomplete examinations as a result of capsule depletion. In 3 of these 13 cases, the capsule was depleted within 5 h of operation, indicating a manufacturing flaw. The average total study time in the remaining 10 cases was 9 h 12 min 9 s. From the pylorus to the last image, the average transit time was 8 h 26 min 4 s. The examination was discontinued sooner than planned in 3 cases due to the patient's request. In 2 cases, there was capsule retention due to Crohn's-like ulceration, accompanied by a narrow bowel lumen (Table 6). These problems were resolved spontaneously without surgery, but with medical treatment. There were no serious adverse events or capsule retention during the study period.

DISCUSSION

There are two main directions in developing capsule endoscopes with active movements: internally and externally guided techniques. Internal guidance means that the locomotive system is integrated into the capsule, but these systems require longer-lasting batteries for full functionality. Its main advantage is a more precise navigation with the help of the internalized locomotive system. External guidance refers to outwardly conducted capsule movements, *e.g.*, with a magnetic control unit or device/moving arm generating the magnetic field. The exceptional advantage of this method is that the magnetic field (and its adjustment) built by the external unit controls the locomotive mechanism, thus making this an energy-saving solution. However, a disadvantage of this technique is that it is limited to more passive, less flexible locomotion. The examining physician controls the capsule outside the body with an external control unit, which decreases the accuracy of the spatial and temporal movements. Locomotion of the capsule endoscope would result in numerous long-term advantages in the diagnostics and therapy of GI diseases (focused biopsies, treatment options, *e.g.*, laser tumor ablation, local targeted release of certain medications, and endoscopic ultrasound applications)[1].

Table 4 Diagnostic yield of magnetically controlled capsule endoscopy

Diagnostic yield	Major	Minor	Total
Total	38 (13.3%)	195 (68.6%)	233 (81.9%)
Gastric	14 (4.9%)	159 (55.9%)	173 (60.8%)
SB	24 (8.4%)	36 (12.7%)	60 (21.1%)

SB: Small bowel.

Table 5 Distribution of pathologies detected by magnetically controlled capsule endoscopy

	Polyp ventriculi	Ulcus ventriculi	Coeliakia	Crohn	Gastritis	Small intestinal diverticula	Angiodysplasia	Aspecific infalmmation in small bowel
Major pathologies	5	9	1	23	159	1	26	9

Table 6 Distribution of different types of transpyloric transit in complete and incomplete small bowel studies

	Cases (*n*)	Mean total transit time	Mean gastric transit time	Mean SB transit time	Transpyloric transit		
					With magnet by automatic protocol	With magnet manually	Without magnet
Total study population	284	5 h 48 min 35 s	0 h 47 min 40 s	3 h 46 min 22 s	56 (19.7%)	63 (22.2%)	165 (58.1%)
Incomplete studies	18 (6.3%)	7 h 13 min 41 s	0 h 52 min 35 s	6 h 19 min 51 s	2	5	11
The capsule depleted (> 5 h)	10 (3.5%)	9 h 12 min 9 s	0 h 46 min 5 s	8 h 26 min 4 s	0	3	7
The capsule depleted (< 5 h)	3 (1%)	2 h 23 min 25 s	0 h 24 min 9 s	1 h 51 min 22 s	1	0	2
The patient requested to terminate	3 (1%)	4 h 45 min 9 s	0 h 50 min 3 s	3 h 55 min 6 s	1	1	1
The capsule stopped because of a disease	2 (0.7%)	8 h 19 min 36 s	2 h 11 min 33 s	6 h 8 min 33 s	0	1	1

SB: Small bowel.

Magnetic assisted capsule endoscopy (MACE) systems have been developed over the past 5-10 years, primarily for research goals. Experiences drawn from previously conducted *in vitro* studies showed that locomotion and precision of the capsule are significantly influenced by the physical characteristics of the generated magnetic field created by the external magnetic unit while travelling in the human body[1].

In 2011, Olympus was the first to introduce a modified MRI machine prototype that moved a MACE system which allowed the operator to successfully guide the capsule in a chosen spatial direction inside the stomach after drinking water. However, the adoption of this diagnostic procedure did not spread worldwide and get medical acceptance[6].

In 2014, IntroMedic developed a navigation (NAVI) magnetic capsule system that could be moved externally with a small, hammer-shaped, external static magnet device. The technology involving a magnet that assisted the physician in manually moving the capsule endoscope appeared viable and valuable in many experimental settings. However, it did not achieve any breakthroughs, as it only allowed sudden and harsh position changes of the capsule. In clinical trials studying the application of the NAVI capsule system using a small cohort, 65%-86% of the mucosal layer of the stomach was visualized accurately using external magnetically controlled locomotion after the ingestion of water. Its diagnostic accuracy was similar to that of traditional gastroscopy[9]. Using a similar type of NAVI capsule system, CE was performed on the large intestines, where magnetic locomotion directed the capsule from the cecum to the sigmoid colon. At the same time, a colonoscopy probe was inserted to monitor capsule movements to provide dilatation[10]. In iron deficiency anemia, after routine colonoscopy of 49 patients, the performance of a MACE system was compared with the IntroMedic Navi system in providing a diagnostic examination of the stomach and small intestine in one sitting.

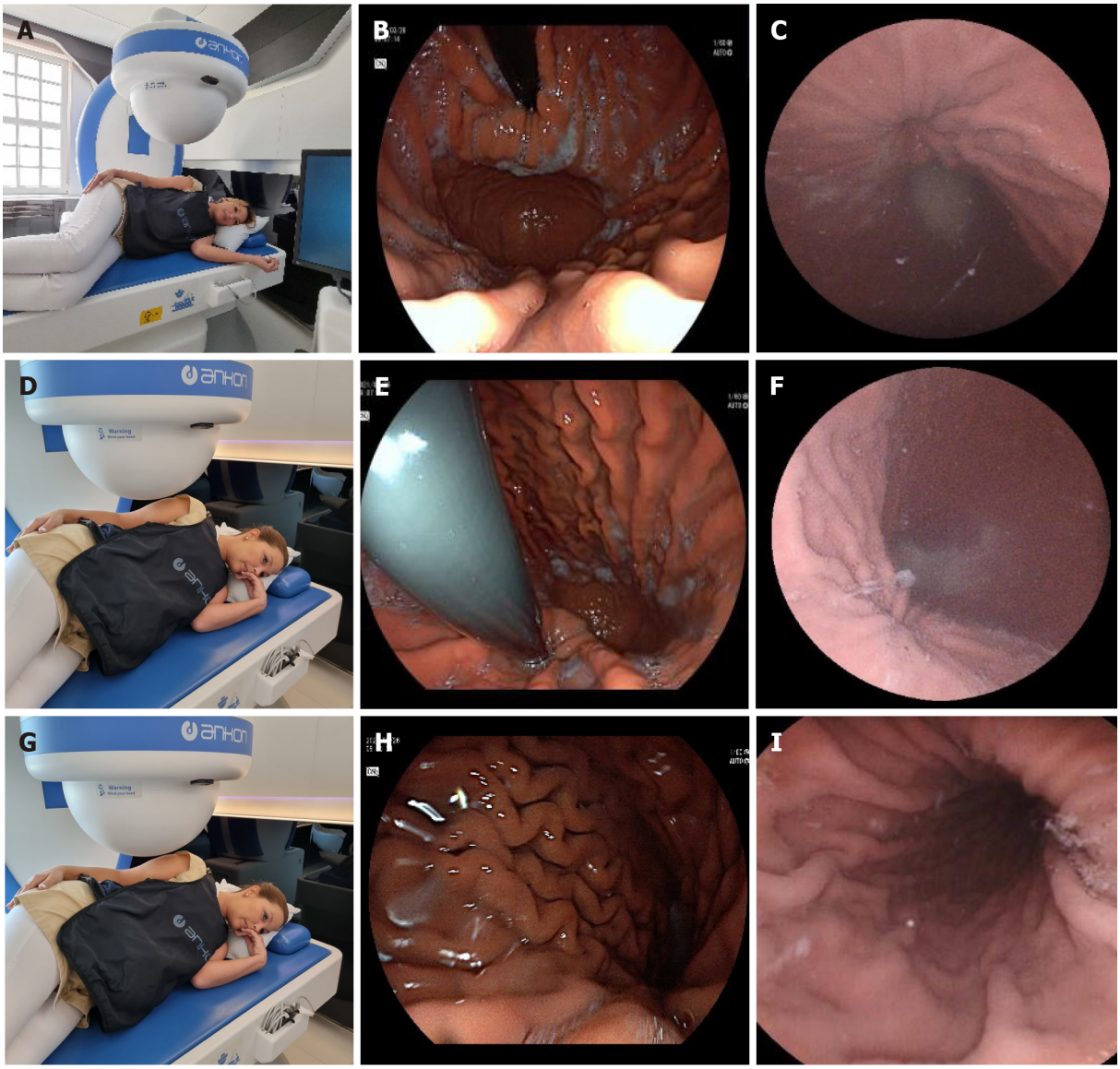

DOI: 10.3748/wjg.v28.i20.2227

Figure 7 Stations I-III at the left lateral decubitus position. A: Patients' position (Station I); B: Cardia by a gastroscope (Station I); C: Cardia by CE (Station I); D: Patients' position (Station II); E: Cardia by a gastroscope (Station II); F: Cardia by CE (Station II); G: Patients' position (Station III); H: Corpus by a gastroscope (Station III); I: Corpus by a capsule (Station III).

According to the results, MACE detected more pathologies than by gastroscopy alone, and no significant difference in diagnostic sensitivity was found between the methods when examining the upper GI tract[11].

Precise locomotion of the magnetic capsule inside the GI tract by manual control is not possible due to the variable density of tissues and variable distance of the capsule, *e.g.*, in the stomach from the external magnet. Moreover, exact spatial location of the capsule, its relation to the surrounding organs, or the ante-/retrograde orientation cannot be judged accurately. Therefore, a control mechanism is needed alongside the magnetic capsule, which is based on external robotics that enable the physician's input to be executed (*i.e.*, joystick: in forward, backward, upward, downward, and sideways directions). By pre-programming instruction sequences (script) in the computing control unit to examine the stomach from the fundus to the antrum, we created a reproducible examination of the complete inner mucosal lining of the stomach, which lowered the variability among investigations. If the examining physician notices significant pathology, he/she can intervene and move the examination to manual control and revisit the alteration; doing so increases the number of images taken of the lesion and optimizes the diagnostic accuracy of the study.

NaviCam was the first magnetically controlled capsule system that enables bidirectional data transmission and robotic control. The capsule functions at 1-6 fps and its spatial orientation with continuous monitoring of energy levels are transmitted *via* the recording vest to control the data and screen of the computing unit. At the console, we can control the precise locomotion of the capsule, image capturing speed, and brightness, as well as turn it on or off.

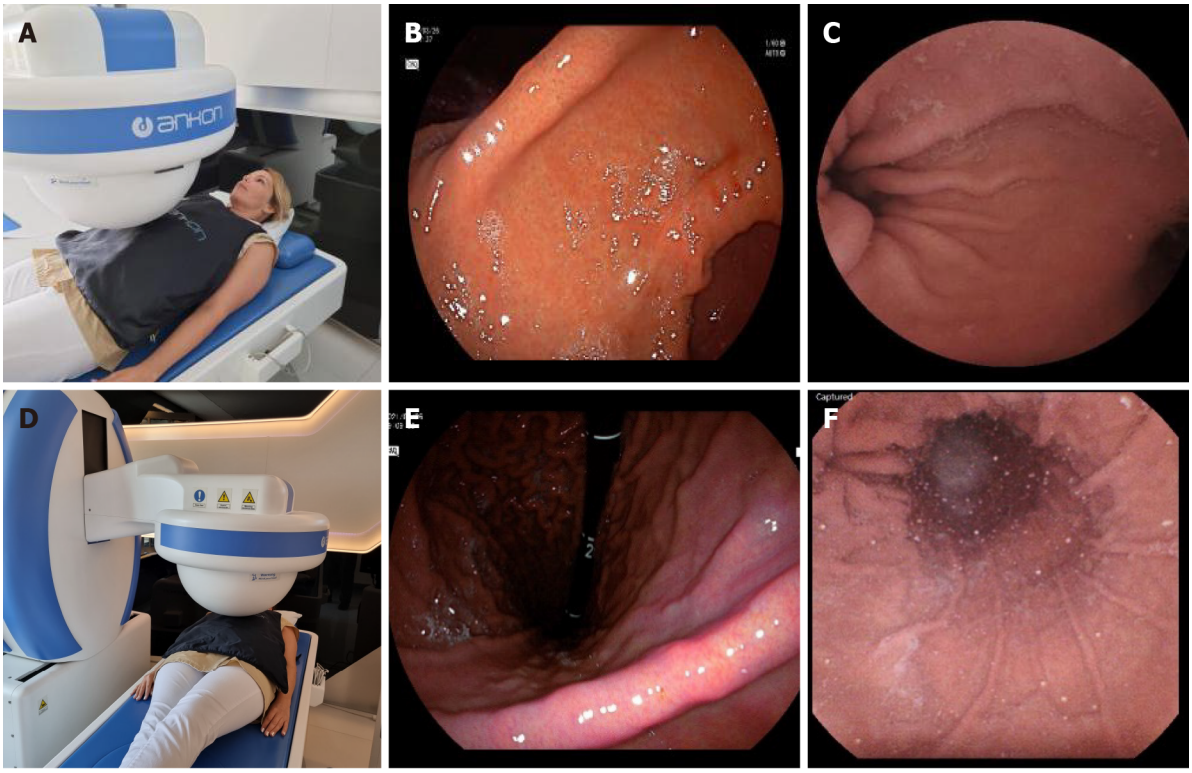

DOI: 10.3748/wjg.v28.i20.2227 **Copyright** © The Author(s) 2022.

Figure 8 Stations IV and V in the supine position. A: Patients' position (Station IV); B: Angular incisure by a gastroscope (Station IV); C: Angular incisure by CE (Station IV); A: Patients' position (Station V); B: Angular incisure by a gastroscope (Station V); C: Angular incisure by CE (Station V).

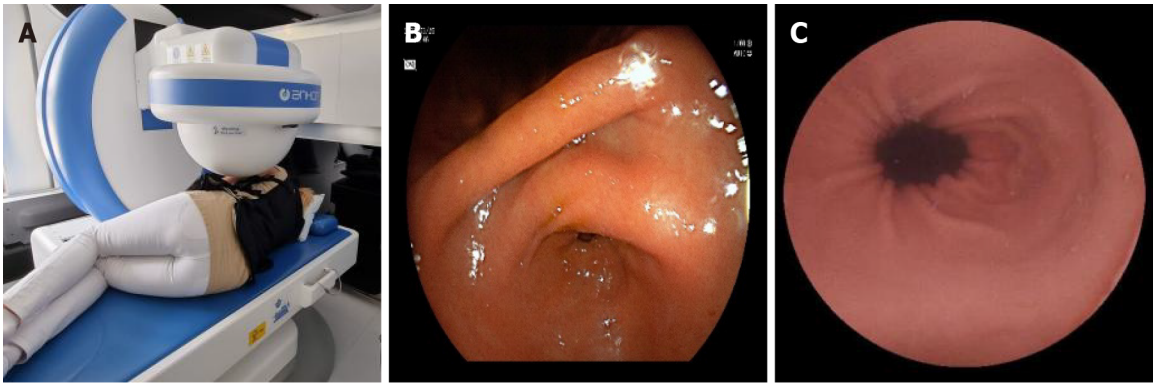

DOI: 10.3748/wjg.v28.i20.2227 **Copyright** © The Author(s) 2022.

Figure 9 Station at the right lateral decubitus patient position. A: Patients' position (Station VI); B: Antrum canal of stomach by gastroscope (Station VI); C: Antrum canal of stomach by CE (Station VI).

We combined manual and automatic, robotic capsule control to optimize the gastric procedure. As we previously published in an *in vitro* setting, complete 100% visualization of the inner surface of a plastic stomach model with the medium and large stomach autoscan program module and with the freehand controlling method could be successfully achieved in all cases. With the small and medium stomach mode, we could observe only 97.5% of the inner surface, because of the incomplete visualization of the prepyloric region. With freehand method, we needed nearly twice as much average time (749 s) to make a complete examination, compared to the robotic maneuvering with autoscan program (390 s). In an everyday praxis, in each patient position, the following stations and capsule positioning were performed after running the 3 different autoscan programs[12,13].

CE is a potentially patient-friendly and noncontact/infection-free diagnostic modality of screening for gastric diseases, which may result in complete and excellent examinations of the stomach. During the coronavirus disease 2019 pandemic, direct contact with the patients in the practice is a potential risk factor for infections. Non-contact medicine is a possibility for further examinations, such as remote control of CE[14]. The prevalence of focal gastric lesions (polyps, gastric ulcers, submucosal tumors, *etc*.)

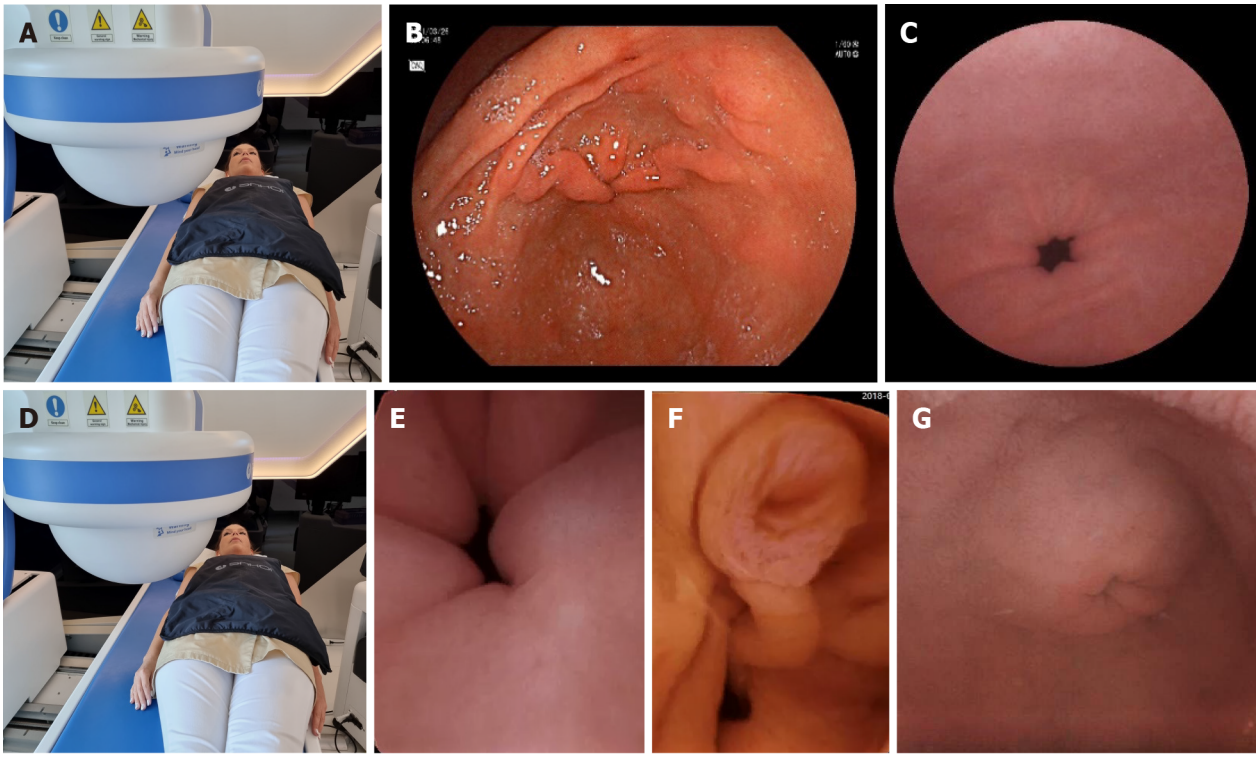

DOI: 10.3748/wjg.v28.i20.2227

Figure 10 Stations VII and VIII in the supine position. A: Patient's position (Station VII); B: Antrum canal of stomach by gastroscope (Station VII); C: Antrum canal of stomach by CE (Station VII); D: Patient's position (Station VIII); E: Pyloric ring (Station VIII); F: Ampulla of Vater (Station VIII); G: Pylorus from the duodenal bulb with a capsule (Station VIII).

increases with age, and they may be detected with MCCE as effectively as with gastroscopy[8]. The sensitivity is between 90% and 92%, and the specificity is between 94% and 96.7%[15]. Several studies proved that, altogether, reliable preparation (gastric cleanliness), careful examination, and MCCE are pivotal for adequate gastric visualization and, therefore, for the detection of superficial gastric neoplasms[16]. In a large multicenter gastric cancer screening trial conducted in China seven asymptomatic patients out of 3182 were diagnosed with advanced cancer by MCCE. Cancer prevalence was highest in the gastric body (3 cases), followed by 2 cases in the cardia and 2 in the antrum, while 1-1 cases were detected in the region of the angulus, in the fundus and in the esophagus. All were confirmed to be adenocarcinoma pathologically. These results indicate that screening with MCCE may be useful in high family risk populations or people aged over 50 years old as a gastric cancer screening modality[8].

Magnetic steering may also impact TTs, as delayed gastric transit of the CE (especially in patients with gastroparesis) may lead to an incomplete SB exam. This method may increase the papilla detection rate as well. In addition to magnetic steering, there are several other independent factors, such as male gender and higher BMI, which increase gastric TTs and decrease SB TTs, thus impacting the time required for CE completion[10]. Despite the fact that delayed gastric TT may cause incomplete SBCE, we should avoid esophago-gastro-duodenoscopy to resolve temporary gastric capsule retention and instead use MCCE[17].

The visual diagnosis of the presence of *H. pylori* with standard white light endoscopy (WLI) has a relatively low accuracy, especially in population with a low pretest probability. Moreover, WLI endoscopy correlates poorly with histopathological findings of *H. pylori* induced gastritis too. Recently, low quality retrospective studies proposed the theory, that with the application of a special electronic chromoendoscopy, linked color imaging, diffuse reddish appearance of the mucosa in the gastric body and fundic glands correlates with the presence of HP[18].

In our study we found no correlation between the HP status and the activity and type of gastritis observed on MCCE as follows, but not included this into the Table 2, since it would be relevant in another publication, focusing HP status and gastritis on MCCE.

MCCE is an excellent method to visualize the entire gastric mucosal surface up to 100% precision in healthy volunteers[5]. In a previous study of 75 consecutive patients, we demonstrated that with our combined method with automatic and manual control, a complete visualization of the cardia, fundus, corpus, angulus, antrum, and duodenal bulb was 95.4%, 100%, 100%, 100%, 100% and 100%, respectively. The ampulla of Vater was detected and observed in 20 patients (26%). Moreover, the visualization of the distal esophagus and the Z-line was possible in 67/75 patients (89%), which was

assessed as complete in 23, and partially complete in 44 patients. The mean stationary time for MCCE in the distal esophagus was 1 min and 32 s[19].

The use of MCCE needs to be considered in western and eastern countries, as there are two different scenarios, depending on the different levels of prevalence of UGI diseases and gastric cancer in each country. Nowadays, MCCE is mostly used for the detection of malignant and premalignant gastric lesions, which are more prevalent in eastern countries. However, the present technology opens the door to further, new technologies; subsequent developments would allow MCCE technology to be extended to other regions of the GI tract, *e.g.*, the esophagus, which may facilitate the detection of more relevant lesions, such as Barrett metaplasia in western countries as well. With second-generation MCCE, visualization of the esophagus, Z-line, and duodenal papilla would be improved, according to a study by Jiang *et al*[20] Furthermore, the gastric TT could shorten by one-third, which was nearly achieved by conventional endoscopy with an examination of approximately 10 min.

It is known that the current gold standard gastroscopy has some clear disadvantages, as it is commonly uncomfortable for patients, and therefore it is mostly performed under sedation, which carries definite procedure related risks. MCCE, as a patient-friendly, non-invasive test, might be an alternative for patients who refuse to undergo gastroscopy and increase patients' adherence for screening. Furthermore, MCCE of the stomach was recently approved by the Chinese Food and Drug Association for the following diagnostic indications: (1) As an alternative diagnostic tool for patients who refuse to undergo gastroscopy; (2) Screening of gastric diseases as a part of physical examination; (3) Screening for gastric cancer; (4) To diagnose various causes of GI inflammation; (5) To perform follow-up for diseases like gastric varices, gastric ulcer, atrophic gastritis, and polyps after surgical or endoscopic removal[21].

There is no similar study in the literature, as we performed a complete upper GI capsule examination, including the stomach and the SB with the same capsule endoscope during MCCE. Denzer *et al*[22] published a blinded, prospective trial from two French centers with the Intromedic manually controlled MCCE. A total of 189 patients were enrolled into this multicenter study. Lesions were defined as major (requiring biopsy or removal) or minor ones. The final gold-standard was unblinded conventional gastroscopy with biopsy, under sedation with propofol. Twenty-three major lesions were found in 21 patients and in this population, the capsule accuracy was 90.5% as compared to gastroscopy. Of the remaining 168 patients, 94% had minor and mostly multiple lesions; the capsule accuracy was 88.1%. All patients preferred MCCE over gastroscopy[22].

One of the risk factors of incomplete SB capsule endoscopy is a prolonged gastric transit time, which could be considered as a limitation of our combined gastric and SB study protocol. In our patient population, the average gastric transit time with magnetic transpyloric, manual control was 26 min. In contrast, in those cases where the magnetic transpyloric control failed, after examining the stomach, we left the capsule to propel through the pylorus by spontaneous peristaltic activity. In these patient groups, the average gastric transit time took 1 h and 9 min. In 10 cases out of 18 incomplete SB studies caused by battery low energy, this event occurred in 3 patients with manual magnetic passage and in 7 patients with spontaneous transpyloric passage[23].

Visibility and identification of landmarks are important factors to consider in accurate examination of stomach using MCCE. Gastric landmarks and typical stations described in the methods were always forced to achieve during combined automatic and manual maneuvering. For improving the learning curve of our gastroenterologist, we started to train the examinations in a plastic stomach model. In our previously published abstract, we described the improvement of the learning curves with manual magnetic controls both in experts and in trainees[1]. In this study, we find significant differences in the examination time of the complete inner surface mapping between trainees and experts, and moreover automatic protocols were faster and equally accurate as experts to achieve a complete inner surface mapping.

The problem how to minimalize bubbles and mucoid secretions is an existing problem in real life studies. To improve visibility, we established a unique preparation process with a combination of bicarbonate, Pronase B, and simethicone combined with a patient body rotation technique[2]. Moreover, in our described stations, we rotate our patients from left lateral to supine, then from supine top right lateral, and finally from right lateral to supine position during MCCE study. During this protocol, the gastric mucoid secretions also moving into different parts of the stomach due to the gravity making visible all the landmarks and the majority of the mucosal abnormalities. Application of prokinetics or motilin agonist erythromycin might also be an option in future studies to improve the visibility and reduce gastric lake content[24,25].

An inherent limitation of our present study that we performed gastroscopy only in a few patients with major gastric pathologies to accomplish final diagnosis and biopsy; and therefore, we could not assess the accuracy of MCCE in all patients compared to gastroscopy. However, several previous studies demonstrated excellent diagnostic value and high accuracy. In a recent meta-analysis of Zhang *et al*[26] four studies with 612 patients were included, in which the results of blinded MCCE and gastroscopy were compared. MCCE demonstrated a pooled sensitivity and specificity of 91% (95%CI: 0.87-0.93) and 90% (95%CI: 0.75-0.96), respectively. The diagnostic accuracy of MCCE was 91% (95%CI: 0.88-0.94) for assessing gastric diseases.

CONCLUSION

MCCE is an effective and safe diagnostic method for evaluating gastric and SB mucosal lesions while being utilized as a single upper GI capsule endoscope in patients referred for SBCE evaluation. MCCE using the novel Ankon capsule endoscopic technique is a proper diagnostic method for evaluating the gastric mucosa. It is a promising non-invasive screening tool that may be applied in future monitoring of patients with high gastric cancer family risk to decrease morbidity and mortality of benign and malignant upper GI disorders.

ARTICLE HIGHLIGHTS

Research background

While capsule endoscopy (CE) is the gold standard diagnostic method of detecting small bowel diseases and disorders, a novel magnetically controlled capsule endoscopy (MCCE) system provides non-invasive evaluation of the gastric mucosal surface, which can be performed without sedation or discomfort.

Research motivation

During standard small bowel capsule endoscopy (SBCE), passive movement of the CE may cause areas of the complex anatomy of the gastric mucosa to remain unexplored, whereas the precision of MCCE capsule movements inside the stomach promises better visualization of the entire mucosa.

Research objectives

To evaluate the Ankon MCCE system's feasibility, safety and diagnostic yield in patients with gastric or small bowel disorders.

Research methods

Of outpatients who were referred for SBCE, 284 (male/female: 149/135) were prospectively enrolled and evaluated by MCCE. The stomach was examined in the supine, left, and right lateral decubitus positions without sedation. Next, all patients underwent a complete small bowel CE study protocol. The gastric mucosa was explored with the Ankon MCCE system with active magnetic control of the capsule endoscope in the stomach, applying three standardized pre-programmed computerized algorithms in combination with manual control of the magnetic movements.

Research results

The urea breath test revealed *Helicobacter pylori* positivity in 32.7% of patients. The mean gastric and small bowel transit times with MCCE were 47 min 40 s and 3 h 46 min 22 s, respectively. The average total time of upper GI MCCE examination was 5 h 48 min 35 s min. Active magnetic movement of the Ankon capsule through the pylorus was successful in 41.9% of patients. Overall diagnostic yield for detecting abnormalities in the stomach and small bowel was 81.9% (68.6% minor; 13.3% major pathologies); 25.8% of abnormalities were in the small bowel; 74.2% were in the stomach. The diagnostic yield for stomach/small bowel was 55.9%/12.7% for minor and 4.9%/8.4% for major pathologies.

Research conclusions

MCCE is a feasible, safe diagnostic method for evaluating gastric mucosal lesions and is a promising non-invasive screening tool to decrease morbidity and mortality in upper gastrointestinal diseases.

Research perspectives

MCCE is promising as a non-invasive screening tool that may be applied in future monitoring of patients for evaluating gastric mucosal lesions and decreasing morbidity and mortality of benign and malignant upper GI disorders.

ACKNOWLEDGEMENTS

Acknowledgements: special thanks for Zoltán Tóbiás MD for the graphical work and visual explanations of different gastric stations and Kata Tőgl our nurse manager for assistance and modelling the patients positioning during magnetically controlled capsule endoscopy.

FOOTNOTES

Author contributions: Szalai M, Madácsy L and Finta Á performed the capsule endoscopy examinations; Szalai M, Helle K, Finta Á, Oczella L and Madácsy L performed the data collection; Szalai M, Helle K, Lovász BD, Finta Á, Rosztóczy A, Oczella L and Madácsy L drafted the manuscript; Oczella L enrolled participants; Szalai M and Madá csy L reviewed capsule endoscopy images as expert endoscopists with high experience in capsule endoscope; Rosztó czy A and Madácsy L planned the study concept, consulted with the authors, performed manuscript database validation, supervised the manuscript preparation and writing, and acted as the submission's guarantor; All authors finally read and approved the manuscript.

Institutional review board statement: This study was approved by the Ethical Committee of the University of Szeged (registry No. 5/17.04.26) and registered in the trial registry: ClinicalTrials.gov (Identifier: NCT03234725). The present study was conducted according to the World Medical Association's Declaration of Helsinki provisions in 1995.

Informed consent statement: All involved participants gave their informed consent (in written form) prior to study inclusion. Patients agreed to participate in the present study, undergo capsule endoscopy and Helicobacter pylori breaths tests by written informed consent. All details that might disclose the identity of the subjects under study are anonymized. The institutional review board of University of Szeged waived the requirement to obtain informed consents from patients.

Conflict-of-interest statement: No conflict-of-interest.

Data sharing statement: Data (deidentified participant data) are available upon reasonable request. Contact details: endomabt1@gmail.com; László Madácsy (0000-0002-7589-6193). No additional information or data is available.

STROBE statement: The authors have read the STROBE Statement-checklist of items, and the manuscript was prepared and revised according to the STROBE Statement-checklist of items.

Country/Territory of origin: Hungary

ORCID number: Milán Szalai 0000-0002-5314-7693; Krisztina Helle 0000-0002-5477-2618; Barbara Dorottya Lovasz 0000-0003-0894-5669; Ádám Finta 0000-0002-2455-1056; András Rosztóczy 0000-0002-8597-8934; László Oczella 0000-0003-1454-4917; Laszlo Madacsy 0000-0002-7589-6193.

Corresponding Author's Membership in Professional Societies: Hungarian Society of Gastroenterology, 45326.

S-Editor: Zhang H
L-Editor: A
P-Editor: Zhang H

REFERENCES

1 **Adler SN**. The history of time for capsule endoscopy. *Ann Transl Med* 2017; **5**: 194 [PMID: 28567374 DOI: 10.21037/atm.2017.03.90]
2 **Eliakim R**, Yassin K, Shlomi I, Suissa A, Eisen GM. A novel diagnostic tool for detecting oesophageal pathology: the PillCam oesophageal video capsule. *Aliment Pharmacol Ther* 2004; **20**: 1083-1089 [PMID: 15569110 DOI: 10.1111/j.1365-2036.2004.02206.x]
3 **Iddan G**, Meron G, Glukhovsky A, Swain P. Wireless capsule endoscopy. *Nature* 2000; **405**: 417 [PMID: 10839527 DOI: 10.1038/35013140]
4 **Keller J**, Fibbe C, Volke F, Gerber J, Mosse AC, Reimann-Zawadzki M, Rabinovitz E, Layer P, Schmitt D, Andresen V, Rosien U, Swain P. Inspection of the human stomach using remote-controlled capsule endoscopy: a feasibility study in healthy volunteers (with videos). *Gastrointest Endosc* 2011; **73**: 22-28 [PMID: 21067740 DOI: 10.1016/j.gie.2010.08.053]
5 **Liao Z**, Duan XD, Xin L, Bo LM, Wang XH, Xiao GH, Hu LH, Zhuang SL, Li ZS. Feasibility and safety of magnetic-controlled capsule endoscopy system in examination of human stomach: a pilot study in healthy volunteers. *J Interv Gastroenterol* 2012; **2**: 155-160 [PMID: 23687601 DOI: 10.4161/jig.23751]
6 **Rey JF**, Ogata H, Hosoe N, Ohtsuka K, Ogata N, Ikeda K, Aihara H, Pangtay I, Hibi T, Kudo S, Tajiri H. Feasibility of stomach exploration with a guided capsule endoscope. *Endoscopy* 2010; **42**: 541-545 [PMID: 20593331 DOI: 10.1055/s-0030-1255521]
7 **Rey JF**, Ogata H, Hosoe N, Ohtsuka K, Ogata N, Ikeda K, Aihara H, Pangtay I, Hibi T, Kudo SE, Tajiri H. Blinded nonrandomized comparative study of gastric examination with a magnetically guided capsule endoscope and standard videoendoscope. *Gastrointest Endosc* 2012; **75**: 373-381 [PMID: 22154417 DOI: 10.1016/j.gie.2011.09.030]

8 **Zhao AJ**, Qian YY, Sun H, Hou X, Pan J, Liu X, Zhou W, Chen YZ, Jiang X, Li ZS, Liao Z. Screening for gastric cancer with magnetically controlled capsule gastroscopy in asymptomatic individuals. *Gastrointest Endosc* 2018; **88**: 466-474.e1 [PMID: 29753039 DOI: 10.1016/j.gie.2018.05.003]

9 **Nam SJ**, Lee HS, Lim YJ. Evaluation of Gastric Disease with Capsule Endoscopy. *Clin Endosc* 2018; **51**: 323-328 [PMID: 30078305 DOI: 10.5946/ce.2018.092]

10 **Gu H**, Zheng H, Cui X, Huang Y, Jiang B. Maneuverability and safety of a magnetic-controlled capsule endoscopy system to examine the human colon under real-time monitoring by colonoscopy: a pilot study (with video). *Gastrointest Endosc* 2017; **85**: 438-443 [PMID: 27480288 DOI: 10.1016/j.gie.2016.07.053]

11 **Ching HL**, Hale MF, Kurien M, Campbell JA, Chetcuti Zammit S, Healy A, Thurston V, Hebden JM, Sidhu R, McAlindon ME. Diagnostic yield of magnetically assisted capsule endoscopy versus gastroscopy in recurrent and refractory iron deficiency anemia. *Endoscopy* 2019; **51**: 409-418 [PMID: 30360012 DOI: 10.1055/a-0750-5682]

12 **Szalai M**, Oczella L, Lovasz BD, Madacsy L. Surface mapping in plasctic gastric model assisted by a robotic autoscan program with new magnetically controlled gastroc capsule endoscopy system compared to manual controlling. *United European Gastroenterol J* 2018; 865

13 **Jiang X**, Qian YY, Liu X, Pan J, Zou WB, Zhou W, Luo YY, Chen YZ, Li ZS, Liao Z. Impact of magnetic steering on gastric transit time of a capsule endoscopy (with video). *Gastrointest Endosc* 2018; **88**: 746-754 [PMID: 30005825 DOI: 10.1016/j.gie.2018.06.031]

14 **Pan J**, Li Z, Liao Z. Noncontact endoscopy for infection-free gastric examination during the COVID-19 pandemic. *VideoGIE* 2020; **5**: 402-403.e1 [PMID: 32391446 DOI: 10.1016/j.vgie.2020.04.026]

15 **Liao Z**, Hou X, Lin-Hu EQ, Sheng JQ, Ge ZZ, Jiang B, Hou XH, Liu JY, Li Z, Huang QY, Zhao XJ, Li N, Gao YJ, Zhang Y, Zhou JQ, Wang XY, Liu J, Xie XP, Yang CM, Liu HL, Sun XT, Zou WB, Li ZS. Accuracy of Magnetically Controlled Capsule Endoscopy, Compared With Conventional Gastroscopy, in Detection of Gastric Diseases. *Clin Gastroenterol Hepatol* 2016; **14**: 1266-1273.e1 [PMID: 27211503 DOI: 10.1016/j.cgh.2016.05.013]

16 **Qian YY**, Zhu SG, Hou X, Zhou W, An W, Su XJ, McAlindon ME, Li ZS, Liao Z. Preliminary study of magnetically controlled capsule gastroscopy for diagnosing superficial gastric neoplasia. *Dig Liver Dis* 2018; **50**: 1041-1046 [PMID: 29779696 DOI: 10.1016/j.dld.2018.04.013]

17 **Luo YY**, Pan J, Chen YZ, Jiang X, Zou WB, Qian YY, Zhou W, Liu X, Li ZS, Liao Z. Magnetic Steering of Capsule Endoscopy Improves Small Bowel Capsule Endoscopy Completion Rate. *Dig Dis Sci* 2019; **64**: 1908-1915 [PMID: 30725289 DOI: 10.1007/s10620-019-5479-z]

18 **Madacsy L**, Lovasz BD, Zsobrak K, Szalai M, Oczella L. Feasibility and safety of robotocally controlled magnetic capsule endoscopy in the visualization of the upper gastrointestinal tract. *United European Gastroenterol J* 2018; 1484

19 **Dohi O**, Yagi N, Onozawa Y, Kimura-Tsuchiya R, Majima A, Kitaichi T, Horii Y, Suzuki K, Tomie A, Okayama T, Yoshida N, Kamada K, Katada K, Uchiyama K, Ishikawa T, Takagi T, Handa O, Konishi H, Naito Y, Itoh Y. Linked color imaging improves endoscopic diagnosis of active Helicobacter pylori infection. *Endosc Int Open* 2016; **4**: E800-E805 [PMID: 27556101 DOI: 10.1055/s-0042-109049]

20 **Jiang B**, Qian YY, Pan J, Jiang X, Wang YC, Zhu JH, Zou WB, Zhou W, Li ZS, Liao Z. Second-generation magnetically controlled capsule gastroscopy with improved image resolution and frame rate: a randomized controlled clinical trial (with video). *Gastrointest Endosc* 2020; **91**: 1379-1387 [PMID: 31981648 DOI: 10.1016/j.gie.2020.01.027]

21 **Chinese Digestive Endoscopist Committee**, Chinese Endoscopist Association, the Health Management and Physical Examination Committee of Digestive Endoscopy; Capsule Endoscopy Collaboration Group of Chinese Society of Digestive Endoscopy; Chinese Anti-Cancer Association, the Society of Oncological Endoscopy; Chinese Society of Health Management. [The China expert consensus of clinical practice for magnetically controlled capsule gastroscopy(2017, Shanghai)]. *Zhonghua Nei Ke Za Zhi* 2017; **56**: 876-884 [PMID: 29136725 DOI: 10.3760/cma.j.issn.0578-1426.2017.11.023]

22 **Denzer UW**, Rösch T, Hoytat B, Abdel-Hamid M, Hebuterne X, Vanbiervielt G, Filippi J, Ogata H, Hosoe N, Ohtsuka K, Ogata N, Ikeda K, Aihara H, Kudo SE, Tajiri H, Treszl A, Wegscheider K, Greff M, Rey JF. Magnetically guided capsule versus conventional gastroscopy for upper abdominal complaints: a prospective blinded study. *J Clin Gastroenterol* 2015; **49**: 101-107 [PMID: 24618504 DOI: 10.1097/MCG.0000000000000110]

23 **Westerhof J**, Weersma RK, Koornstra JJ. Risk factors for incomplete small-bowel capsule endoscopy. *Gastrointest Endosc* 2009; **69**: 74-80 [PMID: 18691709 DOI: 10.1016/j.gie.2008.04.034]

24 **Szalai M**, Oczella L, Lovasz BD, Madacsy L. Surface mapping in plastic gastric model assisted by a robotic autoscan program with a new magnetically controlled gastric capsule endoscopy system compared to manual controlling. *United European Gastroenterol J* 2018; 415-A415

25 **Schmiedt P**, Szalai M, Oczella L, Zsobrak K, Lovasz BD, Dubravcsik Z, Madacsy L. A new preparation method for improving gastric mucosal visibility and cleanliness during magnetically assisted capsule endoscopy: A prospective study. *Endoscopy* 2019; **51**: S7

26 **Zhang H**, Chen J, Li J, Huang C, Li M, Wu W, Jiang J. Use of magnetically controlled capsule endoscopy for the diagnosis of gastric diseases in adults: a systematic review and meta-analysis. Dig Med Res 2020; 3: 42 [DOI: 10.21037/dmr-20-141]

World Journal of Gastroenterology

Submit a Manuscript: https://www.f6publishing.com

World J Gastroenterol 2022 May 28; 28(20): 2243-2247

DOI: 10.3748/wjg.v28.i20.2243

ISSN 1007-9327 (print) ISSN 2219-2840 (online)

CASE REPORT

Endoscopic management of intramural spontaneous duodenal hematoma: A case report

Giorgio Valerii, Vittorio Maria Ormando, Carlo Cellini, Luca Sacco, Carmelo Barbera

Specialty type: Gastroenterology and hepatology

Provenance and peer review: Unsolicited article; Externally peer reviewed.

Peer-review model: Single blind

Peer-review report's scientific quality classification

Grade A (Excellent): 0
Grade B (Very good): B
Grade C (Good): C
Grade D (Fair): 0
Grade E (Poor): 0

P-Reviewer: Kumar R, India; Tanpowpong P, Thailand

Received: November 28, 2021
Peer-review started: November 28, 2021
First decision: January 8, 2022
Revised: January 12, 2022
Accepted: April 21, 2022
Article in press: April 21, 2022
Published online: May 28, 2022

Giorgio Valerii, Carlo Cellini, Carmelo Barbera, Gastroenterology and Endoscopy Unit, Ospedale G. Mazzini, Teramo 64100, Italy

Vittorio Maria Ormando, Gastroenterology and Endoscopy Unit, AORN San Giuseppe Moscati, Avellino 83100, Italy

Luca Sacco, Surgery Unit, Ospedale G. Mazzini, Teramo 64100, Italy

Corresponding author: Giorgio Valerii, MD, PhD, Doctor, Gastroenterology and Endoscopy Unit, Ospedale G. Mazzini, Piazza Italia, 1, Teramo 64100, Italy. gioval83@hotmail.it

Abstract

BACKGROUND

Intramural duodenal hematoma is a rare condition described for the first time in 1838. This condition is usually associated with blunt abdominal trauma in children. Other non-traumatic risk factors for spontaneous duodenal haematoma include several pancreatic diseases, coagulation disorders, malignancy, collagenosis, peptic ulcers, vasculitis and upper endoscopy procedures. In adults the most common risk factor reported is anticoagulation therapy. The clinical presentation may vary from mild abdominal pain to acute abdomen and intestinal obstruction or gastrointestinal bleeding.

CASE SUMMARY

The aim of this case summary is to show a case of intramural spontaneous hematoma with symptoms of intestinal obstruction that was properly drained endoscopically by an innovative system lumen-apposing metal stent Hot AXIOS™ stent (Boston Scientific Corp., Marlborough, MA, United States).

CONCLUSION

Endoscopic lumen-apposing metal stent Hot AXIOS™ stent is a safe and feasible treatment of duodenal intramural hematoma in our case.

Key Words: Duodenal hematoma; Several pancreatic diseases; Endoscopy complication; AXIOS™ stent; Case report

Core Tip: The present case explored the feasibility, safety and efficacy of endoscopic ultrasound-guided drainage of spontaneous duodenal hematoma. The new lumen-apposing self-expandable metallic stent Hot AXIOS™ could be considered a valid alternative to conventional endoscopic incision of the hematoma by using a needle-knife, a biopsy forceps or surgical drainage and percutaneous drainage to relieve pain and a persistent duodenal ulcer.

Citation: Valerii G, Ormando VM, Cellini C, Sacco L, Barbera C. Endoscopic management of intramural spontaneous duodenal hematoma: A case report. *World J Gastroenterol* 2022; 28(20): 2243-2247
URL: https://www.wjgnet.com/1007-9327/full/v28/i20/2243.htm
DOI: https://dx.doi.org/10.3748/wjg.v28.i20.2243

INTRODUCTION

Intramural duodenal hematoma (IDH) is a rare intestinal condition described for the first time at autopsy in 1838[1], and the first source in the PubMed database accessing the MEDLINE database (http://www.ncbi.nlm.nih.gov/pubmed/) dates from 1952[2].

This condition is usually associated with blunt abdominal trauma in children[3] and upper endoscopy procedures (duodenal biopsy or injection therapy for bleeding peptic ulcers) or various non-traumatic conditions in adults (> 70% of cases). These include several pancreatic diseases even if the association remains unclear, such as certain coagulation disorders (anticoagulant therapy, haemophilia, Von Willebrand disease, Henoch-Schönlein purpura), malignancy, collagenosis, peptic ulcers and vasculitis[4-7].

Clinical symptoms for IDH may vary from vague abdominal pain to acute abdomen, intestinal obstruction or gastrointestinal bleeding[3,8], and diagnosis is subsequently confirmed by magnetic resonance imaging or computed tomography (CT) and upper gastrointestinal endoscopy (UGIE).

Most IDH cases resolve spontaneously or with correction of abnormal coagulation. Percutaneous drainage or surgery may be needed in some refractory IDH cases, malignancy, perforation and intestinal tract obstruction.

Here we present the use of the innovative lumen apposing metal stent catheter (LAMS) Hot AXIOS™ (Boston Scientific Corp., Marlborough, MA, United States) in the case of spontaneous IDH with intestinal substenosis, which was non-responsive to conservative management, in a patient without risk factors. This innovative device, with a lumen apposing self-expandable metal stent fitted onto an electrocautery-enhanced tip catheter, is safe and feasible in gallbladder drainage, choledochoduodenostomy and drainage of pancreatic fluid collections. In recent years, Hot AXIOS™ has also been used for off-label indications including gastrojejunostomy, gastro-gastrostomy and drainage of postsurgical collections. Herein we report the use of Hot AXIOS™ in the rare digestive disorder spontaneous IDH.

CASE PRESENTATION

Chief complaints

A 51-year-old man was admitted to the hospital with abdominal pain, bloating and vomiting.

History of present illness

The clinical data suggested a diagnosis of intestinal obstruction.

History of past illness

The patient did not report comorbidities or recent abdominal trauma without relevant previous medical history and in particular without having taken anti-platelet medication.

Personal and family history

He did not have relevant family history.

Physical examination

Physical examination on admission revealed slight tenderness over the epigastric region and right flank.

Laboratory examinations

Initial biochemical analysis indicated neutrophilic leukocytosis (13.07 × 10^9/L) and an increased level of C-reactive protein without alterations of serum haemoglobin, D-dimer, platelet function and

coagulation parameters.

Imaging examinations

A contrast-enhanced abdominal CT scan revealed an IDH (Figure 1A). On admission UGIE and then endoscopic ultrasound (EUS) confirmed submucosal swelling of the second part of the duodenum that measured approximately 90 mm along the long axis with substenosis of the duodenal lumen (Figure 1B).

MULTIDISCIPLINARY EXPERT CONSULTATION

A conservative approach was attempted with clinical observation and empirical antibiotic therapy. The patient was discharged in good clinical condition after 8 d of intravenous antibiotic therapy.

FINAL DIAGNOSIS

Intramural spontaneous duodenal hematoma.

TREATMENT

After 48 h the patient was readmitted to the hospital due to clinical relapse. Biochemical analysis indicated a significant increase of both leukocytosis and C-reactive protein, and the radiological evaluation confirmed the previous diagnosis. After 10 d a multidisciplinary evaluation was performed, and minimally invasive endoscopic treatment was proposed.

EUS-guided drainage was performed with the Hot AXIOS™ system. A direct LAMS 15 mm × 10 mm was inserted into the submucosa lumen with an electrocautery-enhanced tip catheter and released under complete EUS control after the second flange was deployed in the duodenal lumen (Figure 2A). UGIE control confirmed the correct LAMS placement, and hematinic material associated with slightly purulent drainage was observed (Figure 2B).

OUTCOME AND FOLLOW-UP

A control CT scan demonstrated the presence of LAMS and the complete drainage of the intramural collection (Figure 2C). The patient was discharged in good clinical condition after 7 d. After an additional 2 wk he repeated UGIE, which revealed a complete resolution of the duodenal bulging, and the LAMS was contextually removed with complete closure of the mucosal defect with a clip. At the 30-d follow-up the patient was completely asymptomatic.

DISCUSSION

IDH is a rare condition usually caused by trauma, anticoagulant therapy, rupture of a duodenal aneurysm or biopsy[4-7,9]. Rare cases of IDH have also been described as a consequence of acute pancreatitis[3] or after endoscopic retrograde cholangiopancreatography procedures[10].

CT and magnetic resonance imaging represent the most sensitive diagnostic exams for IDH. Radiological exams have a role both for diagnosis as well as follow-up of small bowel hematoma within 2 wk[11,12]. Once IDH is confirmed, conservative management with fasting and total parenteral nutrition should be given[13]. Traditionally, in the case of persistent IDH, surgical drainage[14,15] and percutaneous drainage were performed[16], both causing great trauma for the patient. The indications for surgical intervention are not well clarified, certainly in the case of occlusive symptoms over 7-10 d or where there is evidence of perforation with a generalized peritonitis[17].

To date there are few described cases of endoscopic drainage of duodenal hematoma. This consists of endoscopic incision of the hematoma using a needle-knife or a biopsy forceps in order to obtain rapid submucosal decompression[18,19] with improvement of abnormal laboratory findings and abdominal pain in up to 1 wk. The persistence of duodenal ulcer at the site of endoscopic incision has also been described with a complete resolution only after 1 mo[18].

In our case we had a patient with an unremarkable previous medical history, with no risk factors for IDH who presented with intestinal pseudo-obstruction symptoms and leukocytosis without evidence of pancreatitis. We first attempted a conservative approach according to the existing data, but after recurrence of symptoms an endoscopic approach was proposed.

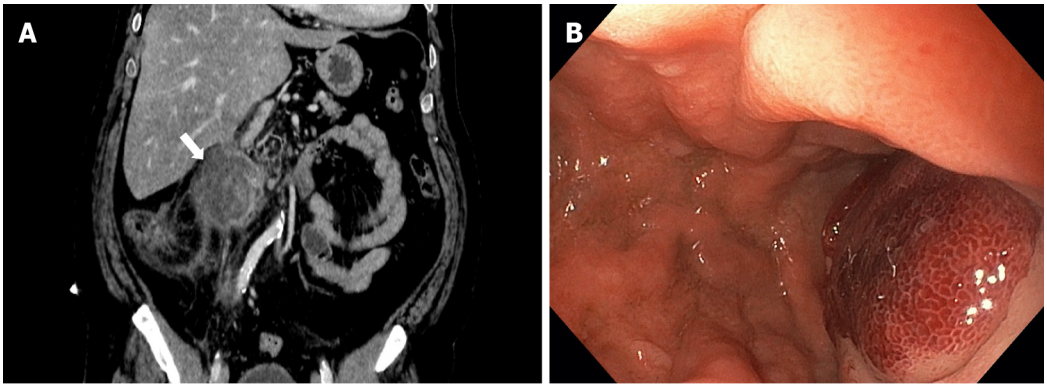

DOI: 10.3748/wjg.v28.i20.2243 **Copyright** © The Author(s) 2022.

Figure 1 Intramural duodenal hematoma. A: Contrast-enhanced abdominal computed tomography in coronal section; B: Endoscopic visualization with substenosis of duodenal lumen.

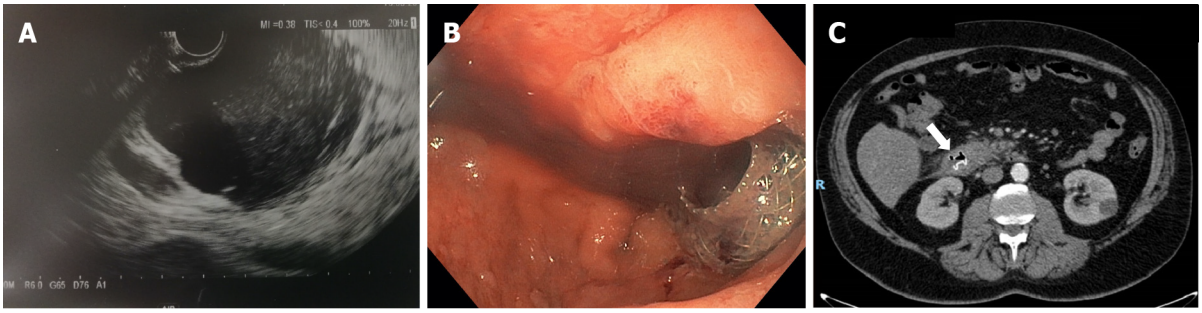

DOI: 10.3748/wjg.v28.i20.2243 **Copyright** © The Author(s) 2022.

Figure 2 Intramural duodenal hematoma after endoscopic treatment. A: Endoscopic ultrasonography (EUS) image showed deployment of the distal flange of a cautery-tipped lumen apposing metal stent (LAMS) in the intramural duodenal hematoma under EUS guidance; B: Endoscopic views showed the proximal flange of the LAMS; C: Control abdominal computed tomography confirmed the correct position of the LAMS.

The Hot AXIOS™ lumen-apposing stent is a novel double-flanged covered, self-expanding metal stent, safe and effective in gallbladder drainage, choledochoduodenostomy and drainage of pancreatic fluid collections. In the recent years, Hot AXIOS™ stents have also been used for off-label indications including gastrojejunostomy, gastro-gastrostomy and drainage of postsurgical collections.

Here we present the use of Hot AXIOS™ in a rare but possible digestive disorder with a rapid and complete resolution of this insidious clinical entity, as confirmed by CT scan and with only 7 d length of stay without abnormal laboratory findings and abdominal pain after the procedure.

CONCLUSION

In our experience Hot AXIOS™ is a safe and effective endoscopic procedure for the treatment of IDH, reserved for patients who are not responsive to conservative management. However, it should be performed by expert endoscopists trained in EUS and radiological procedures. To reduce the rate of postoperative complications and improve clinical outcome a previous careful clinical evaluation focusing on coagulopathies is mandatory.

FOOTNOTES

Author contributions: All authors contributed to writing this case report.

Informed consent statement: Informed written consent was obtained from the patient for publication of this report and any accompanying images.

Conflict-of-interest statement: All authors declare no conflict of interest for this case report.

CARE Checklist (2016) statement: The authors have read the CARE Checklist (2016), and the manuscript was

prepared and revised according to the CARE Checklist (2016).

Country/Territory of origin: Italy

ORCID number: Giorgio Valerii 0000-0001-8268-2022; Vittorio Maria Ormando 0000-0003-4481-755X; Carlo Cellini 0000-0001-7210-0439; Luca Sacco 0000-0003-1007-9894; Carmelo Barbera 0000-0002-4051-4976.

S-Editor: Yan JP
L-Editor: Filipodia
P-Editor: Yan JP

REFERENCES

1 **McLauchlan J**. False aneurysmaltumouroccupyingnearly the whole of the duodenum. *Lancet* 1838; 2243-2247 [DOI: 10.1016/S0140-6736(02)95675-8]
2 **Dey DL**. Acute duodenal obstruction due to an intramural haematoma. *Med J Aust* 1952; **1**: 708 [PMID: 14940187 DOI: 10.5694/j.1326-5377.1952.tb84095.x]
3 **Kumar R**, Athwal PSS, Kumar M, Devi K, Kahlon S. Spontaneous Intramural Duodenal Hematoma: A Rare Complication of Pancreatitis. *Cureus* 2020; **12**: e8491 [PMID: 32656009 DOI: 10.7759/cureus.8491]
4 **Chang CM**, Huang HH, How CK. Acute pancreatitis with an intramural duodenal hematoma. *Intern Med* 2015; **54**: 755-757 [PMID: 25832937 DOI: 10.2169/internalmedicine.54.3147]
5 **Eichele DD**, Ross M, Tang P, Hutchins GF, Mailliard M. Spontaneous intramural duodenal hematoma in type 2B von Willebrand disease. *World J Gastroenterol* 2013; **19**: 7205-7208 [PMID: 24222967 DOI: 10.3748/wjg.v19.i41.7205]
6 **Frostick SP**, Collin J, Daar AS, Kettlewell M, Nolan DJ. Non-traumatic intramural haematoma: an unusual cause of duodenal obstruction. *Br J Surg* 1984; **71**: 313-314 [PMID: 6608393 DOI: 10.1002/bjs.1800710421]
7 **Tseng CY**, Fan JS, Yang SC, Huang HH, Chen JD, Yen DH, Huang CI. Anticoagulant-induced intramural intestinal hemorrhage. *Am J Emerg Med* 2010; **28**: 937-940 [PMID: 20887911 DOI: 10.1016/j.ajem.2009.08.002]
8 **Kang EA**, Han SJ, Chun J, Lee HJ, Chung H, Im JP, Kim SG, Kim JS, Yoon H, Shin CM, Park YS, Kim N, Lee DH, Jung HC. Clinical features and outcomes in spontaneous intramural small bowel hematoma: Cohort study and literature review. *Intest Res* 2019; **17**: 135-143 [PMID: 30301344 DOI: 10.5217/ir.2018.00085]
9 **Iuchtman M**, Steiner T, Faierman T, Breitgand A, Bartal G. Post-traumatic intramural duodenal hematoma in children. *Isr Med Assoc J* 2006; **8**: 95-97 [PMID: 16544730]
10 **Pan YM**, Wang TT, Wu J, Hu B. Endoscopic drainage for duodenal hematoma following endoscopic retrograde cholangiopancreatography: a case report. *World J Gastroenterol* 2013; **19**: 2118-2121 [PMID: 23599635 DOI: 10.3748/wjg.v19.i13.2118]
11 **Abbas MA**, Collins JM, Olden KW, Kelly KA. Spontaneous intramural small-bowel hematoma: clinical presentation and long-term outcome. *Arch Surg* 2002; **137**: 306-310 [PMID: 11888455 DOI: 10.1001/archsurg.137.3.306]
12 **Zhou H**, Ma X, Sheng M, Lai C, Fu J. Evolution of intramural duodenal hematomas on magnetic resonance imaging. *Pediatr Radiol* 2018; **48**: 1593-1599 [PMID: 30109380 DOI: 10.1007/s00247-018-4178-9]
13 **Eurboonyanun C**, Somsap K, Ruangwannasak S, Sripanaskul A. Spontaneous Intramural Duodenal Hematoma: Pancreatitis, Obstructive Jaundice, and Upper Intestinal Obstruction. *Case Rep Surg* 2016; **2016**: 5321081 [PMID: 27891286 DOI: 10.1155/2016/5321081]
14 **Banieghbal B**, Vermaak C, Beale P. Laparoscopic drainage of a post-traumatic intramural duodenal hematoma in a child. *J Laparoendosc Adv Surg Tech A* 2008; **18**: 469-472 [PMID: 18503387 DOI: 10.1089/lap.2007.0147]
15 **Chirkov RN**, Abakumov MM, Blokhin VN. [Diagnostics and surgical treatment of traumatic intramural duodenal haematomes]. *Khirurgiia (Mosk)* 2008; 33-36 [PMID: 18577968]
16 **Kwon CI**, Choi KH, Ko EH, Lee JH, Song YJ, Ko KH, Hong SP, Park PW. [A case of duodenal intramural hematoma treated by percutaneous external drainage]. *Korean J Gastroenterol* 2007; **49**: 45-49 [PMID: 18167434]
17 **Jewett TC Jr**, Caldarola V, Karp MP, Allen JE, Cooney DR. Intramural hematoma of the duodenum. *Arch Surg* 1988; **123**: 54-58 [PMID: 3257385 DOI: 10.1001/archsurg.1988.01400250064011]
18 **Kwon CI**, Ko KH, Kim HY, Hong SP, Hwang SG, Park PW, Rim KS. Bowel obstruction caused by an intramural duodenal hematoma: a case report of endoscopic incision and drainage. *J Korean Med Sci* 2009; **24**: 179-183 [PMID: 19270837 DOI: 10.3346/jkms.2009.24.1.179]
19 **Lee JY**, Chung JS, Kim TH. Successful endoscopic decompression for intramural duodenal hematoma with gastric outlet obstruction complicating acute pancreatitis. *Clin Endosc* 2012; **45**: 202-204 [PMID: 22977802 DOI: 10.5946/ce.2012.45.3.202]

World Journal of Gastroenterology

Submit a Manuscript: https://www.f6publishing.com

World J Gastroenterol 2022 May 28; 28(20): 2248-2250

DOI: 10.3748/wjg.v28.i20.2248

ISSN 1007-9327 (print) ISSN 2219-2840 (online)

LETTER TO THE EDITOR

Future prospect of "Gut microbiome composition can predict the response to nivolumab in advanced hepatocellular carcinoma patients"

Yong-Bo Kang, Yue Cai

Specialty type: Gastroenterology and hepatology

Provenance and peer review: Unsolicited article; Externally peer reviewed.

Peer-review model: Single blind

Peer-review report's scientific quality classification

Grade A (Excellent): A
Grade B (Very good): B
Grade C (Good): 0
Grade D (Fair): 0
Grade E (Poor): 0

P-Reviewer: Gorrell MD, Australia; Yu L, Singapore

Received: December 10, 2021
Peer-review started: December 10, 2021
First decision: January 8, 2022
Revised: January 14, 2021
Accepted: April 24, 2022
Article in press: April 24, 2022
Published online: May 28, 2022

Yong-Bo Kang, Yue Cai, Department of Microbiology and Immunology, School of Basic Medical Sciences, Shanxi Medical University, Jinzhong 030600, Shanxi Province, China

Corresponding author: Yong-Bo Kang, PhD, Associate Professor, Department of Microbiology and Immunology, School of Basic Medical Sciences, Shanxi Medical University, Wenhua Street, Jinzhong 030600, Shanxi Province, China. 657151276@qq.com

Abstract

Recently, we read the article "Gut microbiome composition can predict the response to nivolumab in advanced hepatocellular carcinoma patients" with interest, and it is preliminary suggested that gut microbiota is closely related to therapeutic effect of nivolumab. Based on the meaningful results of this article, several valuable research directions are proposed to enhance the therapeutic effect of immune checkpoint inhibitors on advanced hepatocellular carcinoma.

Key Words: Gut microbiome; Immunotherapy; Immune checkpoint inhibitor resistance; Probiotics; Faecal microbiota transplantation; Hepatocellular carcinoma; Prognosis

Core Tip: We read the article "Gut microbiome composition can predict the response to nivolumab in advanced hepatocellular carcinoma patients" with interest, and it is preliminary suggested that the gut microbiota is closely related to therapeutic effect of nivolumab. Future research should pay attention to the relationship between the gut microbiota and therapeutic effect of immune checkpoint inhibitors (ICIs) on advanced hepatocellular carcinoma and the way of regulating the gut microbiota to improve the therapeutic effect of ICIs.

Citation: Kang YB, Cai Y. Future prospect of "Gut microbiome composition can predict the response to nivolumab in advanced hepatocellular carcinoma patients". *World J Gastroenterol* 2022; 28(20): 2248-2250
URL: https://www.wjgnet.com/1007-9327/full/v28/i20/2248.htm
DOI: https://dx.doi.org/10.3748/wjg.v28.i20.2248

TO THE EDITOR

We read with interest the article "Gut microbiome composition can predict the response to nivolumab in advanced hepatocellular carcinoma patients"[1], in which the authors analyzed and summarized the correlation between gut bacterial composition and the prognosis of nivolumab therapy in hepatocellular carcinoma (HCC) patients. The highlight of this article was that gut microbiota composition and diversity of responders differed significantly from those of non-responders following nivolumab therapy. Several intestinal bacterial species such as *Citrobacter freundii, Azospirillum species*, and *Enterococcus durans* were specific to the responders. Moreover, a higher *Prevotella/Bacteroides* ratio and the presence of *Akkermansia species* can serve as predictive markers of response. Altogether, the study not only demonstrated that the therapeutic effect of nivolumab has something to do with the composition of the gut microbiota in advanced HCC patients, but also provided some inspiration for future research direction.

In our opinion, it is of importance to underline that the relationship between the therapeutic effect of various immune checkpoint inhibitors (ICIs) such as pembrolizumab, nivolumab atezolizumab, durvalumab, and avelumab on HCC and the gut microbiota. At present, the response rates to ICIs are very low in advanced HCC. To be specific, the response rate to ICI monotherapy is merely 15%-23%, which is increased to approximately 30% after combination treatment[2]. How to improve the effectiveness of ICI treatment is essential and has been extensively investigated. While the human gut microbiota has been shown to be associated with clinical responses to ICIs in HCC[3], the available data in this field remain limited and the relevant scientific work is only in the initial stage. Thus, more research is required in the future. First, clinical studies with large sample sizes are needed to further clarify the relationship between the gut microbiota and the therapeutic effect of various ICIs. At the same time, which types of gut microbiota are suitable for which ICIs should also be figured out. Furthermore, construction based on the gut microbiota can function as a prognostic marker for the response to various ICI therapies. These results will provide clinicians with a valuable reference for rational use of ICIs and personalized precision therapy. Second, the mechanism by which the gut microbiota promotes the therapeutic effect of various ICIs needs to be further studied, with the focus on key pathways such as intestinal mucosal barrier function, bacterial metabolites, and microorganism-related molecular patterns, thus being conducive to discovering how to enhance the therapeutic effect of various ICIs by targeting the gut microbiota. Third, probiotics, prebiotics, synbiotics, and antibiotics may represent innovative, safe, and low-cost strategies for promoting the therapeutic effect of various ICIs[4]. In this respect, it is of necessity to determine which beneficial bacteria and harmful bacteria are bound up with the therapeutic effects of which ICIs. Meanwhile, it will also be significant to confirm how probiotics, prebiotics, synbiotics, and antibiotics alter the composition of the gut microbiota and how relevant it is to the therapeutic effect of various ICIs. In other words, these results will contribute to the identification of probiotics, prebiotics, synbiotics, and antibiotics that may increase the efficacy of ICIs when being used in combination. Last but not least, faecal microbiota transplantation (FMT) may be a direct and superior approach to enhancing the therapeutic effect of various ICIs through modulating the gut microbiota in human beings. Considering that, it is extremely valuable to explore the therapeutic method of FMT in combination with ICIs. Besides, the optimal gut microbiota composition for enhancing the therapeutic effect of various ICIs should be recognized. On this basis, it is of great importance to choose the right donors[5].

In summary, based on the meaningful research results of this article, it is expected that readers can pay attention to the relationship between the gut microbiota and therapeutic effect of ICIs on advanced HCC and the method of regulating the gut microbiota to improve the therapeutic effect of ICIs.

FOOTNOTES

Author contributions: Kang YB and Cai Y wrote the letter and conceived the manuscript; Kang YB supervised the manuscript drafting and reviewed the literature data; and all authors contributed important intellectual content during manuscript drafting or revision.

Conflict-of-interest statement: There is no conflict to declare.

Country/Territory of origin: China

ORCID number: Yong-Bo Kang 0000-0002-1584-5546; Yue Cai 0000-0001-6314-0463.

S-Editor: Wang JJ
L-Editor: Wang TQ
P-Editor: Wang JJ

REFERENCES

1 **Chung MW**, Kim MJ, Won EJ, Lee YJ, Yun YW, Cho SB, Joo YE, Hwang JE, Bae WK, Chung IJ, Shin MG, Shin JH. Gut microbiome composition can predict the response to nivolumab in advanced hepatocellular carcinoma patients. *World J Gastroenterol* 2021; **27**: 7340-7349 [PMID: 34876793 DOI: 10.3748/wjg.v27.i42.7340]
2 **Pinter M**, Jain RK, Duda DG. The Current Landscape of Immune Checkpoint Blockade in Hepatocellular Carcinoma: A Review. *JAMA Oncol* 2021; **7**: 113-123 [PMID: 33090190 DOI: 10.1001/jamaoncol.2020.3381]
3 **Li L**, Ye J. Characterization of gut microbiota in patients with primary hepatocellular carcinoma received immune checkpoint inhibitors: A Chinese population-based study. *Medicine (Baltimore)* 2020; **99**: e21788 [PMID: 32925716 DOI: 10.1097/MD.0000000000021788]
4 **Kang Y**, Cai Y, Yang Y. The gut microbiome and hepatocellular carcinoma: Implications for early diagnostic biomarkers and novel therapies. *Liver Cancer* 2021 [DOI: 10.1159/000521358]
5 **Kang YB**, Cai Y. Faecal microbiota transplantation enhances efficacy of immune checkpoint inhibitors therapy against cancer. *World J Gastroenterol* 2021; **27**: 5362-5375 [PMID: 34539138 DOI: 10.3748/wjg.v27.i32.5362]

Published by **Baishideng Publishing Group Inc**
7041 Koll Center Parkway, Suite 160, Pleasanton, CA 94566, USA
Telephone: +1-925-3991568
E-mail: bpgoffice@wjgnet.com
Help Desk: https://www.f6publishing.com/helpdesk
https://www.wjgnet.com